

Department of

Biotechnology and Biosciences

PhD program

Converging Technologies for Biomolecular Systems (TeCSBI)

Cycle XXXIII

Microbial cell factories for biobased processes: the concept of cascading applied to different biomasses and bioproducts in the context of bioeconomy

Candidate: **Bertacchi Stefano**

Registration number: 725932

Tutor: Prof. Paola Branduardi

Coordinator: Prof. Paola Branduardi

This dissertation has been approved by the promoters.

Composition of the doctoral committee

Prof. Paola Branduardi (promoter)	University of Milano Bicocca (Italy)
Prof. Diethard Mattanovich (opponent)	University of BOKU of Vienna (Austria)
Prof. Stefano Castiglione	University of Salerno (Italy)
Prof. Francisca Lottersberger	Linköping University (Sweden)

The researched presented in this thesis was performed at the Department of Biotechnology and Biosciences of the University of Milano Bicocca, Italy, and supported by Food Social Sensor Network (FOOD NET). Part of the work was performed at the Faculty of Technology of the University of Oulu (Finland) and funded by the European Institution of Innovation & Technology (EIT) KIC-RawMaterials project ADMA2 (Practical training between Academia and Industry during doctoral studies).

© 2021 **Stefano Bertacchi**

All rights reserved. No part of this publication may be reproduced, stored in a retrieval system, or transmitted, in any form or by any means, electronically, mechanically, by photocopying, recording or otherwise, without the prior written permission of the author.

Index

Abstract_____ 1

Introduction

Bioeconomy and the concept of cascading_____ 3

Biorefineries, residual biomasses and microbial cell factories_____ 5

Enzymatic hydrolysis of lignocellulosic biomasses_____ 8

Bioprospecting microbial cell factories: from bacteria to yeasts_____ 11

Bioproducts: carotenoids, folates and biogas_____ 16

Chapter 1

Camelina sativa meal hydrolysate as sustainable biomass for the production of carotenoids by *Rhodospiridium toruloides*_____ 33

Chapter 2

Optimization of carotenoids production from *Camelina sativa* meal hydrolysate by *Rhodospiridium toruloides*_____ 57

Chapter 3

Enzymatic hydrolysate of cinnamon waste material as feedstock for the microbial production of carotenoids_____ 77

Chapter 4

Assessment of folates forms produced by wild type and engineered *Saccharomyces cerevisiae* yeast cells_____ 99

Chapter 5

Implementation of mathematical modelling of a bio-based methane production from manure_____ 119

Conclusions	<u>135</u>
Acknowledgments	<u>141</u>
Academic and outreach activities	<u>143</u>
Awards and scholarships	<u>145</u>
Publications	<u>147</u>

Abstract

Bioeconomy involves processes based on renewable biomasses: in this scenario, the development of second-generation processes, based on residual biomasses such as industrial by-products (*e.g.* from the food, agriculture, forestry sectors), can accomplish all the principles of sustainability. Since microorganisms have the potential to transform these biomasses into products of industrial interest, the work focused on the valorization of residual biomasses (*i.e.* *Camelina* meal and cinnamon waste materials, manure), and on the identification and possible modification of microbial cell factories (*i.e.* *Rhodospiridium toruloides*, *Saccharomyces cerevisiae*, anaerobic consortia) for the synthesis of molecules of industrial relevance (*i.e.* carotenoids, folates). Following the logic of cascading, high added value compounds can be obtained in relatively low amounts and using increasingly expensive raw materials, whereas bulk chemicals (*i.e.* biogas) must be obtained from low value feedstocks (*i.e.* manure).

The first substrate studied as feedstock was the *Camelina sativa* meal, which, despite its potential, had never been considered as a raw material for the development of a bioprocess. Different concentrations of *Camelina sativa* meal were tested for enzymatic hydrolysis by different concentrations of the industrial cocktail NS22119, to release sugars for the growth of the microorganism. The process was optimized in terms of enzymes added and total solid loadings, identifying the use of 9% w/v of *Camelina* meal and 0.56% w/w_{*Camelina* meal} of enzymatic cocktail as able to increase the specific productivity of carotenoids by *R. toruloides*. The hydrolyzate of *Camelina sativa* meal was then provided to the microorganism by a separate hydrolysis and fermentation (SHF) or a simultaneous saccharification and fermentation (SSF) process. In all the cases *R. toruloides* was able to grow and accumulate carotenoids, at a concentration comparable with those reported in the literature from other residual biomasses. SHF production was further tested in bioreactor to acquire quantitative data under industrially relevant conditions. Overall, we demonstrated the potential use of the *Camelina sativa* meal as raw material for

bioprocesses based on *R. toruloides*, an oily yeast naturally able of accumulating carotenoids.

A second activity concerned the exploitation of cinnamon (*Cinnamomum verum*): since its cellulose content, we applied the principles exposed for the *Camelina* meal to the waste deriving from the extraction of polyphenols from cinnamon as well. The hydrolysis via enzymatic cocktail was tested at different operating pH, successfully resulting in released sugars available for the growth of microorganisms. Since cinnamon possess antimicrobial properties, an on-plate testing of different yeast species was carried out: in the presence of cinnamon extract waste hydrolysate, all the tested species proved to be able to grow, meaning that the initial extraction diminishes the levels of antimicrobial species in the residues. In the case of *R. toruloides*, it was able to produce carotenoids both on plate and in liquid media derived from cinnamon waste.

Another class of high added-value molecules we focused on were folates: the yeast *S. cerevisiae* was engineered in order to increase the production of these molecules of pharmacological relevance. Modulation of the shikimate and folate pathways were proposed to assess their effect on the different forms of folates produced from glucose.

Finally, the production of biomethane from manure by microbial consortia was evaluated using a computational model: we updated existing equations to better describe microbial conversion of sugars into biomethane and modified specific process parameters to simulate and predict possible increases in production.

Overall, this work explored different aspects of the concept of cascading applied to several biomasses, microbial cell factories and products.

Introduction

Bioeconomy and the concept of cascading

The Earth Overshoot Day (EOV) is calculated as the moment of the year when humans have already utilized the total amount of resources produced by the planet in one year: the earlier this date the more unsustainably resources are deployed, therefore impoverishing the planet for future generations [1]. In 1987 EOV was at the end of October, whereas in 2019 at the end of July, witnessing a strong increase in the consumption of natural resources in the last decades. This fact is strongly related to the skyrocketing of fossil resources deployment, together with their detrimental effects on the environment and human health [2]. One of the main paths to detach from our fossil resources dependence is the exploitation of newly generated resources, whose renewability is time-scale compatible with their consumption. Biomasses are therefore good candidates for such purposes, to be exploited in a society where the Sustainable Development Goals, proposed by the United Nations [3], are (or should be) the driving forces for governance, citizens and scientific research towards “greener” societies (Figure 1).



Figure 1 Postage stamp issued by the Republic of San Marino in 2016 as part of the “Europa postage stamp” series. In 2016 the chosen topic was the environment: the winning design “Think green” from Cyprus was used by all European countries involved in this joint issue, in order to underline the commitment of European citizens towards bioeconomy. Stamp from private collection.

Indeed, bioeconomy is already a worldwide business that involves the exploitation of different types of biomasses: agriculture, feed, pulp and paper, food and beverage, fisheries, and forestry are the most involved sectors within bioeconomy boundaries [4].

Bioeconomy is a key protagonist in fostering environment-driven measures across countries, and, as announced by the European Commission, it “needs to have sustainability and circularity at its heart” [5]. In this scenario, it is possible to identify several keywords closely related to bioeconomy development, such as wastes and residues, bioenergy and biofuels, bio-based products, cascading, and biorefineries [6].

Specifically, cascading aims to examine the potential of specific biomasses, and the possible outcomes that could match the the three pillars of sustainability: economic, environmental and social. Bio-based resources have to be considered for their sequential use during time, in respect to their decreasing quality, to enable the resource to endure longer in the system: this definition of “cascading-in-time” perfectly fits in the circular economy scenario [7] (Figure 2).

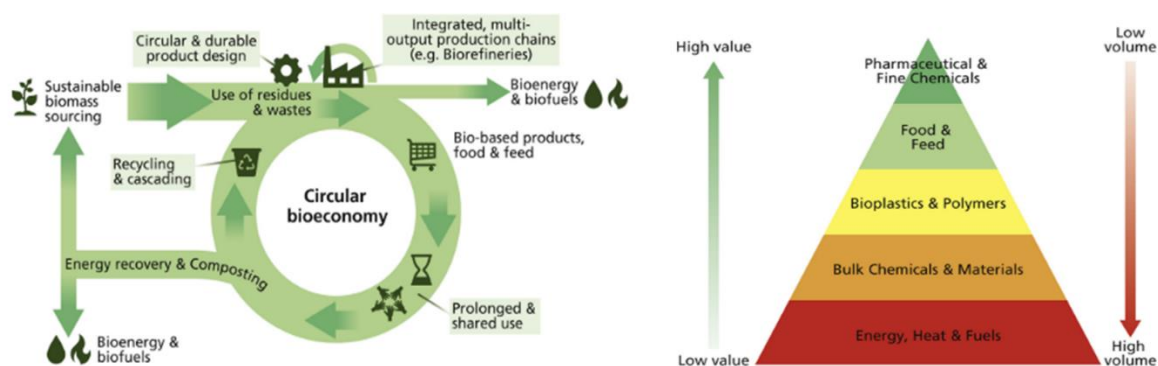


Figure 2. The circular bioeconomy and its elements (left) and Bio-based value pyramid, from [6].

Furthermore, “cascading-in-value” concept focuses in maximizing the value of the biomass throughout the cascade chain, in order to obtain added values related, for example, to the abundance of the original feedstock [6,7]. In a nutshell, considering the so called “bio-based pyramid” (Figure 2), pharma and cosmetic-related compounds have a high market value, being fine chemicals, whereas bulk chemicals and biofuels have a low price with a high volumetric demand [6,8]. Therefore, the original biomass value and availability have to be considered as well, since low-quality feedstocks, such as manure, can be deployed for low-cost products with large market demand, such as biogas, whereas residual biomasses with limited applications (*e.g.* feed sector) or refined sugars (*e.g.* glucose) can be used for the production of fine chemicals, such as vitamins. Based on the logic of cascading [7,9], the

present Doctorate work focused on the exploitation of renewable biomasses (mainly of residual origin) for the development of microbial-based processes, to produce fine and bulk chemicals, in the logic of biorefinery.

The concept of biorefineries is indeed aimed at revolutionizing the industrial sector to sustainably meet the requirements of the growing population with limited resources. Key players in this context are second generation biorefineries, based mainly on lignocellulose, a biomass with huge potential particularly owing to its abundance, availability, relatively low cost and non-competition with the food sector [10].

Biorefineries, residual biomasses and microbial cell factories

Biorefineries can be described as “the sustainable processing of biomass into a spectrum of marketable products (food, feed, materials, chemicals) and energy (fuels, power, heat)” [9]. Biorefineries indeed are aimed to provide a broad portfolio of products alongside classical bio-based molecules such as biofuels or biogas [6,11,12]. Consistently, they are considered as one of the key technologies in circular bioeconomy, presenting different opportunities and challenges across countries, as they need to be organically integrated in the territories’ landscape and infrastructure. In order to widen possible outcomes of biorefineries and in some cases minimize environmental impacts, it is possible to exploit microorganisms, the so-called microbial cell factories, whose role is to convert the provided biomass into the desired product(s) [13,14]. Microbes are naturally able to produce molecules of industrial interest and to exploit biomasses; plus genetic engineering and synthetic biology can improve both the characteristics [15–18]. Nonetheless, since the use of genetically modified microorganisms (GMMs) is strictly regulated, particularly in Europe, their industrial applications are still limited, especially in fields related to food and feed [19]. Metabolic features of microbes can in fact valorize residual biomasses like seaweeds-derived ones, whose sugar components could be further used for microbial fermentation, even after the extraction of valuable compounds (*e.g.* specialty lipids) from the seaweeds themselves, perfectly matching the cascading concept [20]. Indeed, microbial cell factories can provide products that lay at opposite boundaries of the cascading pyramid, from high-

value molecules such as terpenoid flavors and fragrances [21] to low-value ones, like biofuels [22]. The product portfolio provided by microbial biodiversity permits in fact to address cascading principles, exploiting various types of biomasses [23].

Consequently, biorefineries based on microorganisms are strongly dependent on the biomass used, since it will act as nutritional source for microbial cells, thus the access to nutrients in those sources must be guaranteed. Both first and second generation biorefineries often rely on sugar-based biomasses, such as edible crops (*e.g.* corn, sugarcane) and lignocellulose, respectively, whose polysaccharides need to be hydrolyzed to release simpler molecules that are used by the cells more easily. This goal can be achieved by either chemical or enzymatic hydrolysis, the latter being preferred since generally it can be performed under conditions that are more compatible with the microbial growth. For example, acid hydrolysis is limited by the need of neutralizing the pH afterwards, by the generation of inhibitory compounds (*e.g.* furfurals) and by the disposal of the acid itself that negatively affects the environmental impact of biorefineries [24,25]. Consequently, it is crucial that nutrients released from biomasses can match microbial requirements. In the case of lignocellulosic biomasses (LCBs), constituted by cellulose, hemicellulose and lignin in different ratios, a pre-treatment step aimed to open-up the recalcitrant macromolecular structure is often followed by enzymatic hydrolysis [26], as enzymes are operating under conditions that are more compatible with microbial growth. Different hydrolyses can generate different mixtures of sugars and other nutrients, both in terms of composition and relative quantities. Remarkably, enzymes, as loyal allies to unlock the real potential of second generation biomasses, can be applied using two different processes such as separate hydrolysis and fermentation (SHF) and simultaneous saccharification and fermentation (SSF) in order to match microbial cell factories characteristics [27] (Figure 3).

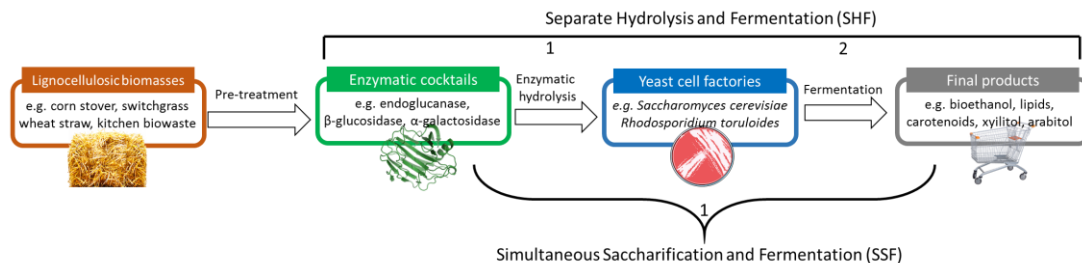


Figure 3: Overview of the processes/factors involved in conversion of lignocellulosic biomass into final products. Pre-treatment is often needed to weaken the intertwined structure of LCBs, prior to enzymatic hydrolysis. In SHF two steps (hydrolysis and fermentation) are apart among them, whereas they are combined in a single one in SSF.

Annually, about 1.3 billion tons of lignocellulosic biomasses are generated all around the world, although only 3% are being exploited to produce biochemicals, bioenergy and non-food related bio-products [28]. Main examples of LCBs are plant straw, coconut husk, corn stover, and sugarcane bagasse, vegetable and woody materials in general. The structure of lignocellulose is intertwined by three main biological polymers, namely lignin (20-30%), hemicellulose (20-40%) and cellulose (40-50%) [29] held together by different types non-covalent bonds and covalent cross-linkages. Cellulose, the most abundant LCB polymer, is composed of β -D-glucose units linked by β -(1,4) glycosidic bonds, with cellobiose as the fundamental repeating dimeric unit. Around 500-1400 glucose molecules compose the cellulose chains forming the microfibrils that are embedded in the lignocellulosic matrix: this in turn makes it resistant to enzymatic hydrolysis [30]. Hemicelluloses are composed of heterogeneous groups of biopolymers containing various monosaccharide subunits to form xylans, xyloglucan, mannans and glucomannans [31]. They are amorphous with very little physical strength and act as a physical barrier for enzyme accessibility. Lignin, responsible for the hydrophobicity and structural rigidity, binds hemicelluloses to cellulose in the cell wall [30]. Cellulose and hemicelluloses are linked together through hydrogen bonds, while lignin is covalently linked to hemicelluloses to form lignin-carbohydrate complex (LCC).

Given the uneven and complex nature of LCBs, their exploitation in biorefineries propaedeutically involves steps aimed to degrade such matrixes, with the goal to easily release the sugar content within, and to provide the hydrolysate as growth medium to

microbial cell factories. Therefore, both pre-treatment and hydrolysis are pivotal to the development of second-generation biorefineries.

Enzymatic hydrolysis of lignocellulosic biomasses

As aforementioned, enzymatic cocktails are a preferred option compared to chemical hydrolysis of LCBs, in order to match better microbial growth requirements. Nevertheless, before the addition of enzymes, the so-called pre-treatment step is often applied to destabilize the recalcitrant structure of LCB. Depending on the type of LCB used and the end product of interest, there are several physical, chemical, thermal and biological pre-treatment methods, that can also be used in combination [29]. Classic types of pre-treatments involve acid or alkaline based methods, steam explosion and hydrothermal processing, that in turn may release inhibitory compounds for both enzymes and microbes, such as phenolic compounds, weak acids and furan aldehydes (*i.e.* furfural and hydroxymethylfurfural) [28,29]. Despite it might be easier to choose among techniques the one most suitable considering the sole LCB or the plant equipment, the subsequent steps need to be considered as well, since they can have a negative impact [28]. Knowing that, there are several examples, and many more are going to appear in a near future, of protocols where these factors are taken into utmost consideration, showing the possibility to reach efficient hydrolysis and microbial fermentation by exploiting enzymatic cocktails (and microbial cell factories too) that are less sensitive to those inhibitors.

Considering the main components of LCBs, cellulose is hydrolyzed to cellobiose and glucose, whereas hemicellulose gives rise to diverse pentose and hexose sugars: cellulases and hemicellulases are used respectively, often combined in cocktails [32]. Multiple factors such as temperature, pH, rate of mixing, substrate concentration, enzyme loading and addition of surfactants influence monomeric sugar yields from LCBs [33]. According to the International Union of Biochemistry and Molecular Biology (IUBMB) most of the (hemi)cellulases and other polysaccharide degrading enzymes are grouped in the family of O-glycoside hydrolases (GH) and further sub-classified into different families based on primary structure of catalytic domains [32]. Given the variation between LCBs from

different sources, and the heterogeneity that arises following the pre-treatment, biodiversity of GHs is pivotal to address the hydrolysis of the different component of these matrixes. The complete degradation of cellulose can occur by combined and simultaneous action of three distinct classes of cellulolytic enzymes namely, endoglucanases, cellobiohydrolases and β -glucosidases. Endoglucanases are involved in the cleavage of internal β -glucosidic bonds thereby providing to cellobiohydrolases accessible cellulose chain ends, releasing cellobiose that is further hydrolyzed to glucose by β -glucosidase [34]. On the other hand, considering that hemicellulose is not composed by a single monomer and contains several different bonds as mentioned, its composition may instead vary a lot depending on the LCB considered and therefore hemicellulolytic enzymes are more diverse. Since the intertwined nature of lignocellulose, to detach sugars from the lignin moiety and to reduce the inhibitory effect of lignin itself different it is crucial to have combinations of hydrolytic and accessory enzyme, both in terms of types and ratios [35]. Enzymatic cocktails have a pivotal role in improving the efficiency of biomass hydrolysis by reducing the amount of enzymes and time required to convert all the carbohydrates into fermentable sugars and having the possibility to function at high substrate loadings [36]. The formulation of cocktails can be in fact designed to exploit synergistic effect of enzymes such as cellulase, xylanase and pectinase.

Considering the relationship between enzymatic hydrolysis and microbial fermentation, in the last decades two main types of processes have been developed: simultaneous saccharification and fermentation (SSF) and separate hydrolysis and fermentation (SHF). They can be simply described as processes where enzymes and cells are working together or in separated vessels, respectively. The two processes have several pros and cons in terms of efficiency, duration, presence/release of inhibitory molecules, and downstream process of the final product [27,37,38]. There are several examples in literature of second generation bioethanol production by *Saccharomyces cerevisiae*, the main microbial cell factory exploited for this purpose [37,39,40], based on SHF or SSF processes. An obvious advantage of SHF is the possibility to choose the optimal conditions for both enzymatic hydrolysis and fermentation steps as they occur temporally and spatially separated. For example, temperature is a key parameter since efficient enzymatic cocktails often have

optimum activity at around 50 °C, whereas microbial fermentations very often use mesophilic microorganisms displaying optimal temperatures comprised between 25 °C and 35 °C [37,38,41]. In addition, in a SHF process it is possible to eliminate by centrifugation the non-hydrolyzed components, called water insoluble solids (WIS), that may impair subsequently microbial growth and production, because of the toxicity of some of their components, such as the phenolic moiety, that may impair cellular redox balance [42], as well as because of a poor homogenization of the liquid medium [43]. Separation of WIS is also advantageous if not indispensable when the final product is intracellular [44]. Nevertheless, SHF also displays drawbacks, such as higher capital expenditures (CAPEX – the money spent by a company to handle with long-term assets) because of the need of different vessels and prolonged process times (augmenting also the risk of undesired fermentations), which in turn may impair the economical sustainability of the process itself [27,38]. Another relevant issue in SHF is the enzyme inhibition caused by the mono- and disaccharides released, while the downside of an optimized hydrolysis can be the excessive osmotic stress for the cell factories in batch fermentations.

On the contrary, in SSF cell factories can metabolize sugars co-currently with their release from the biomass, thus mitigating both the osmotic stress and the inhibitory effect of (simple) sugars on the enzymes [27,37,38]. In addition, in SSF processes glucose titer is maintained low by microbial co-consumption, facilitating the consumption of other saccharides as well, otherwise impaired by the catabolic repression caused by glucose itself [37,38]. Considering also that SSF might reduce the overall duration of the process, the number of variables justifies the fact that several works (and several industrial processes as well) are exploring both SHF and SSF to understand which one better matches their expectations [45–50]. The choice between SSF and SHF is debated also when using high solids loadings (>20% w/v), which can affect cell viability and the action of enzymes; the compromise between the amount of sugars and inhibitors must be considered [49,51]. SSF could additionally be implemented by a presaccharification step, namely a partial enzymatic hydrolysis of cellulose and hemicelluloses contained in the substrate and a enzymatic-assisted disassembly of hemicellulose-lignin moieties. This is aimed to facilitate the subsequent co-current hydrolysis and fermentation, in particular when the microbial

cell factory used is supposed to produce the enzymes (whether endogenous or recombinant) itself [52,53]. The need and the characteristics of the presaccharification step are really dependent on the type of biomass used as feedstock, therefore its deployment could be considered or not to further improve the bioprocess of interest [52,53].

The possibility to choose between different options is a situation even more widened by the huge microbial diversity to draw from in order to develop bioprocesses based on microbial cell factories.

Bioprospecting microbial cell factories: from bacteria to yeasts

Thousands of microorganisms have already been catalogued, despite the majority is yet to be discovered. With the microbial portfolio already available, it is possible to apply a widespread bioprospecting, in order to isolate and select microbial cell factories to be employed in bioprocesses [18]. In addition, genetic engineering and synthetic biology approaches can extend possible products of microbial origin [17]. Nevertheless, these two strategies are inclusive among each other, permitting to unlock innovative phenotypes, and in turn, new bioprocesses [18].

Considering prokaryotes, a great variety of species have been proposed as microbial cell factories, thanks to their apparent simplicity, that provided them with powerful evolutionary tools to colonize basically all known habitats on our planet. Prokaryotes can be exploited as single species for the synthesis of molecules ranging from biofuels and bioplastics to food colorants, cosmetics and pharmaceuticals, providing optionally refined sugars or LCBs [23,54,55]. Several biomasses, especially the cheap ones, are normally contaminated with prokaryotes that naturally can grow on such substrates. Therefore, to completely use them and produce multiple products, industrial processes based on microbial consortia drew more and more attention in the last decades, since their properties arising from the synergistic effect of several species [55]. The combinatory effects of different prokaryotic metabolisms is definitely clear in the case of biogas production from organic material of residual origin, where acetogenic and methanogenic

microbes are a real assembly line to be exploited for human energy needs [55,56]. Among the various prokaryotic microbiotes involved in anaerobic digestion of sludge or manure, core archeal groups are *Methanosarcinales* and *Methanomicrobiales*, whereas main bacterial groups are *Chloroflexi*, *Betaproteobacteria*, *Bacteroidetes* and *Synergistetes* [57,58], although high diversity in members of each specific consortium is responsible for biogas production variations in full-scale anaerobic digesters [59]. Therefore, considering both the complete use of different biomasses and the wide range of product of prokaryotic origin, the use of these microbes definitely matches the cascading principles.

Similarly, eukaryotic biodiversity can be deployed for the cause of bioeconomy as well, to develop microbial-based bioprocesses. Among fungi, several filamentous fungi have been proposed as microbial cell factories able to use waste stream derived biomasses [60,61]. Nonetheless, filamentous fungi are characterized by a multicellular nature and frequently by slow growth that may diminish their performances, especially in terms of productivity [62]. When the accumulation of the final product generates toxicity, as in the case of ethanol among others, this limitation becomes a real impairment to the success of the process. Focusing only on yeasts, it is possible to choose from a huge variety of different species, often with unique features, and compensating some of the drawback of filamentous fungi.

The most widely used eukaryotic microorganism in biorefineries is the yeast *S. cerevisiae*, the main specie responsible for food and beverage production (e.g. fermented beverages), that can be exploited for its natural and engineered features, obtaining products such as bioethanol, organic acids, carotenoids, vitamins and pharmaceuticals [16,18,63,64]. In addition, it can ferment both refined and cellulosic sugars, being therefore a valuable ally to fulfill the principles of cascading in terms of both the substrate and the product. Nevertheless, it shows some limits, such as a narrow substrate preference, that exclude for instance pentose, and its robustness, which is enough for some LCBs, inhibitors and products, but not for other ones [37].

Although *S. cerevisiae* is still the yeast of election both as model system and industrial workhorse, there are plenty of other yeasts to be considered for these purposes [65]. In fact, there is an enormous and mainly unexplored potential among the so called non-

conventional yeasts [14,66,67], essentially because they are less characterized. Their exploitation is limited by the fact that only a few of them are considered into the qualified presumption of safety (QPS) list of the European Food Security Agency (EFSA) [68,69]: soon more will be enlisted too, widening the possible scenarios.

In the presented scenario yeast biodiversity can offer advantages that are not fully exploited and, in some cases, also poorly explored. Prominent examples are the co-consumption of hexose and pentose sugars (which includes both sugar transporters and catalytic enzymes) [70,71], and the native production of enzymes for the hydrolysis of LCB-derived polymers/oligomers [71]. It becomes clear after what disclosed above that enzymatic hydrolyses can bring out these peculiar traits. Once more, despite its high potential *S. cerevisiae* appears limited due to the high preference for glucose. Indeed, the broader substrate range of non-*Saccharomyces* yeasts can be coupled not only to the production of ethanol (which still remains one of the most investigated product when demonstrating industrially relevant products) but also to biodiesel or more generally single cell oil (SCO), as in the case of oleaginous yeasts [72–74]. Testing the ability of yeast species as putative cell factories using a certain feedstock is therefore pivotal, to explore the potential provided by a bioprospecting approach.

Together with the consumption of sugars from LCBs enzymatic hydrolysis, the ability to withstand various growth inhibitors often derived not only from the product but also from the pre-treatment step of LCBs is pivotal [75,76]. In this context, once more yeast diversity can match with feedstock composition, which in turn is dependent from the enzymatic cocktail that was used. Oleaginous yeasts are often displaying good resistance towards classic inhibitors present in LCBs hydrolysates [74,76,77]. Non-*Saccharomyces* yeasts are therefore an important biological reservoir of biodiversity that can be applied to the development of second-generation biorefineries, in order to widen our horizons beyond the common exploitation of *S. cerevisiae* for bioethanol production, and to maximize the portfolio of enzymatic cocktails available on the market.

In the last years, some yeast species, including *Rhodospiridium toruloides*, *Lipomyces starkeyi*, and *Yarrowia lipolytica* have become popular and are currently used on an industrial scale. These species are called oleaginous yeasts, since their natural ability to

accumulate intracellular lipids can be exploited mainly for the production of biodiesel [61,72,73,78]. Together with the “*ex novo*” lipid biosynthetic pathway, that starts from hydrophobic substrates (oils, alkane, etc.), these species possess also a “*de novo*” pathway, starting from sugars and related molecules, therefore being the one of interest when exploiting LCBs [79]. Among oleaginous yeasts, several species are able to metabolize LCBs derived sugars, being therefore attractive cell factories for second generation biorefineries [72–74,76].

Relevant parts of the work described in the present Doctoral work has been focused on the use of *R. toruloides*, whose features and characteristics, together with its applications as microbial cell factory in biorefineries, have been recently reviewed [80,81]. *R. toruloides* is a heterothallic yeast, isolated in 1922 from the air of the city of Dailan (China), originally named *Torula rubescen* [82], and today classified in the *Pucciniomycotina* clade. Since species of this group are polyphyletic, a recent phylogenetic classification proposed to rename *Rhodospordium* as *Rhodotorula* [83]. In nature, *R. toruloides* is also found in diverse types of environment such as soil, seawater, acid sewage and plant leaves. *R. toruloides* can indeed metabolize different kind of substrates, like mono- and disaccharides such as sucrose, maltose, cellobiose, trehalose, raffinose, and D-galacturonic acid, and alcohols such as ethanol, glycerol, mannitol and sorbitol [74,76,77], therefore being an attractive cell factory to be deployed in second generation biorefineries. *R. toruloides* consumes pentose sugars of LCB origin, like xylose, by the classic fungal pathway comprising xylose reductase (XR) and xylitol dehydrogenase (XDH) activity, producing also D-arabitol in the process [84,85]. In addition, (Figure 4), it is a natural producer of carotenoids, such as β -carotene, γ -carotene, torulene, and torularhodin, and neutral lipids, accumulated under nutrient-limiting conditions as a carbon storage mechanism [81,86]. This specie, often called “pink yeast” because of carotenoids, produces also enzymes, such as esterases and phenylalanine ammonia-lyase (PAL), which are of interest for the drug and the green chemistry industrial sectors [81,87]. *R. toruloides* also possesses a good resistance towards classic inhibitors derived from the hydrolysis and pretreatment of LCBs, such as furfural, acetic acid, and phenolic compounds [74,77]. In addition to its natural abilities, *R. toruloides* can be genetically modified to produce several other molecules, such

as fatty alcohols, fatty acids methyl esters (FAME) and various mono- and polyunsaturated fatty acids, together with compounds derived from branching of the isoprenoids pathway [81,88]. When compared with other oleaginous yeasts, *R. toruloides* is desirable since it accumulates up to 65% of the dry cell weight as lipids under nitrogen-limited conditions, whereas *Y. lipolytica*, the most used for this goal, naturally produces around 30% without additional engineering [81]. *R. toruloides* synthesis of carotenoids is also similar in terms of production to those of species of the genera *Rhodotorula*, *Sporidiobolus*, and *Xanthophyllomyces / Phaffia* accounted for being top producer organisms: nevertheless, genetic tools to modify *R. toruloides* are more advanced [81]. These tools include random DNA insertion by *Agrobacterium tumefaciens*-mediated transformation (ATMT) [89], RNA interference [90], and genome editing by CRISPR/Cas9 system [91,92].

Since the possibility to obtain different product from a single species, when expanding to other microbes with a bioprospecting approach it is fundamental to examine in depth the characters of such compounds, in order to evaluate the bioprocesses in the light of the cascading principles.

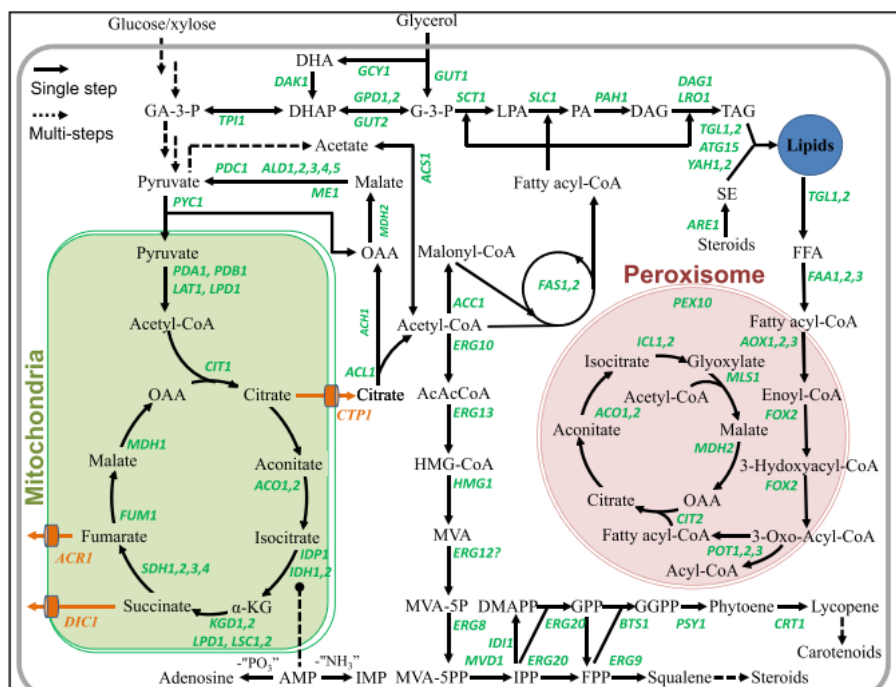


Figure 4 The primary metabolic pathways of *R. toruloides*. Key genes involved in glycolysis, pentose phosphate pathway, TCA cycle in mitochondria, biosynthesis and degradation of fatty acids,

triacylglycerols and phospholipids, isoprenoid biosynthesis, glyoxylate cycle pathway, and the β -oxidation pathways in peroxisomes are highlighted in green. Abbreviations: GA-3-P, glyceraldehyde 3-phosphate; DHA, dihydroxyacetone; DHAP, dihydroxyacetone phosphate; G-3-P, glycerol-3-phosphate; LPA, lysophosphatidic acid; PA, phosphatidic acid; DAG, diacylglycerol; TAG, triacylglycerol; SE, steryl ester; FFA, free fatty acid; OAA, oxaloacetate; AHG, α -ketoglutarate; AcAcCoA, aceto-acetyl-CoA; HMG-CoA, hydroxymethylglutaryl-CoA; MVA, mevalonate; MVA5P, mevalonate-5-phosphate; MVA5PP, mevalonate-5-diphosphate; IPP, isopentenyl diphosphate; DMAPP, dimethylallyl diphosphate; GPP, geranyl diphosphate; FPP, farnesyl diphosphate; GGPP, geranylgeranyl diphosphate; AMP, adenosine monophosphate; IMP, inosine monophosphate. From [80].

Bioproducts: carotenoids, folates and biogas

As aforementioned, heat and electricity are the main products obtained from renewable biomasses, but the involvement of microbial cell factories expanded that portfolio, with a plethora of other fine and bulk chemicals. Alongside (ligno)cellulosic bioethanol, solvents (*e.g.* butanediol, propendiol, isobutanol), carboxylic acids (*e.g.* lactic acid, acetic acid, itaconic acid), amino acids (*e.g.* lysine, glutamic acid), terpenes (*e.g.* squalene, carotenoids) have been proposed by the means of natural or engineered microbial cell factories, with examples already on the market [11]. These molecules have different added values from low (biofuels, solvents) to high (terpenes) ones, therefore, in the context of the cascading principles [6,7] the biomasses to be exploited for such purposes can vary in terms of costs and availability. This Doctoral work has been focused on three main products of renewable origin, namely carotenoids, folates and biogas.

The global market value for carotenoids was estimated to be \$1.5B in 2017 and is expected to reach \$2.0B by 2022, with a compound annual growth rate of 5.7% [93–95]. Carotenoids display several benefits for human health, related to their antioxidant properties, with anticancer and anti-inflammatory activity as well [94]. In fact, food and dietary supplements are the second ranked sector for revenue from carotenoids, being animal feed the first one with 41% of total revenue [94,96]. Ruminants are indeed entirely dependent on feed as a source of carotenoids, since they cannot produce them autonomously [97]. Other applications involve the pharmaceutical, the cosmetic and the food dye sectors

[94,98]. Carotenoids have also been recently tested for their antimicrobial activity against both bacteria and fungi [99].

Carotenoids are lipophilic tetraterpenes (C₄₀) divided in two main groups, namely carotenes and xanthophylls, being the first compounds with only hydrocarbons in their chemical structure (*e.g.* lycopene, β -carotene, torulene), and the second being oxygenated, with different functional groups such as hydroxy (*e.g.* lutein and zeaxanthin) and keto (*e.g.* astaxanthin) [98,100]. The end group of carotenoids can be either acyclic, like in the case of lycopene, of cyclic, like β -carotene or astaxanthin [98,101] (Figure 5). Known carotenoids, their properties, functions and natural producers have been listed in a recent database [102].

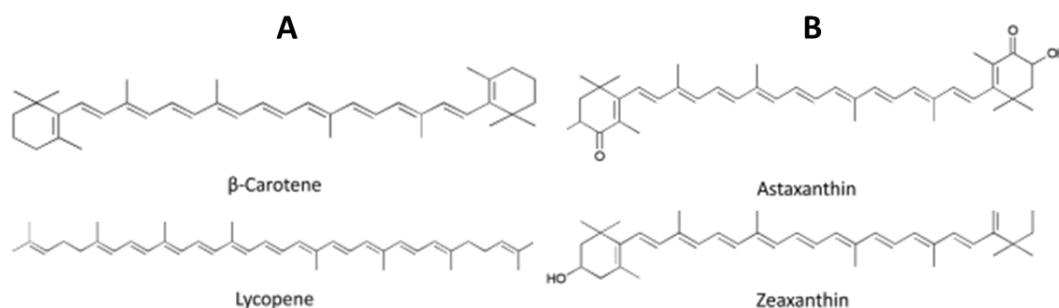


Figure 5 A. Structure of some carotenes (A) and xanthophylls (B) present in the human diet. Modified from [101].

All carotenogenic organisms (both eukaryotic and prokaryotic) biosynthesize carotenoids via the C₅ isoprenoid precursors isopentenyl pyrophosphate (IPP) and dimethylallyl pyrophosphate (DMAPP), predominantly produced utilizing the mevalonate (MVA) pathway or the 2-C-methyl- d-erythritol 4-phosphate (MEP) pathway [94]. The presence of conjugated double bonds is the reason why carotenoids appear colored from yellow to orange/red (410–510 nm) to the human eye [99,101]. Thanks to this feature, carotenoids have several natural roles related to light exposure, such as being directly deployed for photosynthesis and protection from photo-protection stress. For example, halophilic microbes like the microalga *Dunaliella salina* or the archaea *Halobacterium salinarium* live in body of water with high salinity and low depth, and therefore produce carotenoids to

counter the high exposure to light typical of their natural habitat [103]. Together with natural producers from all the three Domains of life, several other non-carotenogenic microbes can be genetically modified for this purpose, like *Escherichia coli*, *S. cerevisiae* and *Y. lipolytica* [95].

Among carotenoids, β -carotene has a relevant importance, since its role as pro-vitamin A involved in several biological processes. This compound is cleaved to vitamin A by mono or dioxygenase leading to the biosynthesis of retinoids molecules, which promote body growth, visual function, differentiation of epithelial tissue, and also embryonic development for pregnant women [96]. Vitamin A deficiency is a worldwide problem, especially in developing African and Asian countries, since it can lead to eye damage and even death in children [104]. It is not therefore a surprise that several attempts have been made to enrich food with β -carotene as additive, or to fortify crops by genetic modification, as in the case of the so-called “golden rice” [105]. Together with this role, β -carotene has other properties related to health since it is a strong antioxidant, it improves immune functions and prevents night blindness and liver fibrosis [94]. In addition, β -carotene is also widely used in the other general sectors where carotenoids are deployed, in particular as feed additive and food colorant [94]. Giving all its applications, the market value of β -carotene reaches \$246.2M, 80%-90% of which is satisfied by chemical manufactory, with Roche and BASF being leading companies in this sector [94,106]. Chemical synthesis by Roche involves enol-ether condensation, whereas BSF utilizes the Wittig condensation for the production of β -carotene. Both these processes start from β -ionone and involve different solvent and chemicals, such as heptane, 2-propanol, sulfuric acid and phosphonium salts, that increase the environmental impact of the synthesis [106,107]. In addition, β -ionone was originally extracted from renewable biomasses such as lemon grass (*Cymbopogon citratus*) or pine (*Pinus caribea*), but currently it derives from acetone, that, in turn, derives from benzene of petrochemical synthesis [106]. Consequently, the demand for naturally produced molecules increased in the last years, fostering the search for new sources.

Natural β -carotene sources are plants like roots (carrots, sweet potatoes), leafy vegetables (spinaches, lettuces), flowers (roses, saffron), and fruits (tomatoes, pumpkins, red

capsicums, oil palm) [96,107]. These edible crops involve first generation biorefineries, and to diverge from them microbial cell factories can be exploited in combination with residual biomasses. Among them, yeasts have been deployed for the production of carotenoids from both defined and complex media, with species like *Rhodotorula glutinis*, *Rhodotorula gracilis*, *Rhodotorula mucilaginosa*, *Xanthophyllomyces dendrorhous* (= *Phaffia rhodozyma*), and *Sporobolomyces ruberrimus* [86,94,99,107,108]. Furthermore, among the top producing species, *R. toruloides*, can be considered a desirable candidate for the reasons explained in the previous section of this Doctoral work. In fact, since the high added value of carotenoids, biomasses with an application, such as *Camelina sativa* meal for the feed sector, can be applied for their exploitation, in the context of the cascading principles. The implementations of processes based on Camelina meal and *R. toruloides* for the production of carotenoids will be disclosed in Chapters 1 and 2. Similarly, in Chapter 3 the feedstock used was instead polyphenol extraction waste from cinnamon (C-PEW). As mentioned, β -carotene is provitamin A, and this role increases its appeal for the market. Similarly, other vitamins B vitamins, are valuable compounds that can be produced using microbial cell factories [16]. Among them folates are a group of water-soluble compounds part of the B vitamin family (B_9), that act as donor of C1 units. Therefore they play essential roles in several cellular pathways: folates are in fact involved for example in DNA synthesis and methylation, protein synthesis and formation of embryonic tissues [109]. Since its importance, it has been deployed as supplement in fortified food in both western and developing countries [110,111]. All the vitamin B_9 commercially available for food supplementation is chemically synthesized in the form of folic acid and may present some drawbacks [112]. Nevertheless, folic acid alone had a market value of \$665M in 2015 [113]. *Saccharomyces cerevisiae* is a natural producer of different folate vitamers, and therefore can be exploited for such purpose in bioprocesses [114,115]. Since the availability of genetic engineering tools, it is possible to modify *S. cerevisiae* to increase the production of folates [116]. Following cascading principles, the high added value of folates permits an initial development of such processes using refined sugars, as described in Chapter 4, as starting point for a successive implementation with sugars of LCB origin.

On the contrary, the low cost of a commodity such as manure, together with its high availability, drives bioeconomy towards its exploitation for the production of bulk chemicals, such as biomethane. Biomethane (CH_4) derives from microbial anaerobic digestion by microbial consortia that produce a mixture of gases called biogas, containing also relevant amounts of CO_2 [55,117,118]. Anaerobic digestion of organic residues to produce biogas comprises different biochemical stages (hydrolysis, acidogenesis, acetogenesis and methanogenesis) carried out by syntrophic microbes [55] that will be discussed in detail in Chapter 5. Biogas can be either used directly as it is (for example *in situ* at the plant facility) or be subjected to process of upgrading, aimed to eliminate CO_2 presence, in order to both increase the calorific value of the mix and to inject purer biomethane into pipelines together with the conventional fossil one for domestic, industrial and transport use [119,120]. The biogas production chain permits the recovery of some residual resources, such as manure and agro-industry wastes, which can be converted into carrier energy [121].

In fact, since the low market value of biogas (from 0.1384 to 0.529 €/m³ [121,122]), its production needs to derive from a very low-cost feedstock as well, in order to guarantee its economic sustainability, following the cascading principles. LCBs can be deployed for such purposes, although their recalcitrance and the presence of inhibitory compounds (*e.g.* phenolic molecules and furfural) impair their applications for the production of biomethane [118].

Among cheap alternatives, manure is a livestock residue (*e.g.* cattle, pig and poultry [56]) with little commercial value, but with high environmental impacts, therefore anaerobic digestion is the best way to mitigate them, generating at the same time energy (in the form of biogas) and biofertilizer (the digestate) [117]. The production of biogas from manure can be obtained either digesting this biomass alone or co-fermenting with other residual biomasses [117]. Manure is still considered the biomass with the highest worldwide potential for the production of biogas, compared to other agricultural or waste side streams [123]. Nevertheless, biogas production still faces several social concerns in term of environmental sustainability: in reality, biogas production proved to be beneficial for the environment, although issues related to direct or indirect emission of methane and NO_x

have to be considered, as well as the need of further data to fully complete life cycle assessment (LCA) analysis [117,123]. It is therefore pivotal to improve biomethane production from methane, and in this context computational and mathematical models [124] can be helpful to foresee microbial behavior in response to process modifications and to further meet cascading principles applied to low value biomasses and products, as explained in Chapter 5.

In conclusion, this Doctoral work focused on the development of bioprocesses based on microbial cell factories and different biomasses, to obtain bioproducts accordingly to the cascading principles (Figure 6). The strategy deployed follows the same pattern, with computational and mathematic modeling that involve little amount of materials and energy, whereas metabolic engineering needs high amount of toil to reach the desired goals. Taken together, the proposed bioprocesses summarize different aspects of the involvement of industrial biotechnology in the bioeconomy scenario.

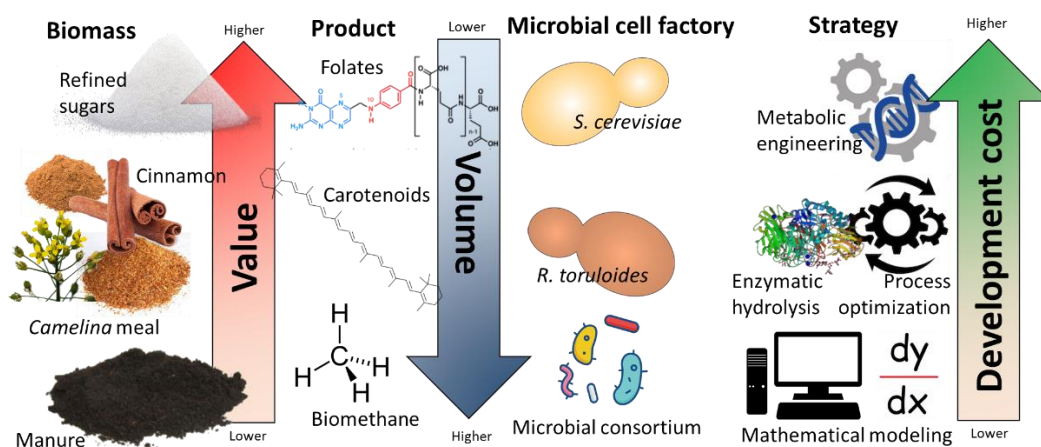


Figure 6 Graphical abstract of the present Doctoral thesis highlighting the cascading principles considered.

References

1. Earth Overshoot Day 2020 - Earth Overshoot Day. <https://www.overshootday.org/>
2. Jackson RB, Friedlingstein P, Andrew RM, Canadell JG, Le Quéré C, Peters GP. Persistent fossil fuel growth threatens the Paris Agreement and planetary health. *Environ. Res. Lett.* Institute of Physics Publishing; 2019. p. 121001.

3. THE 17 GOALS | Sustainable Development. <https://sdgs.un.org/goals>
4. Bracco S, Calicioglu O, Juan MGS, Flammini A. Assessing the contribution of bioeconomy to the total economy: A review of national frameworks. *Sustain.* 2018;10.
5. European Commission. A sustainable Bioeconomy for Europe: strengthening the connection between economy, society and the environment. 2018.
6. Stegmann P, Londo M, Junginger M. The circular bioeconomy: Its elements and role in European bioeconomy clusters. *Resour Conserv Recycl X.* Elsevier; 2020;6:100029.
7. IEA Bioenergy Task40. Cascading of woody biomass: definitions, policies and effects on international trade. *IEA Bioenergy.* 2016;71.
8. Vis M, Reumerman P, Gärtner S. Cascading in the wood sector. 2014.
9. IEA Bioenergy Task42. Sustainable and synergetic processing of biomass into marketable food & feed ingredients, chemicals, materials and energy (fuels, power, heat). *IEA Bioenergy.* 2014;66.
10. Nanda S, Azargohar R, Dalai AK, Kozinski JA. An assessment on the sustainability of lignocellulosic biomass for biorefining. *Renew. Sustain. Energy Rev.* 2015. p. 925–41.
11. Rosales-Calderon O, Arantes V. A review on commercial-scale high-value products that can be produced alongside cellulosic ethanol. *Biotechnol. Biofuels.* BioMed Central; 2019.
12. European Commission. Detailed Case Studies on the Top 20 Innovative Bio-Based Products. *Top 20 Innov. Bio-Based Prod.* 2018. p. 56.
13. Dahiya S, Kumar AN, Shanthi Sravan J, Chatterjee S, Sarkar O, Mohan SV. Food waste biorefinery: Sustainable strategy for circular bioeconomy. *Bioresour Technol.* Elsevier; 2018;248:2–12.
14. Branduardi P. Closing the loop: the power of microbial biotransformations from traditional bioprocesses to biorefineries, and beyond. *Microb Biotechnol.* 2020;0:1–6.
15. Russmayer H, Egermeier M, Kalemasi D, Sauer M. Spotlight on biodiversity of microbial cell factories for glycerol conversion. 2019.
16. Acevedo-Rocha CG, Gronenberg LS, Mack M, Commichau FM, Genee HJ. Microbial cell factories for the sustainable manufacturing of B vitamins. *Curr. Opin. Biotechnol.* Elsevier Ltd; 2019. p. 18–29.

17. Ko YS, Kim JW, Lee JA, Han T, Kim GB, Park JE, et al. Tools and strategies of systems metabolic engineering for the development of microbial cell factories for chemical production. *Chem. Soc. Rev. Royal Society of Chemistry*; 2020. p. 4615–36.
18. Alperstein L, Gardner JM, Sundstrom JF, Sumbly KM, Jiranek V. Yeast bioprospecting versus synthetic biology—which is better for innovative beverage fermentation? *Appl Microbiol Biotechnol. Applied Microbiology and Biotechnology*; 2020;104:1939–53.
19. European Food Safety Authority. Guidance on the risk assessment of genetically modified microorganisms and their products intended for food and feed use. *EFSA J.* 2011;9:1–54.
20. Poblete-Castro I, Hoffmann SL, Becker J, Wittmann C. Cascaded valorization of seaweed using microbial cell factories. *Curr. Opin. Biotechnol. Elsevier Ltd*; 2020. p. 102–13.
21. Schempp FM, Drummond L, Buchhaupt M, Schrader J. Microbial Cell Factories for the Production of Terpenoid Flavor and Fragrance Compounds. *J. Agric. Food Chem.* 2018. p. 2247–58.
22. Gaurav N, Sivasankari S, Kiran GS, Ninawe A, Selvin J. Utilization of bioresources for sustainable biofuels: A Review. *Renew. Sustain. Energy Rev.* 2017. p. 205–14.
23. Liu Y, Nielsen J. Recent trends in metabolic engineering of microbial chemical factories. *Curr Opin Biotechnol.* 2019;60:188–97.
24. Wahlström RM, Suurnäkki A. Enzymatic hydrolysis of lignocellulosic polysaccharides in the presence of ionic liquids. *Green Chem. Royal Society of Chemistry*; 2015;17:694–714.
25. Jönsson LJ, Martín C. Pretreatment of lignocellulose: Formation of inhibitory by-products and strategies for minimizing their effects. *Bioresour. Technol.* 2016.
26. Galbe M, Wallberg O. Pretreatment for biorefineries: A review of common methods for efficient utilisation of lignocellulosic materials. *Biotechnol Biofuels. BioMed Central*; 2019;12:1–26.
27. Kawaguchi H, Hasunuma T, Ogino C, Kondo A. Bioprocessing of bio-based chemicals produced from lignocellulosic feedstocks. *Curr. Opin. Biotechnol. Elsevier Ltd*; 2016. p. 30–9.
28. Baruah J, Nath BK, Sharma R, Kumar S, Deka RC, Baruah DC, et al. Recent trends in the

- pretreatment of lignocellulosic biomass for value-added products. *Front Energy Res.* 2018;6:1–19.
29. Hosseini Koupaie E, Dahadha S, Bazyar Lakeh AA, Azizi A, Elbeshbishy E. Enzymatic pretreatment of lignocellulosic biomass for enhanced biomethane production-A review. *J Environ Manage.* Elsevier; 2019;233:774–84.
30. Zoghalmi A, Paës G. Lignocellulosic Biomass: Understanding Recalcitrance and Predicting Hydrolysis. *Front. Chem.* 2019.
31. McKendry P. Energy production from biomass (part 1): Overview of biomass. *Bioresour Technol.* 2002;83:37–46.
32. Houfani AA, Anders N, Spiess AC, Baldrian P, Benallaoua S. Insights from enzymatic degradation of cellulose and hemicellulose to fermentable sugars– a review. *Biomass and Bioenergy.* Elsevier Ltd; 2020;134:105481.
33. Sarkar N, Ghosh SK, Bannerjee S, Aikat K. Bioethanol production from agricultural wastes: An overview. *Renew Energy.* Elsevier Ltd; 2012;37:19–27.
34. Yennamalli RM, Rader AJ, Kenny AJ, Wolt JD, Sen TZ. Endoglucanases : insights into thermostability for biofuel applications. *Biotechnol Biofuels.* 2017;1–9.
35. Van Dyk JS, Pletschke BI. A review of lignocellulose bioconversion using enzymatic hydrolysis and synergistic cooperation between enzymes-Factors affecting enzymes, conversion and synergy. *Biotechnol Adv.* Elsevier Inc.; 2012;30:1458–80.
36. Adsul M, Sandhu SK, Singhania RR, Gupta R, Puri SK, Mathur A. Designing a cellulolytic enzyme cocktail for the efficient and economical conversion of lignocellulosic biomass to biofuels. *Enzyme Microb. Technol.* 2020.
37. Choudhary J, Singh S, Nain L. Thermotolerant fermenting yeasts for simultaneous saccharification fermentation of lignocellulosic biomass. *Electron. J. Biotechnol.* 2016. p. 82–92.
38. Halder D, Purkait MK. Lignocellulosic conversion into value-added products: A review. *Process Biochem.* 2020. p. 110–33.
39. Aditiya HB, Mahlia TMI, Chong WT, Nur H, Sebayang AH. Second generation bioethanol production: A critical review. *Renew. Sustain. Energy Rev.* 2016.
40. Srivastava N, Rawat R, Singh Oberoi H, Ramteke PW. A review on fuel ethanol

- production from lignocellulosic biomass. *Int J Green Energy*. Taylor & Francis; 2015;12:949–60.
41. Yuan SF, Guo GL, Hwang WS. Ethanol production from dilute-acid steam exploded lignocellulosic feedstocks using an isolated multistress-tolerant *Pichia kudriavzevii* strain. *Microb Biotechnol*. John Wiley and Sons Ltd; 2017;10:1581–90.
42. Panagiotou G, Olsson L. Effect of compounds released during pretreatment of wheat straw on microbial growth and enzymatic hydrolysis rates. *Biotechnol Bioeng*. 2007;96:250–8.
43. Ask M, Olofsson K, Di Felice T, Ruohonen L, Penttilä M, Lidén G, et al. Challenges in enzymatic hydrolysis and fermentation of pretreated *Arundo donax* revealed by a comparison between SHF and SSF. *Process Biochem*. Elsevier Ltd; 2012;47:1452–9.
44. Öhgren K, Bura R, Lesnicki G, Saddler J, Zacchi G. A comparison between simultaneous saccharification and fermentation and separate hydrolysis and fermentation using steam-pretreated corn stover. *Process Biochem*. 2007;42:834–9.
45. Rodrigues THS, de Barros EM, de Sá Brígido J, da Silva WM, Rocha MVP, Gonçalves LRB. The Bioconversion of Pretreated Cashew Apple Bagasse into Ethanol by SHF and SSF Processes. *Appl Biochem Biotechnol*. 2016;178:1167–83.
46. Ben Atitallah I, Antonopoulou G, Ntaikou I, Alexandropoulou M, Nasri M, Mechichi T, et al. On the evaluation of different saccharification schemes for enhanced bioethanol production from potato peels waste via a newly isolated yeast strain of *Wickerhamomyces anomalus*. *Bioresour Technol*. 2019;289.
47. Dahnum D, Tasum SO, Triwahyuni E, Nurdin M, Abimanyu H. Comparison of SHF and SSF processes using enzyme and dry yeast for optimization of bioethanol production from empty fruit bunch. *Energy Procedia*. Elsevier Ltd; 2015. p. 107–16.
48. Mithra MG, Sajeev MS, Padmaja G. Comparison of SHF and SSF Processes under Fed Batch Mode on Ethanol Production from Pretreated Vegetable Processing Residues. *Eur J Sustain Dev Res*. 2019;3.
49. Wu J, Hu J, Zhao S, He M, Hu G, Ge X, et al. Single-cell Protein and Xylitol Production by a Novel Yeast Strain *Candida intermedia* FLO23 from Lignocellulosic Hydrolysates and Xylose. *Appl Biochem Biotechnol*. 2018;185:163–78.

50. Bertacchi S, Bettiga M, Porro D, Branduardi P. *Camelina sativa* meal hydrolysate as sustainable biomass for the production of carotenoids by *Rhodospiridium toruloides*. *Biotechnol Biofuels*. BioMed Central; 2020;13:1–10.
51. Da Silva ASA, Espinheira RP, Teixeira RSS, De Souza MF, Ferreira-Leitão V, Bon EPS. Constraints and advances in high-solids enzymatic hydrolysis of lignocellulosic biomass: A critical review. *Biotechnol. Biofuels*. BioMed Central; 2020. p. 1–28.
52. Mironova GF, Skiba EA, Kukhlenko AA. Optimization of pre-saccharification time during dSSF process in oat-hull bioethanol technology. *3 Biotech*. Springer Verlag; 2019;9:455.
53. Pratto B, Rodrigues MS, Santos-Rocha D, Longati AA, De Sousa Júnior R, Gonçalves Cruz AJ. Experimental optimization and techno-economic analysis of bioethanol production by simultaneous saccharification and fermentation process using sugarcane straw. 2019
54. Lee S, Kang M, Bae JH, Sohn JH, Sung BH. Bacterial Valorization of Lignin: Strains, Enzymes, Conversion Pathways, Biosensors, and Perspectives. *Front Bioeng Biotechnol*. 2019;7:1–18.
55. Jiang LL, Zhou JJ, Quan CS, Xiu ZL. Advances in industrial microbiome based on microbial consortium for biorefinery. *Bioresour. Bioprocess*. Springer; 2017.
56. Kougias PG, Angelidaki I. Biogas and its opportunities—A review. *Front Environ Sci Eng*. 2018;12.
57. Rivière D, Desvignes V, Pelletier E, Chaussonnerie S, Guermazi S, Weissenbach J, et al. Towards the definition of a core of microorganisms involved in anaerobic digestion of sludge. *ISME J*. 2009;3:700–14.
58. Pan J, Ma J, Zhai L, Liu H. Enhanced methane production and syntrophic connection between microorganisms during semi-continuous anaerobic digestion of chicken manure by adding biochar. *J Clean Prod*. Elsevier Ltd; 2019;240:118178.
59. Zhang Q, Wang M, Ma X, Gao Q, Wang T, Shi X, et al. High variations of methanogenic microorganisms drive full-scale anaerobic digestion process. *Environ Int*. Elsevier Ltd; 2019;126:543–51.
60. Ferreira JA, Mahboubi A, Lennartsson PR, Taherzadeh MJ. Waste biorefineries using

filamentous ascomycetes fungi: Present status and future prospects. *Bioresour. Technol.* 2016. p. 334–45.

61. Donot F, Fontana A, Baccou JC, Strub C, Schorr-Galindo S. Single cell oils (SCOs) from oleaginous yeasts and moulds: Production and genetics. 2014.

62. Frengova GI, Beshkova DM. Carotenoids from *Rhodotorula* and *Phaffia*: Yeasts of biotechnological importance. *J. Ind. Microbiol. Biotechnol.* 2009.

63. Li M, Borodina I. Application of synthetic biology for production of chemicals in yeast *Saccharomyces cerevisiae*. *FEMS Yeast Res.* 2015.

64. Hong K-K, Nielsen J. Metabolic engineering of *Saccharomyces cerevisiae*: a key cell factory platform for future biorefineries.

65. Hittinger CT, Rokas A, Bai FY, Boekhout T, Gonçalves P, Jeffries TW, et al. Genomics and the making of yeast biodiversity. *Curr Opin Genet Dev.* 2015;35:100–9.

66. de Souza Varize C, Christofoleti-Furlan RM, de Souza Miranda Muynarsk E, de Melo Pereira GV, Lopes, Lucas Dantas; Basso LC. Biotechnological Applications of Nonconventional Yeasts. *Yeasts Biotechnol.* 2019.

67. Passoth V. Conventional and non-conventional yeasts for the production of biofuels. *Yeast Divers Hum Welf.* Springer Singapore; 2017. p. 385–416.

68. Koutsoumanis K, Allende A, Alvarez-Ordóñez A, Bolton D, Bover-Cid S, Chemaly M, et al. Update of the list of QPS-recommended biological agents intentionally added to food or feed as notified to EFSA 11: suitability of taxonomic units notified to EFSA until September 2019. *EFSA J.* Wiley-Blackwell Publishing Ltd; 2020;18.

69. Koutsoumanis K, Allende A, Alvarez-Ordóñez A, Bolton D, Bover-Cid S, Chemaly M, et al. Scientific Opinion on the update of the list of QPS-recommended biological agents intentionally added to food or feed as notified to EFSA (2017–2019). *EFSA J.* Wiley-Blackwell Publishing Ltd; 2020;18.

70. Mohd Azhar SH, Abdulla R, Jambo SA, Marbawi H, Gansau JA, Mohd Faik AA, et al. Yeasts in sustainable bioethanol production: A review. *Biochem. Biophys. Reports.* Elsevier B.V.; 2017. p. 52–61.

71. Ruchala J, Sibirny AA. Pentose metabolism and conversion to biofuels and high-value chemicals in yeasts. *FEMS Microbiol Rev.* 2020;069:1–44.

72. Sreeharsha RV, Mohan SV. Obscure yet Promising Oleaginous Yeasts for Fuel and Chemical Production. *Trends Biotechnol.* 2020;1–15.
73. Carsanba E, Papanikolaou S, Erten H. Production of oils and fats by oleaginous microorganisms with an emphasis given to the potential of the nonconventional yeast *Yarrowia lipolytica*. *Crit. Rev. Biotechnol.* 2018. p. 1230–43.
74. Poontawee R, Yongmanitchai W, Limtong S. Efficient oleaginous yeasts for lipid production from lignocellulosic sugars and effects of lignocellulose degradation compounds on growth and lipid production. *Process Biochem.* 2017;53:44–60.
75. Pandey AK, Kumar M, Kumari S, Kumari P, Yusuf F, Jakeer S, et al. Evaluation of divergent yeast genera for fermentation-associated stresses and identification of a robust sugarcane distillery waste isolate *Saccharomyces cerevisiae* NGY10 for lignocellulosic ethanol production in SHF and SSF. *Biotechnol Biofuels.* 2019;12.
76. Sitepu I, Selby T, Lin T, Zhu S, Boundy-Mills K. Carbon source utilization and inhibitor tolerance of 45 oleaginous yeast species. *J Ind Microbiol Biotechnol.* 2014;41:1061–70.
77. Osorio-González CS, Hegde K, Brar SK, Kermanshahipour A, Avalos-Ramírez A. Challenges in lipid production from lignocellulosic biomass using *Rhodospiridium* sp.; A look at the role of lignocellulosic inhibitors. *Biofuels, Bioprod. Biorefining.* John Wiley and Sons Ltd; 2019. p. 740–59.
78. Sitepu I, Garay LA, Sestric R, Levin D, Block DE, German JB, et al. Oleaginous yeasts for biodiesel: Current and future trends in biology and production. *Biotechnol Adv.* 2014;
79. Huang C, Luo M-T, Chen X-F, Qi G-X, Xiong L, Lin X-Q, et al. Combined “*de novo*” and “*ex novo*” lipid fermentation in a mix-medium of corncob acid hydrolysate and soybean oil by *Trichosporon dermatis*. *Biotechnol Biofuels.* 2017;10:147.
80. Wen Z, Zhang S, Odoh CK, Jin M, Zhao ZK. *Rhodospiridium toruloides* - A potential red yeast chassis for lipids and beyond. *FEMS Yeast Res.* Oxford University Press; 2020;20:1–12.
81. Park Y-KK, Nicaud J-MM, Ledesma-Amaro R. The Engineering Potential of *Rhodospiridium toruloides* as a Workhorse for Biotechnological Applications. *Trends Biotechnol.* 2018
82. Banno I. Studies on the sexuality of rhodotorula. *J Gen Appl Microbiol.* 1967;

83. Wang QM, Yurkov AM, Göker M, Lumbsch HT, Leavitt SD, Groenewald M, et al. Phylogenetic classification of yeasts and related taxa within Pucciniomycotina. *Stud Mycol.* 2015;81:149–89.
84. Lee JW, Yook S, Koh H, Rao C V., Jin YS. Engineering xylose metabolism in yeasts to produce biofuels and chemicals. *Curr Opin Biotechnol.* Elsevier Ltd; 2021;67:15–25.
85. Pinheiro MJ, Bonturi N, Belouah I, Miranda EA, Lahtvee PJ. Xylose Metabolism and the Effect of Oxidative Stress on Lipid and Carotenoid Production in *Rhodotorula toruloides*: Insights for Future Biorefinery. *Front Bioeng Biotechnol.* 2020;8:1–15.
86. Kot AM, Błazejak S, Gientka I, Kieliszek M, Bryś J. Torulene and torularhodin: “New” fungal carotenoids for industry? *Microb. Cell Fact.* 2018.
87. Lyman M, Urbin S, Strout C, Rubinfeld B. The Oleaginous Red Yeast *Rhodotorula/Rhodospiridium* : A Factory for Industrial Bioproducts . *Yeasts Biotechnol.* IntechOpen; 2019.
88. Yaegashi J, Kirby J, Ito M, Sun J, Dutta T, Mirsiaghi M, et al. *Rhodospiridium toruloides*: A new platform organism for conversion of lignocellulose into terpene biofuels and bioproducts. *Biotechnol Biofuels.* BioMed Central; 2017;10:1–13.
89. Liu Y, Koh CMJ, Yap SA, Du M, Hlaing MM, Ji L. Identification of novel genes in the carotenogenic and oleaginous yeast *Rhodotorula toruloides* through genome-wide insertional mutagenesis. *BMC Microbiol.* BMC Microbiology; 2018;18:1–15.
90. Liu X, Zhang Y, Liu H, Jiao X, Zhang Q, Zhang S, et al. RNA interference in the oleaginous yeast *Rhodospiridium toruloides*. *FEMS Yeast Res.* Oxford University Press; 2019;19:1–10.
91. Jiao X, Zhang Y, Liu X, Zhang Q, Zhang S, Zhao ZK. Developing a CRISPR/Cas9 System for Genome Editing in the Basidiomycetous Yeast *Rhodospiridium toruloides*. *Biotechnol J.* John Wiley & Sons, Ltd; 2019;14:1–7.
92. Schultz JC, Cao M, Zhao H. Development of a CRISPR/Cas9 system for high efficiency multiplexed gene deletion in *Rhodospiridium toruloides*. *Biotechnol Bioeng.* John Wiley and Sons Inc.; 2019;116:2103–9.
93. Wang C, Zhao S, Shao X, Park J Bin, Jeong SH, Park HJ, et al. Challenges and tackles in metabolic engineering for microbial production of carotenoids. *Microb. Cell Fact.* 2019.

94. Saini RK, Keum YS. Microbial platforms to produce commercially vital carotenoids at industrial scale: an updated review of critical issues. *J. Ind. Microbiol. Biotechnol.* Springer International Publishing; 2019. p. 657–74.
95. Yuan S-F, Alper HS. Metabolic engineering of microbial cell factories for production of nutraceuticals. *Microb Cell Fact.* BioMed Central; 2019;18:46.
96. Nagarajan J, Ramanan RN, Raghunandan ME, Galanakis CM, Krishnamurthy NP. Carotenoids. *Nutraceutical Funct. Food Components Eff. Innov. Process. Tech.* Elsevier Inc.; 2017.
97. Food and Agriculture Organization of the United Nations (FAO). Utilization of lipid co-products of the biofuel industry in livestock feed in Biofuel co-products as livestock feed. 2012.
98. Silva Fernandes A, Casagrande do Nascimento T, Jacob-Lopes E, De Rosso VV, Queiroz Zepka L. Carotenoids: A Brief Overview on Its Structure, Biosynthesis, Synthesis, and Applications. *Intech.* 2018;13.
99. Vargas-Sinisterra AF, Ramírez-Castrillón M. Yeast carotenoids: production and activity as antimicrobial biomolecule. *Arch. Microbiol.* Springer Berlin Heidelberg; 2020.
100. Mussagy CU, Winterburn J, Santos-Ebinuma VC, Pereira JFB. Production and extraction of carotenoids produced by microorganisms. *Appl Microbiol Biotechnol.* Applied Microbiology and Biotechnology; 2019;103:1095–114.
101. Mapelli-Brahm P, Barba FJ, Remize F, Garcia C, Fessard A, Mousavi Khaneghah A, et al. The impact of fermentation processes on the production, retention and bioavailability of carotenoids: An overview. *Trends Food Sci Technol.* Elsevier; 2020;99:389–401.
102. Yabuzaki J. Carotenoids Database: structures, chemical fingerprints and distribution among organisms. *Database.* Oxford University Press; 2017;2017:1–11.
103. Waditee-Sirisattha R, Kageyama H, Takabe T. Halophilic microorganism resources and their applications in industrial and environmental biotechnology. *AIMS Microbiol.* American Institute of Mathematical Sciences (AIMS); 2016;2:42–54.
104. Organization WH. Xerophthalmia and night blindness for the assessment of clinical vitamin A deficiency in individuals and populations. 2014;1–6.
105. Paine JA, Shipton CA, Chaggar S, Howells RM, Kennedy MJ, Vernon G, et al.

- Improving the nutritional value of Golden Rice through increased pro-vitamin A content. *Nat Biotechnol.* 2005;
106. Ribeiro BD, Barreto DW, Coelho MAZ. Technological Aspects of β -Carotene Production. *Food Bioprocess Technol.* 2011;4:693–701.
107. Bogacz-Radomska L, Harasym J. β -Carotene-properties and production methods. *Food Qual Saf.* 2018;2:69–74.
108. Mata-Gómez LC, Montañez JC, Méndez-Zavala A, Aguilar CN. Biotechnological production of carotenoids by yeasts: An overview. *Microb Cell Fact.* 2014;13:1–11.
109. Saini RK, Nile SH, Keum YS. Folates: Chemistry, analysis, occurrence, biofortification and bioavailability. *Food Res. Int.* 2016.
110. Hoddinott J. The investment case for folic acid fortification in developing countries. *Ann N Y Acad Sci.* Blackwell Publishing Inc.; 2018;1414:72–81.
111. Pfeiffer CM, Sternberg MR, Zhang M, Fazili Z, Storandt RJ, Crider KS, et al. Folate status in the US population 20 y after the introduction of folic acid fortification. *Am J Clin Nutr.* 2019;110:1088–97.
112. Choi JH, Yates Z, Veysey M, Heo YR, Lucock M. Contemporary issues surrounding folic acid fortification initiatives. *Prev. Nutr. Food Sci.* 2014.
113. Research GV. Folic Acid Market Size, Share | Global Industry Report, 2018-2025. 2016.
114. Hjortmo S, Patring J, Jastrebova J, Andlid T. Inherent biodiversity of folate content and composition in yeasts. *Trends Food Sci Technol.* 2005;
115. Gmelch L, Wirtz D, Witting M, Weber N, Striegel L, Schmitt-Kopplin P, et al. Comprehensive vitamer profiling of folate monoand polyglutamates in baker's yeast (*Saccharomyces cerevisiae*) as a function of different sample preparation procedures. *Metabolites.* 2020;10:1–19.
116. Liu Y, Walkey CJ, Green TJ, Van Vuuren HJJ, Kitts DD. Enhancing the natural folate level in wine using bioengineering and stabilization strategies. *Food Chem.* 2016;
117. Esteves EMM, Herrera AMN, Esteves VPP, Morgado C do RV. Life cycle assessment of manure biogas production: A review. *J Clean Prod.* 2019;219:411–23.
118. Xu N, Liu S, Xin F, Zhou J, Jia H, Xu J, et al. Biomethane production from

lignocellulose: Biomass recalcitrance and its impacts on anaerobic digestion. *Front Bioeng Biotechnol.* Frontiers Media S.A.; 2019;7.

119. Barbera E, Menegon S, Banzato D, D'Alpaos C, Bertucco A. From biogas to biomethane: A process simulation-based techno-economic comparison of different upgrading technologies in the Italian context. *Renew Energy.* Elsevier Ltd; 2019;135:663–73.

120. Adnan AI, Ong MY, Nomanbhay S, Chew KW, Show PL. Technologies for biogas upgrading to biomethane: A review. *Bioengineering.* 2019.

121. D'Adamo I, Falcone PM, Ferella F. A socio-economic analysis of biomethane in the transport sector: The case of Italy. *Waste Manag.* 2019;95:102–15.

122. Cucchiella F, D'Adamo I, Gastaldi M. Biomethane: A renewable resource as vehicle fuel. *Resources.* MDPI AG; 2017;6.

123. Paolini V, Petracchini F, Segreto M, Tomassetti L, Naja N, Cecinato A. Environmental impact of biogas: A short review of current knowledge. *J Environ Sci Heal - Part A Toxic/Hazardous Subst Environ Eng.* Taylor and Francis Inc.; 2018;53:899–906.

124. Simeonov I, Karakashev D. Mathematical Modelling of the Anaerobic Digestion Including the Syntrophic Acetate Oxidation. *IFAC Proc. Vol.* IFAC; 2012.

Chapter 1

Camelina sativa meal hydrolysate as sustainable biomass for the production of carotenoids by *Rhodospiridium toruloides*

From Bertacchi S., Bettiga M., Porro D., Branduardi P. (2020) *Camelina sativa* meal hydrolysate as sustainable biomass for the production of carotenoids by *Rhodospiridium toruloides*. Biotechnology for Biofuels 13.1: 1.10.

Introduction

The continued use of fossil resources poses an ecological, economic, and political problem that has sparked the search for alternative sources of energy, chemicals, and materials. Biorefineries, which transform biomass into energy and chemicals, offer a possible answer, particularly in the form of microbial cell factories. The sustainability of biorefineries is strongly related to the origin, availability, and market of biomass. For example, edible crops have been exploited for decades as feedstocks for the production of several fine and bulk chemicals. However, environmental and social issues, caused by direct or indirect competition with the food sector, discourage the use of agricultural products and land for large-scale production of commodities [1]. At the same time, the existing linear economy's logic of "take, make, dispose" is generating a large amount of waste, including organic matter. For these reasons, biorefineries based on residual biomasses have drawn increasing scientific and industrial interest. Microbial cell factories are especially attractive; however, conventional pretreatments and saccharification processes of residual biomasses often release toxic compounds that can impair microbial growth and synthesis of the target product [2]. These issues need to be factored in when developing robust biorefineries capable of generating high-value molecules from low-cost substrates.

The growing use of oilseed crops for food and biofuels is leading to a surplus of process leftovers that are currently used mainly as animal feed [3] owing to their protein, carbohydrate, and fiber content. A good example is *Camelina* meal (or cake), the main by-product of oil extraction from *Camelina sativa* seeds [4–8], which is a common supplement of cattle and poultry diet. However, the rich composition and relatively low cost (\$0.25/kg) of *Camelina* meal [9], make it attractive for the development of sustainable bio-based processes that would either further valorize its macromolecular components or increase its nutritional value in animal feed. So far, only Mohammad *et al.* [10] have attempted to use *Camelina* meal, mixed with other *Camelina*-derived sugars, for the production of bioethanol, a low value-added molecule, by *Saccharomyces*

cerevisiae. To improve the economic viability of the process, the present study assessed the microbial biotransformation of *Camelina* meal into carotenoids as high value-added products.

The global market value for carotenoids was estimated to be \$1.5B in 2017 and is expected to reach \$2.0B by 2022, with a compound annual growth rate of 5.7% [11–13]. Carotenoids are found mainly in animal feed (41% of total revenue), followed by food and dietary supplements owing to their beneficial effect on human health [12,14]. Ruminants are entirely dependent on feed as a source of carotenoids, since they cannot produce them on their own [3]. Chemical synthesis of carotenoids from synthetic resources meets 80–90% of the market needs, but the increasing demand for naturally produced molecules has sparked the search for new, preferably vegetal sources [12]. β -carotene alone has a market value of \$246.2M. Natural β -carotene can be extracted from carrots and fruits of oil palm, but recent attempts have demonstrated the commercial production of β -carotene in microbial cell factories employing the microalga *Dunaliella salina* or the filamentous fungus *Blakeslea trispora* [12]. Unfortunately, algal carotenoid production is generally expensive and requires large areas for cultivation [15,16], whereas filamentous fungi are frequently characterized by slow growth and a multicellular nature that may impair productivity [17]. Yeasts could potentially improve the overall sustainability of the process. In particular, the oleaginous yeast *Rhodospodium (Rhodotorula) toruloides*, also known as “pink yeast”, naturally accumulates carotenes and xanthophylls, such as β -carotene, torulene, and torularhodin [16,18,19]. *R. toruloides* can use different sugars, such as glucose, cellobiose, sucrose, mannose, xylose, arabinose, and galacturonic acid, as main carbon sources [20]. In addition, *R. toruloides* converts complex substrates, such as carob pulp syrup, sugarcane bagasse, corn stover, and food wastes, into lipids and/or carotenoids [21–24]. Therefore, this yeast is a good candidate for the development of 2nd generation biorefineries.

To produce carotenoids in *R. toruloides*, *Camelina* meal was first saccharified by enzymatic hydrolysis. Then, the released sugars were used as feedstock in Separate Hydrolysis and Fermentation (SHF). An alternative Simultaneous Saccharification and

Fermentation (SSF) process was also assessed. Results indicate that *Camelina* meal and *R. toruloides* can be used for the development of a novel bio-based process for carotenoids production. Moreover, the obtained data will facilitate further optimization of process conditions.

Results and discussion

Evaluation of total sugar content in *Camelina* meal and optimization of enzymatic hydrolysis

The content of water, insoluble components, acetic acid, and sugars in *Camelina* meal was quantified following acid hydrolysis. Acetic acid and sugar were analyzed also after enzymatic hydrolysis, as no enough data exist in literature to assess the use of *Camelina* meal as substrate for microorganisms. As shown in Table 1, almost one third (31%) of *Camelina* meal was composed of sugars. Of these, glucose and fructose accounted for more than two-thirds (w/w) as revealed by high-performance liquid chromatography (HPLC) analysis. Even though acid hydrolysis can be suitable for saccharification, its use is limited by the low final pH, which needs to be neutralized before sugars are added to the cells, and by the release of inhibitory compounds such as furfurals [2,25]. These limitations negatively affect the sustainability of the overall biorefinery process in terms of use and disposal of acid solutions [25]. Therefore, to release monomeric sugars from their polymeric form, an enzymatic instead of an acid hydrolysis was performed under different test conditions (see below). The other main components of *Camelina* meal, as reviewed by [7], are crude proteins and crude fats, which account for 35.2–46.9% and 4.9–11.9% of total biomass, respectively, as well as micronutrients such as vitamins; whereas the insoluble fraction is composed mainly of lignin and ashes. Based on these data, we hypothesized that *Camelina* meal could be a suitable substrate for the growth of *R. toruloides* and carotenoid production.

Table 1 *Camelina* meal hydrolysate composition following acid treatment

<i>Camelina</i> meal composition	
Measured component	Percentage (w/w)
Water	9 ± 1.8%
Acetate	11 ± 1.4%
Insoluble fraction	13 ± 1.4%
Sugars of which	31 ± 1.0%
Glucose	16 ± 0.9%
Fructose	8.3 ± 0.0%
Arabinose	6.9 ± 0.0%
Crude protein	35.2–46.9% [7]
Crude fat	4.9–11.9% [7]

Values are the means of three independent experiments

Table 1: *Camelina* meal hydrolysate composition following acid treatment. Values are the means of three independent experiments.

Enzymatic hydrolysis can be performed under conditions that are generally more compatible with subsequent growth of mesophilic microbial cell factories. Moreover, it can take advantage of a broad range of commercially available enzymatic cocktails [26,27]. Here, this step was optimized by using the commercial cocktail NS22119 (Novozymes A/S), which can release both hexose and pentose sugars. Different initial concentrations of *Camelina* meal were tested to determine the effect of solids loading on sugar release. After autoclaving, the measured pH was 5.5, which was compatible with enzymatic catalysis, as NS22119 is supposed to retain up to 90% of its maximum activity at this pH, according to the indications of the producer. Remarkably, the pH remained constant until the end of hydrolysis, which reduced both the economic and environmental impact of the procedure, as neither neutralization nor additional buffer were required. As shown in Figure 1A, pre-treatment of biomass by autoclaving resulted in the initial concentration of released sugars to range from 1.8 ± 0.03 g/L to 9 ± 0.3 g/L. The values reflected the amount of biomass loaded at the beginning of the experiment. After enzymatic treatment (11.9% w/w *Camelina* meal), the concentration of free sugars rose to at least double the initial amount, independently of the quantity of loaded biomass (Figure 1A). No additional release of sugar was detectable over time from negative control samples, in which 3% or 15% of the initial biomass but no enzyme was incubated

in a shaking water bath at 50°C (Additional Figure S1). The sugar titer increased in the presence of enzymes in a linear manner ($R^2 = 0.98$, $p < 0,001$, calculated with R) until 24 h in respect to the initial quantity of biomass. Hence, the yield of sugars released by enzymatic hydrolysis was constant regardless the concentration of *Camelina* meal (Figure 1B) and the maximum yield of sugars over total biomass was 20% after 24 h. Considering the original amount of carbohydrates, a sugars recovery of 65% was calculated (see Calculations section), which is in accordance with commonly reported values for lignocellulose enzymatic hydrolysis [28,29].

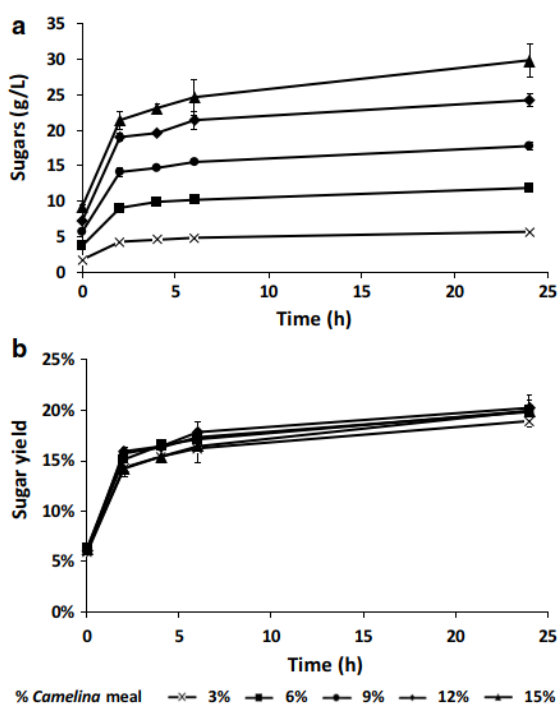


Figure 1: Effect of enzymatic hydrolysis with the NS22119 cocktail (11.9% w/w *Camelina* meal) on different *Camelina* meal concentrations. Time course of sugar released (A) and sugar yield from biomass (B). Values are the means of three independent experiments.

Based on these data, successive experiments were performed using *Camelina* meal at the maximum tested solids loading (15% w/v). To determine if sugar recovery could be further improved in spite of a possible inhibition of enzymatic activity by released products or by biomass itself, two different strategies were designed. In one, the initial quantity of enzymes was doubled from 11.9% to 23.8% w/w *Camelina* meal; in the other, the

mixture was pulsed with a second dose of enzymes (11.9% w/w_{Camelina meal}), thus doubling the total amount, after 6 h of hydrolysis. When the first strategy using double the amount of enzymes was applied, the quantity of sugars released from *Camelina* meal (Figure 2, black bars) did not differ significantly from that of a single enzyme dose (Figure 1A). A similar result was obtained when the second strategy, based on an additional pulse of enzymatic cocktail after 6 h of hydrolysis was applied (Figure 2, white bars). These findings indicate that incomplete saccharification is related more to the intrinsic accessibility of polysaccharides in the biomass than to limitations in catalytic activity. They also suggest that the initial procedure was the preferred one, as it minimized the use of enzymes and thus the overall cost of the process. The enzymatic cocktail exhibited greatest activity during the first hours of hydrolysis; prolonging incubation beyond 6 h to 24 h improved sugar titer by only 20%. Therefore, the conditions for enzymatic hydrolysis of *Camelina* meal were as follows: 15% w/w solids loading, 11.9% w/w_{Camelina meal} of enzymatic cocktail NS22119, reaction time of 6 h, operative temperature of 50°C, and initial pH of 5.5. As underlined before, the pH of the reaction mixture remained constant over time and was conveniently closer to the optimum reported for carotenoids accumulation in *R. toruloides* (pH 5) than to the value suitable for lipid production (pH 4) [30].

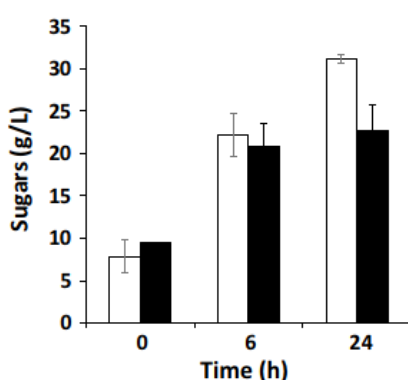


Figure 2: Enzymatic hydrolysis of 15% *Camelina* meal. Sugars released by supplementation with an additional pulse of NS22119 cocktail (11.9% w/w_{Camelina meal}) after 6 h of hydrolysis (white bar) or with a starting double enzymatic cocktail dose (23.8% w/w_{Camelina meal}) (black bar). Values are the means of three independent experiments.

The above settings allowed for about 25 g/L of monomeric sugars to be released and, with a sugar recovery of 53.3%. The fraction of residual non-hydrolyzed carbohydrates could be considered as an added value to the final product, as a feed with *Camelina* meal enriched in carotenoids by fermentation of *R. toruloides* would still contain fibers of nutritional value.

Inhibitory compounds in *Camelina* meal hydrolysate

Compared with traditional acid treatment, enzymatic hydrolysis is efficacious in releasing sugars from lignocelluloses and minimizing the accumulation of inhibitory compounds [31,32]. Nevertheless, there are some drawbacks related to other compounds detached from these complex matrices [2,20]. Acetic acid is the most common inhibitor released by hydrolysis of the hemicellulose fraction composing lignocellulosic biomasses. Acetic acid can easily impair microbial growth and metabolism due to its generic and specific toxicity [33], reducing the key performance indicators of the production process [2,33,34]. Nevertheless, the toxicity of acetic acid is greater at low pH; extracellular pH values higher than its pKa (4.76) reduce its diffusion across the membrane and, therefore, the cellular damage it could trigger [35,36]. In the present study, the operative pH (5.5) was higher than the pKa of acetic acid, thus lowering the detrimental effect of this molecule on cells. Moreover, *R. toruloides* has been shown to withstand acetic acid when added to defined media or even as the sole carbon source at up to 20 g/L at pH 6 [37–39]. During enzymatic hydrolysis, acetic acid titer increased, reaching 1.8 ± 0.01 g/L after 24 h from the start (Additional Figure S2). This amount has been described as bearable by diverse yeasts [34,37,38] including *R. toruloides*.

Considering the above constrains, *Camelina* meal hydrolysate appears to be a suitable feedstock for yeast cell factory-based biorefineries, which would enable the exploitation of yeast biodiversity and engineering strategies to obtain different products of interest.

Carotenoids production from *Camelina* meal hydrolysate in SHF and SSF processes

Having established a protocol for obtaining *Camelina* meal hydrolysate, carotenoids production by SHF was investigated. In the SHF experiment, medium consisted of clarified supernatant collected after 6 h of enzymatic hydrolysis. This medium was sufficient to sustain *R. toruloides* growth, as indicated by the accumulation of biomass and consumption of sugar (Figure 3A, dotted and dashed lines, respectively). The accumulation of carotenoids increased over time, reaching 5 ± 0.7 mg/L after 96 h of fermentation (Figure 3A, white bars), with a yield on consumed sugars of 0.034% (w/w) and on maximum quantity of sugars per biomass of 0.011% (w/w). These data are in accordance with previous reports that *R. toruloides* and carotenogenic microorganisms in general produce carotenoids mostly in response to stressful or sub-optimal conditions such as stationary phase [17,18,40,41]. The period of 96 h was chosen mainly to allow comparison with previous studies, whereby *R. toruloides* was provided with defined media or other/different residual biomasses (Table 2). After 96 h, fewer carotenoids could be extracted from the cells (Additional Figure S3), which could correlate with the export/release of carotenoids from the cells or with an imbalance of nutrients that might promote their consumption/corruption. The carotenoid production achieved here by SHF was competitive with *R. toruloides* grown in shake flasks and supplemented with other complex matrices (Table 2).

Table 2 Carotenoids production by *R. toruloides*

<i>R. toruloides</i> strain	Substrate	Time (h)	β -Carotene (mg/L)	References
ATCC 204091	WE ¹	72	62 \pm 1.70	[23]
	MM ²	100	57 \pm 2.18	
ATCC 10788	YPG ³	288	3.6	[16]
AS 2.1389			4.3	
CBS 5490			6.8	
CCT 0783	SCBH ^b	72	1.2 \pm 0.1	[21]
	cSCBH	94	2.18 \pm 0.2	
NCYC 921 (alias ATCC 10788)	CPS100 ^c	48	0.41	[22]
	CPS75		0.47	
	SCM100 ^d		0.04	
	SCM75		0.18	
DSM 4444	CM SHF ^e	96	5.5 \pm 0.7	This study
	CM SSF + presaccharification		12.6 \pm 2.6	
	CM SSF		16.0 \pm 1.9	

Comparison of data obtained from different media and fermentation modes

¹ WE = waste extract from mandis (road-side vegetable markets)

² MM = minimal media with 5 g/L glucose

³ YPG = 20 g peptone, 10 g yeast extract, 60 g glycerol

^b SCBH = sugarcane bagasse hydrolysate, cSCBH = concentrated SCBH

^c CPS = carob pulp syrup

^d SCM = sugarcane molasse

^e CM = *Camelina* meal

^{1,2} Bioreactor, ^{3, b, c, d, e} shake flasks. Data from other studies are reported with the original digits and standard deviation

Table 2: Carotenoids production by *R. toruloides*. Comparison of data obtained from different media and fermentation modes.

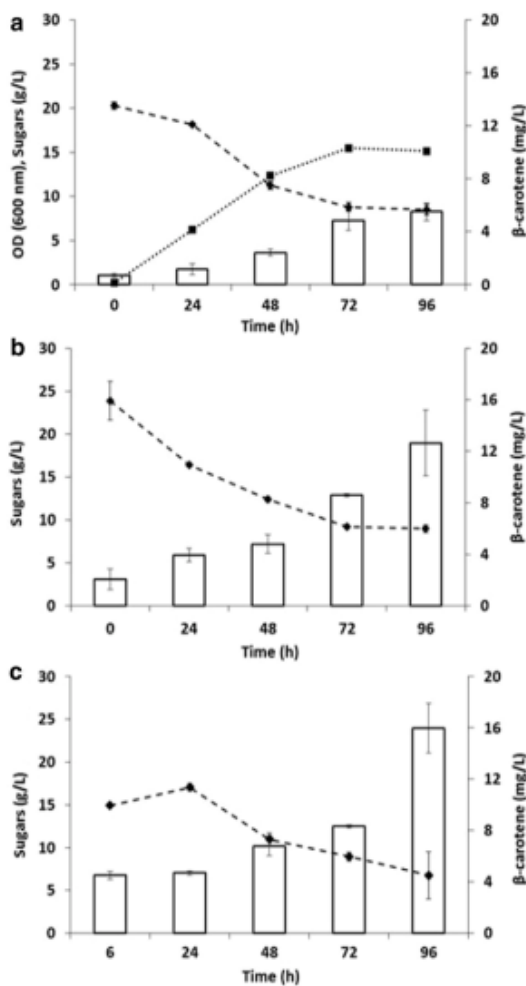


Figure 3: *R. toruloides* production of carotenoids from 15% *Camelina* meal hydrolysate. OD (dotted line), sugars consumption (dashed line), and β -carotene production (white bars) by *R. toruloides* subjected to different processes: SHF (A), SSF + presaccharification (B), and SSF (C). Values are the means of three independent experiments.

To overcome the need for clarifying the medium after enzymatic hydrolysis, we fed the cells the entire *Camelina* meal hydrolysate, including the water-insoluble solids (WIS) fraction left over after enzymatic hydrolysis. WIS may impair microbial growth and production because of the uneven homogenization of the liquid medium caused by the presence of solid components, as well as due to the toxicity of some of their components [28]. Under conditions termed here as “SSF + presaccharification”, *R. toruloides* was able not only of consuming sugars and producing carotenoids (Figure 3B), but it also achieved a higher titer of intracellular carotenoids, reaching 13 ± 2.6 mg/L after 96 h, with a yield

on consumed sugars of 0.108% (w/w) and on maximum quantity of sugars per biomass of 0.028% (w/w). Given that the amount of carotenoids extracted from *Camelina* meal with and without the addition of enzymes remained constant over time, the carotenoids measured in this and in the following experiments in the presence of WIS were due to microbial metabolism (Additional Figure S4).

Often proposed as an alternative to SHF, SSF is characterized by a single combined hydrolysis and microbial fermentation step. The two processes have several pros and cons in terms of efficiency, time, presence/release of inhibitory molecules, and downstream final product [42,43]. SHF and SSF have been proposed and compared for several 2nd generation biorefineries that used *Arundo donax*, grass or wheat straw as feedstocks [28,44,45]. A potential drawback of incubating enzymes and cells in the same environment is the compromise that needs to be reached allowing optimum operating conditions for both of them. In the present study, because 50°C was not a viable temperature for *R. toruloides*, 30°C was selected as the operative temperature. Thus, increased shaking was intended to partially compensate for the reduced activity by augmenting the probability of interactions between the matrix and the enzymes. Remarkably, the release of sugars in these conditions was comparable to that obtained by SHF or SSF + presaccharification (Additional Figure S5). As shown in Figure 3C, after the first 6 h of hydrolysis, the amount of sugars in the medium was lower compared to that obtained by SHF, most likely due to the initial growth (and therefore sugar consumption) of *R. toruloides*. After 24 h, sugar consumption became clearly evident and was accompanied by the accumulation of carotenoids. After 96 h, the carotenoid concentration reached 16 ± 1.9 mg/L, with a maximum amount of sugars per biomass of 0.028% (w/w). In the case of SSF, it is not possible to measure the total sugar released during saccharification because of simultaneous fermentation. Importantly, the amount of carotenoids was significantly higher when WIS were left in the medium (SSF and SSF + presaccharification) compared to simple SHF (*t*-test $p < 0.05$). While sub-lethal concentrations of insoluble solids might impair microbial growth, they could also trigger the accumulation of metabolites important for the microalgae and yeasts own defense

systems [41,46]. For example, β -phenol was shown to trigger carotenoid production in yeast [47].

The titers achieved by SSF indicate the efficacy of concurrent hydrolysis and fermentation, suggesting that a simplified procedure involving a single vessel could be used. Because productivity remained similar over time, the initial sugar released in the presence of cells did not seem to speed up the overall process. Overall, data from SSF and SSF + presaccharification reveal that the often mandatory detoxification step, indicated also for *R. toruloides* [48], is avoidable with this type of residual biomass. Moreover, the final product obtained by both SSF and SSF + presaccharification is a *Camelina* meal enriched with carotenoids, which can be used directly in the animal feed industry.

Therefore, different products, such as pure carotenoids and carotenoids-enriched *Camelina* meal can be recovered from the tested processes. *Camelina* meal in particular, would be an innovative product on the market, as carotenoids are commonly added to animal feed for nutritional and organoleptic reasons [3,12]. In addition, the production of carotenoids from a residual biomass of lower value may increase the economic attractiveness of the proposed process. Based on the logic of cascading [49,50], the present work paves the way for the use of *Camelina* meal as an alternative feedstock in 2nd generation biorefineries exploiting microbial cell factories to produce fine chemicals.

Conclusions

Here, we demonstrate that *Camelina* meal could be employed as residual biomass for the development of novel biorefineries based on microbial cell factories. After enzymatic hydrolysis, this biomass was provided to the oleaginous yeast *R. toruloides* as sole nutrient and energy source, and carotenoids production was assessed. A comparison of different processes revealed that the highest titer of carotenoids was obtained when *R. toruloides* was exposed to WIS and either SSF (16 ± 1.9 mg/L) or SSF + presaccharification (13 ± 2.6 mg/L). The presence of WIS seemed to play a positive role under these conditions, triggering the accumulation of the desired product and showing how common foes of biorefineries can turn into possible allies. To further investigate the pliancy of this

study, we plan to analyze the titer of concurrently accumulated carotenoids (e.g., torulene and torularhodin) and their relative ratio. We also intend to test alternative microbial cell factories to produce other high value-added molecules such as aromas. Moreover, biotransformation will be scaled-up from shake flasks to bioreactors, to generate data useful to calculate the competitiveness of a potential industrial process intended to further valorize *Camelina* meal, following the logic of cascading.

Materials and methods

***Camelina* meal composition**

Flanat Research Italia S.r.l., Rho, Italy, provided *Camelina* meal derived from plants cultivated and harvested in Lombardy in 2018 and 2019. *C. sativa* seeds were processed to collect the oil, while the leftover meal was delivered to the laboratory and stored at -20°C. To measure the water content of *Camelina* meal, 0.9 g and 4.5 g of biomass were dried at 160°C for 3 h, and then weighted again to calculate the amount of evaporated water. The biomass was incubated at 160°C for an additional 3 h, but no further changes in weight compared to the value obtained after the initial treatment were observed. Hence, the initial treatment was deemed sufficient. To analyze chemical composition of *Camelina* meal, the biomass was treated following the protocols for the analysis of structural carbohydrates and lignin in biomass from the National Renewable Energy Laboratory (NREL, <https://www.nrel.gov/docs/gen/fy13/42618.pdf>) with some modifications. Briefly, 300 mg of biomass were diluted in 3 mL H₂SO₄ 72% (v/v), and then incubated at 30°C for 1 h, stirring thoroughly every 10 min. The solution was diluted to 4% (v/v) by adding 84 mL of distilled water, mixed by inversion, and autoclaved at 121°C for 1 h. The hydrolysis solution was vacuum-filtered through a previously weighted filtering crucible, and the insoluble components were measured gravimetrically on the filter paper. The filtered liquid was neutralized with NaOH until pH 5–6 was attained and then the samples were analyzed by HPLC (as described below) after filtration with a 0.22 µm filter (Euroclone, Pero, Milan, Italy). Three independent experiments were performed.

Pretreatment and enzymatic hydrolysis of *Camelina* meal

Enzymatic hydrolysis of *Camelina* meal was performed using the enzyme mixture NS22119, kindly provided by Novozymes (Novozymes A/S, Copenhagen, Denmark). As described by the producer, NS22119 contains a wide range of carbohydrases, including arabinase, β -glucanase, cellulase, hemicellulase, pectinase, and xylanase from *Aspergillus aculeatus*. Without drying the biomass, different quantities of *Camelina* meal were weighted to a concentration of 3%, 6%, 9%, 12%, and 15% (w/v) into glass bottles, steeped in water with a final volume of 30 mL, and then autoclaved at 121°C for 1 h to both sterilize and pre-treat the biomass. Afterwards, enzymes were added directly to the bottles and incubated at pH 5.5 and at 50°C in a water bath under mild agitation (105 rpm). A 1-mL aliquot was collected every 2, 4, 6, and 24 h from the start, and sugar content was analyzed by HPLC (see below). The following enzyme concentrations were tested: 11.9% w/w_{Camelina meal}, 23.8% w/w_{Camelina meal}, and 11.9 % w/w_{Camelina meal} at 0 h plus at 6 h. Three independent experiments were performed. Low enzyme doses were intended to mimic commercially feasible hydrolysis, whereas high doses provided an indication of maximum enzymatically accessible sugar content. When implementing the suggested process at commercial scale, additional testing is recommended to refine the dose response curve and determine the effect of time, solids loading, pretreatment protocol, cellulose conversion, and enzyme dosage.

Microbial strain and media

R. toruloides (DSM 4444) was purchased from DSMZ (German Collection of Microorganisms and Cell Cultures, GmbH) and stored in cryotubes at -80°C in 20% glycerol (v/v). The composition of the medium for the pre-inoculum was as follows (per liter): 1 g yeast extract, 1.31 g (NH₄)₂SO₄, 0.95 g Na₂HPO₄, 2.7 g KH₂PO₄, and 0.2 g Mg₂SO₄·7H₂O. The medium was supplemented with 15 g/L of glycerol as main carbon source and a 100× trace mineral stock solution consisting of (per liter): 4 g CaCl₂·2H₂O, 0.55 g FeSO₄·7H₂O, 0.52 g citric acid, 0.10 g ZnSO₄·7H₂O, 0.076 g MnSO₄·H₂O, and 100 μ L 18 M H₂SO₄. Yeast extract was purchased from Biolife Italia S.r.l., Milan, Italy. All other reagents were purchased from Sigma-Aldrich Co., St Louis, MO, USA. After plating on rich

medium, a pre-inoculum was run in rich medium until stationary phase. Then, cells were inoculated at 0.2 OD in shake flasks at 30°C and 160 rpm for both SHF and SSF processes (see below).

SHF and SSF

During both SHF and SSF processes, *R. toruloides* was grown in shake flasks at pH 5.5, supplemented with *Camelina* meal hydrolysate, with or without WIS. After 6 h of enzymatic hydrolysis at 50°C, the hydrolysate was centrifuged at 4000 rpm for 10 min to separate the water-soluble components from WIS. Then, for SHF, the liquid fraction was collected and transferred into a shake flask for microbial growth at 30°C. Alternatively, for the SSF + saccharification process, *Camelina* hydrolysate was provided directly to *R. toruloides* as growth medium, regardless of the presence of WIS. For the SSF process, *Camelina* meal was directly steeped and autoclaved in a shake flask, then supplemented with the enzymatic cocktail at 11.9% w/w_{*Camelina* meal} and 0.2 OD of cells, and incubated at 30°C and 160 rpm. Three independent experiments for each setting were performed.

Carotenoids extraction

Carotenoids were analyzed by acetone extraction from *R. toruloides* cells with a protocol adapted from [51]. Briefly, 1 mL of culture broth was collected and harvested by centrifugation at 7000 rpm for 7 min at 4°C, and the pellet was then resuspended in 1 mL acetone and broken using glass beads by thorough agitation with a FastPrep-24™ (MP Biomedicals, LLC, Santa Ana, CA, USA). Carotenoids were extracted in the acetone phase, the suspension was centrifuged, and the supernatant collected. The extraction was repeated with fresh acetone until the biomass was colorless. Carotenoid content was measured spectrophotometrically (see below).

Analytical methods

HPLC analyses were performed to quantify the amount of glucose, sucrose, arabinose, fructose, and acetic acid. Briefly, 1-mL samples from each of the three different streams of production (enzymatically hydrolyzed *Camelina* meal, SHF or SSF) were collected and

centrifuged twice (7000 rpm, 7 min, and 4°C), and then analyzed by HPLC using a Rezex ROA-Organic Acid column (Phenomenex, Torrance, CA, USA). The eluent was 0.01 M H₂SO₄ pumped at 0.5 mL min⁻¹ and column temperature was 35°C. Separated components were detected by a refractive index detector and peaks were identified by comparing with known standards (Sigma-Aldrich).

Optical density (OD) of *R. toruloides* was measured spectrophotometrically at 600 nm.

The pH was measured with indicator strips at the beginning and at the end of enzymatic hydrolysis to assess suitability of the initial conditions and to foresee possible toxic effects of the final medium.

The titer of carotenoids extracted in acetone from *R. toruloides* was determined spectrophotometrically (UV-1800; Shimadzu, Kyoto, Japan) based on the maximum absorption peak for β-carotene (455 nm). A calibration curve with standard concentration of β-carotene was obtained.

Calculations and statistical analyses

Sugar recovery (here S_r) was calculated as percentage of sugar yield obtained by enzymatic hydrolysis (here Y_{EH}) compared with the yield obtained from total acid hydrolysis of biomass (here Y_{AH}) (Equation 1). Carotenoids yield on consumed sugars (here $Y_{c/s}$) and carotenoids yield on maximum quantity of sugars per biomass (here $Y_{c/b}$) measured with acid hydrolysis were calculated by Equations 2 and 3, respectively.

$$1) S_r = Y_{EH} / Y_{AH} \times 100$$

$$2) Y_{c/s} = C_p / \Delta sug \times 100$$

$$3) Y_{c/b} = C_p / S_b \times 100$$

Where Δsug corresponds to consumed sugars, S_b to maximum quantity of sugars in the biomass, and C_p to carotenoids produced.

For statistical analysis heteroscedastic two-tailed *t*-test was applied.

List of abbreviations

HPLC: high-performance liquid chromatography; OD: optical density; SHF: Separate Hydrolysis and Fermentation; SSF: Simultaneous Saccharification and Fermentation; WIS: water-insoluble solids.

Supplementary figures

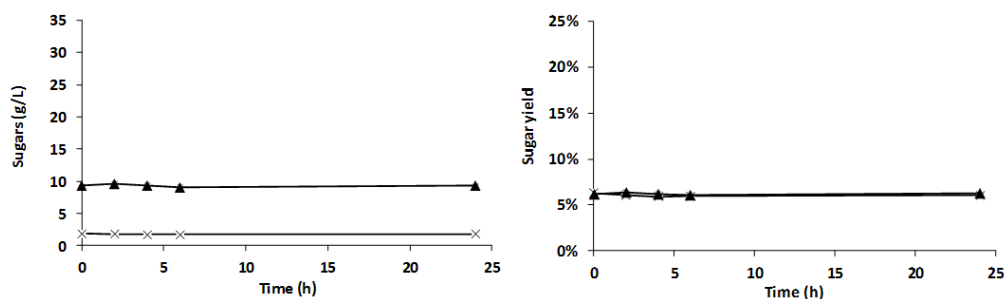


Figure S1. Effect of enzymatic hydrolysis conditions on different concentrations of *Camelina* meal without addition of the NS22119 cocktail.

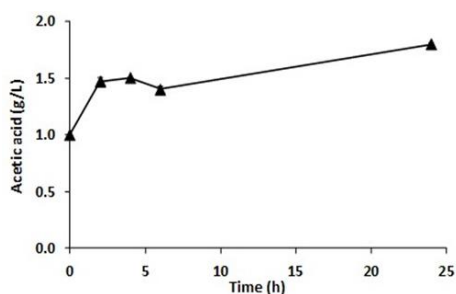


Figure S2: Acetic acid released during enzymatic hydrolysis. The concentration of acetic acid released from 15% *Camelina* meal by treatment with the NS22119 cocktail (11.9% w/w *Camelina* meal) was evaluated over time.

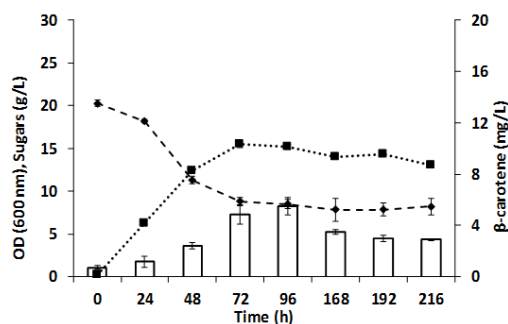


Figure S3. *R. toruloides* production of carotenoids from 15% (w/v) *Camelina* meal hydrolysate. OD (dotted line), sugars consumption (dashed line), and β -carotene production (white bars) by *R. toruloides* during the SHF process are shown.

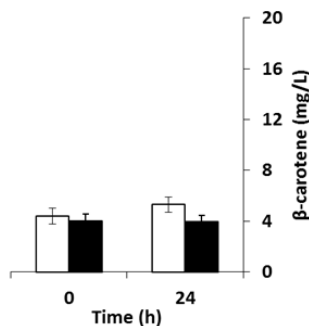


Figure S4. Carotenoids extraction from *Camelina* meal hydrolysate.

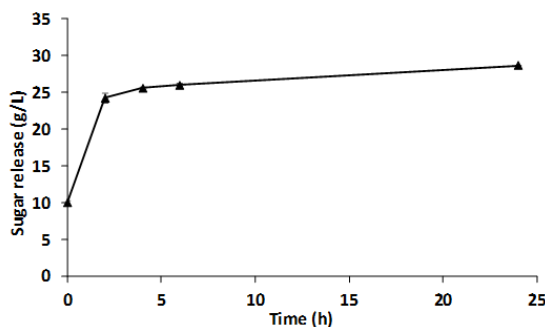


Figure S5: Effect of enzymatic hydrolysis on 15% *Camelina* meal by the NS22119 cocktail (11.9% w/w *Camelina* meal) at 30°C.

References

1. Azapagic A. Sustainability considerations for integrated biorefineries. Trends Biotechnol. Elsevier Ltd; 2014;32:1–4.
2. Jönsson LJ, Martín C. Pretreatment of lignocellulose: Formation of inhibitory by-products and strategies for minimizing their effects. Bioresour. Technol. 2016.
3. Food and Agriculture Organization of the United Nations (FAO). Utilization of lipid co-products of the biofuel industry in livestock feed in Biofuel co-products as livestock feed. 2012.
4. Zubr J. Carbohydrates, vitamins and minerals of *Camelina sativa* seed. Nutr Food Sci. 2010;40:523–31.
5. Cherian G. *Camelina sativa* in poultry diets : opportunities and challenges. Biofuel co-products as Livest Feed – Oppor challenges. 2012;
6. Murphy EJ. *Camelina* (*Camelina sativa*). Ind Oil Crop. 2016.
7. Dharavath RN, Singh S, Chaturvedi S, Luqman S. *Camelina sativa* (L.) Crantz A

mercantile crop with speckled pharmacological activities. *Ann Phytomedicine An Int J. Marwah Infotech*; 2016;5:6–26.

8. Sizmaz O, Gunturkun OB, Zentek J. A Point on Nutritive Value of *Camelina* Meal for Broilers : A Review. *Int J Vet Sci*. 2016;5:114–7.

9. Li X, Mupondwa E. Production and value-chain integration of *Camelina Sativa* as a dedicated bioenergy feedstock in the Canadian prairies. *Eur Biomass Conf Exhib Proc*. 2016.

10. Mohammad BT, Al-Shannag M, Alnaief M, Singh L, Singasaas E, Alkasrawi M. Production of Multiple Biofuels from Whole *Camelina* Material: A Renewable Energy Crop. *BioResources*. 2018;

11. Wang C, Zhao S, Shao X, Park J Bin, Jeong SH, Park HJ, et al. Challenges and tackles in metabolic engineering for microbial production of carotenoids. *Microb. Cell Fact*. 2019.

12. Saini RK, Keum YS. Microbial platforms to produce commercially vital carotenoids at industrial scale: an updated review of critical issues. *J. Ind. Microbiol. Biotechnol*. Springer International Publishing; 2019. p. 657–74.

13. Yuan S-F, Alper HS. Metabolic engineering of microbial cell factories for production of nutraceuticals. *Microb Cell Fact*. *BioMed Central*; 2019;18:46.

14. Nagarajan J, Ramanan RN, Raghunandan ME, Galanakis CM, Krishnamurthy NP. Carotenoids. *Nutraceutical Funct. Food Components Eff. Innov. Process. Tech*. Elsevier Inc.; 2017.

15. Guedes AC, Amaro HM, Malcata FX. Microalgae as sources of carotenoids. *Mar. Drugs*. 2011.

16. Lee JIL, Chen L, Shi J, Trzcinski A, Chen WN. Metabolomic profiling of *Rhodospiridium toruloides* grown on glycerol for carotenoid production during different growth phases. *J Agric Food Chem*. 2014;

17. Frengova GI, Beshkova DM. Carotenoids from *Rhodotorula* and *Phaffia*: Yeasts of biotechnological importance. *J. Ind. Microbiol. Biotechnol*. 2009.

18. Kot AM, Błazejak S, Gientka I, Kieliszek M, Bryś J. Torulene and torularhodin: “New” fungal carotenoids for industry? *Microb. Cell Fact*. 2018.

19. Park Y-KK, Nicaud J-MM, Ledesma-Amaro R. The Engineering Potential of *Rhodospiridium toruloides* as a Workhorse for Biotechnological Applications. *Trends Biotechnol*. 2018

20. Sitepu I, Selby T, Lin T, Zhu S, Boundy-Mills K. Carbon source utilization and inhibitor tolerance of 45 oleaginous yeast species. *J Ind Microbiol Biotechnol*. 2014;41:1061–70.

21. Bonturi N, Crucello A, Viana AJC, Miranda EA. Microbial oil production in sugarcane bagasse hemicellulosic hydrolysate without nutrient supplementation by a *Rhodospiridium toruloides* adapted strain. *Process Biochem.* Elsevier; 2017;57:16–25.
22. Freitas C, Parreira TM, Roseiro J, Reis A, Da Silva TL. Selecting low-cost carbon sources for carotenoid and lipid production by the pink yeast *Rhodospiridium toruloides* NCYC 921 using flow cytometry. *Bioresour Technol.* 2014;
23. Singh G, Sinha S, Bandyopadhyay KK, Lawrence M, Paul D. Triauxic growth of an oleaginous red yeast *Rhodospiridium toruloides* on waste “extract” for enhanced and concomitant lipid and β -carotene production. *Microb Cell Fact.* 2018;
24. Dai X, Shen H, Li Q, Rasool K, Wang Q, Yu X, et al. Microbial Lipid Production from Corn Stover by the Oleaginous Yeast *Rhodospiridium toruloides* Using the PreSSLP Process. *Energies.* Multidisciplinary Digital Publishing Institute; 2019;12:1053.
25. Wahlström RM, Suurnäkki A. Enzymatic hydrolysis of lignocellulosic polysaccharides in the presence of ionic liquids. *Green Chem.* Royal Society of Chemistry; 2015;17:694–714.
26. Khare SK, Pandey A, Larroche C. Current perspectives in enzymatic saccharification of lignocellulosic biomass. *Biochem Eng J.* 2015;102:38–44.
27. Arevalo-Gallegos A, Ahmad Z, Asgher M, Parra-Saldivar R, Iqbal HMN. Lignocellulose: A sustainable material to produce value-added products with a zero waste approach—A review. *Int J Biol Macromol.* Elsevier B.V.; 2017;99:308–18.
28. Ask M, Olofsson K, Di Felice T, Ruohonen L, Penttilä M, Lidén G, et al. Challenges in enzymatic hydrolysis and fermentation of pretreated *Arundo donax* revealed by a comparison between SHF and SSF. *Process Biochem.* Elsevier Ltd; 2012;47:1452–9.
29. Kim JK, Yang J, Park SY, Yu JH, Kim KH. Cellulase recycling in high-solids enzymatic hydrolysis of pretreated empty fruit bunches. *Biotechnol Biofuels.* BioMed Central; 2019;12:1–9.
30. Dias C, Sousa S, Caldeira J, Reis A, Lopes da Silva T. New dual-stage pH control fed-batch cultivation strategy for the improvement of lipids and carotenoids production by the red yeast *Rhodospiridium toruloides* NCYC 921. *Bioresour Technol.* Elsevier; 2015;189:309–18.
31. Merino ST, Cherry J. Progress and challenges in enzyme development for biomass utilization. *Adv Biochem Eng Biotechnol.* 2007;
32. Lenihan P, Orozco A, O’Neill E, Ahmad MNM, Rooney DW, Walker GM. Dilute acid hydrolysis of lignocellulosic biomass. *Chem Eng J.* 2010;
33. Sousa MJ, Ludovico P, Rodrigues F, Leo C, Crte-Real M. Stress and Cell Death in Yeast Induced by Acetic Acid. *Cell Metab - Cell Homeost Stress Response.* 2012.

34. Martani F, Marano F, Bertacchi S, Porro D, Branduardi P. The *Saccharomyces cerevisiae* poly(A) binding protein Pab1 as a target for eliciting stress tolerant phenotypes. *Sci Rep.* 2015;5.
35. Guldfeldt LU, Arneborg N. Measurement of the effects of acetic acid and extracellular pH on intracellular pH of nonfermenting, individual *Saccharomyces cerevisiae* cells by fluorescence microscopy. *Appl Environ Microbiol.* 1998;
36. Pampulha ME, Loureiro-Dias MC. Energetics of the effect of acetic acid on growth of *Saccharomyces cerevisiae*. *FEMS Microbiol Lett.* 2000;
37. Zhao X, Peng F, Du W, Liu C, Liu D. Effects of some inhibitors on the growth and lipid accumulation of oleaginous yeast *Rhodospiridium toruloides* and preparation of biodiesel by enzymatic transesterification of the lipid. *Bioprocess Biosyst Eng.* 2012;
38. Huang XF, Liu JN, Lu LJ, Peng KM, Yang GX, Liu J. Culture strategies for lipid production using acetic acid as sole carbon source by *Rhodospiridium toruloides*. *Bioresour Technol.* 2016;
39. Hu C, Zhao X, Zhao J, Wu S, Zhao ZK. Effects of biomass hydrolysis by-products on oleaginous yeast *Rhodospiridium toruloides*. *Bioresour Technol.* Elsevier; 2009;100:4843–7.
40. Singh G, Jawed A, Paul D, Bandyopadhyay KK, Kumari A, Haque S. Concomitant production of lipids and carotenoids in *Rhodospiridium toruloides* under osmotic stress using response surface methodology. *Front Microbiol.* 2016;
41. Mata-Gómez LC, Montañez JC, Méndez-Zavala A, Aguilar CN. Biotechnological production of carotenoids by yeasts: An overview. *Microb. Cell Fact.* 2014.
42. Aditiya HB, Mahlia TMI, Chong WT, Nur H, Sebayang AH. Second generation bioethanol production: A critical review. *Renew. Sustain. Energy Rev.* 2016.
43. Srivastava N, Rawat R, Singh Oberoi H, Ramteke PW. A review on fuel ethanol production from lignocellulosic biomass. *Int J Green Energy.* Taylor & Francis; 2015;12:949–60.
44. Burman NW, Sheridan CM, Harding KG. Lignocellulosic bioethanol production from grasses pre-treated with acid mine drainage: Modeling and comparison of SHF and SSF. *Bioresour Technol Reports.* 2019;7.
45. Tomás-Pejó E, Oliva JM, Ballesteros M, Olsson L. Comparison of SHF and SSF processes from steam-exploded wheat straw for ethanol production by xylose-fermenting and robust glucose-fermenting *Saccharomyces cerevisiae* strains. *Biotechnol Bioeng.* 2008;100:1122–31.
46. Sun X-M, Ren L-J, Zhao Q-Y, Ji X-J, Huang H. Microalgae for the production of lipid and

carotenoids: a review with focus on stress regulation and adaptation. *Biotechnol Biofuels*. BioMed Central; 2018;11:272.

47. Kim BK, Park PK, Chae HJ, Kim EY. Effect of phenol on β -carotene content in total carotenoids production in cultivation of *Rhodotorula glutinis*. *Korean J Chem Eng*. 2004;21:689–92.

48. Matsakas L, Novak K, Enman J, Christakopoulos P, Rova U. Acetate-detoxification of wood hydrolysates with alkali tolerant *Bacillus* sp. as a strategy to enhance the lipid production from *Rhodospiridium toruloides*. *Bioresour Technol*. 2017;

49. IEA Bioenergy Task42. Sustainable and synergetic processing of biomass into marketable food & feed ingredients, chemicals, materials and energy (fuels, power, heat). *IEA Bioenergy*. 2014;66.

50. IEA Bioenergy Task40. Cascading of woody biomass: definitions, policies and effects on international trade. *IEA Bioenergy*. 2016;71.

51. Saenge C, Cheirsilp B, Suksaroge TT, Bourtoom T. Potential use of oleaginous red yeast *Rhodotorula glutinis* for the bioconversion of crude glycerol from biodiesel plant to lipids and carotenoids. *Process Biochem*. Elsevier Ltd; 2011;46:210–8.

Chapter 2

2

Optimization of carotenoids
production from *Camelina*
sativa meal hydrolysate
by *Rhodospiridium*
toruloides

From Bertacchi S., Cantù C., Branduardi P. (2021) **Manuscript in preparation.**

Introduction

The widespread use of fossil resources is known to be detrimental towards the environment and human health [1], therefore alternatives as the development of bioprocesses based on renewable biomasses are desirable. Nonetheless, the use of biomasses has still to become competitive towards the classic petrochemical sector, in terms of economics and production volumes, despite this gap is not equal for every product or process. Indeed, in light of the principles of cascading, several commodities are requested by the market of reference in low amounts, such as compounds related to pharmaceutical, nutrition and cosmetic sectors [2–4]. Their high added value makes these molecules attractive for the scouting of bioprocesses based on biomasses that already have certain, yet limited, applications. In order to increase the environmental sustainability as well, waste biomasses, such as those originated from residual agro-industrial streams (often called lignocellulosic biomasses, LCBs) must be preferred. Such biomasses can be valorized in second generation biorefineries, often by the means of microbial cell factories, whose metabolism can transform carbon and energy sources of LCB origin into valuable compounds of interest [5].

In this scenario, we focused our attention on the exploitation of *Camelina* meal, the main by-product of oil extraction from *Camelina sativa* seeds [6–8]. This biomass is currently used as feed supplement: since its macromolecular components and relatively low cost (\$0.25/kg) [9,10], it is an attractive biomass for the development of sustainable bioprocesses. As we previously described in [11], it is possible to hydrolyse different amounts of *Camelina* meal by the use of an enzymatic cocktail, to be preferred to the conventional acid hydrolysis of LCBs. Furthermore, *Camelina* meal hydrolysate can be provided as sole component of the growth medium to the yeast *Rhodosporidium (Rhodotorula) toruloides*, and used in different types of processes, namely separated saccharification and fermentation (SHF) or simultaneous saccharification and fermentation (SSF) [11].

R. toruloides is naturally able to accumulate carotenoids, such as β -carotene, torulene, and torularhodin [12–14], optionally using residual biomasses as feedstock [15–17]. Recalling the cascading principles, carotenoids are high added value products, with a global market value expected to reach \$2.0B by 2022 and mainly deployed in animal feed, cosmetic, food and dietary supplements [18–21].

In order to increase the appeal of such process, in this work we propose optimizations aimed to reduce costs in terms of material use and fermentation timing, and to improve production, yield, and productivity.

Enzymatic cocktails, although being valuable ally in the hydrolysis of LCBs and in the release of fermentable sugars, have costs that decisively impact second generation biorefineries, since the maximum hydrolysis yield is often not likely the economical optimum as well [22,23]. Similarly, total solid loading is a parameter that could impact on production costs [24], therefore its optimization should be considered as well. Furthermore, the industrial implementation of a bioprocess needs a scale-up, which may bring to the rise of hurdles and complications [25,26]: at lab scale, whenever possible, we need to acquire quantitative data in bioreactor under industrially relevant conditions.

In the present work, we considered separately enzymatic loading and the amount of total solid loading as variable of the hydrolysis to be modulated in order to release sufficient quantity of sugars for the growth of *R. toruloides*. Combining the two best options in a SHF process, *R. toruloides* specific productivity of carotenoids resulted increased if compared with the initial setting. With these data we run fermentations at bioreactor scale and explored SSF and SHF to obtain quantitative data on carotenoids production by *R. toruloides* from *Camelina* meal, with the aim of promoting the industrial applications of this residual, yet underestimated, biomass.

Results and discussion

Optimization of the enzyme loading for *Camelina* meal hydrolysis

Glycosidic enzymes are cost items when assessing the economics of a bioprocess, since reducing the loading of enzymatic cocktails can be crucial to reduce overall costs.

Nevertheless, the yield of the sugars released must be considered to evaluate the performances of the enzymatic hydrolysis itself and the subsequent cellular production of interest. Here we evaluated the effect of reducing the amount of enzymatic cocktail (11.9% $w/w_{Camelina\ meal}$) previously used for the hydrolysis of 15% (w/v) of *Camelina* meal, leading to carotenoid production by *R. toruloides* [11].

Enzyme loadings were decreased from 11.9% to 0.56% $w/w_{Camelina\ meal}$, pairing with the lower dose the specific usage indications by the manufacturer. As shown in Figure 1 (left bars), a significant reduction in sugar release could be measured when comparing 11.90% and 8.93% $w/w_{Camelina\ meal}$ to the lower enzymatic loadings. This can be related to the inhibitory effect of the biomass on enzymatic hydrolysis, both in terms of compounds released by the pre-treatment and the requisition by LCBs on the enzymes themselves. Nevertheless, from 5.95% to 0.56% $w/w_{Camelina\ meal}$ of enzymes no significant difference could be observed, as also the lowest dose resulted in the release of about 15 g/L of total sugar.

If we consider only the sugars preferentially metabolized by *R. toruloides* (Figure S1, S2) [16,27] as carbon and energy source (*i.e.* sucrose, glucose and fructose; Figure 1, central bars), a similar observation can be drawn in terms of trends. Nevertheless, comparing the first with the second set of bars, it is clear that higher amounts of enzymes mainly promoted the release of sugars such as arabinose and galacturonic acid, as starting from 5.95% of enzyme loading the sum of glucose fructose and sucrose does not significantly differ from the quantity released from the use of higher amounts of enzymes. Arabinose and galacturonic acid are not promptly consumed by *R. toruloides* when the other sugars are present (Figure S1) [11,28]. Furthermore, considering only glucose, that is the first to be consumed by *R. toruloides* and imposes catabolite repression on the other sugars, (Figure S1, S2), the total release is overall similar with all the different loadings (Figure 1, right bars). Therefore, a reduction in the enzymatic loading by 95% (from 11.90% to 0.56% $w/w_{Camelina\ meal}$) provided a comparable amount of glucose (and fructose plus sucrose too) in the *Camelina* meal hydrolysate, thus suggesting a way for to reducing the cost of the process, which should be further tested and implemented.

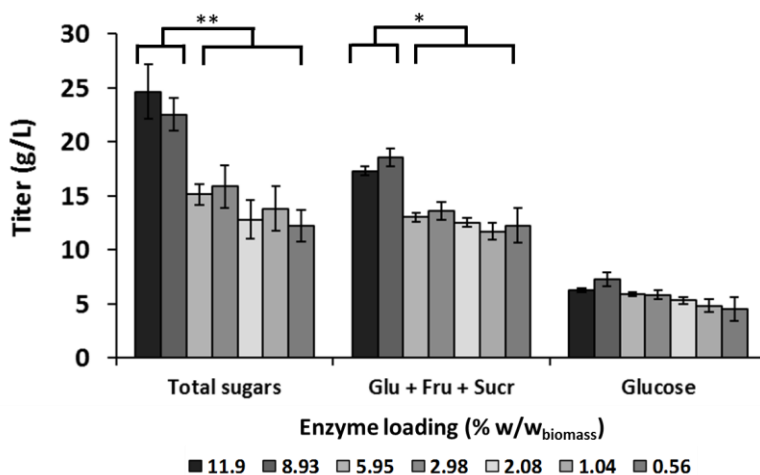


Figure 1: Sugar release (Titer, g/L) from 15% w/v of *Camelina* meal by NS22119 enzymatic cocktail at different loadings, in terms of total amount (intended as sum of sucrose, glucose, fructose, arabinose and galacturonic acid), sum of sucrose, glucose and fructose, and sole glucose. Values are the means of three independent experiments. ** $p < 0.02$, * $p < 0.05$

Effect of *Camelina* meal solid loadings on the production of carotenoids by *R. toruloides*

We previously demonstrated that *R. toruloides* was able to grow and accumulate carotenoids when provided with 15% w/v *Camelina* meal hydrolyzed with 11.9% w/w_{biomass} of enzymatic cocktail [11]. Maintaining this enzyme loading, we here explored to increase the amount of solid loading to understand the impact on sugar release, and how this would affect *R. toruloides* in a separated hydrolysis and fermentation (SHF) process.

From the enzymatic hydrolysis of 20% w/v *Camelina* meal 35.1 ± 0.07 g/L of total sugars were obtained, higher than those released from 15% w/v (24.6 ± 2.53 g/L, $p < 0.05$), but with very similar yield in respect to the total sugars (17.5 ± 0.04% and 16.4 ± 1.69% respectively). Therefore, the increased solid loading did not impair enzymatic hydrolysis. Surprisingly, as shown in Figure 2A, the growth of *R. toruloides* was reduced when provided with 20% w/v *Camelina* hydrolysate compared to 15% w/v in terms of number of cells/ml. Arguably, this can be related to the intracellular accumulation of lipids, since cellular dry weight (CDW) increased in this condition compared to the others tested (data not shown). *R. toruloides* is in fact an oleaginous yeast able to produce both carotenoids and neutral

lipids [13,14,17], and the accumulation of the latter may affect the OD detection. Nevertheless, with 20% w/v *Camelina* meal the production of carotenoids resulted significantly lower compared to the use of 15% w/v of initial biomass (Figure 2B), suggesting that providing higher quantities of initial sugars is not beneficial for the obtainment of the product of interest. Since their scavenger nature, carotenoids are produced by cell as response to environmental and cellular stresses, such as the stationary phase. We might argue that, as the presence of higher amount of sugars delayed the entrance to this phase (Figure 2A), carotenoids accumulation was delayed as well.

Given these data, we decided to move toward the opposite direction, namely lowering the amount of biomass, and, therefore, of sugars initially provided to cells. In this context cells could be in a starving situation, therefore being prompt to anticipate the stationary phase, and consequently accumulate carotenoids earlier and possibly in higher amounts. The tested solid loadings were 3%, 6%, 9% and 12% w/v, with enzymatic cocktail NS22119 able to release increasingly amount of sugars [11]. The derived growth media were able to support the growth of *R. toruloides*, with an increasingly anticipated entrance in stationary phase (Figure 2A). Interestingly, the use of 6% w/v of substrate sustained a higher growth in terms of OD compared to 9% and 12% w/v, probably due to lower amounts of inhibitors in the media. Nevertheless, 3% w/v of substrate provided also low sugar titers, reducing the final cellular OD. Figure 2B shows the production of carotenoids over time, for each of the biomass amounts tested in SHF processes with *R. toruloides*. Carotenoids accumulation is quite low after 24 h, increasing with the respective entrance into stationary phases. In particular, the most interesting conditions are 9% and 12% w/v, where carotenoids production obtained after 48 h of fermentation are comparable to the production obtained with 15% w/v but only after 72 h of growth. Consequently, the best productivities were reached using 9% and 12% *Camelina* meal hydrolysate ($p < 0.05$) (Figure 2C). Figure 2D shows that, the carotenoids yield on 9% w/v after 48 h resulted significantly higher compared to the yield on 12% w/v ($p < 0.05$) but not if compared with the yield with the 6% w/v, although their difference is at the limit of significativity (probably due to the uneven nature of the hydrolysates). Moving to productivity after 48 h of growth, this was

significantly higher with 9% w/v compared to 6% w/v *Camelina* meal ($2.1 \pm 0.32 \times 10^{-5} \text{ h}^{-1}$ and $0.5 \pm 0.11 \times 10^{-5} \text{ h}^{-1}$, $p < 0.02$), therefore supporting the inferior performance of the latter.

Therefore, considering *Camelina* meal solid loading as the variable parameter of the process, optimized conditions for carotenoids synthesis were the use of 9% w/v of biomass and 48 h of fermentation, with the following performances: production = $6.1 \pm 0.85 \text{ g/L}$, productivity = $0.13 \pm 0.017 \text{ g/L/h}$, yield on CWD = $0.1 \pm 0.02\%$, yield on consumed sugars = $0.1 \pm 0.01\%$, yield on total sugars provided = $0.02 \pm 0.003\%$. This result is remarkable if we consider that it was hardly possible to foresee such results giving data previously reported [11], highlighting once more the importance to test different conditions when developing bioprocesses, changing single parameters and assessing their effect on the final product.

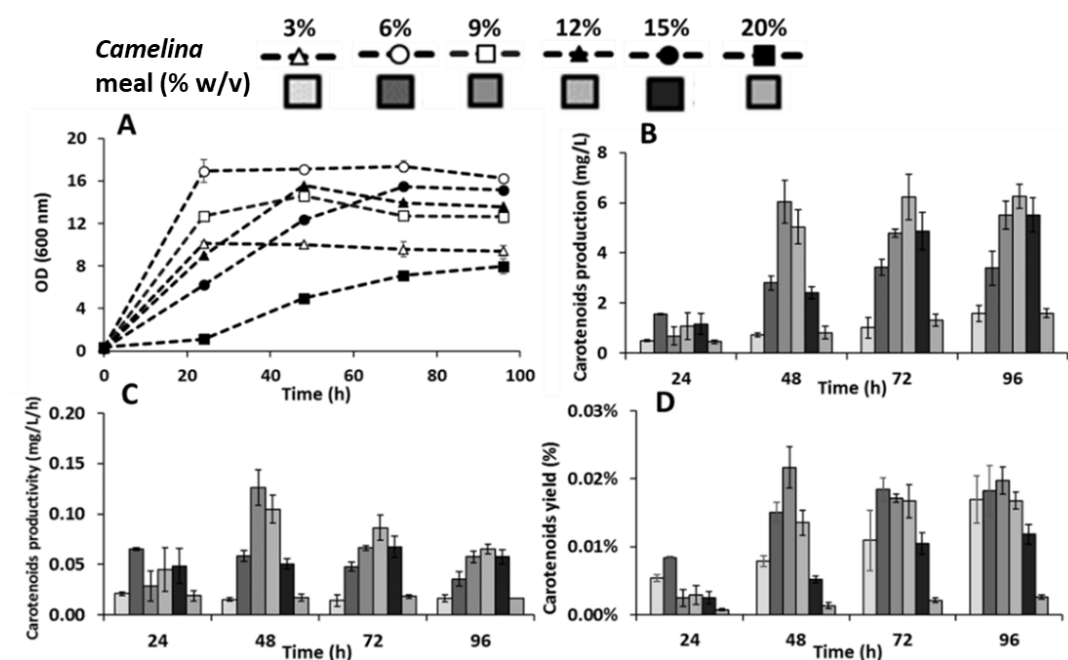


Figure 2: Modulation of solid loading of *Camelina* meal (from 3% to 20% w/v, hydrolysed with NS22119 11.9% w/w_{biomass}) and its effect on *R. toruloides* growth and carotenoids production. Growth in terms of OD (panel A), carotenoids production (panel B), productivity (panel C) and yield (panel D).

Combinatory effect of optimized enzymes and biomass titers on the production of carotenoids by *R. toruloides*

After showing the possibility to reduce the enzymatic loading and the solid loading of *Camelina* meal, we then combined the two strategies in a single process. Therefore, we run a SHF process in which *R. toruloides* was provided with 9% w/v of *Camelina* meal hydrolysed by NS22119 enzymatic cocktail 0.56% w/w_{*Camelina* meal} as growth medium. The results in terms of OD, sugar consumption and carotenoids production are shown in Figure 3: samples were collected until 48 h in the light of data shown in the previous section. *R. toruloides* did not consume all the sugars provided, arguably due to the depletion of fundamental micronutrients in the medium [11]. Furthermore, the reduction of enzymes and the consequent reduction in sugar titer contributed to anticipate the maximum carotenoid accumulation (2.2 ± 0.33 g/L) to 24 h. Although this value was inferior compared to that obtain from the use of 11.90% w/w_{*Camelina* meal} and 48 h of fermentation, no significant difference could be observed in terms of specific productivity after 24 h when 0.56% w/w_{*Camelina* meal} were used (0.1 ± 0.01 g/L/h and $2 \pm 0.3 \times 10^{-5}$ h⁻¹, respectively). Despite a techno-economic analysis (including downstream processing and possible related issues) was not performed yet, it is reasonable to conclude that reduction in both process time and enzymatic loading would in turn drastically reduce the overall cost of the process, maintaining relevant production parameters for carotenoids. Therefore, optimized conditions for the synthesis of carotenoids by *R. toruloides* were the use of 9% (w/v) *Camelina* meal hydrolysed with 0.56% w/w_{*Camelina* meal} of NS22119 as medium for 24 h of growth in a SHF process. Furthermore, in these conditions the specific growth rate (μ) of *R. toruloides* was calculated to be 0.25 h⁻¹, with a duplication time of 2.74 h (Figure S3). Entrance in lag phase was evaluated to be reached after about 5 h from start, whereas the entrance in stationary phase after 21 h, coherently with what disclosed in Figure 3.

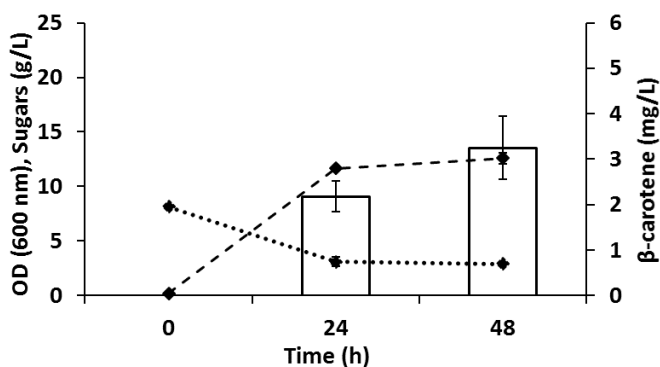


Figure 3: *R. toruloides* growth in SHF process with 9% (w/v) *Camelina* meal hydrolysed with 0.56% w/w_{*Camelina* meal} of NS22119 as growth medium: OD (dashed line), sugar consumption (dotted line), carotenoids production (white bars). Values are the means of three independent experiments.

We further explored the use of such conditions in SSF and SSF + presaccharification processes, to evaluate the effect of the presence of water insoluble components (WIS), which, being potentially stressful compounds for the cells, may trigger the production of scavenger molecules as carotenoids. Figure 4 shows that *R. toruloides* was able to consume sugars and to produce carotenoids in both settings, reaching the maximum after 48 h of growth (4.6 ± 0.21 g/L for SSF + presaccharification, 4.9 ± 0.39 g/L for SSF). The delayed production compared to SHF may be related to the harsher conditions that cells had to face in the presence of WIS. In fact they may impair microbial growth and production due to uneven homogenization of the liquid medium, as well as to the toxicity of some of their components [29]. Overall, WIS do not interfere with the production of carotenoids by *R. toruloides*. Consequently, it is possible to imagine different types of bioprocesses based on *Camelina* meal, with SHF or SSF to be display considering various factors of industrial relevance, such as time, costs, number of vessels for hydrolysis and fermentation, and final product. Fermentations in the presence of WIS lead to a *Camelina* meal enriched in carotenoids, which may be directly used as feed supplement. Furthermore, these data show that results obtained from SHF can be predictive of the corresponding SSF process.

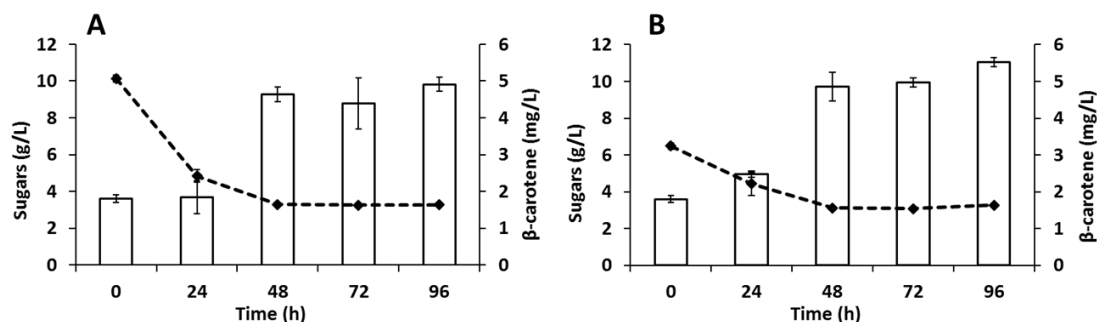


Figure 4: *R. toruloides* growth with 9% (w/v) *Camelina* meal hydrolysed with 0.56% w/w *Camelina* meal of NS22119 as growth medium in a SSF + presaccharification (panel A) and SSF (panel B) process: sugar consumption (dotted line), carotenoids production (white bars). Values are the means of three independent experiments.

Carotenoids production in batch bioreactors

To test the reliability of the protocols in larger volume and to acquire data for quantitative analysis, we moved the process to stirred tank bioreactor. As starting point, the volume of the enzymatic hydrolysis was increased to 1 L: due to the uneven nature of lignocellulosic biomasses and their inhibitory effect towards enzymatic activity, scaling up this step may lead to a decrease in hydrolysis yield. Remarkably, after 6 h of hydrolysis of 9% w/v of *Camelina* meal by NS22119 0.56% w/w *Camelina* meal the amount of released sugars (7.2 ± 0.84 g/L, see T0 Figure 3) was comparable with that obtained from lower volumes of hydrolysis, demonstrating the scalability of the first step of the process.

The obtained medium was used to test the production of carotenoids in batch bioreactors, where *R. toruloides* cells were inoculated at initial OD of 0.4, pH 5.6 ± 0.09 and oxygenation of 25%. Cells reached the stationary phase already after T16, as shown by the profile of the optical density and the cellular dry weight (Figure 5A). This is also in line with the kinetic parameters calculated for *R. toruloides* grown in shake flasks in the same medium (see previous section). Bioreactor cultivation permitted also to monitor pH and dissolved oxygen (Figure 5A): the first increased over time to reach the value of 6.7 ± 0.03 at T48, whereas the second increased after T16 (up to 80%), witnessing a strong decrease in cellular growth, as from the reduction of oxygen consumption. The increase in pH could be related to the accumulation of ammonia in the medium, initially consumed by cells (Figure 5B), but then produced probably as a consequence of amino acid catabolism triggered in

response to starvation. In fact, as shown in Figure 5B, cells already consumed sugars and nitrogen (in the form of primary amines) at T16, although the incomplete consumption of both (that remained till the end of the fermentation) may be related to the depletion in the medium of micronutrients pivotal to cellular sustainment.

The exhaustion of nutrients, the increase in pH and pO_2 and the growth curve profiles (in terms of OD and CDW) suggest an early entrance in stationary phase, which is of interest as aforementioned for the production of secondary metabolites such as carotenoids.

Consistently, regarding the production of carotenoids, from T16 on there was no statistically significant increase in their accumulation, reaching 3.6 ± 0.69 mg/L after T24 (Figure 5B), with a productivity (0.13 ± 0.03 mg/L/h) comparable with the one obtained in the same conditions in shake flasks (Figure 3). Therefore, shake flask tests showed to be predictable on the behavior of *R. toruloides* in bioreactor. The data here disclosed are the first reports of bioreactor scale fermentation of *Camelina* meal hydrolysate, and therefore they can pave the way for further optimization. To maximize the production of interest several modifications influencing lipid and carotenoid production in yeasts, like C/N ratio, initial CDW, pH and oxygenation [30–33], can be operated.

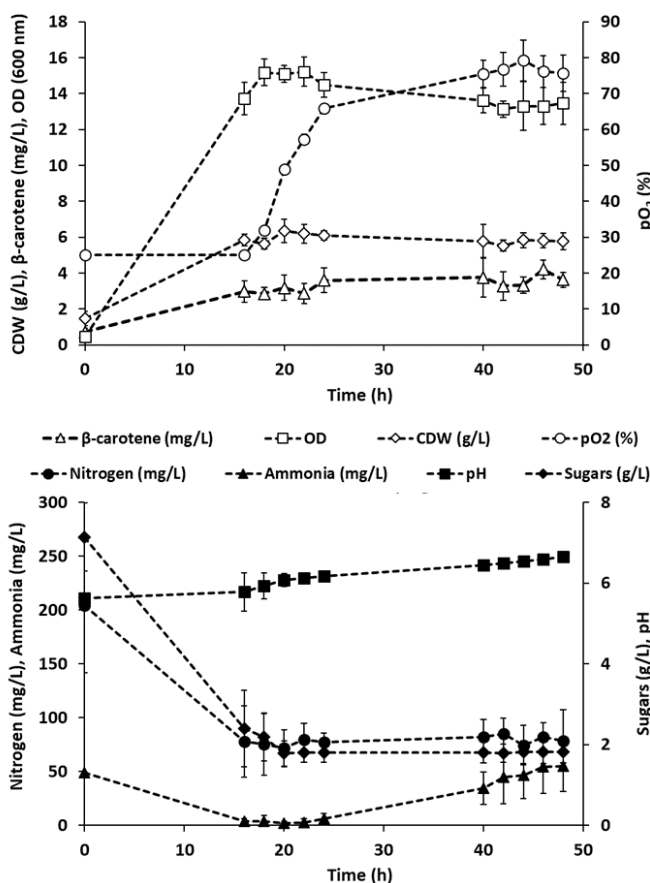


Figure 5: *R. toruloides* growth with 9% (w/v) *Camelina* meal hydrolysed with 0.56% w/w *Camelina* meal of NS22119 as growth medium in stirred tank bioreactor (batch mode). Profile over time of β -carotene production (empty triangles), optical density (empty squares), cellular dry weight (empty diamonds), pO_2 (empty circles) – panel A; nitrogen titer (full circles), ammonia titer (full triangles), sugars titer (full diamonds) and pH (full squares) – panel B.

Conclusions

In the present work we demonstrate that the bioprocess involving the use of *Camelina* meal hydrolysate for the production of carotenoids by *R. toruloides* can be optimized in terms of different parameters. In fact, by dropping the enzymatic titer by 95% the hydrolysis was still efficient in releasing the main sugars consumed by this yeast in this medium (*i.e.* glucose, fructose, sucrose). In parallel we also modified the amount of total solid loading, exploring both higher and lower biomass titer than the original (15% w/v), in order to select the best option considering production, yield and productivity. Combining the optimized conditions for these two parameters, SHF was performed with 9% w/v

Camelina meal hydrolysed by NS22119 0.56% w/w_{*Camelina* meal}. In these conditions *R. toruloides* was able to accumulate 2.2 ± 0.33 g/L of carotenoids in 24 h, with a specific productivity of $2 \pm 0.3 \times 10^{-5}$ h⁻¹. Furthermore, this SHF process in shake flask proved to be predictable of the behavior in SSF and SSF + presaccharification, and when the process was performed in batch bioreactors as well. The preliminary data from bioreactor fermentation pave the way for additional optimization of the process itself. Based on the logic of cascading [3,34], the present work further fostered the use of *Camelina* meal as an alternative feedstock in second generation biorefineries exploiting microbial cell factories to produce fine chemicals.

Materials and methods

***Camelina* meal hydrolysis**

Flanat Research Italia S.r.l., Rho, Italy, provided *Camelina* meal derived from plants cultivated and harvested in Lombardy in 2018 and 2019. *C. sativa* seeds were processed to collect the oil, while the leftover meal was delivered to the laboratory and stored at -20 °C. Enzymatic hydrolysis of *Camelina* meal was performed using the enzyme mixture NS22119, kindly provided by Novozymes (Novozymes A/S, Copenhagen, Denmark) as described in [11]. Without drying the biomass, different quantities of *Camelina* meal were weighted to a concentration of 3%, 6%, 9%, 12%, 15% and 20% (w/v) into glass bottles, steeped in water with a final volume of 30 mL, and then autoclaved at 121 °C for 1 h to both sterilize and pre-treat the biomass. Afterwards, enzymes were added directly to the biomass and incubated at 50°C in a water bath under mild agitation (105 rpm). The following enzyme concentrations were tested: 11.9%, 8.93%, 5.95%, 2.98%, 2.08%, 1.04%, and 0.56% w/w_{*Camelina* meal}. Three independent experiments were performed.

Microbial strain, media and fermentations

R. toruloides (DSM 4444) was purchased from DSMZ (German Collection of Microorganisms and Cell Cultures, GmbH) and stored in cryotubes at -80 °C in 20% glycerol (v/v). The composition of the medium for the pre-inoculum was as follows (per liter): 1 g yeast

extract, 1.31 g $(\text{NH}_4)_2\text{SO}_4$, 0.95 g Na_2HPO_4 , 2.7 g KH_2PO_4 , and 0.2 g $\text{Mg}_2\text{SO}_4 \cdot 7\text{H}_2\text{O}$. The medium was supplemented with 15 g/L of glycerol as main carbon source and a 100× trace mineral stock solution consisting of (per liter): 4 g $\text{CaCl}_2 \cdot 2\text{H}_2\text{O}$, 0.55 g $\text{FeSO}_4 \cdot 7\text{H}_2\text{O}$, 0.52 g citric acid, 0.10 g $\text{ZnSO}_4 \cdot 7\text{H}_2\text{O}$, 0.076 g $\text{MnSO}_4 \cdot \text{H}_2\text{O}$, and 100 μL 18 M H_2SO_4 . Yeast extract was purchased from Biolife Italia S.r.l., Milan, Italy. All other reagents were purchased from Sigma-Aldrich Co., St Louis, MO, USA.

For shake flasks fermentations, after plating on rich medium, a pre-inoculum was run until stationary phase. Then, cells were inoculated at 0.2 OD at 30°C and 160 rpm for both SHF and SSF processes (see below).

SHF and SSF

During both SHF and SSF processes, *R. toruloides* was grown in shake flasks supplemented with *Camelina* meal hydrolysate, with or without WIS. After 6 h of enzymatic hydrolysis at 50 °C, the hydrolysate was centrifuged at 4000 rpm for 10 min to separate the water-soluble components from WIS. Then, for SHF, the liquid fraction was collected and transferred into a shake flask or a stirred tank bioreactor for microbial growth at 30°C. Alternatively, for the SSF + saccharification process, *Camelina* hydrolysate was provided directly to *R. toruloides* as growth medium, regardless of the presence of WIS. For the SSF process, *Camelina* meal was directly steeped and autoclaved in a shake flask, then supplemented with the enzymatic cocktail at 0.56% w/w_{*Camelina* meal} and 0.2 OD of cells, and incubated at 30°C and 160 rpm. These conditions were also used to calculate specific growth rate of *R. toruloides*. Three independent experiments for each setting were performed.

Batch bioreactor fermentation

Enzymatic hydrolysis of 1 L of *Camelina* meal 9% w/v was performed in 2 L shake flasks by the action of NS22119 0.56% w/w_{*Camelina* meal}, for 6 h at 50 °C and 130 rpm, in order to increase the homogenization of the solid component in the liquid. The hydrolysate was

then centrifuged in an Avanti J-20 (Beckman Coulter Brea, California, USA), at 4 °C and 8000 rpm for 10 min and the supernatant collected and stored at 4 °C until use.

Regarding *R. toruloides* inoculum, from cryotubes cells were inoculated in 250 mL flasks with 50 mL of culture medium, as pre-seeding for the inoculation in 1 L flasks with 200 mL of the culture medium, and seed cultures were placed at 30 °C and 160 rpm for 24 h. Exponential phase shake flasks cultures were used to inoculate bioreactors to a final optical density (OD_{600}) of 0.4. Briefly, cells were centrifuged at 6000 rpm for 10 min, washed twice with water, and finally resuspended in 10 mL of sterilized water. The batch experiments were conducted in 2 L stirred tank bioreactors (BIOSTAT® A plus, Sartorius Stedim Biotech GmbH, Goettingen, Germany) equipped with Visiferm DO ECS 225 for pO₂ measurement and Easyferm Plus K8 200 for pH measurement (both from Hamilton Bonaduz AG, Bonaduz, Switzerland). The batch fermentation was carried out with 1 L of *Camelina* meal hydrolysate, and aeration rate, agitation, and temperature set to 1 vvm, 300 rpm (in cascade to 25% of dissolved oxygen), and 30 °C, respectively. Three independent experiments were performed.

Carotenoids extraction

Carotenoids were analyzed by acetone extraction from *R. toruloides* cells with a protocol adapted from [35]. Briefly, 1 mL of culture broth was collected and harvested by centrifugation at 7000 rpm for 7 min at 4°C, and the pellet was then resuspended in 1 mL acetone and broken using glass beads by thorough agitation with a FastPrep-24™ (MP Biomedicals, LLC, Santa Ana, CA, USA). Carotenoids were extracted in the acetone phase, the suspension was centrifuged, and the supernatant collected. The extraction was repeated with fresh acetone until the biomass was colorless. Carotenoid content was measured spectrophotometrically (see below).

Analytical methods

HPLC analyses were performed to quantify the amount of glucose, sucrose, arabinose, fructose, galacturonic acid, and acetic acid. Briefly, 1-mL samples from each of the three

different streams of production (enzymatically hydrolyzed *Camelina* meal, SHF or SSF) were collected and centrifuged twice (7000 rpm, 7 min, and 4°C), and then analyzed by HPLC using a Rezex ROA-Organic Acid column (Phenomenex, Torrance, CA, USA). The eluent was 0.01 M H₂SO₄ pumped at 0.5 mL min⁻¹ and column temperature was 35 °C. Separated components were detected by a refractive index detector and peaks were identified by comparing with known standards (Sigma-Aldrich).

Optical density (OD) of *R. toruloides* was measured spectrophotometrically at 600 nm. Cellular dry weight (CDW) was measured gravimetrically after drying 1 mL of cell culture (Concentrator 5301, Eppendorf AG, Germany).

Primary Amino Nitrogen Assay Kit (PANOPA) and Urea/Ammonia Assay Kit (K-URAMR, Megazyme International Limited, Bray, Ireland) were used to determine the amount of primary amines, ammonia and urea in the *Camelina* meal hydrolysate.

The titer of carotenoids extracted in acetone from *R. toruloides* was determined spectrophotometrically (UV-1800; Shimadzu, Kyoto, Japan) based on the maximum absorption peak for β-carotene (455 nm). A calibration curve with standard concentration of β-carotene was obtained.

Calculations and statistical analyses

Carotenoids yield on consumed sugars (here $Y_{c/s}$) and carotenoids yield on maximum quantity of sugars per biomass (here $Y_{c/b}$) measured with acid hydrolysis in [11] were calculated by Equations 1 and 2, respectively. Specific productivity (q_p) was calculated by Equation 3. Specific growth rate (μ) was calculated mathematically by equation obtained from plotting values of OD vs time on Excel (Figure S3). Duplication time (T_d) was calculated by Equation 4.

$$1) Y_{c/s} = \frac{C_p}{\Delta sug} \times 100$$

$$2) Y_{c/b} = \frac{C_p}{S_b} \times 100$$

$$3) q_p = \frac{C_p/t}{CDW}$$

$$4) t_d = \frac{\ln 2}{\mu}$$

Where Δsug corresponds to consumed sugars, S_b to maximum quantity of sugars in the biomass, C_p to carotenoids produced, and $C_{p/s}$ to carotenoids productivity.

For statistical analysis heteroscedastic two-tailed t -test was applied.

List of abbreviations

CDW: cellular dry weight; HPLC: high-performance liquid chromatography; OD: optical density; SHF: Separate Hydrolysis and Fermentation; SSF: Simultaneous Saccharification and Fermentation; WIS: water-insoluble solids.

Supplementary figures

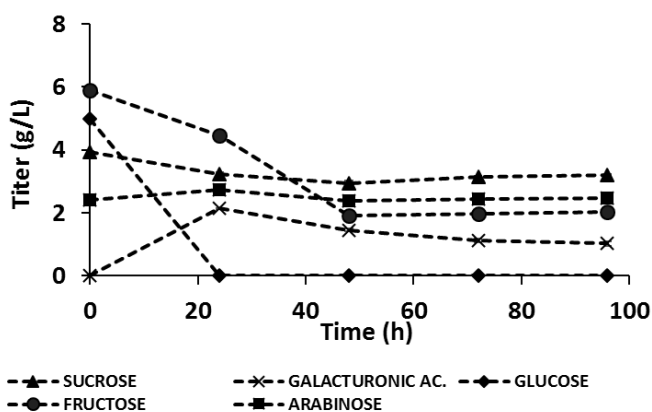


Figure S1. Sugar consumption profile during *R. toruloides* growth in shake flask fermentation when provided with 9% (w/v) *Camelina* meal hydrolysed with 11.9% w/w *Camelina* meal of NS22119.

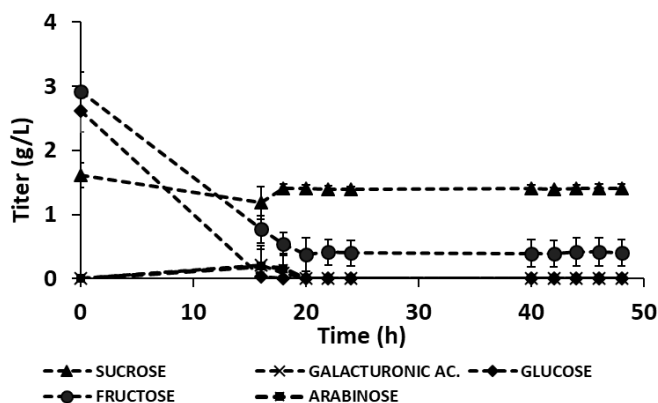


Figure S2. Sugar consumption profile during *R. toruloides* growth in batch bioreactor fermentation when provided with 9% (w/v) *Camelina* meal hydrolysed with 0.56% w/w *Camelina* meal of NS22119.

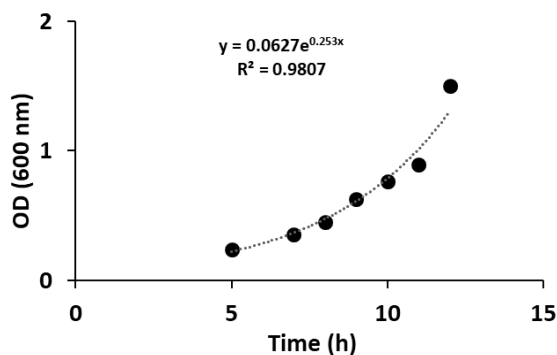


Figure S3. Optical density profile during *R. toruloides* grow in shake flask fermentation when provided with 9% (w/v) *Camelina* meal hydrolysed with 0.56% w/w *Camelina* meal of NS22119.

References

1. Jackson RB, Friedlingstein P, Andrew RM, Canadell JG, Le Quéré C, Peters GP. Persistent fossil fuel growth threatens the Paris Agreement and planetary health. *Environ. Res. Lett.* Institute of Physics Publishing; 2019. p. 121001.
2. Stegmann P, Londo M, Junginger M. The circular bioeconomy: Its elements and role in European bioeconomy clusters. *Resour Conserv Recycl X.* Elsevier; 2020;6:100029.
3. IEA Bioenergy Task40. Cascading of woody biomass: definitions, policies and effects on international trade. IEA Bioenergy. 2016;71.
4. Vis M, Reumerman P, Gärtner S. Cascading in the wood sector. 2014.
5. Branduardi P. Closing the loop: the power of microbial biotransformations from traditional bioprocesses to biorefineries, and beyond. *Microb Biotechnol.* 2020;0:1–6.
6. Zubr J. Carbohydrates, vitamins and minerals of *Camelina sativa* seed. *Nutr Food Sci.* 2010;40:523–31.
7. Murphy EJ. *Camelina (Camelina sativa)*. *Ind Oil Crop.* 2016.
8. Dharavath RN, Singh S, Chaturvedi S, Luqman S. *Camelina sativa* (L.) Crantz A mercantile crop with speckled pharmacological activities. *Ann Phytomedicine An Int J.* Marwah Infotech; 2016;5:6–26.
9. Cherian G. *Camelina sativa* in poultry diets : opportunities and challenges. Biofuel co-products as Livest Feed – Oppor challenges. 2012;
10. Li X, Mupondwa E. Production and value-chain integration of *Camelina Sativa* as a dedicated bioenergy feedstock in the Canadian prairies. *Eur Biomass Conf Exhib Proc.* 2016.

11. Bertacchi S, Bettiga M, Porro D, Branduardi P. *Camelina sativa* meal hydrolysate as sustainable biomass for the production of carotenoids by *Rhodospiridium toruloides*. *Biotechnol Biofuels*. BioMed Central; 2020;13:1–10.
12. Lee JIL, Chen L, Shi J, Trzcinski A, Chen WN. Metabolomic profiling of *Rhodospiridium toruloides* grown on glycerol for carotenoid production during different growth phases. *J Agric Food Chem*. 2014;
13. Kot AM, Błazejak S, Gientka I, Kieliszek M, Bryś J. Torulene and torularhodin: “New” fungal carotenoids for industry? *Microb. Cell Fact*. 2018.
14. Park Y-KK, Nicaud J-MM, Ledesma-Amaro R. The Engineering Potential of *Rhodospiridium toruloides* as a Workhorse for Biotechnological Applications. *Trends Biotechnol*. 2018.
15. Freitas C, Parreira TM, Roseiro J, Reis A, Da Silva TL. Selecting low-cost carbon sources for carotenoid and lipid production by the pink yeast *Rhodospiridium toruloides* NCYC 921 using flow cytometry. *Bioresour Technol*. 2014;
16. Singh G, Sinha S, Bandyopadhyay KK, Lawrence M, Paul D. Triauxic growth of an oleaginous red yeast *Rhodospiridium toruloides* on waste “extract” for enhanced and concomitant lipid and β -carotene production. *Microb Cell Fact*. 2018;
17. Wen Z, Zhang S, Odoh CK, Jin M, Zhao ZK. *Rhodospiridium toruloides* - A potential red yeast chassis for lipids and beyond. *FEMS Yeast Res*. Oxford University Press; 2020;20:1–12.
18. Wang C, Zhao S, Shao X, Park J Bin, Jeong SH, Park HJ, et al. Challenges and tackles in metabolic engineering for microbial production of carotenoids. *Microb. Cell Fact*. 2019.
19. Saini RK, Keum YS. Microbial platforms to produce commercially vital carotenoids at industrial scale: an updated review of critical issues. *J. Ind. Microbiol. Biotechnol*. Springer International Publishing; 2019. p. 657–74.
20. Yuan S-F, Alper HS. Metabolic engineering of microbial cell factories for production of nutraceuticals. *Microb Cell Fact*. BioMed Central; 2019;18:46.
21. Nagarajan J, Ramanan RN, Raghunandan ME, Galanakis CM, Krishnamurthy NP. Carotenoids. *Nutraceutical Funct. Food Components Eff. Innov. Process. Tech*. Elsevier Inc.; 2017.
22. Pihlajaniemi V, Ellilä S, Poikkimäki S, Nappa M, Rinne M, Lantto R, et al. Comparison of pretreatments and cost-optimization of enzymatic hydrolysis for production of single cell protein from grass silage fibre. *Bioresour Technol Reports*. Elsevier Ltd; 2020.
23. Aden A, Foust T. Technoeconomic analysis of the dilute sulfuric acid and enzymatic hydrolysis process for the conversion of corn stover to ethanol. *Cellulose*. 2009.

24. Larnaudie V, Ferrari MD, Lareo C. Techno-economic analysis of a liquid hot water pretreated switchgrass biorefinery: Effect of solids loading and enzyme dosage on enzymatic hydrolysis. *Biomass and Bioenergy*. Elsevier Ltd; 2019.
25. Humphrey A. Shake Flask to Fermentor: What Have We Learned? *Biotechnol Prog. AIChE*; 1998;14:3–7.
26. Crater JS, Lievens JC. Scale-up of industrial microbial processes. *FEMS Microbiol Lett*. 2018;365:138.
27. Gancedo JM. Yeast Carbon Catabolite Repression. *Microbiol. Mol. Biol. Rev.* 1998.
28. Wiebe MG, Koivuranta K, Penttilä M, Ruohonen L. Lipid production in batch and fed-batch cultures of *Rhodospiridium toruloides* from 5 and 6 carbon carbohydrates. *BMC Biotechnol. BioMed Central*; 2012.
29. Ask M, Olofsson K, Di Felice T, Ruohonen L, Penttilä M, Lidén G, et al. Challenges in enzymatic hydrolysis and fermentation of pretreated *Arundo donax* revealed by a comparison between SHF and SSF. *Process Biochem. Elsevier Ltd*; 2012;47:1452–9.
30. Júnior H, Lopes S, Bonturi N, Lahtvee P, Kerkhoven EJ. C/N ratio and carbon source-dependent lipid production profiling in *Rhodotorula toruloides*. *Appl Microbiol Biotechnol. Applied Microbiology and Biotechnology*; 2020.
31. Dias C, Sousa S, Caldeira J, Reis A, Lopes da Silva T. New dual-stage pH control fed-batch cultivation strategy for the improvement of lipids and carotenoids production by the red yeast *Rhodospiridium toruloides* NCYC 921. *Bioresour Technol. Elsevier*; 2015;189:309–18.
32. Bento TFSR, Viana VFM, Carneiro LM, Silva PA. Influence of Agitation and Aeration on Single Cell Oil Production by *Rhodotorula glutinis* from Glycerol. *J Sustain Bioenergy Syst*. 2019;9:29–43.
33. Pinheiro MJ, Bonturi N, Belouah I, Miranda EA, Lahtvee PJ. Xylose Metabolism and the Effect of Oxidative Stress on Lipid and Carotenoid Production in *Rhodotorula toruloides*: Insights for Future Biorefinery. *Front Bioeng Biotechnol*. 2020;8:1–15.
34. IEA Bioenergy Task42. Sustainable and synergetic processing of biomass into marketable food & feed ingredients, chemicals, materials and energy (fuels, power, heat). *IEA Bioenergy*. 2014;66.
35. Saenge C, Cheirsilp B, Suksaroge TT, Bourtoom T. Potential use of oleaginous red yeast *Rhodotorula glutinis* for the bioconversion of crude glycerol from biodiesel plant to lipids and carotenoids. *Process Biochem. Elsevier Ltd*; 2011;46:210–8.

Chapter 3

Enzymatic hydrolysate of cinnamon waste material as feedstock for the microbial production of carotenoids

3

From Bertacchi S., Pagliari S., Cantù C., Bruni I., Labra M., Branduardi P. (2021) **Enzymatic hydrolysate of cinnamon waste material as feedstock for the microbial production of carotenoids**. Special issue *Industrial Microbiology and Bioprocess Technology* of the *International Journal of Environmental Research and Public Health*. 2021; 18(3):1146.

Introduction

Biobased processes involve the exploitation of different renewable biomasses that possess a faster turnover compared to fossil resources and therefore have a reduced impact on the environment. The forestry, agriculture, and food industries are the main sectors involved in bioeconomy worldwide [1]. Sustainability and circularity are key features in this scenario, with the obtainment of products and energy from biomasses: indeed, the main aim of biorefineries is to exploit such resources as alternatives to fossil ones [2]. Agricultural biomasses are generally related to staple crops (e.g., cereals, tubers, corn, and sugarcane), which can satisfy the issue of circularity but cannot match all the criteria of sustainability. Therefore, there is an increasing need for utilizing side-stream materials that can be valorized in second-generation biorefineries, often by means of the so-called microbial cell factories [3,4]. These side-streams materials can be derived not only from staple crop processing but also from minor crops (for example, spice crops), which are often directly used in the food industry.

One of the main interesting strategies to ennoble minor crops consists in the extraction of bioactive molecules by using chemical or biotechnological processes with low environmental impact [5,6]. In the case of the presence of residual biomasses after processing, these are mostly used to produce energy, which is a low-added value product usually obtained starting from abundant biomasses to compensate costs and market requirements.

Embedded in this approach, there is the aim to transform the entire biomass into a resource, potentially exploiting all the different portions of the plant: depending on composition and volumes, different innovative processes can be developed to obtain high added-value compounds, especially from these minor crops.

Given these considerations, in this work, we focused our attention on cinnamon (*Cinnamomum verum* J.Presl sin. *C. zeylanicum* Blume), a plant of Asian origin that has been exploited as a spice for centuries, with many nutraceutical properties and largely adopted as a food ingredient. At the botanical level, cinnamon bark is widely used by

industries for the extraction of essential oils and secondary metabolites such as polyphenols to be used in food preparation, fragrances, and perfumes [7]. In these sectors, cinnamon can be deployed as an additive for both exploiting its antimicrobial properties and increasing the nutritional values of foods [8–10]. The global demand for cinnamon has been increasing during the last years also due to its possible antioxidant, anti-inflammatory, and antitumoral applications [11]. As a result of industrial processing, large quantities of waste vegetable matrix rich in cellulose and lignin [12] are obtained annually. Nevertheless, this loss has the potential to become a new resource as feedstock for the development of bioprocesses based on so-called microbial cell factories.

Indeed, microorganisms can transform different raw materials of plant (or animal) origin into valuable molecules such as biofuels, chemical platforms, biopolymers, and nutraceuticals [13]. Because of its lignocellulosic nature, the cellulose and hemicellulose content of cinnamon is an unmissable opportunity to be exploited as the main carbon and energy source for microbial growth possibly related to the biosynthesis of interest, given that other residual bioactive compounds are not expressing their antimicrobial properties. In fact, because of the presence of several antimicrobial molecules (*i.e.*, cinnamaldehyde and cinnamic acid [14,15]), cinnamon-derived biomasses have never been considered as feedstock to be deployed in bioprocesses based on microbial cell factories; therefore, their biotechnological potential still needs to be explored.

For these reasons, the aim of this study focuses on the development of a novel bioprocess (*i*) by establishing and optimizing enzymatic hydrolysis of the cinnamon bark (CB) and of the derived residual biomass (polyphenols extraction waste, C-PEW) with varying chemico-physical parameters; (*ii*) by evaluating the criticisms in bioprocesses such as inhibitory molecules for microbial and, in particular, antifungal growth; and (*iii*) by identifying a potential cell factory and a product of interest.

With respect to the process developed, the oleaginous yeast *Rhodospiridium toruloides* was identified as a cell factory. It is naturally able to produce and accumulate carotenoids, valuable compounds with vast markets, with the food and feed sectors being the prominent ones [16–18]. In the present work, the enzymatic hydrolysis of C-PEW was

matched with the ability of *R. toruloides* to produce carotenoids, and a separate hydrolysis and fermentation (SHF) process was run. The obtainment of 2.0 ± 0.23 mg/L of carotenoids starting from 9% (w/v) of initial biomass with a yield of $0.0053 \pm 0.0006\%$ on total sugars provided is a successful proof of concept of the possibility to provide an additional added value to the original biomass beyond the conventional extraction of nutraceuticals from cinnamon. Lastly, considering the promising results obtained on carotenoids production, other potential cell factories were tested for their ability to grow on C-PEW hydrolysate, expanding the industrial implications of our findings.

Results and discussion

Evaluation of total composition of the CB and C-PEW by acid hydrolysis

The provided cinnamon bark (CB) and the related waste material derived from polyphenol extraction (C-PEW) were subjected to total acid hydrolysis to assess their composition in terms of water, insoluble components, acetate, and sugars. Insoluble components and acetate are among the main growth inhibitors commonly linked to residual biomasses, whereas sugars act as the main carbon and energy sources for microbial cell factories. As shown in Table 1, CB and C-PEW showed similar compositions among all the analyzed constituents, consistent with the fact that the components previously extracted (i.e., polyphenols) constitute only a limited amount of the whole biomass. These data are also in accordance with the few previously reported examples from both *C. verum* (formerly *C. zeylanicum*) and *C. cassia* [11,19]. Remarkably, the vast majority of sugars is composed by glucose (more than 65% w/w), being up to 27% w/w of the total biomass.

Total Acid Hydrolysis of Cinnamon		
Component	Cinnamon Bark (CB)	Cinnamon Waste Material (C-PEW)
Water	19.4 ± 1.34%	/
Insoluble fraction	41.1 ± 1.26%	44.5 ± 1.86%
Acetate	1.5 ± 1.03%	2.8 ± 0.13%
Sugars of which	37.3 ± 0.83%	41.5 ± 1.28%
Glucose	25.2 ± 0.53%	27.2 ± 0.99%
Fructose	9.1 ± 0.15%	10.7 ± 0.32%
Arabinose	3.0 ± 0.19%	3.6 ± 0.04%

Table 1: Total hydrolysis of cinnamon. Cinnamon bark and waste extract hydrolysate composition following acid treatment.

Total acid hydrolysis was then no longer used for the experiments as it creates conditions that are detrimental (if not incompatible) with microbial growth and requires processing conditions that have a higher environmental impact if compared with enzymatic hydrolysis. In addition, its use is limited by the release of inhibitory compounds and a very low final pH that would need a neutralization step prior to use as the growth media [20,21].

Enzymatic hydrolysis of CB and C-PEW and composition of the hydrolysates

After assessing the composition of both CB and C-PEW, enzymatic hydrolysis of such biomasses was performed. To the best of our knowledge, there is only a single accessible peer-reviewed example of enzymatic hydrolysis of cinnamon or cinnamon-derived biomasses [19], and it is not related to the development of a microbial-based bioprocess. We first assessed the effect of enzymatic cocktail NS22119 11.9% w/w_{biomass} on CB or C-PEW 9% w/v: the exceeding amount of enzyme was proposed to maximize the hydrolysis of this novel substrate. The pH of both CB and C-PEW were measured between the pre-treatment and the hydrolysis step obtaining pH of 4.5 and 3.5, respectively. Both these values are lower than the optimum of the enzymatic cocktail (pH 6, as described by the manufacturer); therefore, we tested the saccharification at both the initial and the optimal pH.

As shown in Figure 1A, the enzymatic cocktail hydrolyzed CB at both pH during the first hours of saccharification. Prolonging the incubation beyond 6 h up to 24 h did not significantly increase the sugar release (data not shown): these observations are in accordance with previous applications of this enzymatic cocktail on a different residual biomass [18]. As shown in Table 2, in both cases, glucose is the main sugar released, in accordance with the data obtained from the total acid hydrolysis (Table 1). Figure 1A shows that the release of sugars from CB is higher (13%) when performed at pH 6 ($p < 0.05$). Despite a technoeconomic analysis not yet performed, it is reasonable to conclude that this increase would not justify the additional neutralization step, considering that the difference was constituted by about 1 g/L of total sugars.

As shown in Figure 1B, increasing the pH did not affect the enzymatic hydrolysis of C-PEW. In addition, the sugar released from CB and C-PEW, at their original pH, are comparable: this means that polyphenol extraction did not impair the enzymatic activity. In order to reduce the use of neutralizing agents and therefore the operative steps, increasing both the economic and environmental sustainability of the process, the hydrolysis of C-PEW at pH 3.5 was chosen as the preferred one. In these conditions, considering the original sugar content, the yield of sugars from C-PEW was 33% on the total available, with a yield of glucose of 36.7% on the total available (see the Calculation subsection in the Materials and Methods section). In addition, 8.1 ± 2.1 mg/L of ammonia and 4.5 ± 1.35 mg/L of urea, which may act as nitrogen sources, were detected in the C-PEW hydrolysate.

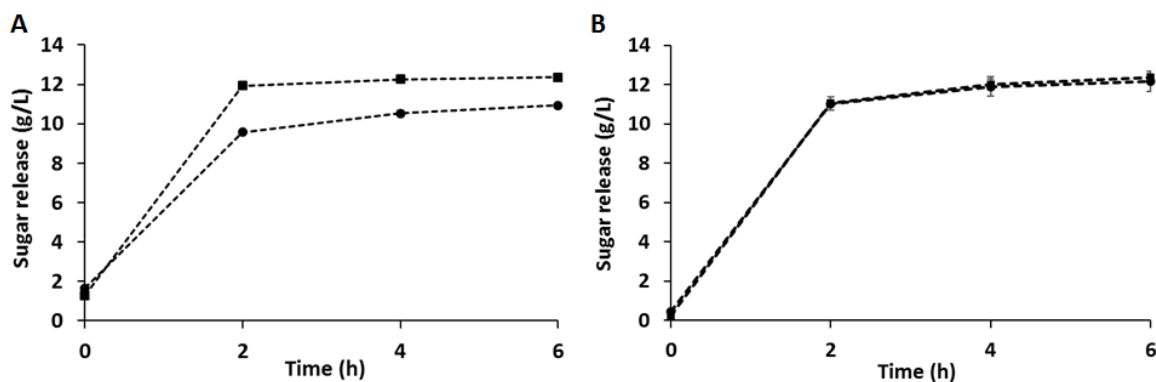


Figure 1. Enzymatic hydrolysis of cinnamon derived biomasses: the effect of the NS22119 cocktail (11.9% w/w_{biomass}) on 9% w/v cinnamon bark (CB) (A) and cinnamon waste material after polyphenol extraction (C-PEW) (B) at pH 6 (squares) or at their original pH after pretreatment (pH 4.5 for panel A, pH 3.5 for panel B) (circles). The values are the means of three independent experiments. In panel A, standard deviations are included, despite being hardly visible as numerically very small.

Enzymatic Hydrolysis of Cinnamon-Derived Biomasses	Cinnamon Bark (CB)				Cinnamon Waste Material (C-PEW)				
	Component Titer (g/L)	pH 4.5	Yield	pH 6	Yield	pH 3.5	Yield	pH 6	Yield
Sucrose	0.9 ± 0.01	-	1.06 ± 0.00		0.8 ± 0.04	-	0.9 ± 0.01	-	
Glucose	7.5 ± 0.09	32.98%	8.2 ± 0.08	36.07%	8.8 ± 0.42	36.7%	9.0 ± 0.12	35.9%	
Fructose	2.6 ± 0.05	30.73%	2.4 ± 0.01	28.44%	1.8 ± 0.05	18.6%	1.8 ± 0.06	18.6%	
Arabinose	-	-	0.8 ± 0.01	25.65%	0.8 ± 0.02	8.4%	0.7 ± 0.06	5.6%	
Total sugars	10.9 ± 0.11	32.4%	12.4 ± 0.10	36.67%	12.2 ± 0.52	33%	12.4 ± 0.23	32.5%	

Table 2: Effect of pH on enzymatic hydrolysis. Titer of sugars released by the NS22119 cocktail (11.9% w/w_{biomass}) on 9% w/v CB or C-PEW at different pH after 6 h of treatment. Values are the means of three independent experiments.

The presence of aromatic compounds typical of cinnamon was evaluated too because of their known antimicrobial activity, concentrated in their essential oils. For example, cinnamaldehyde is known to possess a fungicidal activity [11,22,23]. Therefore, we investigated its presence together with cinnamic acid, p-coumaric acid, and 4-hydroxybenzoic acid in the hydrolysate without adjusting pH, since these molecules may impair microbial growth as well [20], reducing in return the applications of biomasses derived from the cinnamon supply chain. As shown in Table 3, cinnamaldehyde and cinnamic acid were the main aromatic compounds detected in the hydrolysate of CB. When compared with the same biomass hydrolyzed without the pretreatment, a reduction in the titer of most of these molecules can be observed: heat is indeed known to have this kind of effect on such volatile compounds [11,24,25]. The titer of cinnamic acid and cinnamaldehyde detected in the C-PEW hydrolysate was inferior compared to the CB one (Table 3): this observation is consistent with the polyphenol extraction that cinnamon was subjected to.

Taken together, these data confirmed that the C-PEW hydrolysate was comparable (in terms of sugars released) with the hydrolysate of the original edible biomass (CB), with an important reduced amount of growth inhibitors. Therefore, we excluded CB from the

following experiments. Indeed, since C-PEW is a residual biomass not further valorized, it is a suitable feedstock to be considered in a microbial-based bioprocess: its hydrolysis can provide glucose as the main accessible carbon source, even without pH corrections.

Aromatic Compounds in Cinnamon-Derived Hydrolysates	CB Hydrolysate ZZZ(W/O Autoclave Pre-Treatment)	CB Hydrolysate	C-PEW Hydrolysate
Component	Titer (mg/L)	Titer (mg/L)	Titer (mg/L)
4-hydroxybenzoic acid	-	1.8 ± 0.52	4.8 ± 0.47
p-coumaric acid	6.7 ± 0.24	2.5 ± 1.27	0.8 ± 0.16
Cinnamic acid	35.6 ± 0.51	23.2 ± 2.88	6.7 ± 1.29
Cinnamaldehyde	155.5 ± 12.55	73.4 ± 2.82	5.5 ± 0.96

Table 3: Aromatic compounds of cinnamon origin. Evaluation of the presence of aromatic compounds typical of cinnamon in CB or C-PEW hydrolysates. Values are the means of three independent experiments.

Production of carotenoids from C-PEW hydrolysate

In order to valorize C-PEW as feedstock biomass in a bioprocess, we focused our attention on the yeast *Rhodospiridium toruloides*, known for being able to withstand residual biomasses when used as feedstock for both their growth and the production of carotenoids [16,18]. When tested on plates prepared with C-PEW as the growth medium, *R. toruloides* was able to grow and accumulate pigments (see section 3.4); therefore, we tested the production in shake flasks as well. The type of process chosen was a separate hydrolysis and fermentation (SHF) in order to eliminate the water insoluble components (WIS) from the media. Figure 2 shows the growth of *R. toruloides* on sugars released from C-PEW hydrolysis at pH 3.5 and the co-current production of carotenoids. In particular, we could observe that the production reached its maximum after 48 hours in concomitance with the beginning of the stationary phase. These data are in accordance with previous reports that carotenogenic microorganisms like *R. toruloides* produce carotenoids mainly in response to stressful or suboptimal conditions such as the stationary phase itself. In addition, only a limited amount of sugars was consumed: to analyze this phenomenon, we provided to *R. toruloides* the synthetic medium supplemented with the same amount of sugars present in C-PEW hydrolysate, setting the pH value at 3.5 or 5.5 (optimal for this yeast). As shown in Figure S1, *R. toruloides* was

able to completely consume the sugars and to reach a higher CDW than in C-PEW hydrolysate regardless of the initial pH. The reduced growth and sugar consumption observed in the C-PEW hydrolysate could be ascribed to the low initial amount of nitrogen source, which resulted in depletion after 48 hours (Figure S2), in correspondence to the stationary phase of growth. As the inhibitory compounds typical of cinnamon origin were not detected after 24 h, nitrogen depletion should be considered the main bottleneck for *R. toruloides* growth in C-PEW hydrolysate.

In SHF conditions with 9% (w/v) C-PEW hydrolysate, *R. toruloides* was able to accumulate up to 2.0 ± 0.23 mg/L of carotenoids after 48 h of growth, with a productivity of 0.04 ± 0.005 g/L/h and yields of $0.09 \pm 0.007\%$ on CDW, of $0.11 \pm 0.013\%$ on consumed sugars, and of $0.005 \pm 0.0006\%$ on the total sugars provided. When considering high added-value products, yields are not crucial but important to describe the process itself and to understand how to further improve it. In fact, although this titer of carotenoids is comparable with other recently reported bioprocesses based on the combination of *R. toruloides* and residual biomasses, like *Camelina sativa* meal, carob pulp syrup, sugarcane bagasse, and molasses [18,26,27], the possibility to increase glucose consumption might ameliorate the result obtained here.

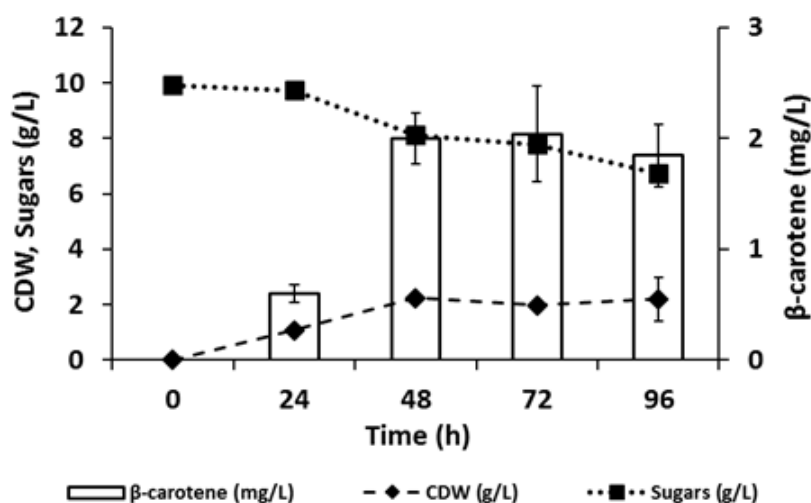


Figure 2: Production of carotenoids from C-PEW hydrolysate by *R. toruloides*. Cellular dry weight (CDW) in dashed line, total sugars in dotted line, β -carotene in white bars. Values are the means of three independent experiments.

This work focused on the valorization of cinnamon by-products by their exploitation as a substrate for microorganisms. Industries in this sector must eliminate large amounts of residues each year from the processing of cinnamon extraction of polyphenols and other residual biomasses derived from biomolecule extraction. Although this waste disposal cost may not be excessively high, it is important to consider it in the scenario of the reconversion to a circular economic model fostered by the European Union, promoting increasing attention towards the exploitation of industrial products following a biorefinery model, which aims to obtain more products starting from a single biomass [28–30]. This is also in line with the ambitious aims and goals of the Green Deal [31], where every activity can contribute to reaching the declared “carbon neutral” status. Additionally, other microbial cell factories might be deployed in bioprocesses involved in the conversion of C-PEW to compounds of industrial relevance, such as, as a matter of example, lipids and shikimate from species such as *Cryptococcus curvatus* and *Scheffersomyces stipitis*.

Testing the growth of other fungal cell factories on C-PEW hydrolysate

In order to widen the possible outcomes of the exploitation of C-PEW, we tested the ability of other yeast cell factories to grow on such biomass. Testing of possible candidates was needed since, to the best of our knowledge, there were no previous examples of cinnamon use for such purposes. In addition, cinnamon is known to possess a potent antimicrobial activity [11]; therefore, putative cell factories must be tested and selected for their ability to grow on this new medium. In fact, cinnamon antimicrobial activity has been studied with regard to several pathogenic microorganisms: in particular, the minimal inhibitory concentrations of cinnamaldehyde were 125 ± 25 g/L for *Candida albicans*, 88 ± 13 g/L for *Aspergillus niger*, 300 ± 0 g/L for *Escherichia coli*, and 250 ± 50 g/L for *Staphylococcus aureus* [32]. Nevertheless, considering the titers of antimicrobial compounds typical of cinnamon found in C-PEW (Table 2), their amount may be considered neglectable or anyhow bearable by different fungal cell factories.

We focused our attention on the fungal species enlisted in Figure 3 (further details in the Materials and Methods section): all of them are classified as yeasts except for *Aureobasidium pullulans*, that is considered a yeast-like fungus [33]. The choice to test fungal clades that involve yeasts is related to the fact that those microorganisms are reliable and robust cell factories, able to convert residual biomasses into valuable compounds or to be used as chassis for further genetic modification, expanding the portfolio of putative products [34,35]. Although bacteria could be considered relevant microbial cell factories too, the higher general tolerance of yeasts towards low pH, likewise the biomass of interest, led them to be excluded in this study. As shown in Figure 3, all the tested strains were able to grow on agar plates containing C-PEW at pH 3.5, with a qualitative slower growth by *Komagataella phaffii* compared to the other tested species. These observations clearly highlight that C-PEW can be used as feedstock by a variety of fungal cell factories that possess peculiar characteristics of industrial interest. *A. pullulans* naturally produces antimicrobial compounds, industrial enzymes, and polymers such as pullulans and poly(β -L-malic acid) [33]. *K. marxianus*, *K. pastoris*, and *S. cerevisiae* are known to be chassis for recombinant molecules with several available tools for this purpose [36–38], therefore expanding the potential uses of C-PEW. *Z. bailii* and *Z. parabailii* were selected due to their ability to grow at low pH and to withstand weak organic acid: the availability of technologies for these species is increasing their applicability [39,40]. *S. stipitis* is known for producing shikimate, which can act as building blocks for high-value aromatics [41]. *C. curvatus* and *Rhodotorula glutinis* (together with *R. toruloides*) are oleaginous yeasts able to accumulate from 20% w/w lipids of their dry cell mass [42,43]. Therefore, the obtained single cell oils (SCOs) can be exploited for several applications, from biodiesel to waxes, as an alternative to both petrochemical and vegetable oil industries [44,45]. In addition, *R. glutinis* and *R. toruloides* are natural producers of carotenoids [17,46], a group of molecules widely used in the feed, food, dietary supplements, and dye industries with high market demand [47] that perfectly matches the bioeconomic logic of cascading [48]. Both these carotenogenic yeasts were able to produce carotenoids when fed with cinnamon waste material hydrolysate since

their pinkish color was clearly visible (Figure 3). Due to the positive test of all these species, we can infer that they would be able to reproduce the same features in batch mode as well, providing a great added value to the residual biomass obtained from cinnamon processing.

Taken together, the data obtained showed that a broad range of fungal species are phenotypically able to grow on the hydrolysate of cinnamon waste material and that therefore they can be considered a starting material for bioprocesses to obtain molecules of industrial relevance, from carotenoids to recombinant proteins.

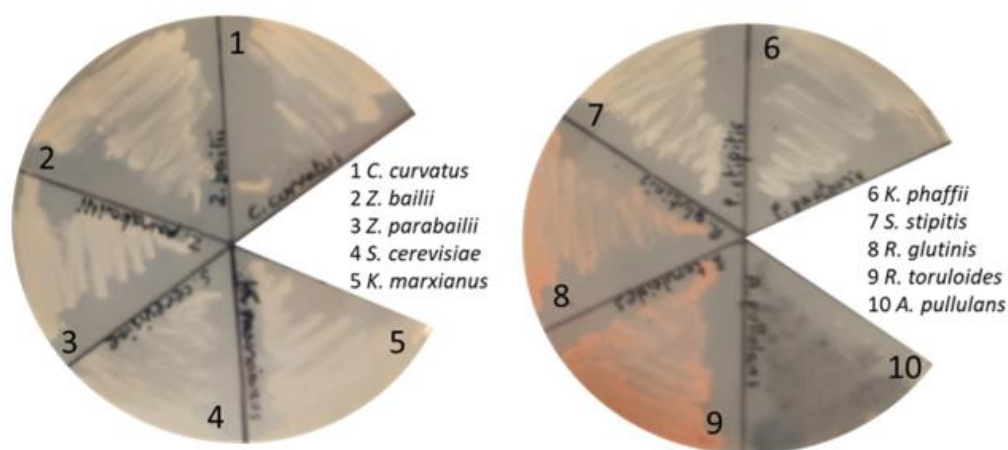


Figure 3. Testing of different fungal cell factories on agar plates containing only the enzymatic hydrolysate of 9% w/v C-PEW (pH 3.5) as a nutrient source: the picture was taken after 72 h of growth at 30 °C.

Conclusions

The agri-food sector is leading to the accumulation of relevant amounts of residual biomasses, which are mainly burned for energy, used as animal feed, or disposed of as wastes. Nevertheless, these biomasses often contain energy-rich molecules that can still be exploited to obtain high-value products. Furthermore, the valorization of these biomasses fosters the transition from linear economies to circular ones, where the life cycle of natural resources is extended thanks to their further processing to extract additional values. In this work, we focused our attention on the waste material of the cinnamon supply chain, obtained from the polyphenol extraction (called C-PEW), which is

not used for any purpose at the moment. Here, for the first time, a cinnamon-derived biomass was hydrolyzed using a commercial enzymatic cocktail, with a 33% yield of sugars on the total available, demonstrating its potentiality as feedstock for a bioprocess based on microbial cell factories.

We focused our attention on the yeast *Rhodospiridium toruloides*, naturally able to produce carotenoids and high-value molecules used in the food, the feed, the dye, and the cosmetic sectors. Since most of the carotenoid market is satisfied by chemical synthesis, there is an increasing demand for molecules of renewable origin. Here, in a separated hydrolysis and fermentation (SHF) process, *R. toruloides* was able to consume sugars from C-PEW and to accumulate up to 2.0 ± 0.23 mg/L of carotenoids. Although the obtained titer was comparable with those of other processes based on residual biomasses valorized by *R. toruloides*, the low sugar consumption in these conditions was a limiting element. An additional nitrogen source, preferentially of residual origin, might be considered to overcome this shortcoming.

In this work, it is shown for the first time the possibility to develop bioprocesses based on cinnamon-derived biomasses to provide additional production streams, such as carotenoids, to be applied as additive in sectors in which industries dealing with this residual biomass are already involved, thus increasing the value thereof. The successful test of several microorganisms of industrial relevance for their ability to grow on C-PEW hydrolysate (withstanding its low pH and anti-microbial compounds) widens the possible exploitations of this residual biomass. In addition, several new synthetic biology tools are becoming available for non-Saccharomyces fungal species, thus expanding the ability of these microbes to be tailored for industrial processes. In this case, a desirable implementation should be the engineering of *R. toruloides* to withstand antifungal molecules and to produce fine chemicals of industrial relevance. This in turn would increase the appeal of cinnamon derived biomasses, although it is a currently underrated feedstock for microbial cell factories.

Overall, this work can pave the way for further development of bioprocesses based on the exploitation of a side-stream biomass derived from the cinnamon industry, that

usually would be disposed of as waste material, in order to produce not only high-value added products such as carotenoids in *R. toruloides* but also compounds from other yeast cell factories in the scenario of the cascading principles of biorefineries.

Materials and methods

Plant biomass: feedstock preparation and composition

Epo S.r.l., Milano, Italy, provided cinnamon bark (*Cinnamomum verum* J.Presl, sin. *C. zeylanicum* Blume) grown in Madagascar. The cinnamon bark (CB) was stored at 25 °C away from heat and light sources until its use. Before extraction, the cinnamon bark was pulverized with an electric laboratory grinder. The cinnamon bark underwent an extraction process with water at 60 °C as described by [49] to obtain polyphenols. This extraction protocol was comparable with the one used by Epo S.r.l. in order to simulate their industrial process and to obtain realistic waste material at the laboratory scale. At the end of the process, the cinnamon waste material after polyphenol extraction (C-PEW) was recovered, dried out to eliminate the water derived from the extraction, and stored at -20 °C until its use. To measure the water percentage of CB, 0.9 g of biomass was dried out at 160 °C for 3 h and then weighed again to calculate the amount of evaporated water. The biomass was heat-incubated for additional 3 h to assess a lack of further changes in weight compared to the initial treatment. To analyze the chemical composition of CB and C-PEW, the biomass was processed following the protocol for the analysis of structural carbohydrates and lignin in the biomass of the National Renewable Energy Laboratory (NREL, <https://www.nrel.gov/docs/gen/fy13/42618.pdf>) with modifications as follows: 300 mg of biomass were diluted in 3 mL H₂SO₄ 72% (v/v), and then incubated at 30 °C for 1 h, stirring thoroughly every 10 min. The solution was diluted to 4% (v/v) by adding 84 mL of distilled water, mixed by inversion and autoclaved (121 °C, 1 h). The hydrolysis mixture was vacuum filtered through one of the previously weighted filtering crucibles, and the insoluble components were measured gravimetrically on the filter paper. The filtered liquid was neutralized with NaOH to pH 5–6, and then, the

samples were analyzed by High-Performance Liquid Chromatography (HPLC) (as described below). Three independent experimental replicates were performed.

Pretreatment and Enzymatic hydrolysis of cinnamon bark and waste material

Enzymatic hydrolysis of the cinnamon bark powder and waste material was performed using the enzyme cocktail NS22119, kindly provided by Novozymes (Novozymes A/S, Copenhagen, Denmark). As described by the manufacturer, NS22119 contains a wide range of carbohydrases, including arabinase, β -glucanase, cellulase, hemicellulase, pectinase, and xylanase from *Aspergillus aculeatus*; 9% (w/v) of cinnamon bark and waste material were steeped in water with a final volume of 30 mL and then autoclaved (121 °C, 1 h) in order to both sterilize and pretreat the biomass. Although mild physical pretreatment by autoclaving is less effective than chemical pretreatments, we decided not to involve their use because the overall processing, starting from the phenolic extraction that occurs upstream (and generate this waste), is intended to minimize environmental impacts.

Afterwards, the enzymes (11.9% w/w_{biomass}) were added directly in the solution and incubated at pH 5.5 and at 50 °C in a water bath under agitation (105 rpm). One milliliter of the sample was collected every 2, 4, and 6 h from the start, and the sugar content was analyzed by HPLC (see below). A high dosage provides an indication of the maximum enzymatically accessible sugar content, although low enzyme dosages provide a target for commercially feasible hydrolysis for further developments. Three independent experiments were performed.

Microbial strains and media

S. cerevisiae CEN.PK 102-5B was obtained from Peter Kötter (Institut für Mikrobiologie der Johann Wolfgang Goethe Universität, Frankfurt, Germany). The other strains used were *Komagataella phaffii* X-33 (formerly *Pichia pastoris*, ThermoFisher Scientific, Massachusetts, USA); *Scheffersomyces stipitis* CBS 6054 (CBS Fungal Biodiversity Centre, The Netherlands); *Zygosaccharomyces bailii* ATCC 8766 and *Zygosaccharomyces parabailii*

ATCC 60483 (ATCC Virginia, USA); *Rhodospiridium toruloides* DSM 4444, *Rhodotorula glutinis* DSM 10134, *Cryptococcus curvatus* DSM 70022, and *Aureobasidium pullulans* DSM P268 from DSMZ (German Collection of Microorganisms and Cell Cultures, GmbH); and *Kluyveromyces marxianus* NBRC1777 (Biological Resource Center, NITE, NBRC, Japan). All the strains were stored in cryotubes at $-80\text{ }^{\circ}\text{C}$ in 20% glycerol (v/v) and were pre-inoculated at $30\text{ }^{\circ}\text{C}$ on rich medium plates: 1% yeast extract (Biolife Italia S.r.l., Milan, Italy), 2% peptone, and 2% glucose (Sigma-Aldrich Co., St Louis, MO, USA). The enzymatic hydrolysate from C-PEW was used for formulating the media for the plates in order to test the ability of the aforementioned strains to grow in such substrates. This feature was qualitatively assessed after 72 h of growth at $30\text{ }^{\circ}\text{C}$.

***R. toruloides* cultivation and carotenoids production**

R. toruloides was pre-inoculated in a synthetic medium constituting (per liter) 1 g of the yeast extract, 1.31 g of $(\text{NH}_4)_2\text{SO}_4$, 0.95 g of Na_2HPO_4 , 2.7 g of KH_2PO_4 , and 0.2 g of $\text{Mg}_2\text{SO}_4 \cdot 7\text{H}_2\text{O}$ and was supplemented with 15 g/L of glycerol as the main carbon source and a 100 \times trace mineral stock solution as follows (per liter): 4 g of $\text{CaCl}_2 \cdot 2\text{H}_2\text{O}$, 0.55 g of $\text{FeSO}_4 \cdot 7\text{H}_2\text{O}$, 0.52 g of citric acid, 0.10 g of $\text{ZnSO}_4 \cdot 7\text{H}_2\text{O}$, 0.076 g of $\text{MnSO}_4 \cdot \text{H}_2\text{O}$, and 100 μL of 18 M H_2SO_4 . The yeast extract was purchased from Biolife Italia S.r.l., Milan, Italy. All other reagents were purchased from Sigma-Aldrich Co., St Louis, MO, USA. Pre-inoculum was run in that medium until stationary phase; then, cells were inoculated at an optical density (OD, 600 nm) of 0.2 in shake flasks at $30\text{ }^{\circ}\text{C}$ and 160 rpm with C-PEW hydrolysate. After enzymatic hydrolysis, C-PEW hydrolysate was centrifuged at 4000 rpm for 10 min to separate the water insoluble components: the liquid medium obtained was used for the growth and the production of carotenoids by *R. toruloides*. Three independent experiments were performed.

Analytical methods

HPLC analyses were performed to quantify the amount of glucose, sucrose, arabinose, fructose, and acetic acid. One milliliter of the liquid fraction was collected from each

enzymatic hydrolysis, centrifuged twice (7000 rpm, 7 min, and 4 °C), and then analyzed at the HPLC using a Rezex ROA-Organic Acid (Phenomenex). The eluent was 0.01 M H₂SO₄ pumped at 0.5 mL min⁻¹, and column temperature was 35 °C. Separated components were detected by a refractive-index detector, and peaks were identified by comparison with known standards (Sigma-Aldrich, St Louis, MO, USA). HPLC analyses were performed to quantify also the amount of cinnamic acid, cinnamaldehyde, 4-hydroxybenzoic acid, and p-coumaric acid using the analysis protocol reported by [50]. The extracts were previously filtered with a 0.22 μm polytetrafluoroethylene (PTFE) filter. The column used for this chromatographic stroke was an Agilent Zorbax SB-C18 (4.6 × 250 mm, 5 μm) composed of carbon chains of 18 carbon atoms and set to a temperature of 30 °C. Two mobile phases were used: phase A (aqueous solution of phosphoric acid H₃PO₄ at pH 3) and phase B (acetonitrile CH₃CN, 99.98% pure, HPLC grade). The volume of samples injected for analysis was 50 μL. The biomolecules were monitored by setting the diode array detector (DAD) detection signal to 280 nm.

The cellular dry weight (CDW) was measured gravimetrically after drying 1 mL of cell culture (Concentrator 5301, Eppendorf AG, Germany). The titer of carotenoids extracted in acetone from *R. toruloides*, as reported in [18], was determined spectrophotometrically (UV1800; Shimadzu, Kyoto, Japan) based on the maximum absorption peak for β-carotene (455 nm). A calibration curve with standard concentration of β-carotene was used for quantification.

A Urea/Ammonia Assay Kit (K-URAMR, Megazyme International Limited, Bray, Ireland) was used to determine the amount of ammonia and urea in the C-PEW hydrolysate.

The pH was measured with indicator strips in order to assess if the conditions were suitable for the enzymatic hydrolysis and to foresee possible detrimental effects on microbial growth of the final media.

Calculations

Sugar recovery (S_r) was calculated as a percentage of the sugar yield by enzymatic hydrolysis (Y_{EH}) when compared with the yield obtained from the total acid hydrolysis of the biomass (Y_{AH}).

$$S_r = Y_{EH}/Y_{AH} \times 100$$

For statistical analysis, heteroscedastic two-tailed t test was applied.

Supplementary figures

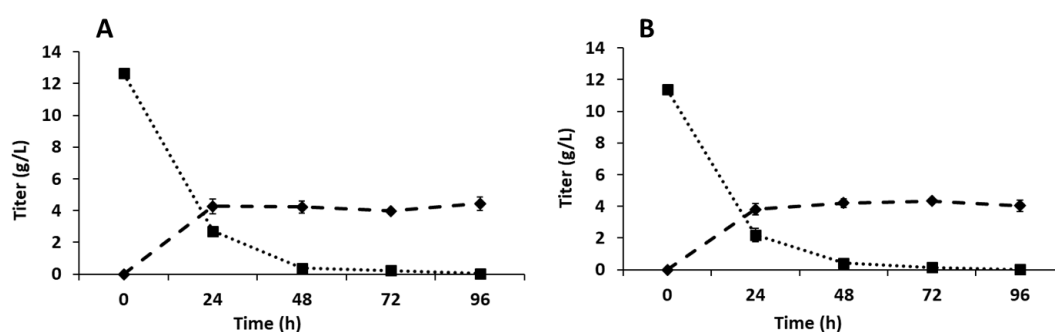


Figure S1. Growth of *R. toruloides* on synthetic media at pH 3.5 (panel A) and pH 5.5 (panel B). Cellular dry weight (CDW) in dashed line, total sugars in dotted line. Values are the means of three independent experiments.

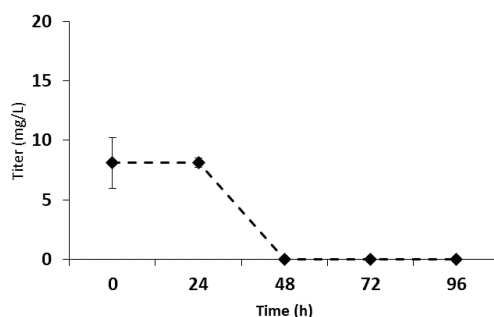


Figure S2. Ammonium titer during *R. toruloides* growth on C-PEW hydrolysate. Values are the means of three independent experiments.

References

1. Bracco S, Calicioglu O, Juan MGS, Flammini A. Assessing the contribution of bioeconomy to the total economy: A review of national frameworks. *Sustain.* 2018;10.

2. IEA Bioenergy Task42. Sustainable and synergetic processing of biomass into marketable food & feed ingredients, chemicals, materials and energy (fuels, power, heat). IEA Bioenergy. 2014;66.
3. Dahiya S, Kumar AN, Shanthi Sravan J, Chatterjee S, Sarkar O, Mohan SV. Food waste biorefinery: Sustainable strategy for circular bioeconomy. *Bioresour Technol*. Elsevier; 2018;248:2–12.
4. Branduardi P. Closing the loop: the power of microbial biotransformations from traditional bioprocesses to biorefineries, and beyond. *Microb Biotechnol*. 2020;0:1–6.
5. Magoni C, Bruni I, Guzzetti L, Dell'Agli M, Sangiovanni E, Piazza S, et al. Valorizing coffee pulp by-products as anti-inflammatory ingredient of food supplements acting on IL-8 release. *Food Res Int*. Elsevier; 2018;112:129–35.
6. Cavini S, Guzzetti L, Givoia F, Regonesi ME, Di Gennaro P, Magoni C, et al. Artichoke (*Cynara cardunculus* var. *scolymus* L.) by-products as a source of inulin: how to valorise an agricultural supply chain extracting an added-value compound. *Nat Prod Res*. Taylor & Francis; 2020;0:1–5.
7. Goel B, Mishra S. Medicinal and Nutritional Perspective of Cinnamon: A Mini-review. *European J Med Plants*. 2020;
8. Muhammad DRA, Tuenter E, Patria GD, Foubert K, Pieters L, Dewettinck K. Phytochemical composition and antioxidant activity of *Cinnamomum burmannii* Blume extracts and their potential application in white chocolate. *Food Chem*. Elsevier; 2021;340:127983.
9. Clemente I, Aznar M, Silva F, Nerín C. Antimicrobial properties and mode of action of mustard and cinnamon essential oils and their combination against foodborne bacteria. *Innov Food Sci Emerg Technol*. Elsevier Ltd; 2016;36:26–33.
10. Nabavi SF, Di Lorenzo A, Izadi M, Sobarzo-Sánchez E, Daglia M, Nabavi SM. Antibacterial effects of cinnamon: From farm to food, cosmetic and pharmaceutical industries. *Nutrients*. 2015;7:7729–48.
11. Ribeiro-Santos R, Andrade M, Madella D, Martinazzo AP, de Aquino Garcia Moura L, de Melo NR, et al. Revisiting an ancient spice with medicinal purposes: Cinnamon. *Trends Food Sci Technol*. 2017;62:154–69.
12. Mehta MJ, Kumar A. Green and Efficient Processing of *Cinnamomum cassia* Bark by Using Ionic Liquids: Extraction of Essential Oil and Construction of UV-Resistant Composite Films from Residual Biomass. *Chem - An Asian J*. 2017;
13. Lee SY, Kim HU, Chae TU, Cho JS, Kim JW, Shin JH, et al. A comprehensive metabolic map for production of bio-based chemicals. *Nat Catal*. Springer US; 2019;2:18–33.

14. Hameed IH, Altameme HJ, Mohammed GJ. Evaluation of antifungal and antibacterial activity and analysis of bioactive phytochemical compounds of *Cinnamomum zeylanicum* (Cinnamon bark) using gas chromatography-mass spectrometry. *Orient J Chem.* 2016;
15. OuYang Q, Duan X, Li L, Tao N. Cinnamaldehyde exerts its antifungal activity by disrupting the cell wall integrity of *Geotrichum citri-aurantii*. *Front Microbiol.* 2019;
16. Wen Z, Zhang S, Odoh CK, Jin M, Zhao ZK. *Rhodospiridium toruloides* - A potential red yeast chassis for lipids and beyond. *FEMS Yeast Res.* Oxford University Press; 2020;20:1–12.
17. Park Y-KK, Nicaud J-MM, Ledesma-Amaro R. The Engineering Potential of *Rhodospiridium toruloides* as a Workhorse for Biotechnological Applications. *Trends Biotechnol.* 2018
18. Bertacchi S, Bettiga M, Porro D, Branduardi P. *Camelina sativa* meal hydrolysate as sustainable biomass for the production of carotenoids by *Rhodospiridium toruloides*. *Biotechnol Biofuels.* BioMed Central; 2020;13:1–10.
19. Tang P, Hao E, Deng J, Hou X, Zhang Z, Xie J. Boost anti-oxidant activity of yogurt with extract and hydrolysate of cinnamon residues. *Chinese Herb Med.* Elsevier BV; 2019;11:417–22.
20. Jönsson LJ, Martín C. Pretreatment of lignocellulose: Formation of inhibitory by-products and strategies for minimizing their effects. *Bioresour. Technol.* 2016.
21. Wahlström RM, Suurnäkki A. Enzymatic hydrolysis of lignocellulosic polysaccharides in the presence of ionic liquids. *Green Chem.* Royal Society of Chemistry; 2015;17:694–714.
22. Ainane A, Elkouali M. Cosmetic bio-product based on cinnamon essential oil "*Cinnamomum verum*" for the treatment of mycoses: preparation, chemical analysis and antimicrobial activity. *MOJ Toxicol.* 2019;6–10.
23. Shreaz S, Wani WA, Behbehani JM, Raja V, Irshad M, Karched M, et al. Cinnamaldehyde and its derivatives, a novel class of antifungal agents. *Fitoterapia.* Elsevier B.V.; 2016;112:116–31.
24. Benkeblia N. Free-radical scavenging capacity and antioxidant properties of some selected Onions (*Allium cepa* L.) and garlic (*Allium sativum* L.) extracts. *Brazilian Arch Biol Technol.* 2005;48:753–9.
25. Settharaksa S, Jongjareonrak A, Hmadhlu P, Chansuwan W, Siripongvutikorn S. Flavonoid, phenolic contents and antioxidant properties of thai hot curry paste extract and its ingredients as affected of pH, solvent types and high temperature. *Int Food Res J.* 2012;19:1581–7.
26. Bonturi N, Crucello A, Viana AJC, Miranda EA. Microbial oil production in sugarcane

- bagasse hemicellulosic hydrolysate without nutrient supplementation by a *Rhodospordium toruloides* adapted strain. *Process Biochem.* Elsevier; 2017;57:16–25.
27. Freitas C, Parreira TM, Roseiro J, Reis A, Da Silva TL. Selecting low-cost carbon sources for carotenoid and lipid production by the pink yeast *Rhodospordium toruloides* NCYC 921 using flow cytometry. *Bioresour Technol.* 2014;
28. Zabaniotou A. Redesigning a bioenergy sector in EU in the transition to circular waste-based Bioeconomy-A multidisciplinary review. *J Clean Prod.* 2018;
29. European Commission. Financing the green transition: The European Green Deal Investment Plan and Just Transition Mechanism. 2020;3.
30. United Nations Goal 9. Build Resilient Infrastructure, Promote Inclusive and Sustainable Industrialization, and Foster Innovation. *Sustain. Dev. Goals.* 2020. p. 1–6.
31. A European Green Deal | European Commission (accessed on 10 December 2020). Available from: https://ec.europa.eu/info/strategy/priorities-2019-2024/european-green-deal_en
32. Ooi LSM, Li Y, Kam SL, Wang H, Wong EYL, Ooi VEC. Antimicrobial activities of Cinnamon oil and cinnamaldehyde from the Chinese medicinal herb *Cinnamomum cassia* Blume. *Am J Chin Med.* 2006;34:511–22.
33. Prasongsuk S, Lotrakul P, Ali I, Bankeeree W, Punnapayak H. The current status of *Aureobasidium pullulans* in biotechnology. *Folia Microbiol.* 2018. p. 129–40.
34. Nandy SK, Srivastava RK. A review on sustainable yeast biotechnological processes and applications. *Microbiol Res.* Elsevier; 2018;207:83–90.
35. Xu X, Liu Y, Du G, Ledesma-Amaro R, Liu L. Microbial Chassis Development for Natural Product Biosynthesis. *Trends Biotechnol.* 2020;1–18.
36. Fischer JE, Glieder A. Current advances in engineering tools for *Pichia pastoris*. *Curr Opin Biotechnol.* 2019;59:175–81.
37. Li M, Borodina I. Application of synthetic biology for production of chemicals in yeast *Saccharomyces cerevisiae*. *FEMS Yeast Res.* 2015.
38. Varela JA, Gethins L, Stanton C, Ross P, Morrissey JP. Applications of *Kluyveromyces marxianus* in Biotechnology. *Yeast Divers Hum Welf.* 2017;1–486.
39. Kuanyshev N, Adamo GM, Porro D, Branduardi P. The spoilage yeast *Zygosaccharomyces bailii* : Foe or friend? *Yeast.* John Wiley and Sons Ltd; 2017;34:359–70.
40. Suh SO, Gujjari P, Beres C, Beck B, Zhou J. Proposal of *Zygosaccharomyces parabailii*

sp. nov. and *Zygosaccharomyces pseudobailii* sp. nov., novel species closely related to *Zygosaccharomyces bailii*. *Int J Syst Evol Microbiol.* 2013;63:1922–9.

41. Gao M, Cao M, Suástegui M, Walker J, Quiroz NR, Wu Y, et al. Innovating a nonconventional yeast platform for producing shikimate as the building block of high-value aromatics. *ACS Synth Biol.* 2017;6:29–38.

42. Carsanba E, Papanikolaou S, Erten H. Production of oils and fats by oleaginous microorganisms with an emphasis given to the potential of the nonconventional yeast *Yarrowia lipolytica*. *Crit. Rev. Biotechnol.* 2018. p. 1230–43.

43. Sreeharsha RV, Mohan SV. Obscure yet Promising Oleaginous Yeasts for Fuel and Chemical Production. *Trends Biotechnol.* 2020;1–15.

44. Donot F, Fontana A, Baccou JC, Strub C, Schorr-Galindo S. Single cell oils (SCOs) from oleaginous yeasts and moulds: Production and genetics. 2014

45. Uemura H. Synthesis and production of unsaturated and polyunsaturated fatty acids in yeast: Current state and perspectives. *Appl. Microbiol. Biotechnol.* 2012. p. 1–12.

46. Frengova GI, Beshkova DM. Carotenoids from *Rhodotorula* and *Phaffia*: Yeasts of biotechnological importance. *J. Ind. Microbiol. Biotechnol.* 2009.

47. Nagarajan J, Ramanan RN, Raghunandan ME, Galanakis CM, Krishnamurthy NP. Carotenoids. *Nutraceutical Funct. Food Components Eff. Innov. Process. Tech.* Elsevier Inc.; 2017.

48. IEA Bioenergy Task40. Cascading of woody biomass: definitions, policies and effects on international trade. *IEA Bioenergy.* 2016;71.

49. Cheng DM, Kuhn P, Poulev A, Rojo LE, Lila MA, Raskin I. In vivo and in vitro antidiabetic effects of aqueous cinnamon extract and cinnamon polyphenol-enhanced food matrix. *Food Chem.* 2012;

50. Safafar H, Wagenen J Van, Møller P, Jacobsen C. Carotenoids, phenolic compounds and tocopherols contribute to the antioxidative properties of some microalgae species grown on industrial wastewater. *Mar Drugs.* 2015;

Chapter 4

Assessment of folates forms produced by wild type and engineered *Saccharomyces* *cerevisiae* yeast cells

4

From Mastella L.*, Bertacchi S.*, Berterame NM.*, Bertolesi T, Branduardi P. (2021) **Assessment of folates forms produced by wild type and *engineered Saccharomyces cerevisiae* yeast cells.** Submitted to FEMS Yeast Research. *these authors contributed equally to the work.

Introduction

Folates are a group of water-soluble compounds part of the B vitamin family (B₉). They share a common structure consisting in a pteridine ring linked to a molecule of para-amino-benzoic acid (pABA) by a methylene bridge, and a glutamic acid molecule. The vitamers of folate differ for the state of oxidation (folic acid, di-hydrofolate, tetrahydrofolate), for carbon substitutions (*i.e.* methyl, formyl, methylene, or methenyl) and for the presence of a diverse number of glutamate units linked together in a poly-glutamate tail (Figure 1). Folates act as donor of C1 units, thus playing an essential role in a wide range of biochemical pathways such as: DNA synthesis and methylation [1]; protein synthesis [2]; homocysteine metabolism [3]; red blood cells formation [4]; formation of embryonic tissues [5].

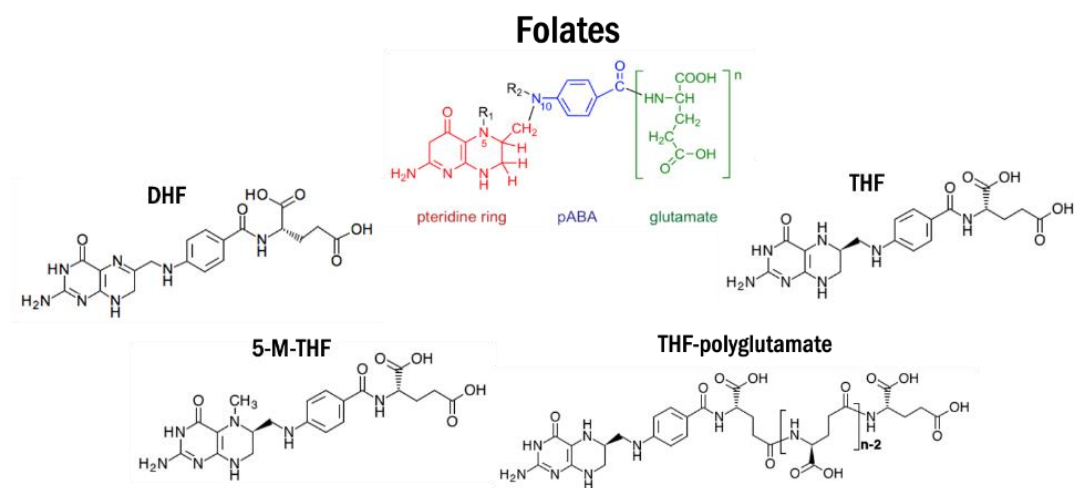


Figure 1: Schematic representation of the general structure of a folate molecule, in which the three fundamental parts are distinct with different colours. The pteridine ring (red) deriving from GTP, the pABA (blue) produced from chorismate, and the glutamate (green). The vitamers of folate (black) differ for the state of oxidation (DHF, THF), for carbon substitutions (5-M-THF, Folinic Acid, 5-10-MTHF) and for the presence of several glutamates linked together in a poly-glutamate tail (THF-poly-glutamate), as represented by the other molecules in the figure.

Due to the central role of folate in human primary metabolism, its deficiency leads to several detrimental physiological disorders including: anemia [6]; cardiovascular diseases;

neural tube defects (TNDs) and colon cancer [3,7]. As vitamin B₉ is biosynthesized *de novo* only by plants and some microorganisms, it is an essential component for animal nutrition, obtainable either by diet or food supplementation. Folates are present in a variety of foods: green leafy vegetables, dark green vegetables (such as broccoli and Brussels sprouts), orange juice, beans, and other legumes [8]. In addition, fruits, dairy products, poultry and eggs are also important sources of folates [9]. As prescribed by the National Institutes of Health (NIH), in the USA the recommended dietary allowance (RDA) for folates in adults is 400 µg dietary folate equivalents (DFE), whereas the folate RDA in the European Union is 240 µg DFE [10]; a higher intake (600–1000 µg DFE) is advised for pregnant women [6]. As reviewed by [11] folate deficiency is a global health problem, therefore the two main strategies developed to increase folate content in foods are biofortification and food supplementation. Several examples of folate biofortification in plants (*e.g.* rice, tomato, wheat and beans) are reported in literature [12], as well as in dairy products and fermented food by using folate-producing lactic acid bacteria (LABs) [13]. However, there are some concerns regarding the use of bio-fortified food, as folate stability during food processing and preservation remains problematic; by contrast, folates food supplementation seems a good alternative overcome this limitation [14]. Unfortunately, all the vitamin B₉ commercially available is chemically synthesized in the form of folic acid, which seems to have not the desired biological effects, as it can mask symptoms of vitamin B₁₂ deficiency which is linked to an increase of prostate cancer risk, whereas natural folates do not display these collateral effects [14]. For these reasons, the production of natural folates by microbial fermentation appears desirable. Moreover, the current improvements on the development of microbial hosts able to exploit residual biomasses would make the overall process more sustainable compared to the chemical synthesis.

We focused our attention on *Saccharomyces cerevisiae*, which, in addition of being a microbial cell factory widely used in biotechnological processes, is also a natural producer of different folate vitamers [15], and a microorganism certified as GRAS. Yeast's folate biosynthetic pathway is well characterized: it consists in the biosynthesis of the pteridine

ring starting from GTP, common precursor of the riboflavin biosynthetic pathway, its condensation with para-amino benzoic acid (pABA), deriving from chorismate, and the addition of glutamate residue(s) (Figure 2).

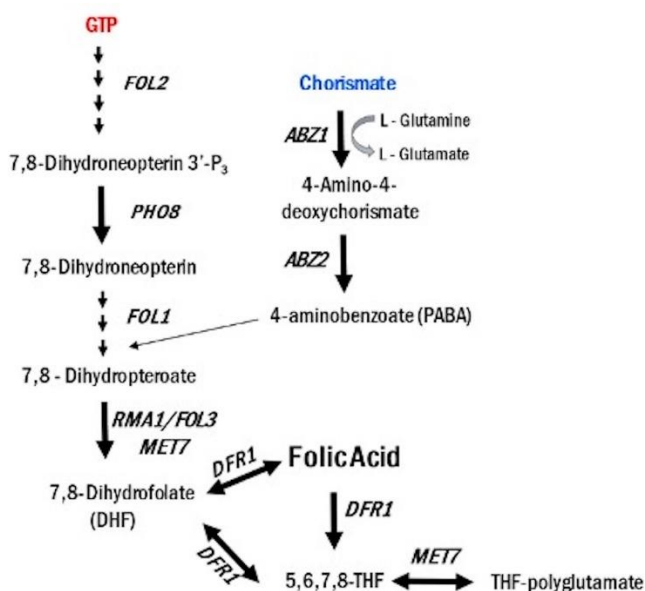


Figure 2: Schematic representation of the metabolic pathways involved in folate biosynthesis. *FOL2*: GTP cyclohydrolase I; *ABZ1*: 4-amino-4-deoxychorismate synthase; *ABZ2*: 4-amino-4-deoxychorismate lyase; *FOL3*: Dihydrofolate synthase; *DFR1*: dihydrofolate reductase.

Genetic modification approaches have been proposed in yeast to boost the flux of the main metabolites involved in the biosynthesis of folate towards its accumulation [16–18]. Nevertheless, in these studies genetic manipulations were performed in different yeast genetic backgrounds, and the production of vitamin B₉ was evaluated either at the intracellular or extracellular level, without a systematic analysis for distinguishing among the various chemical forms of vitamin B₉. Without combining these pieces of information, it is difficult to establish the real potential of *S. cerevisiae* in terms of folates production. For these reasons, in the present work genes involved in the folate and in the shikimate biosynthesis pathways (*i.e.* *FOL2*, *ARO4*^{K229L}, *AroL*, *ARO2*), were expressed separately or in combination. From the resulting engineered strains, sharing the same parental genetic background, we measured intracellular and extracellular levels of free and poly-glutamate folates. This allowed us to describe the contribution of the different overexpression on

the quantity and quality of the folate forms produced and as a consequence to indicate the metabolic steps to unlock for further improving the productions of bioactive folates.

Results and discussion

Engineering of yeast strains and evaluation of free extracellular folates production

In order to evaluate how folate and shikimate biosynthesis pathways can contribute to the modulation of yeast folates production, in terms of quantity, localization and vitameric forms, the overexpression of several genes involved in those pathways was evaluated. In brief, there are two main branches of reactions leading to the synthesis of folate skeleton, non-considering the glutamate moiety: one modifies the GTP to contribute with the pteridine module, and the other one modifies the chorismate as biosynthetic intermediate (Figure 1). The overexpression of *FOL2*, involved in the first biosynthetic step of the pteridine moiety (Figure 1), is a reasonable target for increasing the overall folate levels, as explored in the wine yeast Enoferm M2 [18]. Considering the other branch, what is reported in literature relates to the reactions involved in the conversion of chorismate into pABA. Chorismate derives from the shikimate pathway, which branches to the production of other metabolites, such as aromatic amino acids. As a consequence, it is well known that the enzymes of this biosynthetic route are highly regulated, both at transcriptional and translational/post-translational level [19]. The first step of the pathway is catalysed by 2-dehydro-3-deoxy-D-arabino-heptulosonate-7-phosphate (DAHP) synthase (EC 2.5.1.54): the two isoenzymes in *S. cerevisiae* are encoded by the *ARO4* and *ARO3* genes. Aro4p and Aro3p enzymes are feedback-inhibited by tyrosine and phenylalanine, respectively [19]. To enhance the level of activity, the mutated version *ARO4*^{K229L}, a feedback-resistant variant of DAHP synthase [20], was introduced in the CEN.PK strain. In *S. cerevisiae*, DAHP is then converted into 5-O-(1-Carboxyvinyl)-3-phosphoshikimate by the pentafunctional enzyme codified by *ARO1*, while in other organisms such as *E. coli* the five steps are catalysed by monofunctional enzymes [21]. In literature it is reported that the enzyme involved in the third step (the

conversion of shikimate into shikimate-3-phosphate) has the highest flux-control among the five steps [21]. Therefore, *AroL* from *E. coli*, encoding the shikimate kinase, was overexpressed in the CEN.PK strain. In addition, we overexpressed the *ARO2* gene, involved in the last step of the shikimate pathway, in which the 5-P-(L-Carboxyvinyl)-3-phosphoshikimate is converted into chorismate. Thereby we obtained the so-called SHIK strain, in which the genes *ScARO4*^{K229L}, *EcAroL* and *ScARO2* were overexpressed simultaneously (Figure 3). Furthermore, we combined the overexpression of *FOL2* in our engineered strain, obtaining the FOL SHIK strain, to evaluate possible effects (Table 1) of the simultaneous deregulation of the two branches of the folate biosynthesis pathway. All the overexpressions were confirmed by RT-qPCR (Figure S1).

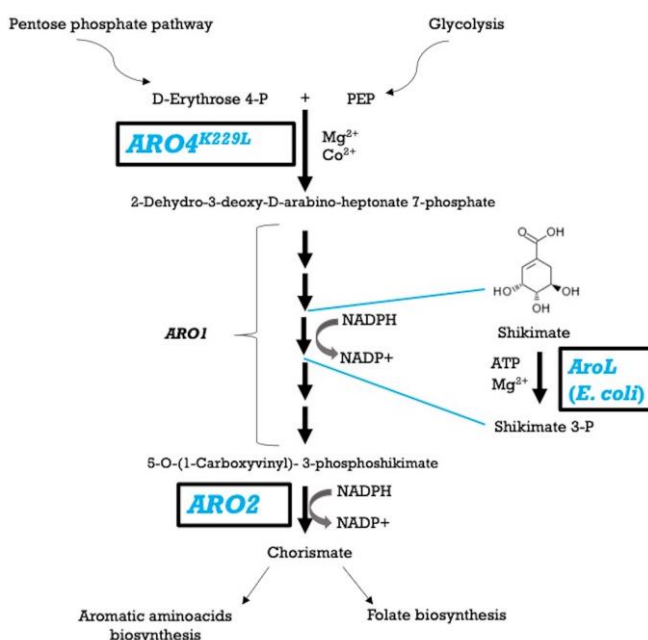


Figure 3 Schematic representation of the shikimate pathway. The intermediates and genes involved are explicated and the genes *ARO4*^{K229L}, *AroL* and *ARO2* highlighted in blue have been overexpressed in this study.

Free extracellular folates accumulation was evaluated over time by microbiological assay (see Materials and methods) in the parental (wild type, WT), FOL, SHIK and FOL SHIK strains grown in Verduyn minimal medium in the absence of vitamin B9. We started from

the evaluation of this form of folate released in the medium as this is what was mainly reported in previous works, therefore allowing a direct comparison.

Figure 4 shows that the highest titer of extracellular free folate corresponds to the stationary phase (48 h from the inoculum, where no further changes of OD measurements were observed, data not shown); therefore, in this work we focused on measuring samples collected in this growth phase. The FOL strain reached 19 ± 3.19 ng/mL of free extracellular folates (red bar), displaying a 7-fold increase in the accumulation compared to the folate production measured in the WT strain.

Similarly, we analyzed the free folate titers from strains overexpressing the genes regulating the shikimate pathway, which was not investigated before: the data show that the deregulation of the upstream steps for the chorismate synthesis did not lead to an increase in free folates production compared to the wild type (Figure 4, blue bars). In agreement with these data, the combined deregulation of the two branches (FOL SHIK strain, Figure 4, orange bars) did not exceed significantly the production of free extracellular folate observed in the FOL strain.

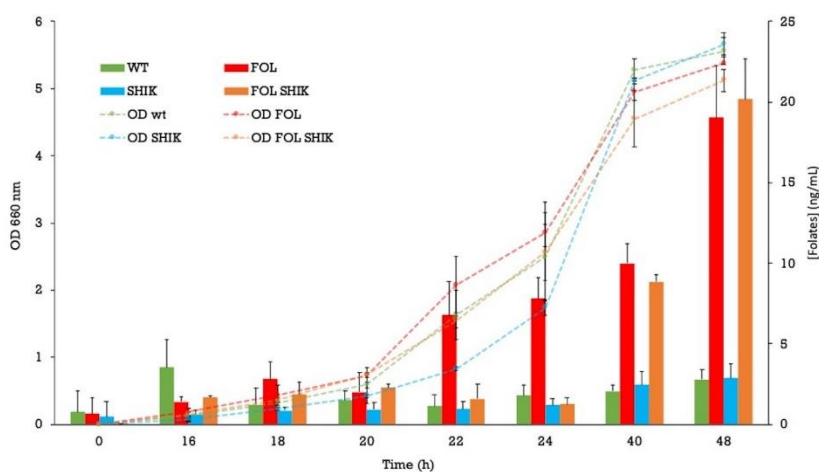


Figure 4: Growth kinetics (lines) and extracellular free folate production time (bars) by WT (green), FOL (red), SHIK (blue) and FOL SHIK (orange) strains. Values are the means of three independent experiments.

Production of extracellular poly-glutamate folates and free folates in engineered strains in different media

To exhaustively evaluate the effects of genetic manipulations and to understand how to further improve folates production, the analysis should include both intracellular and extracellular measurements of both free and poly-glutamate folates, possibly from the same genetic background. Our strains can constitute a valuable basis for these measurements, which can complement the data currently available in literature. Figure 5A shows the extracellular production of both free (white bars) and poly-glutamate folates (grey bars) after 48 h of growth in Verduyn medium, measured in all the engineered strains and compared to the parental one. This characterization shows that the extracellular poly-glutamate accumulation is similar in all the strains, and therefore the difference in total folate is to be ascribable mainly to free folates, which constitute the minor fraction of the whole folates pool. Thus, we also clarified that the *FOL2* overexpression is crucial to increase only the free folates forms.

Since pABA is an important moiety for the formation of folate, its presence in Verduyn medium (0.2 µg/mL) could mask the effect of the overexpression of the shikimate pathway in SHIK and FOL SHIK strains. It is indeed possible that the chorismate is channeled into alternative metabolic pathways, such as the biosynthesis of aromatic amino acids and ubiquinone, while pABA present in the medium is used for folate production. Hence, we repeated the experiments in Verduyn medium without pABA supplementation (Figure 5B).

As reported in Figure S3, in this condition the behavior of the various strains is different among themselves. In fact, only the SHIK and the FOL SHIK strains showed a similar growth regardless the presence of pABA, whereas the WT and FOL strains' growth were considerably reduced in the absence of pABA. Thus, in this condition the overexpression of the shikimate pathway seems pivotal to guarantee a similar growth to that observed when pABA was added to the media. Nevertheless, the engineered strains did increase the extracellular concentration of poly-glutamate folates, when compared to the WT. Remarkably, under the same conditions, free extracellular folates were not detected after 48 h of growth, while the increase in poly-glutamate folates was significant in both SHIK and FOL SHIK strains, compared to both WT and FOL strains (Figure 5).

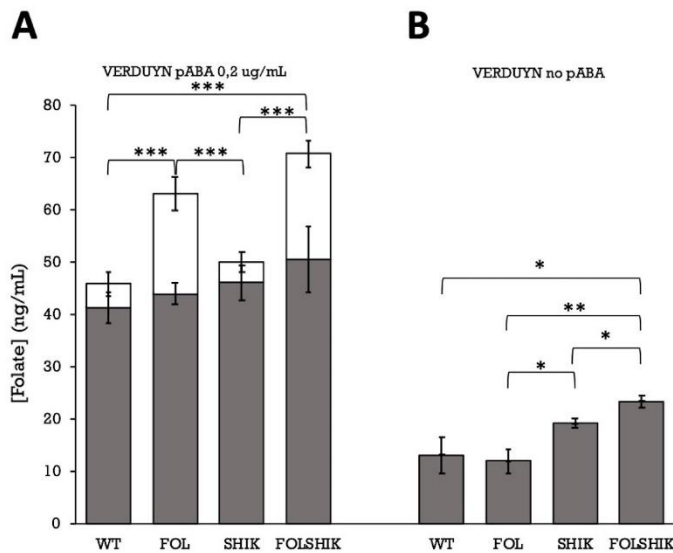


Figure 5: Extracellular production of free (white bars) and poly-glutamate (grey bars) folates. In panel A data obtained in normal Verdruyn medium are displayed, while panel B shows folates production in Verdruyn without pABA. Values are the means of three independent experiments. * $p \leq 0.05$; ** $p \leq 0.005$; *** $p \leq 0.0005$.

Intracellular free and poly-glutamate folates production in engineered strains in different media

Figure 6 displays intracellular poly-glutamate (grey bars, panel A) and free (white bars, panel B) folates accumulation in minimal Verdruyn media supplemented or not with pABA. Firstly, the overall levels of intracellular folates are much higher than those measured extracellularly, coherently with the importance of the vitamin B9 for cells. Therefore, it is arguable that only a minor fraction is excreted, although up to now there are no reports describing a possible transporter system or mechanism involved. The other important observation relates to the quantification, which is affected by the large distribution of values, possibly affected by sampling method.

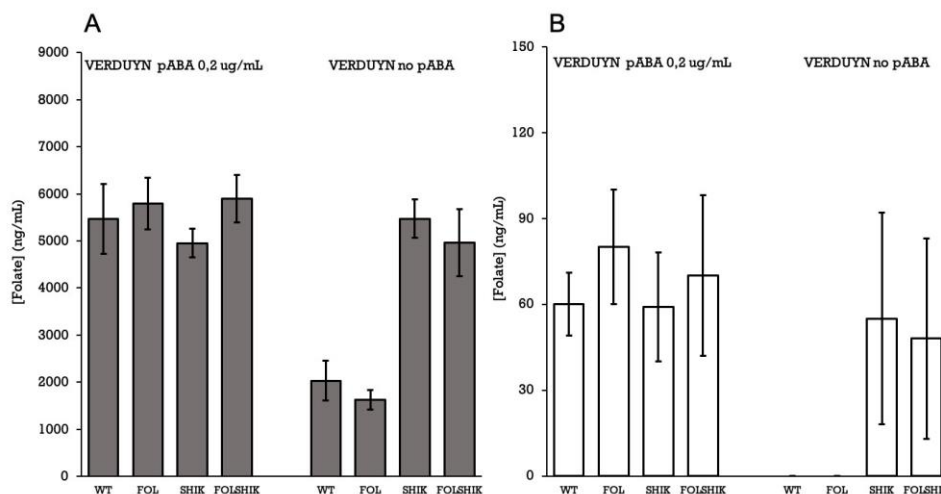


Figure 6: Intracellular production of free (white bars) and poly-glutamate (grey bars) folates. Panel A shows data obtained in normal Verduyn medium, while panel B shows folates production in Verduyn without pABA. Values are the means of three independent experiments.

It can be anyhow commented that the highest amounts of folates produced by the strains were represented by the poly-glutamate intracellular forms. In Verduyn medium the strains tested produced a similar quantity of intracellular folates, independently from the overexpressions considered. Consistently with our hypothesis, in a medium not supplemented with pABA the strains SHIK and FOL SHIK were able to reach the same titer of folates produced from cells growing in standard Verduyn medium (Figure 6). On the other hand, the *FOL2* overexpression is not enough for compensating both the growth and the folate production in Verduyn medium without pABA.

Taken together this data suggest that the shikimate pathway represents a bottleneck for increasing folate production in *S. cerevisiae*. The effect of the overexpression of genes related to this pathway (in the SHIK and FOL SHIK strains) becomes evident when pABA is not present in the media. Therefore, since pABA supplementation may mask the effect of the tested genetic modifications, the de-regulation of pathways subtracting chorismate (a direct precursor of pABA) can be a path to explore. As we demonstrated, the measurement of all folate forms, defining their cellular location (intra- or extracellular) and poly-glutamation level, is pivotal in order to achieve an informative description of the engineered strains.

Following the same approach, the obtained strains can be further engineered to decrease the competitive pathways towards folates production, such as the ones leading to the biosynthesis of aromatic amino acids, and to increase the pools of GTP and chorismate.

Conclusions

Folates are involved in one-carbon metabolism and thus play essential roles in a wide range of biochemical pathways. Due to the central role of folate, its deficiency leads to several physiological disorders. Indeed, folate supplementation of food has been implemented by most countries to efficiently fight folate deficiency [22]. Unfortunately, all the vitamin B₉ commercially available for food supplementation is chemically synthesized in the form of folic acid and may present some drawbacks [14]. For these reasons, we decided to evaluate the production of natural folates by microbial fermentation. *Saccharomyces cerevisiae*, widely used in biotechnological processes, was here exploited as natural producer of the different folate vitamers. Three genes involved in the shikimate pathway, *ARO4*^{K229L}, *AroL* and *ARO2*, were co-overexpressed to increase the production of chorismate, a possible bottleneck in the vitamin B₉ biosynthesis. Simultaneously, *FOL2* was co-overexpressed in the FOL SHIK strain. A complete characterization of both intracellular and extracellular free and poly-glutamate production of engineered *S. cerevisiae* strains originated from the same genetic background has been proposed, for the first time, in this work. Data shows that *FOL2* overexpression increases only the free extracellular folate forms, while it does not change all the other forms taken into account, such as intracellular ones. Furthermore, the shikimate pathway overexpression is pivotal in a medium not containing pABA, highlighting the importance of such moiety (and of its metabolism) as bottleneck to unlock the production of folates in yeasts. Therefore, the modulation of intracellular quantity of pABA by deregulating pathways related to the shikimate node (for example by subtracting chorismate) can be targeted for further modifications. This study demonstrates that by metabolic engineering and medium composition it is possible to modulate folates form, their distribution and accumulation in yeast. Moreover, possible

bottlenecks have been determined. In the future, synthetic biology strategies will be pursued, in combination with the definition of key elements in culture media, to improve folates yield, production and productivity, with the goal to develop sustainable bioprocesses for the synthesis of this essential vitamin.

Materials and methods

Yeast strains and growth conditions

S. cerevisiae parental and engineered strains used in this study are listed in Table 1. Yeast transformations were performed according to the LiAc/PEG/ss-DNA protocol [23] with integrative plasmids constructed as described in the next paragraphs. Transformants were selected for the complementation of the different auxotrophies and the integrations of the constructs were confirmed by PCR analysis. For each set of transformation at least three independent transformants were initially tested, showing no significant differences among them.

Yeast cultures were grown in Verduyn medium (Verduyn, Postma *et al.* 1992) with 2% (w/v) D-glucose as carbon source. All strains were grown in shake flasks at 30 °C and 160 rpm, with a flask volume:medium ratio of 5:1. Cells were inoculated at an initial optical density (OD) of 0.001, and growth was monitored spectrophotometrically (UV-1800; Shimadzu, Kyoto, Japan) at 660 nm. The free folate production was evaluated indirectly by a microbiological assay exploiting *Lactobacillus rhamnosus* as the test microorganism (Horne and Patterson 1988), as described in the dedicated section below. The same protocol was used for the evaluation of the total folates by previously pre-treating samples with enzymatic deconjugation protocol to remove the poly-glutamate residues as described below.

Strains	Relevant genotype	Plasmid	Reference
CEN.PK 102-5B	<i>MATa his3Δ1, ura 3–52, leu2-3,112 MAL2–8c SUC2</i>	-	Peter Kötter
Parental strain	CEN.PK 102-5B	pYX012; pYX022; pYX042	This study
FOL	CEN.PK 102-5B	pYX012; pYX022; pYX042 <i>FOL2</i>	This study
SHIK	CEN.PK 102-5B	pYX012 <i>ARO4</i> ^{K229L} <i>AroL ARO2</i> ; pYX022; pYX042	This study
FOL SHIK	CEN.PK 102-5B	pYX012 <i>ARO4</i> ^{K229L} <i>AroL ARO2</i> ; pYX022; pYX042 <i>FOL2</i>	This study

Table 1: List of the strains used in this study

Gene amplification and plasmids construction

All the primers used for gene amplifications and the obtained PCR products are listed in Table 2. The mutant gene *ARO4*^{K229L} was obtained using *S. cerevisiae ARO4* from the genomic DNA of the CEN.PK strain, extracted by standard methods [24] as template. Two different sets of primers (Fw flank*a*-*ARO4* and Rev *ARO4*^{K229L}; Fw *ARO4*^{K229L} and Rev *ARO4*-flank*b*, Table 2) were designed and used to introduce the desired mutations (685A>T and 686A>T), and specific flanks complementary to the Triose Phosphate Isomerase gene promoter (TPI_p) and terminator (TPI_{ter}) regions present in the pYX012 vector (R&D Systems Wiesbaden, Germany) were also inserted. The two fragments obtained by PCRs were then assembled using the Gibson Assembly Cloning Kit (New England Biolabs, Ipswich, Massachusetts, USA) into the pYX012 vector, previously linearized with *EcoRI*, obtaining the pYX012*ARO4*^{K229L} vector.

S. cerevisiae ARO2 and *FOL2* coding sequences were amplified by PCR using the genomic DNA from CEN.PK strain as a template. *E. coli AroL* coding sequence was amplified by PCR using as template the genomic DNA of the DH5α strain, extracted by standard methods [25]. The *ARO2* PCR product, amplified with FW *EcoRI ARO2* and Rev *BamHI ARO2* primers, was digested with *EcoRI* and *BamHI* and ligated within the pYX042 vector (R&D Systems Wiesbaden, Germany) previously digested with the same enzymes, obtaining the pYX042*ARO2* vector. The *FOL2* PCR product, amplified with FW *EcoRVFOL2* and Rev *BamHIFOL2* primers, was digested with *EcoRV* and *BamHI* and ligated with the pYX042 vector, previously digested with the same enzymes. The obtained vector pYX042*FOL2*,

harboring *FOL2* under the control of the TPI_p , was linearized with *ClaI* and directly used for yeast transformations. The *AroL* PCR product, amplified with FW *EcoRI* *AroL* and Rev *BamHI* *AroL* primers, was digested with *EcoRI* and *BamHI* and ligated with the pYX022 vector (R&D Systems Wiesbaden, Germany), previously digested with the same enzymes, obtaining the pYX022*AroL* vector.

The “flank*a*-*ARO4*^{K229L}- TPI_{ter} -flank3”, “flank3- TPI_p -*AroL*- TPI_{ter} -flank4” and “flank4- TPI_p -*ARO2*- TPI_{ter} -flank5” fragments were obtained by PCR using as a template pYX012*ARO4*^{K229L}, pYX042*ARO2* and pYX022*AroL*, respectively and using the primers described in Table 2. These fragments were then assembled into the pYX012 vector, previously linearized with *EcoRI*. The obtained vector pYX012*ARO4*^{K229L}*AroL* *ARO2*, harboring all the genes under the control of TPI_p , was linearized with *BsmI* and directly used for yeast transformations.

All the genes were sequenced, and they resulted identical to the deposited *S. cerevisiae* or *E. coli* target sequences (*ARO2* Gene ID: 852729; *FOL2* Gene ID: 853183; *AroL* Gene ID: 945031)

The *ARO4*^{K229L} gene was identical to the deposited *S. cerevisiae* target sequence (Gene ID: 852551) except for the desired mutations (685A>T and 686A>T).

Name	Sequence (5'-3')	DNA template for PCR	PCR product
Fw flank <i>a</i> - <i>ARO4</i> Rev <i>ARO4</i> ^{K229L}	<u>CTACAAAAACACATACAGGTCAGAAATGAGTGAATCTC</u> AGCAACACCATGCAAAGTAACACC	<i>S. cerevisiae</i> gDNA	<i>ARO4</i> ^{K229L} first 725 bp
Fw <i>ARO4</i> ^{K229L} Rev <i>ARO4</i> -flank <i>b</i>	GGTGTACTTTGCATGGTGTGCT CCCTAGGATCCATGGTGTGTACGTTACATATCA	<i>S. cerevisiae</i> gDNA	<i>ARO4</i> ^{K229L} last 485 bp
Fw <i>EcoRI</i> <i>ARO2</i> Rev <i>BamHI</i> <i>ARO2</i>	ATTAGAATTCGCATGTCAACGTTTGGGAA AATGGATCCTCTTAATGAACACGGATC	<i>S. cerevisiae</i> gDNA	<i>ARO2</i> (ORF)
FW <i>EcoRV</i> <i>FOL2</i> Rev <i>BamHI</i> <i>FOL2</i>	TACAGGATATCATGCATAACATCCAATTAGT AATGGATCCTCAAATACTTCTTCTCCTA	<i>S. cerevisiae</i> gDNA	<i>FOL2</i> (ORF)
FW <i>EcoRI</i> <i>AroL</i> Rev <i>BamHI</i> <i>AroL</i>	ATTCGAATTCGATGACACAACCTCTTT AATGGATCCAAAATCACAATTGATCGTC	<i>E. coli</i> gDNA	<i>AroL</i> (ORF)
Fw flank <i>a</i> - <i>ARO4</i> Rev <i>ARO4</i> TPI_{ter} -flank1	<u>CTACAAAAACACATACAGGTCAGAAATGAGTGAATCTC</u> <u>GAGATAGAAATTTGACATTCCTAGACAAAAGACAAAAAAGGG</u>	pYX012 <i>ARO4</i> ^{K229L}	flank <i>a</i> - <i>ARO4</i> ^{K229L} - TPI_{ter} -flank3
Fw flank1- TPI_p <i>AroL</i> Rev <i>AroL</i> TPI_{ter} -flank2	<u>GAATGTCAAATTTCTATCCTTTTCGTCITCAAGAATTGGGGATCTA</u> <u>GTATTTAGTTAGTACTTAAGGAACAAAAGCTGGAGCTAGACAAAGAC</u>	pYX022 <i>AroL</i>	flank3- TPI_p - <i>AroL</i> - TPI_{ter} -flank4
Fw flank2- TPI_p <i>ARO2</i> Rev <i>ARO2</i> TPI_{ter} -flank3	<u>CTTAAGTACTAACTAAATACCGTCTTCAAGAATTGGGGATCTACGTATG</u> <u>GGGCCCTAGGATCCATGGTGGGAACAAAAGCTGGAGCTAGACAAAG</u>	pYX042 <i>ARO2</i>	flank4- TPI_p - <i>ARO2</i> - TPI_{ter} -flank5

Table 1: List of the primers used in this study

Real Time - qPCR

Quantitative PCR was performed in order to assay *FOL2*, *ARO4*, *AroL* and *ARO2* overexpression. Aliquots of yeast cells were collected from cultures in exponential phase, and total RNA prepared using a *ZR Fungal/Bacterial RNA MiniPrep™ Kit* (ZYMO RESEARCH, Irvine, USA). Reverse transcription was performed on 1 µg of total RNA as a template, using *iScript™ cDNA Synthesis Kit* (BIO-RAD, Hercules, USA). RT-qPCR was carried out to amplify *FOL2*, *ARO4*, *AroL* and *ARO2* cDNAs using *LunaScript RT SuperMix Kit* (New England Biolabs, Ipswich, USA). Actin cDNA was also amplified for normalization. Relative expression was calculated using the $\Delta\Delta C_t$ method.

Folate microbiological assay

The extracellular or intracellular amounts of free folates (folate forms with at maximum three glutamyl residues) produced by the yeast strains were determined indirectly by microbiological assay, using *L. rhamnosus* (NRRL culture collection, B-442) as test microorganism. This bacterium is able to grow proportionally to the initial concentration of folic acid present in the medium: this allows to build a calibration curve that correlates the final OD reached by *L. rhamnosus* to the concentration of folates in the samples [26]. As reference, folic acid (Sigma-Aldrich, St. Louis, USA) was firstly dissolved in 1 M NaOH at the initial concentration of 5 mg/mL and then, after serial dilutions in 0.1 M potassium phosphate buffer (pH 6.4) with 1% (w/v) ascorbic acid, a stock of folic acid 1 ng/mL was prepared and used for the calibration curve at concentrations ranging from 0 to 0.2 ng/mL. Prior to the assay, the culture of *L. rhamnosus* was prepared as follows: the lyophilized cells were resuspended in 1 mL of Folic Acid Casei Medium (FACM, HiMedia Laboratories, Mumbai, India) supplemented with folic acid 0.3 µg/L, previously dissolved in 1 M NaOH. 50 µL of cells were inoculated in 30 mL of FACM medium with folic acid 0.3 µg/L in flask hermetically closed and were incubated at 37 °C under agitation (160 rpm). After 24 hours from the inoculum, aliquots of cell culture and glycerol (100%) in a ratio of 1:1 were prepared and stored in sterile tubes at -80 °C until use for folate determination.

For the use in the microbiological assay, the inoculum of *L. rhamnosus* was prepared by mixing one volume of the thawed bacterial suspension with four volumes of sterile 9 g/L NaCl solution [26].

The microbiological assay was performed in 96-well microtiter plates, following a protocol adapted from [27]. The wells were filled by adding: 100 μ L of twofold-concentrated FACM, 100 μ L of an unknown or reference sample in 0.1 M potassium phosphate buffer (pH 6.4) containing 1% (w/v) ascorbic acid and 20 μ L of the *L. rhamnosus* inoculum. The plates were incubated at 37 °C and the turbidity was measured after 18 hours (T 18 h) from the inoculum of *L. rhamnosus* using a multiscan spectrophotometer set at 595 nm (VICTOR™ X3, PerkinElmer). Control wells were inoculated without *L. rhamnosus* to check for the FACM medium absorbance, then subtracted to the absorbance of the samples. The correlation between the OD_{595nm} at T 18 h and the initial concentration of free folates in the wells was described by a second-degree polynomial equation (Figure S1).

The yeast samples collected during growth kinetics were split in supernatant and pellet by centrifugation. For the extracellular evaluation, the supernatant was mixed for 1/10 volume with 1 M potassium phosphate buffer (pH 6.4) containing 10% (w/v) ascorbic acid. From this, serial dilution in 0.1 M potassium phosphate buffer (pH 6.4) containing 1% (w/v) ascorbic acid were prepared and 100 μ L from each dilution were used for the microbiological assay detection. Regarding the intracellular evaluation, the pellet was washed twice in 1 mL deionized water and then resuspended in 1 mL of 0.1 M potassium phosphate buffer (pH 6.4) containing 1% (w/v) ascorbic acid. The samples were incubated at 50 °C for 5 minutes to release the intracellular folates now available for the detection with the microbiological assay as previously described.

Since the microbiological assay is responsive only to free folates forms, the analysis of the total folate concentration (including forms with long chain of poly-glutamates) was performed after an enzymatic deconjugation of the folate samples with rat serum (Sigma-Aldrich, St. Louis, USA) as source for γ -glutamyl hydrolase activity. Prior to use, rat serum was subjected to a pre-treatment in order to remove endogenous folates, as follows: 1/10 volume of activated charcoal, was mixed to the serum, stirred for 1 hour on ice-

water bath, centrifuged and filtered through 0.22 μm sterile syringe filter (Primo[®] Syringe Filter EUROCLONE) [28]. The clarified rat serum was added to the folate samples at the final concentration of 20% (v/v). After 3 hours of incubation at 37 °C, the enzyme was inactivated by heating for 5 min at 100 °C. The samples were cooled down and after centrifugation at 14000 rpm for 20 min at 4 °C the supernatant was collected and used for the microbiological assay, as described above.

Statistical analysis

All statistical analyses, where P-values are indicated, were performed using a two-tails, unpaired, heteroscedastic Student's t-test.

List of abbreviations

DAHP: 2-dehydro-3-deoxy-D-arabino-heptulosonate-7-phosphate; DFE: Dietary Folate Equivalents; FACM: Folic Acid Casei Medium; GRAS: Generally Recognize As Safe; GTP: Guanosine triphosphate; LABs: Lactic Acid Bacteria; LiAc: Lithium acetate; NIH: National Institutes of Health; OD: Optical Density; pABA: para Amino Benzoic Acid; PCR: Polymerase Chain Reaction; PEG: polyethyleneglycol; RDA: Recommended Dietary Allowance; rpm: revolutions per minute; RT-qPCR: Real Time quantitative Polymerase Chain Reaction; TNDs: Neural Tube Defects; TPI: Triose Phosphate Isomerase gene.

Supplementary figures

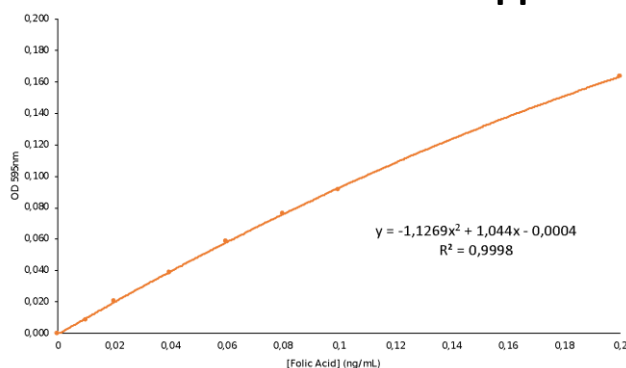


Figure S1: Calibration curve obtained by growing *Lactobacillus rhamnosus* in FACM medium with different concentrations of folic acid.

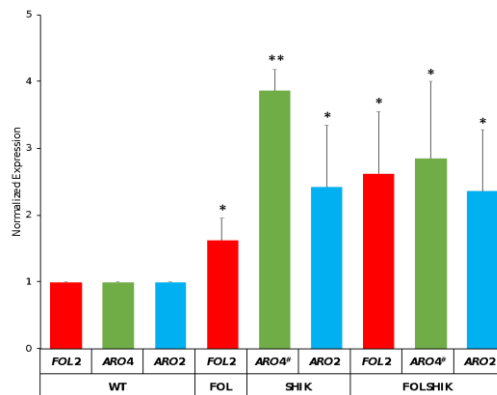


Figure S2: The graphs show the mRNA normalized expression of the different genes (*FOL2*, *ARO4* and *ARO2*) overexpressed in the different strains obtained in this study. Values are the means of three independent experiments.

* $p \leq 0,05$; ** $p \leq 0,005$; *** $p \leq 0,0005$

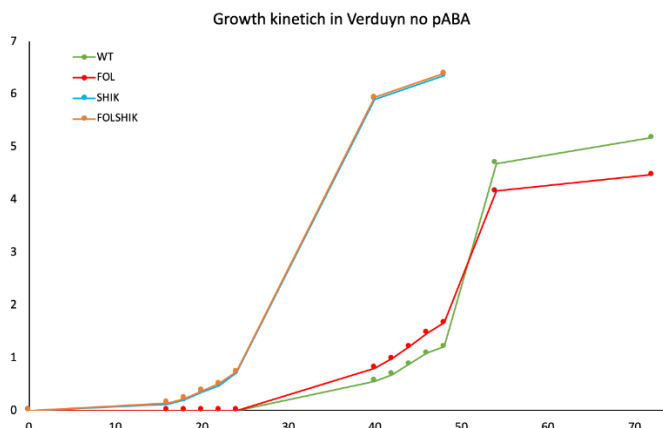


Figure S3: Growth kinetics by WT (green), FOL (red), SHIK (blue) and FOL SHIK (orange) strains in Verduyn without pABA. Values are the means of three independent experiments.

References

1. Crider KS, Yang TP, Berry RJ, Bailey LB. Folate and DNA methylation: A review of molecular mechanisms and the evidence for Folate's role. *Adv. Nutr.* 2012.
2. McBreairty LE, Robinson JL, Harding S V., Randell EW, Brunton JA, Bertolo RF. Betaine is as effective as folate at re-synthesizing methionine for protein synthesis during moderate methionine deficiency in piglets. *Eur J Nutr.* 2016;
3. Blom HJ, Smulders Y. Overview of homocysteine and folate metabolism. With special references to cardiovascular disease and neural tube defects. *J. Inherit. Metab. Dis.* 2011.
4. Koury MJ, Ponka P. New insights into erythropoiesis: The roles of folate, vitamin B 12,

and iron. *Annu. Rev. Nutr.* 2004.

5. Moyers S, Bailey LB. Fetal malformations and folate metabolism: Review of recent evidence. *Nutr. Rev.* 2001.

6. Strobbe S, Van Der Straeten D. Folate biofortification in food crops. *Curr. Opin. Biotechnol.* 2017.

7. Ferrari A, Tardin Torrezan G, Maria Carraro D, Aguiar Junior S. Association of Folate and Vitamins Involved in the 1-Carbon Cycle with Polymorphisms in the Methylenetetrahydrofolate Reductase Gene (MTHFR) and Global DNA Methylation in Patients with Colorectal Cancer. *Nutrients.* 2019;

8. Jägerstad M, Jastrebova J. Occurrence, stability, and determination of formyl folates in foods. *J. Agric. Food Chem.* 2013.

9. USDA National Nutrient Database for Standard Reference, Legacy Release | Ag Data Commons.

10. EFSA. Scientific Opinion on the essential composition of infant and follow-on formulae. *EFSA J.* 2014;12:1–106.

11. McLean E, de Benoist B, Allen LH. Review of the magnitude of folate and vitamin B12 deficiencies worldwide. *Food Nutr Bull.* 2008.

12. Saini RK, Nile SH, Keum YS. Folates: Chemistry, analysis, occurrence, biofortification and bioavailability. *Food Res. Int.* 2016.

13. Saubade F, Hemery YM, Guyot JP, Humblot C. Lactic acid fermentation as a tool for increasing the folate content of foods. *Crit Rev Food Sci Nutr.* 2017;

14. Choi JH, Yates Z, Veysey M, Heo YR, Lucock M. Contemporary issues surrounding folic acid fortification initiatives. *Prev. Nutr. Food Sci.* 2014.

15. Hjortmo S, Patring J, Jastrebova J, Andlid T. Inherent biodiversity of folate content and composition in yeasts. *Trends Food Sci Technol.* 2005;

16. Hjortmo S, Patring J, Andlid T. Growth rate and medium composition strongly affect folate content in *Saccharomyces cerevisiae*. *Int J Food Microbiol.* 2008;

17. Gientka I, Duszkiwicz-Reinhard W. P-Aminobenzoic acid (PABA) changes folate content in cell biomass of *saccharomyces cerevisiae*. *Polish J Food Nutr Sci.* 2010;

18. Liu Y, Walkey CJ, Green TJ, Van Vuuren HJJ, Kitts DD. Enhancing the natural folate level in wine using bioengineering and stabilization strategies. *Food Chem.* 2016;

19. Luttik MAH, Vuralhan Z, Suir E, Braus GH, Pronk JT, Daran JM. Alleviation of feedback inhibition in *Saccharomyces cerevisiae* aromatic amino acid biosynthesis: Quantification

of metabolic impact. *Metab Eng.* 2008;

20. Hartmann M, Schneider TR, Pfeil A, Heinrich G, Lipscomb WN, Braus GH. Evolution of feedback-inhibited barrel isoenzymes by gene duplication and a single mutation. *PNAS* Febr. 2003.

21. Rodriguez A, Kildegaard KR, Li M, Borodina I, Nielsen J. Establishment of a yeast platform strain for production of p-coumaric acid through metabolic engineering of aromatic amino acid biosynthesis. *Metab Eng.* 2015;

22. Arth A, Kancherla V, Pachón H, Zimmerman S, Johnson Q, Oakley GP. A 2015 global update on folic acid-preventable spina bifida and anencephaly. *Birth Defects Res Part A - Clin Mol Teratol.* 2016;

23. Gietz RD, Woods RA. Transformation of yeast by lithium acetate/single-stranded carrier DNA/polyethylene glycol method. *Methods Enzymol.* 2002;

24. Sambrook J, Russel, D W. *Molecular Cloning, 3-Volume Set : A Laboratory Manual.* Cold Spring Harboc Lab. Press. 2000.

25. He F. *E. coli Genomic DNA Extraction.* BIO-PROTOCOL. 2011;

26. Horne DW, Patterson D. *Lactobacillus casei* microbiological assay of folic acid derivatives in 96-well microtiter plates. *Clin Chem.* 1988;

27. Sybesma W, Starrenburg M, Tijsseling L, Hoefnagel MHN, Hugenholtz J. Effects of cultivation conditions on folate production by lactic acid bacteria. *Appl Environ Microbiol.* 2003;

28. Shohag MJI, Wei Y, Yu N, Lu L, Zhang J, He Z, et al. Folate Content and Composition of Vegetables Commonly Consumed in China. *J Food Sci.* 2012;

Chapter 5

Implementation of mathematical modelling of a bio-based methane production from manure

This research project has been supported by the European Institution of Innovation & Technology (EIT) KIC-RawMaterials project ADMA2 (Practical training between Academia and Industry during doctoral studies). The data here disclosed were obtained during abroad secondment at the Department of Environmental and Chemical Engineering, Faculty of Technology, University of Oulu (Finland). Industrial partner was Biometa Finland Oy. The work then continued remotely. Manuscript in preparation in collaboration with Anu Sirviö, Mika Ruusunen, Aki Sorsa and Paola Branduardi.

Introduction

At the end of the first decade of XXI century, the European Union (EU) Renewable Energy Directive 2009/28/EC required that by 2020 each member state had to rely on renewable energy for 20% of the total needs and 10% for transport alone [1]. Unfortunately, only Sweden and Austria have reached that target [2]; consequently, there is a urgent and binding need to push forward the use of alternatives to common fossil resources. Natural gas, namely methane (CH_4), is a prominent target to be substituted with renewable alternatives, as it is still widely used in the EU for industrial, domestic and transport sectors. Its direct replacement is biomethane, which is the final product of anaerobic fermentation of organic matter, as part of the gaseous mixture called biogas. Biogas is in fact a blend mainly of CH_4 and CO_2 : it can be deployed directly as source of energy, but the presence of the already fully oxidized CO_2 reduces the overall calorific value. For this reason, several “upgrading” processes exist, aimed at purifying biomethane from biogas, to expand its use also to domestic and transport sectors via injection into the conventional pipelines [3,4]. Among the various residual biomasses used in order to match the low market value of biomethane [2,5], manure plays a prominent role. It is a livestock side stream with a high environmental impact that can be reduced by further manipulations, as its exploitation for bioenergy and biofertilizers production [6]. Manure possess a huge potential in terms of worldwide production of biogas, exceeding other biomasses such as sewage sludge, organic fraction of municipal solid waste, and agricultural residues [7]. Since the increasing growth of the European market of biomethane, leaded by Germany, several countries from both northern (*e.g.* Finland) and southern (*e.g.* Italy) Europe are interested in developing this sector, to fulfill the aforementioned goals of the EU in the years [2,8]. To make the production profitable, considering the reduced margin between cost and price, is essential but not trivial. For these reasons a quantitative description of the microbiological system sustaining the process is essential: the development of mathematical models can support this description and predict possible improvements, which can be crucial for the viability of the biomethane sector.

Biogas production in anaerobic digestors generally follows four sequential phases carried out by the metabolism of the microbial consortium therein. Biopolymers are initially hydrolysed into simple or simpler monomers and oligomers (mainly sugars, stage I - hydrolysis), then fermented into alcohols, CO₂, volatile fatty acids (VFAs, *e.g.* propionate, butyrate, acetate) and H₂ (stage II - acidogenesis) [9]. These molecules are then converted into acetic acid (stage III - acetogenesis), sequentially transformed into biomethane (CH₄) (stage IV - methanogenesis) (Figure 1) [9]. These reactions are carried out by different species of microbes, whose symbiosis and syntrophy in the consortium is the key for the anaerobic digester to function. In a simplified model of these reactions, described in Figure 1, stage I is carried out by glucose-fermenting acidogens, able to both hydrolyse the fibers contained in manure (undigested by the animals) and transform glucose into VFAs. Propionate and butyrate-degrading acetogens accumulate acetic acid from corresponding VFAs, whereas acetoclastic methanogens complete the reaction to biomethane [10,11].

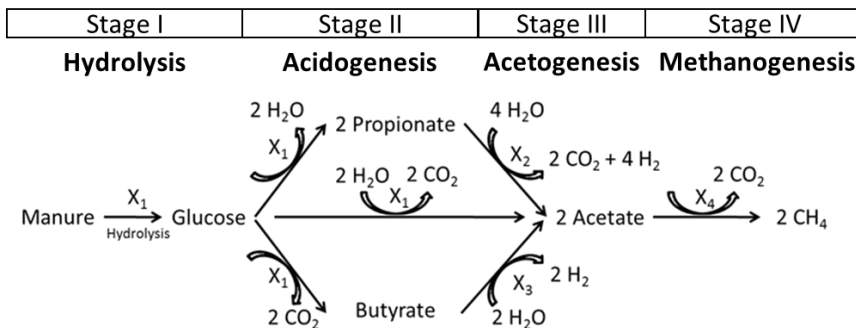


Figure 1 Simplified biochemical model of anaerobic digestion of manure by the consortium of glucose-fermenting acidogens (X_1), propionate-degrading acetogens (X_2), butyrate-degrading acetogens (X_3) and acetoclastic methanogens (X_4).

From the process of the waste-derived biomethane it was possible to create a mathematical model based on differential equations, able to foresee predict the behavior of the process itself if specific parameters are modified, as described for example in [10]. The goal of the present work was to update this model with observations from the microbiological nature of the process, and to evaluate which industrial relevant parameters could impact the most on the final production of biomethane by the simulated microbial consortium.

Results and discussion

Biochemical description of the model

Microbial metabolism reflects microbial biodiversity: different species often display different abilities in utilizing the same carbon source. Since the heterogenous nature of microbial consortia, understanding the main reactions occurring within is of utmost industrial interest [9]. As mentioned, the production of biomethane from biogas is constituted by four main phases, that, although being sequential to each other, follow different metabolic branches. In fact, as shown in Figure 1, different routes can lead to the accumulation of acetate, then transformed into biomethane by acetoclastic methanogens. A direct metabolism from glucose to acetate is in fact combined by the alternative production of butyrate or propionate, later converted into acetate as well. The three metabolisms could be described stoichiometrically with the chemical equations enlisted in Table 1.

Equation	Estimated $\Delta_r G'^{\circ}$ (kJ/mol)	K'_{eq}
1) Glucose + 2 H ₂ O \rightleftharpoons 4 CO ₂ + 2 CH ₄ + 4 H ₂	-148.6 ± 35.0	1.1 × 10 ²⁶
2) Glucose + 2 NAD ⁺ + 2 H ₂ O \rightleftharpoons 4 CO ₂ + 2 CH ₄ + 2 H ₂ + 2 NADH	-217.7 ± 28.6	1.5 × 10 ³⁸
3) Glucose + 4 NAD ⁺ + 2 H ₂ O \rightleftharpoons 4 CO ₂ + 2 CH ₄ + 4 NADH	-286.9 ± 26.3	1.9 × 10 ⁵⁰

Table 1 Stoichiometric description of the reactions occurring during anaerobic digestion from glucose to acetate, via propionate (1) or butyrate (2) production, or direct fermentation to acetate (3), with kinetic parameters of such reactions.

The analysis of these equations make clear that with the direct fermentation of glucose into acetate, NAD⁺ becomes the electron sink of the reaction (equation 3, Table 1), whereas H₂ is the receiver of the four electrons (equation 1, Table 1) when propionate-degrading acetogens are involved. Accordingly, butyrate as mid-step involved the use of both H₂ and NAD⁺ as electron sink of the fermentation (equation 2, Table 1). Considering kinetic parameters such as the estimated Gibbs free energy ($\Delta_r G'^{\circ}$) and equilibrium constant (K'_{eq}) it was clear that the direct fermentation of glucose into acetate is the most thermodynamically favorite, suggesting that the microorganisms involved in such metabolism are pivotal for the accumulation of biomethane. Bioaugmentation of acetate-

type fermentation species have in fact been proposed to ameliorate anaerobic digestion of residual biomasses into biomethane [12].

Updating the anaerobic digestion mathematical model

The differential equations describing the anaerobic digestion of manure into biomethane from [10] (originally developed for the use of activated sludge from the municipal wastewater treatment plants) were recreated on Simulink in a simplified version, by omitting hydrogenotropic methanogens, since their yield of methane production was calculated to be inferior to acetoclastic methanogens (0.8 and 4 g/g biomass respectively [10]). In fact, acetoclastic methanogens are responsible for most of the biomethane produced during anaerobic digestion (up to 70% of the total) [13]. The equations and the parameters within are described in “Materials and methods” section. Given the considerations arising from the previous paragraphs, we decided to quantify with the model the influence of the metabolism of acetate-type fermentation microbes (X_1) on the production of biomethane. We singularly simulated the nullification of acetate production yields by X_1 , X_2 and X_3 (Y_{acet/X_1} , Y_{acet/X_2} and Y_{acet/X_3} , respectively). In the latter two cases biomethane yield (Q) did not decrease significantly from the original one ($Q = 0.45$ L/L_{medium}/d, Figure 2A), whereas $Y_{\text{acet}/X_1} = 0$ resulted in $Q = 0.18$ L/L_{medium}/d, witnessing the importance of the metabolism of X_1 on the overall process. We then expanded the simulation by nullifying the yield of glucose consumption by X_1 ($Y_{\text{glu}/X_1} = 0$) to eliminate completely the action of this specie. Surprisingly, although a strong reduction of Q should have been expected, the simulation resulted in an infinite production of biomethane in the first days of fermentation (Figure 2B), underlying some inaccuracy in the model itself. In the model X_1 both hydrolysed fibers and fermented glucose into VFA, therefore the subsequent production of biomethane is strongly dependent on its activity. Since Y_{glu/X_1} represents the ability of X_1 to consume glucose and therefore to growth, the fact that its simulated nullification was so beneficial for the production of biomethane was at least suspicious from a microbiological point of view.

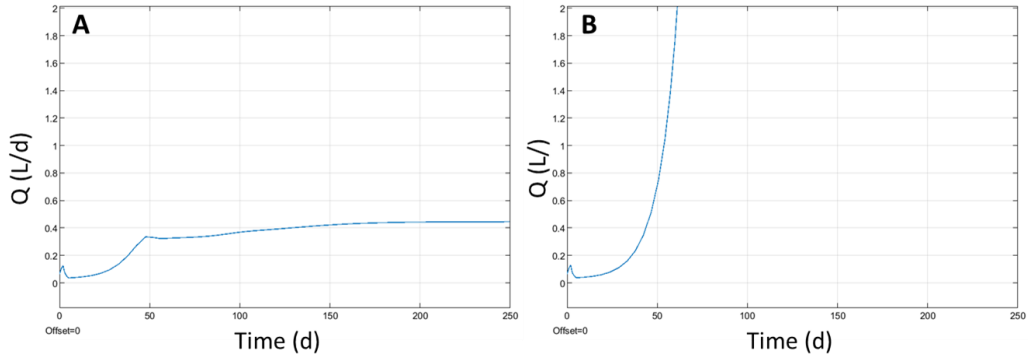


Figure 2 Simulation of biomethane yield (Q) during time using parameters from [10] (panel A) and with $Y_{glu/X1} = 0$ (panel B).

Analyzing the equations of the model (see “Materials and methods”) it became clear the mathematical reason of such behavior. $Y_{glu/X1}$ appears in equation 3, as negative contributor to the titer of glucose in the digester. The nullification of $Y_{glu/X1}$ therefore increased the amount of glucose, that in turn increased μ_1 and the titer of X_1 (equation 1), and subsequently the titer of the of microbial species as well. The paradox laid on the fact that although X_1 was simulated of not being able to consume glucose, it was still growing and producing VFA, while microbiologically the opposite should occur. In order to meet this fundamental requirement, we modified the equations describing microbial growth (2, 4, 6, 8) by adding the corresponding yield of substrate consumption as follows.

$$\begin{aligned} \frac{dX_1}{dt} &= Y_{glu/X1} \cdot (\mu_1 - b_1) X_1 - D \cdot X_1 \quad (2) & \frac{dX_3}{dt} &= Y_{but/X1} \cdot (\mu_3 - b_3) X_3 - D \cdot X_3 \quad (6) \\ \frac{dX_2}{dt} &= Y_{prop/X1} \cdot (\mu_2 - b_2) X_2 - D \cdot X_2 \quad (4) & \frac{dX_4}{dt} &= Y_{acet/X4} \cdot (\mu_4 - b_4) X_4 - D \cdot X_4 \quad (8) \end{aligned}$$

With the updated equations, the original parameter values permitted a simulation with $Q = 0.9698 \text{ L/L}_{\text{medium}}/\text{d}$ as result, whereas the nullification of $Y_{glu/X1}$ reduced the value to $Q = 0.1104 \text{ L/L}_{\text{medium}}/\text{d}$, in accordance with the modifications proposed for the model (Figure 3). The value of Q was not nullified as well because of the acetate present in the influent (S_{i4}), transformed by X_4 into biomethane according to equations 9 and 10. Furthermore, the value of Q obtained with this new version of the model was higher compared to the original [10], although inserting the same constant values and being those validated

experimentally. Nevertheless, the goal of this work was to provide an updated version of the model that could be a closer description of the microbial consortium responsible for the anaerobic digestion.

The second aim was to investigate how the yield of biomethane could be modified as a matter of specific implementations of the process to be suggested to an industrial partner, rather than to validate the model itself with wet data in these first stages of investigation.

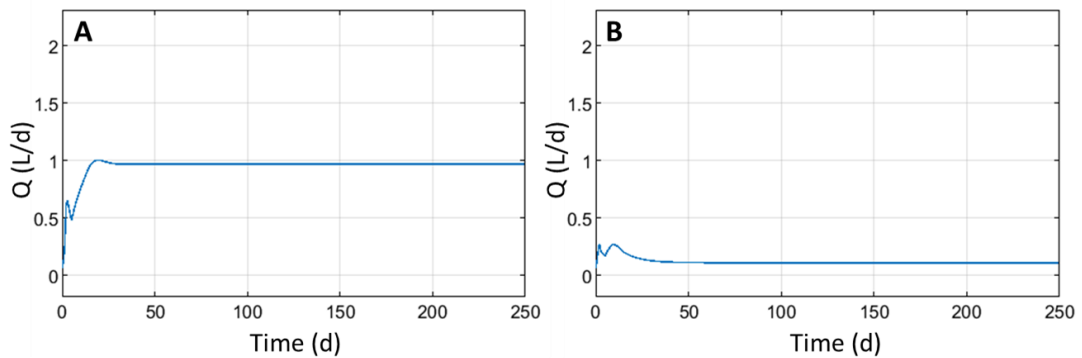


Figure 3 Simulation of biomethane yield (Q) during time with updated equations using parameters from [10] (panel A) and with $Y_{glu/X1} = 0$ (panel B).

Simulation studies on the anaerobic digestion model

After updating the model by introducing the yield of substrate consumption in the equations, it was possible to describe the growth of the various microbial species present in the model (X_1, X_2, X_3, X_4). As starting point, dilution rate (D) was modified according to the maximum value available at the plant of the industrial partner of the project ($D = 0.14 \text{ d}^{-1}$), with 5000 L as operative volume. The updated set of values resulted in $Q = 1.198 \text{ L/L}_{\text{medium}}/\text{d}$, displayed in Figure 4 together with other parameters, such as substrate, glucose and VFA titer, microbial titer and specific growth rate. From now on 60 d was used as stoppage time, since the maximum Q was already reached.

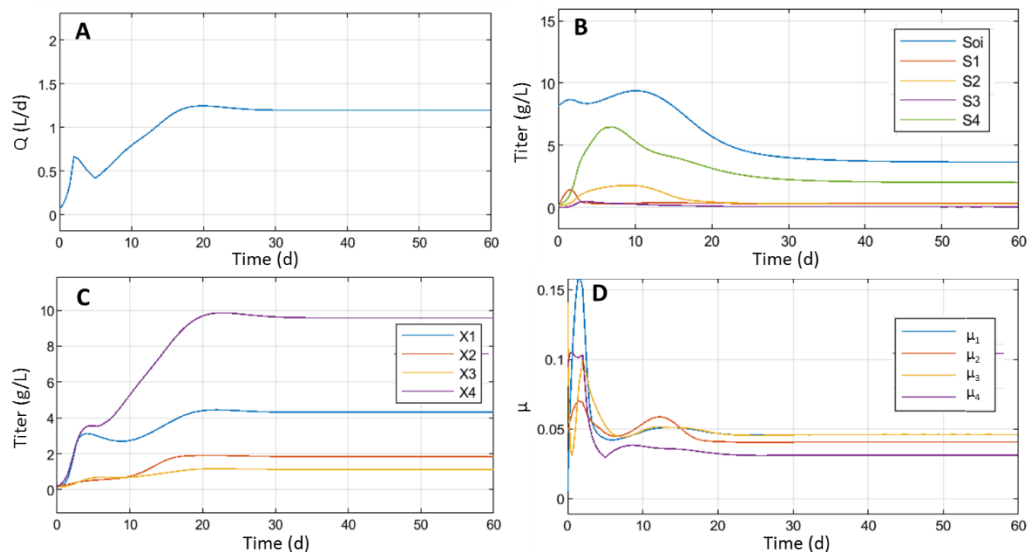


Figure 4 Simulation of biomethane yield (panel A), compound titers (panel B), microbial titers (panel C) and microbial specific growth rates (panel D) during time with updated equations and $D = 0.14 \text{ d}^{-1}$.

Thanks to the simulation by Toolbox Simulink it was possible to analyze the production of biomethane (Q) as a function of different parameter in the model. Starting from dilution rate (D), the function could be described by a second-grade equation ($y = -9.9166x^2 + 8.8125x + 0.124$, $R^2 = 0.99$), underlying the limit of the dilution that can cause wash out. With the equation it was also possible to calculate the dilution rate that provided the higher production of biomethane ($D = 0.4458 \text{ d}^{-1}$, $Q = 2.062 \text{ L/L}_{\text{medium}}/\text{d}$): the ability to foresee this value is clearly an advantage of the use of mathematical modeling. Nevertheless, the technical limitations of the plant available at the production site of the industrial partner of the project obliged to maintain $D = 0.14 \text{ d}^{-1}$ in the model.

Q was found to be a linear function of some parameters of the model (listed in Table 2), since their mathematical relationships could be described with first-grade equations. Nevertheless, the angular coefficient was not sufficient for comparisons, since the parameters have different orders of magnitudes among themselves. Therefore, we decided to compare the ratios between the single ratios of each parameter value and of the corresponding Q (Table 2), to understand how much an increase in the parameter value affect the increase of biomethane production (see “Materials and Methods” section).

Parameter	Value	Ratio	Q value	Q ratio	Q ratio/parameter ratio
Y_{acet/X_1}	20		1.198		
	40	2	1.933	1.62	0.81
	60	3	2.548	2.13	0.71
S_{1i} (g/L)	5.1		1.198		
	10.2	2	1.504	1.26	0.63
	15.3	3	1.807	1.51	0.50
S_{0i} (g/L)	30.6		1.198		
	61.2	2	2.001	1.67	0.84
	91.8	3	2.796	2.33	0.78
Y_e	0.55		1.198		
	1.1	2	2.001	1.67	0.84
	1.65	3	2.796	2.33	0.78

Table 2 Effect of the increment of the value of some parameters of the anaerobic digestion model on the value of biomethane production (Q).

Giving the importance of X_1 metabolism in anaerobic digestion, in particular for the production of acetate, Y_{acet/X_1} was modified to assess its impact on Q. Similarly, values for the initial concentration of glucose in the influent (S_{1i}) were considered, to simulate the effect of the addition of another residual biomass containing glucose. Finally, the concentration of insoluble organic compounds (S_{0i}), and the coefficient of decomposition (Y_e), counting which part of the insoluble organic compounds are transformed to soluble compounds, were considered as well. Table 2 shows that none of the modified parameters caused the same increase in Q and that the more the value was increased the lower was the effect on the corresponding ratio. In addition, implementation of S_{1i} had the minor effects, showing that additional glucose would not greatly impact on Q. On the other hand, S_{0i} and Y_e showed to be crucial for a relevant implementation of Q; unsurprisingly same increment of S_{0i} and Y_e produced the same values of Q, since they are both factors of equation 1.

Nevertheless, increasing the initial concentration of insoluble organic compounds could be problematic from a technical point of view, and furthermore organic loading rates exceeding the decomposition or the hydrolysis rates can determine a decline in methane production [5,14,15]. On the other hand, the coefficient of decomposition is a parameter that could be targeted more easily as it can be modified by pretreating the biomass with enzymes or composting [16,17]. Remarkably, when Q was considered as a function of the hydrolytic rate (β), a logarithmic equation was obtained ($R^2 = 0.91$), showing that an improvement in the ability of the microbial consortium to hydrolyse fibers was not going to be proportionally beneficial in the production of biomethane (Figure S1). These observations from the simulation of anaerobic digestion of manure may pave the way for further implementation of the real industrial process, and in turn, to the validation of the modified equations from the original ADM-1.

Conclusions

The quest for more sustainable energy source is intertwined with the development of technologies able to valorize renewable biomasses, with increased appeal if residual ones are used. Among those, animal manure is one of the most promising, because of abundance, low cost and intrinsic potential to be fermented into biogas. Biogas in fact can be directly used as source of energy or upgraded to biomethane, to be used in different sectors. In order to optimize anaerobic digestion of manure several settings and parameters could be modified, such as bioreactor type, pH and temperature, as well as organic loading rate [14]. Since the complex nature of a process dependent on heterogenous microbial consortia, the deployment of mathematical modeling of anaerobic digestion could be really helpful to direct possible manipulations. In this respect, in this work we modified equations from ADM-1 model in order to reflect better the microbiological reactions, that we described thermodynamically as well. We furthermore identified the relationship between the production of biomethane and specific process parameters, pinpointing that organic loading was decisive to improve the final product, confirming what is reported in literature also for this specific process. Future analysis will

involve the validation of the new model equations and the values obtained by real experiments in the industrial plant.

Materials and methods

Mathematical model of anaerobic digestion

The model structure presented in [10] was chosen because it is a relatively new modelling approach and this model has been built with laboratory data and further validated running a real process data by the authors. Starting point of that work was the Anaerobic Digestion Model No. 1 (ADM-1) developed by the International Water Association (IWA) for the use of activated sludge from the municipal wastewater treatment plants [11]. ADM-1 model have been successfully proposed for the production of biomethane from different residual sources [15,18]. The original equations taken into consideration modified from [10] were the following.

$$\frac{dS_0}{dt} = -\beta \frac{S_o \cdot X_1}{S_2 + S_3 + S_4 + K_{i0}} + DY_e \cdot S_{oi} + \lambda \left(\sum_{i=1}^6 b_i \cdot X_i \right) - DS_0 \quad (1)$$

$$\frac{dX_3}{dt} = (\mu_3 - b_3)X_3 - D \cdot X_3 \quad (6)$$

$$\frac{dX_1}{dt} = (\mu_1 - b_1)X_1 - D \cdot X_1 \quad (2)$$

$$\frac{dS_3}{dt} = Y_{but/X1} \cdot \mu_1 \cdot X_1 - Y_{but/X3} \cdot \mu_3 \cdot X_3 - D \cdot S_3 + S_{3i} \quad (7)$$

$$\frac{dS_1}{dt} = -Y_{glu/X1} \cdot \mu_1 \cdot X_1 + \beta \cdot \frac{S_o \cdot X_1}{S_2 + S_3 + S_4 + K_{i0}} - D \cdot S_1 + S_{1i} \quad (3)$$

$$\frac{dX_4}{dt} = (\mu_4 - b_4)X_4 - D \cdot X_4 \quad (8)$$

$$\frac{dX_2}{dt} = (\mu_2 - b_2)X_2 - D \cdot X_2 \quad (4)$$

$$\frac{dS_4}{dt} = Y_{acetl/X1} \cdot \mu_1 \cdot X_1 + Y_{acetl/X2} \cdot \mu_2 \cdot X_2 + Y_{acetl/X3} \cdot \mu_3 \cdot X_3 - Y_{acetl/X4} \cdot \mu_4 \cdot X_4 - D \cdot S_4 + S_{4i} \quad (9)$$

$$\frac{dS_2}{dt} = Y_{prop/X1} \cdot \mu_1 \cdot X_1 - Y_{prop/X2} \cdot \mu_2 \cdot X_2 - D \cdot S_2 + S_{2i} \quad (5)$$

$$Q = Y_{CH4/X4} \cdot \mu_4 \cdot X_4 \quad (10)$$

Variables and constant description

Parameters considered for this work were the following obtained from [10], that described anaerobic digestion in a continuously stirred tank reactor.

Variables

Q (L/L_{medium}/d) – biogas yield; S_o (g/L) – concentration of soluble organic compounds, measured as volatile solids; $S_{NH_4^+}$ – concentration of ammonia; S_1 (g/L) – concentration of glucose; S_2 (g/L) – concentration of propionate; S_3 (g/L) – concentration of butyrate; S_4 (g/L) – concentration of acetate.

X_1 (g/L) – concentration of glucose-fermenting acidogens; X_2 (g/L) – concentration of propionate-degrading acetogens; X_3 (g/L) – concentration of butyrate-degrading acetogens; X_4 (g/L) – concentration of acetoclastic methanogens; $\mu_1, \mu_2, \mu_3, \mu_4$ (d⁻¹) – corresponding specific growth rate, described as follow.

$$\mu_1 = \frac{\mu_{\max 1} \cdot S_1}{K_{S1} + S_1}$$

$$\mu_2 = \frac{\mu_{\max 2}}{(1 + K_{s2} / S_2) \cdot (1 + S_4 / K_{i,acet/prop})}$$

$$\mu_3 = \frac{\mu_{\max 3}}{(1 + K_{s3} / S_3) \cdot (1 + S_4 / K_{i,acet/but})}$$

$$\mu_4 = \frac{\mu_{\max 4} \cdot K_{i,NH_4^+} \cdot S_4}{(K_m \cdot X_4 + S_4) \cdot (K_{i,NH_4^+} + S_{NH_4^+})}$$

Constants

D (d⁻¹) = 0.1072 – dilution rate; β (d⁻¹) = 0.31 – hydrolytic rate; $K_{i,o}$ (g/L) = 0.23 – inhibition constant, reflecting the decrease of hydrolytic rate due to VFA accumulation; K_{i,NH_4^+} (g/L) = 0.5 – inhibition constant reflecting the decrease of acetoclastic methanogenesis rate due to ammonia accumulation; $K_{i,acet/prop}$ (g/L) = 0.96 – product inhibition constant, reflecting the decrease of propionate degradation rate due to acetate accumulation; $K_{i,acet/but}$ (g/L) = 0.72 – product inhibition constant, reflecting the decrease of butyrate degradation rate due to acetate accumulation; Y_e = 0.55 – coefficient of decomposition, counting what part of insoluble organic compounds are transformed to soluble compounds; S_{oi} = 30.6 g/L – concentration of insoluble organic compounds, measured as total solids; S_{i1}, S_{i2}, S_{i3} and S_{i4} (g/L) are the concentrations of the corresponding substrates in the influent; S_{i1} = 5.1, S_{i2} = 1.6, S_{i3} = 0.1 and S_{i4} = 3.1.

$K_m = 1.3$ – coefficient in the Contois growth rate model for μ_4 , reflecting the decrease of acetoclastic methanogenesis rate due to biomass accumulation; K_{S1} (g/L) = 4.8 – saturation constant for glucose-fermenting acidogens; K_{S2} (g/L) = 0.93 – saturation constant for propionate-degrading acetogens; K_{S3} (g/L) = 0.176 – saturation constant for butyrate-degrading acetogens

μ_{max1} (d^{-1}) = 0.7 – maximum specific growth rate of glucose-fermenting acidogens at 34 °C; μ_{max2} (d^{-1}) = 0.54 – maximum specific growth rate of propionate-degrading acetogens; μ_{max3} (d^{-1}) = 0.68 – maximum specific growth rate of butyrate-degrading acetogens at 34 °C; μ_{max4} (d^{-1}) = 0.45 – maximum specific growth rate of acetoclastic methanogens at 34 °C; b_i ($i = 1, \dots, 4$) – mortality rates for each of the four bacterial populations (it was supposed that $b_i = 0.05\mu_{maxi}$). It was assumed that a part of the dead cells is transformed into soluble organics with recycling conversion factor λ ($\lambda > 0$ and $\lambda < b_i$).

Yield coefficients of production or consumption: $Y_{glu/X1} = 12.9$ g/g biomass, $Y_{acet/X1} = 20$ g/g biomass, $Y_{prop/X1} = 2.94$ g/g biomass, $Y_{prop/X2} = 10.2$ g/g biomass, $Y_{but/X1} = 3.08$ g/g biomass, $Y_{but/X3} = 11.9$ g/g biomass, $Y_{acet/X2} = 8$ g/g biomass, $Y_{acet/X3} = 1.54$ g/g biomass, $Y_{acet/X4} = 16$ g/g biomass, $Y_{CH4/X4} = 4$ L/g biomass.

Mathematical model of anaerobic digestion

The biochemical reactions from glucose to biomethane described in the model were stoichiometrically balanced and analyzed using the biochemical thermodynamics calculator eQuilibrator [19]. For each equation estimated Gibbs free energy ($\Delta_r G'^{\circ}$) and equilibrium constant (K'_{eq}) were calculated.

Simulation studies

The mathematic model was recreated on Simulink (MathWorks, Massachusetts, USA) and run via data uploaded on MatLab (MathWorks, Massachusetts, USA). Differential equations of the model were modified on Simulink and then run to verify the hypotheses. Similarly, value for some parameters were modified on MatLab and the Simulink model was run to foresee the effect of such modifications on the production of biomethane. Excel (Microsoft,

New Mexico, USA) was then used to calculate equations of the relationship between single parameters and biomethane production.

Supplementary materials

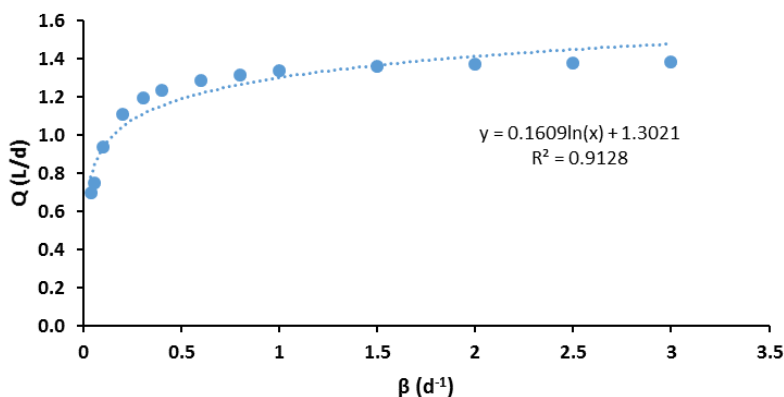


Table 2 Biomethane production (Q) as function of hydrolytic rate (β).

References

1. The European Parliament and the Council of the European Union. Directive 2009/28/EC on the promotion of the use of energy from renewable sources and amending and subsequently repealing Directives 2001/77/EC and 2003/30/EC. 2009.
2. D'Adamo I, Falcone PM, Ferella F. A socio-economic analysis of biomethane in the transport sector: The case of Italy. *Waste Manag.* 2019;95:102–15.
3. Barbera E, Menegon S, Banzato D, D'Alpaos C, Bertucco A. From biogas to biomethane: A process simulation-based techno-economic comparison of different upgrading technologies in the Italian context. *Renew Energy.* Elsevier Ltd; 2019;135:663–73.
4. Adnan AI, Ong MY, Nomanbhay S, Chew KW, Show PL. Technologies for biogas upgrading to biomethane: A review. *Bioengineering.* 2019.
5. Mao C, Feng Y, Wang X, Ren G. Review on research achievements of biogas from anaerobic digestion. *Renew. Sustain. Energy Rev.* Elsevier Ltd; 2015. p. 540–55.
6. Esteves EMM, Herrera AMN, Esteves VPP, Morgado C do RV. Life cycle assessment of manure biogas production: A review. *J Clean Prod.* 2019;219:411–23.
7. Paolini V, Petracchini F, Segreto M, Tomassetti L, Naja N, Cecinato A. Environmental impact of biogas: A short review of current knowledge. *J Environ Sci Heal - Part A Toxic/Hazardous Subst Environ Eng.* Taylor and Francis Inc.; 2018;53:899–906.
8. Zhu T, Curtis J, Clancy M. Promoting agricultural biogas and biomethane production:

Lessons from cross-country studies. *Renew Sustain Energy Rev.* 2019;114.

9. Jiang LL, Zhou JJ, Quan CS, Xiu ZL. Advances in industrial microbiome based on microbial consortium for biorefinery. *Bioresour. Bioprocess.* Springer; 2017.
10. Simeonov I, Karakashev D. Mathematical Modelling of the Anaerobic Digestion Including the Syntrophic Acetate Oxidation. *IFAC Proc. Vol. IFAC*; 2012.
11. Batstone DJ, Keller J, Angelidaki I, Kalyuzhnyi S V., Pavlostathis SG, Rozzi A, et al. The IWA Anaerobic Digestion Model No 1 (ADM1). *Water Sci Technol.* 2002;45:65–73.
12. Zhang J, Guo RB, Qiu YL, Qiao JT, Yuan XZ, Shi XS, et al. Bioaugmentation with an acetate-type fermentation bacterium *Acetobacteroides hydrogenigenes* improves methane production from corn straw. *Bioresour Technol.* Elsevier Ltd; 2015;179:306–13.
13. Simeonov I, Kroumov A. A Mathematical Study of the Impact of Methanogenic and Hydrogenotrophic Steps on Biomethane Production From Organic Wastes. *Effic énergétique - sources d'énergies renouvelables - Prot l'environnement COFRET'12*, Sozopol, Bulg. 2012
14. Khan MA, Ngo HH, Guo WS, Liu Y, Nghiem LD, Hai FI, et al. Optimization of process parameters for production of volatile fatty acid, biohydrogen and methane from anaerobic digestion. *Bioresour Technol.* 2016;219:738–48.
15. Li H, Chen Z, Fu D, Wang Y, Zheng Y, Li Q. Improved ADM1 for modelling C, N in anaerobic digestion process of pig manure and optimization approaches to biogas production. 2019
16. Yang Q, Luo K, Li X ming, Wang D bo, Zheng W, Zeng G ming, et al. Enhanced efficiency of biological excess sludge hydrolysis under anaerobic digestion by additional enzymes. *Bioresour Technol.* 2010;101:2924–30.
17. He XS, Xi BD, Jiang YH, He LS, Li D, Pan HW, et al. Structural transformation study of water-extractable organic matter during the industrial composting of cattle manure. *Microchem J.* 2013;106:160–6.
18. Biernacki P, Steinigeweg S, Borchert A, Uhlenhut F. Application of Anaerobic Digestion Model No. 1 for describing anaerobic digestion of grass, maize, green weed silage, and industrial glycerine. *Bioresour Technol.* 2013;127:188–94.
19. Flamholz A, Noor E, Bar-Even A, Milo R. EQUilibrator - The biochemical thermodynamics calculator. *Nucleic Acids Res.* 2012;40.

Conclusions

In order to detach from mankind dependence on fossil resources, bioeconomy is exploring the potential of renewable biomasses beyond the conventional use in forestry and agriculture. In fact, the components of these raw materials can be valorized for the production of different fine and bulk chemicals. Since the wide range of biomasses to choose from, cascading principles suggest that high-value commodities, needed in low volumes, can be obtained from biomasses available in minor quantity or not entirely exploited in other sectors. On the other hand, low-value compounds must derive from biomasses that have a low-value as well, like residual ones, but largely abundant. In this scenario, different types of bioprocesses can be developed within biorefineries, often deploying microbial cell factories, since their natural metabolism is prone to transform biomass components into various compounds. In addition, genetic engineering and synthetic biology approaches can further improve the ability of these microbial helpers. The strategy to ameliorate bioprocesses must be coherent with the cascading principles as well, since high cost of development, like in the case of genetic modifications, can be sustained only when the final product has an high value; whereas computational simulation, that are generally less expensive, may be useful to foresee the best conditions to be tested. Together with these exemplificative strategies, deployment of other devices of biological origin can be considered, such as the use of enzymatic cocktails, able to release sugars from residual biomasses for the subsequent microbial fermentation, thus unlocking their potential.

Therefore, biodiversity must be a crucial cornerstone for bioprocesses to foster a transition to bioeconomy. For this reason, in this work we explored biodiversity in different terms, namely of biomass, enzymes, microbial cell factories, bioproducts and strategies. With these propositions in mind, the present Doctoral work offers some examples about the utilization of different biomass feedstocks and the tailoring of various microbial cell factories for the scope, displaying strategies in accordance to the cascading principles. The



goal was the production of different fine and bulk chemicals, to show the wide applicability of biobased processes, and therefore the connections between industrial and microbial biotechnology with bioeconomy.

In order to explore biomasses not considered yet for microbial based processes, in Chapter 1 and 2 we described the production of carotenoids from *Camelina* meal hydrolysates (obtained using an enzymatic cocktail) by the yeast *R. toruloides*. Considering the possible future technology transfer, we explored different conditions of industrial relevance to increase productivity and specific productivity, such as different process types and optimization of the amount of enzymatic cocktail added and total solid loading.

Finally, the process demonstrated to be reproducible in bioreactor, both considering the hydrolysis and the fermentation, obtaining quantitative data able to describe the process. The developed bioprocess paves the way to different scenarios, first the exploitation of an underrated residual biomass such as *Camelina* meal, only used for the feed sector. In fact, by the valorization of this biomass through the enzymatic hydrolysis and fermentation with the cell factory *R. toruloides* (combined or separated), it is possible to mine additional value, in terms of production of carotenoids. Since these molecules have application in the feed sector as well, their obtainment from *Camelina* meal potentially matches the two supply chains. Furthermore, the optimizations here disclosed show that this bioprocess can be customized considering the needs of the specific production plant, in terms of biomass availability, enzyme cost, fermentation volume and time, and final product. These adaptable features are pivotal in the bioeconomy scenario, in order to develop resilient processes from various point of view. In addition, in order to increase the appeal of biorefineries, they must be developed considering the overall picture in which they will be integrated, as a single ring of a longer chain, as in the case of the process described in Chapter 1 and 2. Therefore, the multidisciplinary nature of biotechnologists is pivotal to think beyond the development of the process itself.

In Chapter 3 we described a process that particularly fits in this context as well, since polyphenol extraction waste from cinnamon (C-PEW) was successfully hydrolysed and then provided as sole medium for several tested fungal species that are known as microbial cell factories. Among them, *R. toruloides* was able to consume sugars of cinnamon origin and

to produce carotenoids. Two main conclusions could be drawn from these results. First, also in this case the production of carotenoids is in line with the supply chain where the biomass (C-PEW) comes from, since the spice industry is strongly related to food, cosmetics and dye sectors as carotenoids themselves. Specifically, residual biomasses from spices are rarely considered for the development of bioprocesses based on microbial cell factories, since their natural antimicrobial activity. Here we demonstrated that this path is possible and worthwhile for further exploration, considering also the microbial biodiversity that we can source from. The successful on-plate test of several other fungal species underlines that further bioprocess could be developed from the use of biomasses of cinnamon origin, potentially expanding it to other spices. In this context, both the works on cinnamon and *Camelina* meal clearly foster the use of *R. toruloides* as microbial workhorses able to exploit underrated residual biomasses for the production of carotenoids, in tunable and tailored biobased processes.

Nevertheless, among microbial cell factories, the yeast *S. cerevisiae* remains one of the species of election for the production of both fine and bulk chemicals. Since its relevance, industrial biotechnologists should have extensive knowledge regarding this specie, its features and its genetic modification tools. In fact, the principles applied to *S. cerevisiae* during the last decades can be then transposed to other species of putative industrial relevance, although a simplistic approach must be avoided. In this respect, in Chapter 4 we described how exogenous and endogenous genes were inserted in *S. cerevisiae* to modulate the pathways leading from glucose to the production of the main components of folates moieties, thus highlighting how further modifications may increase the production of folates in the forms more useful to human nutrition. In fact, since the importance of folates in daily human intake, their production by sustainable bioprocesses is desirable. This work paves the way to further understanding the biochemical mechanism leading to folates in *S. cerevisiae*, and to implement modifications to these pathways in order to increase the production of folates. Since the wide use of this yeast specie in second generation biorefineries, it is possible to foresee applications of such modified strains in the obtainment of folates from low value substrates as well, in order to overcome and implement the basic principles of cascading.

Finally, industrial biotechnology should be comprehensive of “simpler” processes as well, since they can guarantee relevant outcomes: nonetheless, their simplicity is only illusory, since they often hide complex structure, to be addressed with technological solutions. In Chapter 5 in fact we focused our attention on a bioprocess based on a low-cost substrate and product, namely the production of biogas from manure during anaerobic digestion by microbial consortia. An updated mathematical computational model describing the process was used to forecast the effect of the modification of specific parameters on the production of biomethane, thus providing industrial partner with relevant hints for further improvement. These results are in line with the field of research engaged in optimizing the use of an inexpensive (and polluting) raw material such as manure, to produce biogas, whose biomethane has the potential to substitute the corresponding fossil counterpart, thus nestling this project in the context of bioeconomy and sustainability as well. Considering the cascading principles, computational model implementations are indeed relatively cheaper than the development of an entire set of experiments aimed to understand the key parameters to address modification and subsequently improve the production of biomethane.

Although the utmost importance of these research topics, their complex technical and theoretical details need to be delivered to the different actors of society. In order to show to various stakeholders involved in science development as well (*e.g.* general audience, mass-media, economic, politics), during this doctoral work several activities of Responsible Research and Innovation (RRI), outreach and science communication were performed, by the means of papers, public events, publications (books, articles in newspapers and magazines) and social media (*e.g.* Instagram, Twitter, YouTube), as show in the next sections of this work.

Taken together, this work explored different topics related to the development of biobased processes, like the exploitation of renewable raw materials of various origin, the obtaining of chemicals with different market value and alternative strategies to improve the processes. These are definitely “hot topics” that will surely be increasingly addressed by several stakeholders, from economical to political ones, as well as social. Therefore, this Doctoral work was aimed to further improve the scientific knowledge related to the

exploitation of biomasses (mainly residual ones) to produce fine and bulk chemicals of industrial relevance, revealing at the same time the extraordinary potential of microbial biodiversity. Cascading principles have been the unifying concepts of this work, together with a multidisciplinary approach that is the real strength of industrial biotechnologists. This is paving the way for further application of the bioprocesses in the worldwide scenario of bioeconomy.

Acknowledgments

Many people have helped me during my PhD journey, scientifically, economically and personally. I would like to thank above all Prof. Paola Branduardi for support at all those levels and mentoring during the last years, providing the fertile soil to develop my own idea of biorefinery, and permitting me to explore the various innovative aspects of this sector.

Many thanks to all the present and past members of the BioIndTech Lab research group and in particular to my Master's student Chiara Cantù and Bachelor's student Mariachiara Nova for the fundamental help in developing the research projects here disclosed.

I deeply acknowledge several members of the Department of Biotechnology and Bioscience of University of Milano Bicocca and the Bicocca Center of Science and Technology for Food (Best4Food) members for the fruitful collaboration. In particular, Prof. Massimo Labra for funding opportunities with Food Social Sensor Network (FOOD NET), Dott. Ilaria Bruni and Stefania Pagliari and Chiara Magoni from ZooPlantLab for collaboration.

Similarly, I would like to thank co-authors of published (or published-to-be) scientific paper, Prof. Danilo Porro (University of Milano Bicocca, Italy), Prof. Maurizio Bettiga (University of Chalmers, Sweden) and Prof. John P. Morrissey (University College Cork, Ireland), for helping me as well in dealing with scientific writing. Furthermore, thanks to Prof. Anù Sirvio, Prof. Mika Ruusunen and Prof. Aki Sorsa from University of Oulu (Finland) for welcoming me in the context of the project ADMA2 funded by the European Institution of Innovation & Technology (EIT) KIC-RawMaterials.

I would like to thank the reviewers of this work for revision and comments that have been very useful to improve the manuscript itself, as well as the members of the PhD dissertation committee.

Many thanks of course to friends and family for the never-ending support, as well as to the science communication community for the fruitful collaborations.



Academic and outreach activities

Academic activities

1. **Subject matter scholar** for “Processi Industriali e Bioraffinerie” (BiP) course.
Università degli Studi Milano Bicocca (from 2017).
2. **Reviewer**
Peer-review reviewer for the international journal *Biotechnology for Biofuels* (from 2020).
3. **Master’s thesis Co-supervisor**
Università degli Studi Milano Bicocca
2020 - Chiara Cantù “Sviluppo di bioraffinerie di seconda generazione per la produzione di molecole di interesse per il settore alimentare”.
4. **Bachelor’s thesis Co-supervisor**
Università degli Studi Milano Bicocca
2019 – Mariachiara Nova “Sviluppo di un biosensore per *Vibrio cholerae* utilizzando un sistema di quorum sensing in *E. coli* ricombinante”
2018 – Miryam Bernardi “Dal tutolo al butanolo: viaggio di un bioprocesso consolidato”
2018 – Jacopo Gobbato “Microalga *Chlorella sp.* C2 per lo smaltimento di scarti industriali accoppiato alla produzione di biocarburanti”
2017 – Luca Mastella “Overespressione del gene DGAT2 per la produzione di triacilgliceroli in *Neochloris oleoabundans*”
5. **Teacher for Piano Nazionale Lauree Scientifiche (PLS)** (from 2019). Università degli Studi Milano Bicocca



Seminars

1. Nov 2020 - **Science and Social Media - A biotech approach** – Lecturer for the course Soft skills for the academia and industry of the MS degree course Biotechnology for the Bioeconomy, at **Università degli Studi di Milano**.
2. Nov 2020 - **Development of second generation biorefineries** – Lecturer for Enzyme Engineering and Structural Biology group, **Denmark Technical University (DTU)**.
3. Mar 2020 - **Science and Social Media - A biotech approach** – Lecturer for the course Soft skills for the academia and industry of the MS degree course Biotechnology for the Bioeconomy, at **Università degli Studi di Milano**.

Outreach activities

1. **Women in Sciences - Scienze con la D maiuscola** - Department of Biotechnology and Biosciences, University of Milan - Bicocca.
2. **FameLab 2019** - National Final in Milan.
3. **FameLab 2019** - Semifinal 1 and local Final in Pavia.
4. **European Researcher's Night** ed. 2017 (Meet Me Tonight, Milan) – Stand “Il circo del benessere”

Awards and scholarships

Awards

1. Award “Paola de Paoli – Camillo Marchetti” by Unione Giornalisti Italiani Scientifici (UGIS) for science communication in 2021.
2. Best poster award at the International Forum on Industrial Biotechnologies (IFIB) 2020, with “Enzymatic hydrolysis of residual biomasses for carotenoids production by *Rhodosporidium toruloides*”.
3. First prizes for the best oral presentation of the III-year PhD student during PhD meeting 2020 of the Department of Biotechnology and Biosciences of Università degli Studi di Milano Bicocca from both the scientific committee and the PhD student vote.
4. First Prize of Premio Nazionale di Divulgazione Scientifica 2017 of Associazione Italiana del Libro for Under 35 category with “Geneticamente modificati - Viaggio nel mondo delle biotecnologie” (Hoepli).
5. Finalist for the category “Scientific articles” of Premio Nazionale di Divulgazione Scientifica 2020 dell’Associazione Italiana del Libro, with “Gli sfidanti microbici della plastica” (Macplas n.376).
6. Finalist for the category “Scientific articles” of Premio Nazionale di Divulgazione Scientifica 2019 dell’Associazione Italiana del Libro, with “Le bioplastiche vanno in scena: atto I” (Macplas n.328).
7. Second place at the local final of FameLab 2019, Teatro Politeama Pavia, and consequent qualification to the national grand final.

Scholarships

1. Grant from the European COST Action CA18229 Yeast4Bio for a short-term scientific mission in 2021 at the University of Tartu (Estonia).
2. FEMS bursary for the congress Microbial Stress 2020 from the Federation of European Microbiological Societies (FEMS).
3. Scholarship for research activity titled “Development of sustainable biotechnological processes for the valorization of agricultural and animal waste products” for the duration of 6 months, at the Department of Biotechnology and Biosciences of Università degli Studi di Milano Bicocca. Scholarship renewed for other 24 months.

Publications

Published Papers

1. Bertacchi S., Pagliari S., Cantù C., Bruni I., Labra M., Branduardi P. (2021) **Enzymatic hydrolysate of cinnamon waste material as feedstock for the microbial production of carotenoids**. Special issue Industrial Microbiology and Bioprocess Technology of the *International Journal of Environmental Research and Public Health*. 2021; 18(3):1146.
2. Bertacchi S., Bettiga M., Porro D., Branduardi P. (2020) **Camelina sativa meal hydrolysate as sustainable biomass for the production of carotenoids by Rhodosporidium toruloides**. *Biotechnology for Biofuels* 13.1: 1.10.
3. Brambilla M., Martani F., Bertacchi S., Vitangeli I., Branduardi P. (2019). **The Saccharomyces cerevisiae poly(A) binding protein (Pab1): Master regulator of mRNA metabolism and cell physiology**. *Yeast*, 36(1), 23-34.
4. Magoni C., Campanaro A., Galimberti A., Pesciaroli C., Bertacchi S., Branduardi P., & Labra M. (2018). **RRI Approach for Development and Acceptance of Novel Fish Feed Formulations in Aquaculture**. In *Governance and Sustainability of Responsible Research and Innovation Processes* (pp. 65-70). Springer, Cham.

Papers accepted, submitted or in preparation

1. Mastella L.*, Bertacchi S.*, Berterame NM.*, Bertolesi T., Branduardi P. (2021) **Assessment of folates forms produced by wild type and engineered Saccharomyces cerevisiae yeast cells**. Submitted to FEMS Yeast Research.
2. Bertacchi S.*, Jayaprakash P.* Morrissey J.P., Branduardi P. **Enzymatic hydrolysis of lignocellulosic biomasses matching yeast fermentation requirements in biorefineries: state of the art**. Manuscript in submission.



3. Giustra C.M., Cozza R., Magoni C., Bertacchi S., Torelli A., Labra M., Branduardi P. **Microalgae scenery in Europe: current situation and challenges**. Manuscript in preparation.
4. Bertacchi S., Cantù C., Branduardi P. **Optimization of carotenoids production from *Camelina sativa* meal hydrolysate by *Rhodospiridium torulooides***. Manuscript in preparation.

Patents

1. Porro D., Branduardi P., Bertacchi S., Berterame N.M. **Process for cellular biosynthesis of poly d-lactic acid and poly l-lactic acid** (2018). WO2020025694A1

Books

1. Bertacchi S. **Piccoli geni – Alla scoperta dei microrganismi** (2021). Hoepli Editore, ISBN 9788820399962.
2. Pistore G., Brusaferrò S., Ricciardi W., Villa R. Galassi F.M., Cartabellotta N., Di Grazia S., Cossarizza A., Silenzi A., Gorini G., Bertacchi S. **Il Virus che non Esisteva: Un viaggio nella Scienza che ci tirerà fuori da questa situazione** (2021). ISBN 979-8584657772
3. Bertacchi S. **Geneticamente modificati - Viaggio nel mondo delle biotecnologie** (2017). Hoepli Editore, ISBN 9788820379834.

Publications in newspapers and magazines

1. Bertacchi S. **Alle origini della plastica “naturale”** (2020). Macplas n.379 - notizie per l'industria delle materie plastiche e della gomma.
2. Bertacchi S. **Resilienza scientifica, comunicativa e sociale** (2020). #postdautore Fatti non Fake, blog of Federchimica.
3. Bertacchi S. **Piante geneticamente vaccinate** (2020). Sapere Scienza.



4. Bertacchi S. **Gli sfidanti microbici della plastica - la biodegradazione delle plastiche convenzionali parte II** (2020). Macplas n.376 - notizie per l'industria delle materie plastiche e della gomma.
5. Bertacchi S. **Microbe's got talent - la biodegradazione delle plastiche convenzionali parte I** (2020). Macplas n.375 - notizie per l'industria delle materie plastiche e della gomma.
6. Bertacchi S. **Le bioplastiche danno i numeri** (2019). Macplas n.330 - notizie per l'industria delle materie plastiche e della gomma.
7. Bertacchi S. **Le bioplastiche vanno in scena: atto II** (2019). Macplas n.329 - notizie per l'industria delle materie plastiche e della gomma.
8. Bertacchi S. **Le bioplastiche vanno in scena: atto I** (2019). Macplas n.328 - notizie per l'industria delle materie plastiche e della gomma.
9. Bertacchi S., Labra M., Branduardi P. **Biotrasformazioni in ambito mangimistico: ruolo bioeconomico di innovazione multidisciplinare** (2018). Eurofishmarket.
10. Bertacchi S. **Amore di (bio)plastica**. SAPERE, 2018(2), 10-15.
11. Bertacchi S., Berterame N.M., Branduardi P. **Nano e bio: i due prefissi dei materiali innovativi** (2017) Automazione Oggi.

RESEARCH

Open Access



Camelina sativa meal hydrolysate as sustainable biomass for the production of carotenoids by *Rhodospiridium toruloides*

Stefano Bertacchi¹ , Maurizio Bettiga^{2,3}, Danilo Porro¹ and Paola Branduardi^{1*} 

Abstract

Background: As the circular economy advocates a near total waste reduction, the industry has shown an increased interest toward the exploitation of various residual biomasses. The origin and availability of biomass used as feedstock strongly affect the sustainability of biorefineries, where it is converted in energy and chemicals. Here, we explored the valorization of *Camelina* meal, the leftover residue from *Camelina sativa* oil extraction. In fact, in addition to *Camelina* meal use as animal feed, there is an increasing interest in further valorizing its macromolecular content or its nutritional value.

Results: *Camelina* meal hydrolysates were used as nutrient and energy sources for the fermentation of the carotenoid-producing yeast *Rhodospiridium toruloides* in shake flasks. Total acid hydrolysis revealed that carbohydrates accounted for a maximum of $31 \pm 1.0\%$ of *Camelina* meal. However, because acid hydrolysis is not optimal for subsequent microbial fermentation, an enzymatic hydrolysis protocol was assessed, yielding a maximum sugar recovery of 53.3%. Separate hydrolysis and fermentation (SHF), simultaneous saccharification and fermentation (SSF), and SSF preceded by presaccharification of *Camelina* meal hydrolysate produced 5 ± 0.7 , 16 ± 1.9 , and 13 ± 2.6 mg/L of carotenoids, respectively. Importantly, the presence of water-insoluble solids, which normally inhibit microbial growth, correlated with a higher titer of carotenoids, suggesting that the latter could act as scavengers.

Conclusions: This study paves the way for the exploitation of *Camelina* meal as feedstock in biorefinery processes. The process under development provides an example of how different final products can be obtained from this side stream, such as pure carotenoids and carotenoid-enriched *Camelina* meal, can potentially increase the initial value of the source material. The obtained data will help assess the feasibility of using *Camelina* meal to generate high value-added products.

Keywords: Bio-based products, Renewable resources, Biorefinery, *Camelina* meal, Enzymatic hydrolysis, *Rhodospiridium toruloides*, Carotenoids, Separate hydrolysis and fermentation (SHF), Simultaneous saccharification and fermentation (SSF)

Background

The continued use of fossil resources poses an ecological, economic, and political problem that has sparked the search for alternative sources of energy, chemicals, and materials. Biorefineries, which transform biomass into energy and chemicals, offer a possible answer, particularly in the form of microbial cell factories. The sustainability of biorefineries is strongly related to the origin,

*Correspondence: paola.branduardi@unimib.it

¹ Department of Biotechnology and Biosciences, University of Milano-Bicocca, Piazza della Scienza 2, 20126 Milan, Italy

Full list of author information is available at the end of the article



© The Author(s) 2020. This article is licensed under a Creative Commons Attribution 4.0 International License, which permits use, sharing, adaptation, distribution and reproduction in any medium or format, as long as you give appropriate credit to the original author(s) and the source, provide a link to the Creative Commons licence, and indicate if changes were made. The images or other third party material in this article are included in the article's Creative Commons licence, unless indicated otherwise in a credit line to the material. If material is not included in the article's Creative Commons licence and your intended use is not permitted by statutory regulation or exceeds the permitted use, you will need to obtain permission directly from the copyright holder. To view a copy of this licence, visit <http://creativecommons.org/licenses/by/4.0/>. The Creative Commons Public Domain Dedication waiver (<http://creativecommons.org/publicdomain/zero/1.0/>) applies to the data made available in this article, unless otherwise stated in a credit line to the data.

availability, and market of biomass. For example, edible crops have been exploited for decades as feedstocks for the production of several fine and bulk chemicals. However, environmental and social issues, caused by direct or indirect competition with the food sector, discourage the use of agricultural products and land for large-scale production of commodities [1]. At the same time, the existing linear economy's logic of "take, make, dispose" is generating a large amount of waste, including organic matter. For these reasons, biorefineries based on residual biomasses have drawn increasing scientific and industrial interest. Microbial cell factories are especially attractive; however, conventional pretreatments and saccharification processes of residual biomasses often release toxic compounds that can impair microbial growth and synthesis of the target product [2]. These issues need to be factored in when developing robust biorefineries capable of generating high-value molecules from low-cost substrates.

The growing use of oilseed crops for food and biofuels is leading to a surplus of process leftovers that are currently used mainly as animal feed [3] owing to their protein, carbohydrate, and fiber content. A good example is *Camelina* meal (or cake), the main by-product of oil extraction from *Camelina sativa* seeds [4–8], which is a common supplement of cattle and poultry diet. However, the rich composition and relatively low cost (\$0.25/kg) of *Camelina* meal [9], make it attractive for the development of sustainable bio-based processes that would either further valorize its macromolecular components or increase its nutritional value in animal feed. So far, only Mohammad et al. [10] have attempted to use *Camelina* meal, mixed with other *Camelina*-derived sugars, for the production of bioethanol, a low value-added molecule, by *Saccharomyces cerevisiae*. To improve the economic viability of the process, the present study assessed the microbial biotransformation of *Camelina* meal into carotenoids as high value-added products.

The global market value for carotenoids was estimated to be \$1.5B in 2017 and is expected to reach \$2.0B by 2022, with a compound annual growth rate of 5.7% [11–13]. Carotenoids are found mainly in animal feed (41% of total revenue), followed by food and dietary supplements owing to their beneficial effect on human health [12, 14]. Ruminants are entirely dependent on feed as a source of carotenoids, since they cannot produce them on their own [3]. Chemical synthesis of carotenoids from synthetic resources meets 80–90% of the market needs, but the increasing demand for naturally produced molecules has sparked the search for new, preferably vegetal sources [12]. β -Carotene alone has a market value of \$246.2M. Natural β -carotene can be extracted from carrots and fruits of oil palm, but recent attempts have demonstrated

the commercial production of β -carotene in microbial cell factories employing the microalga *Dunaliella salina* or the filamentous fungus *Blakeslea trispora* [12]. Unfortunately, algal carotenoid production is generally expensive and requires large areas for cultivation [15, 16], whereas filamentous fungi are frequently characterized by slow growth and a multicellular nature that may impair productivity [17]. Yeasts could potentially improve the overall sustainability of the process. In particular, the oleaginous yeast *Rhodospiridium (Rhodotorula) toruloides*, also known as "pink yeast", naturally accumulates carotenes and xanthophylls, such as β -carotene, torulene, and torularhodin [16, 18, 19]. *R. toruloides* can use different sugars, such as glucose, cellobiose, sucrose, mannose, xylose, arabinose, and galacturonic acid, as main carbon sources [20]. In addition, *R. toruloides* converts complex substrates, such as carob pulp syrup, sugarcane bagasse, corn stover, and food wastes, into lipids and/or carotenoids [21–24]. Therefore, this yeast is a good candidate for the development of second-generation biorefineries.

To produce carotenoids in *R. toruloides*, *Camelina* meal was first saccharified by enzymatic hydrolysis. Then, the released sugars were used as feedstock in separate hydrolysis and fermentation (SHF). An alternative simultaneous saccharification and fermentation (SSF) process was also assessed. Results indicate that *Camelina* meal and *R. toruloides* can be used for the development of a novel bio-based process for carotenoids production. Moreover, the obtained data will facilitate further optimization of process conditions.

Results and discussion

Evaluation of total sugar content in *Camelina* meal and optimization of enzymatic hydrolysis

The content of water, insoluble components, acetic acid, and sugars in *Camelina* meal was quantified following acid hydrolysis. Acetic acid and sugars were analyzed also after enzymatic hydrolysis, as no enough data exist in literature to assess the use of *Camelina* meal as substrate for microorganisms. As shown in Table 1, almost one-third (31%) of *Camelina* meal was composed of sugars. Of these, glucose and fructose accounted for more than two-thirds (w/w) as revealed by high-performance liquid chromatography (HPLC) analysis. Even though acid hydrolysis can be suitable for saccharification, its use is limited by the low final pH, which needs to be neutralized before sugars are added to the cells, and by the release of inhibitory compounds such as furfurals [2, 25]. These limitations negatively affect the sustainability of the overall biorefinery process in terms of use and disposal of acid solutions [25]. Therefore, to release monomeric sugars from their polymeric form, an enzymatic instead of an acid hydrolysis was performed under different test

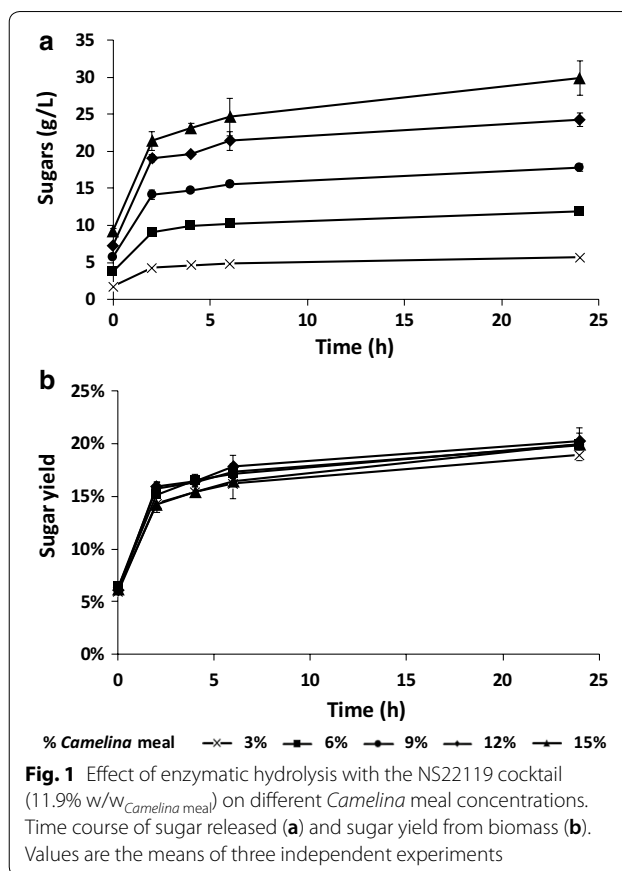
Table 1 *Camelina* meal hydrolysate composition following acid treatment

<i>Camelina</i> meal composition	
Measured component	Percentage (w/w)
Water	9 ± 1.8%
Acetate	11 ± 1.4%
Insoluble fraction	13 ± 1.4%
Sugars of which	31 ± 1.0%
Glucose	16 ± 0.9%
Fructose	8.3 ± 0.0%
Arabinose	6.9 ± 0.0%
Crude protein	35.2–46.9% [7]
Crude fat	4.9–11.9% [7]

Values are the means of three independent experiments

conditions (see below). The other main components of *Camelina* meal, as reviewed by [7], are crude proteins and crude fats, which account for 35.2–46.9% and 4.9–11.9% of total biomass, respectively, as well as micronutrients such as vitamins; whereas the insoluble fraction is composed mainly of lignin and ashes. Based on these data, we hypothesized that *Camelina* meal could be a suitable substrate for the growth of *R. toruloides* and carotenoid production.

Enzymatic hydrolysis can be performed under conditions that are generally more compatible with subsequent growth of mesophilic microbial cell factories. Moreover, it can take advantage of a broad range of commercially available enzymatic cocktails [26, 27]. Here, this step was optimized using the commercial cocktail NS22119 (Novozymes A/S), which can release both hexose and pentose sugars. Different initial concentrations of *Camelina* meal were tested to determine the effect of solids loading on sugar release. After autoclaving, the measured pH was 5.5, which was compatible with enzymatic catalysis, as NS22119 is supposed to retain up to 90% of its maximum activity at this pH, according to the indications of the producer. Remarkably, the pH remained constant until the end of hydrolysis, which reduced both the economic and environmental impact of the procedure, as neither neutralization nor additional buffer was required. As shown in Fig. 1a, pretreatment of biomass by autoclaving resulted in the initial concentration of released sugars to range from 1.8 ± 0.03 to 9 ± 0.3 g/L. The values reflected the amount of biomass loaded at the beginning of the experiment. After enzymatic treatment (11.9% w/w *Camelina* meal), the concentration of free sugars rose to at least double the initial amount, independently of the quantity of loaded biomass (Fig. 1a). No additional release of sugar was detectable over time from negative



control samples, in which 3% or 15% of the initial biomass but no enzyme was incubated in a shaking water bath at 50 °C (Additional file 1: Figure S1). The sugar titer increased in the presence of enzymes in a linear manner ($R^2 = 0.98$, $p < 0.001$, calculated with R) until 24 h in respect to the initial quantity of biomass. Hence, the yield of sugars released by enzymatic hydrolysis was constant regardless the concentration of *Camelina* meal (Fig. 1b) and the maximum yield of sugars over total biomass was 20% after 24 h. Considering the original amount of carbohydrates, a sugar recovery of 65% was calculated (see “Calculations and statistical analyses” section), which is in accordance with commonly reported values for lignocellulose enzymatic hydrolysis [28, 29].

Based on these data, successive experiments were performed using *Camelina* meal at the maximum tested solids loading (15% w/v). To determine if sugar recovery could be further improved in spite of a possible inhibition of enzymatic activity by released products or by biomass itself, two different strategies were designed. In one, the initial quantity of enzymes was doubled from 11.9 to 23.8% w/w *Camelina* meal; in the other, the mixture was pulsed with a second dose of enzymes (11.9% w/w *Camelina* meal), thus doubling the

total amount, after 6 h of hydrolysis. When the first strategy using double the amount of enzymes was applied, the quantity of sugars released from *Camelina* meal (Fig. 2, black bars) did not differ significantly from that of a single enzyme dose (Fig. 1a). A similar result was obtained when the second strategy, based on an additional pulse of enzymatic cocktail, after 6 h of hydrolysis was applied (Fig. 2, white bars). These findings indicate that incomplete saccharification is related more to the intrinsic accessibility of polysaccharides in the biomass than to limitations in catalytic activity. They also suggest that the initial procedure was the preferred one, as it minimized the use of enzymes and thus the overall cost of the process. The enzymatic cocktail exhibited greatest activity during the first hours of hydrolysis; prolonging incubation beyond 6 h to 24 h improved sugar titer by only 20%. Therefore, the conditions for enzymatic hydrolysis of *Camelina* meal were as follows: 15% w/w solids loading, 11.9% w/w_{*Camelina* meal} of enzymatic cocktail NS22119, reaction time of 6 h, operative temperature of 50 °C, and initial pH of 5.5. As underlined before, the pH of the reaction mixture remained constant over time and was conveniently closer to the optimum reported for carotenoids accumulation in *R. toruloides* (pH 5) than to the value suitable for lipid production (pH 4) [30].

The above settings allowed for about 25 g/L of monomeric sugars to be released and with a sugar recovery of 53.3%. The fraction of residual non-hydrolyzed carbohydrates could be considered as an added value to the final product, since a *Camelina* meal enriched in carotenoids by fermentation of *R. toruloides* would still contain fibers of nutritional value.

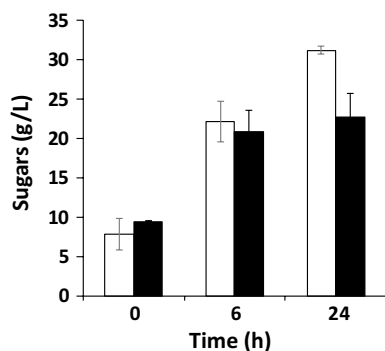


Fig. 2 Enzymatic hydrolysis of 15% *Camelina* meal. Sugars released by supplementation with an additional pulse of NS22119 cocktail (11.9% w/w_{*Camelina* meal}) after 6 h of hydrolysis (white bar) or with a starting double enzymatic cocktail dose (23.8% w/w_{*Camelina* meal}) (black bar). Values are the means of three independent experiments

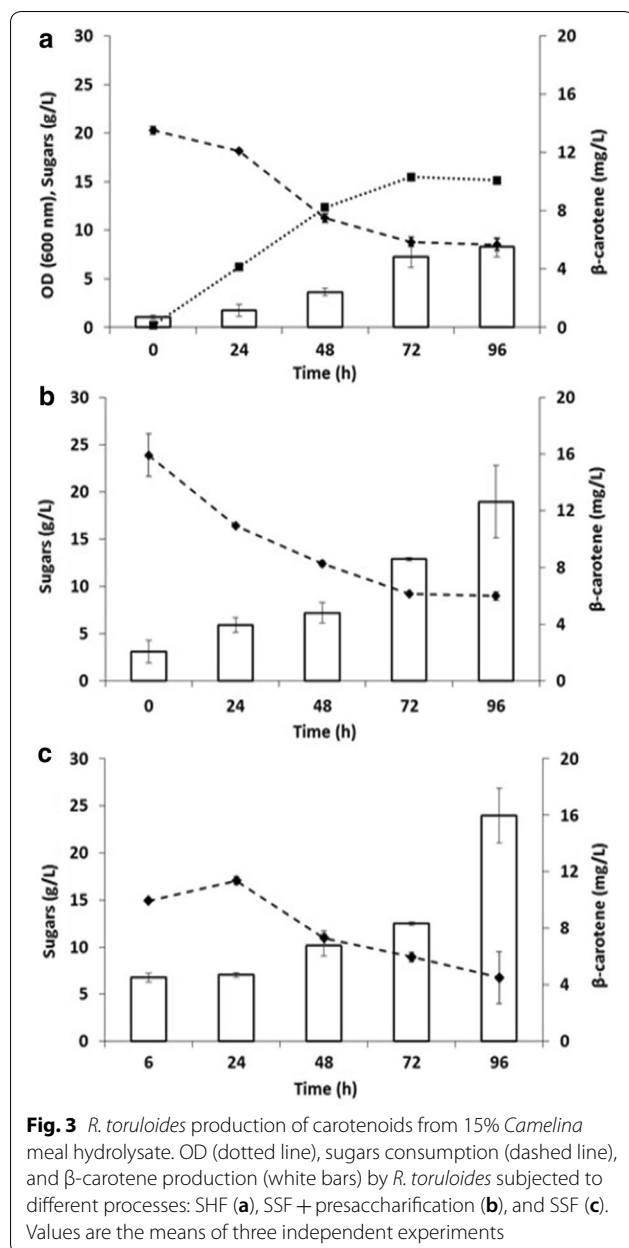
Inhibitory compounds in *Camelina* meal hydrolysate

Compared with traditional acid treatment, enzymatic hydrolysis is efficacious in releasing sugars from lignocelluloses and minimizing the accumulation of inhibitory compounds [31, 32]. Nevertheless, there are some drawbacks related to other compounds detached from these complex matrices [2, 20]. Acetic acid is the most common inhibitor released by hydrolysis of the hemicellulose fraction composing lignocellulosic biomasses. Acetic acid can easily impair microbial growth and metabolism due to its generic and specific toxicity [33], reducing the key performance indicators of the production process [2, 33, 34]. Nevertheless, the toxicity of acetic acid is greater at low pH; extracellular pH values higher than its pK_a (4.76) reduce its diffusion across the membrane and, therefore, the cellular damage it could trigger [35, 36]. In the present study, the operative pH (5.5) was higher than the pK_a of acetic acid, thus lowering the detrimental effect of this molecule on cells. Moreover, *R. toruloides* has been shown to withstand acetic acid when added to defined media or even as the sole carbon source at up to 20 g/L at pH 6 [37–39]. During enzymatic hydrolysis, acetic acid titer increased, reaching 1.8 ± 0.01 g/L after 24 h from the start (Additional file 1: Figure S2). This amount has been described as bearable by diverse yeasts [34, 37, 38] including *R. toruloides*.

Considering the above constrains, *Camelina* meal hydrolysate appears to be a suitable feedstock for yeast cell factory-based biorefineries, which would enable the exploitation of yeast biodiversity and engineering strategies to obtain different products of interest.

Carotenoids production from *Camelina* meal hydrolysate in SHF and SSF processes

Having established a protocol for obtaining *Camelina* meal hydrolysate, carotenoids production by SHF was investigated. In the SHF experiment, medium consisted of clarified supernatant collected after 6 h of enzymatic hydrolysis. This medium was sufficient to sustain *R. toruloides* growth, as indicated by the accumulation of biomass and consumption of sugar (Fig. 3a, dotted and dashed lines, respectively). The accumulation of carotenoids increased over time, reaching 5 ± 0.7 mg/L after 96 h of fermentation (Fig. 3a, white bars), with a yield on consumed sugars of 0.034% (w/w) and on maximum quantity of sugars per biomass of 0.011% (w/w). These data are in accordance with previous reports that *R. toruloides* and carotenogenic microorganisms in general produce carotenoids mostly in response to stressful or sub-optimal conditions such as stationary phase [17, 18, 40, 41]. The period of 96 h was chosen mainly to allow comparison with previous studies, whereby *R. toruloides*



was provided with defined media or other/different residual biomasses (Table 2). After 96 h, fewer carotenoids could be extracted from the cells (Additional file 1: Figure S3), which could correlate with the export/release of carotenoids from the cells or with an imbalance of nutrients that might promote their consumption/corruption. The carotenoid production achieved here by SHF was competitive with *R. toruloides* grown in shake flasks and supplemented with other complex matrices (Table 2).

To overcome the need for clarifying the medium after enzymatic hydrolysis, we fed the cells the entire

Camelina meal hydrolysate, including the water-insoluble solids (WIS) fraction left over after enzymatic hydrolysis. WIS may impair microbial growth and production because of the uneven homogenization of the liquid medium caused by the presence of solid components, as well as due to the toxicity of some of their components [28]. Under conditions termed here as “SSF + presaccharification”, *R. toruloides* was able not only of consuming sugars and producing carotenoids (Fig. 3b), but it also achieved a higher titer of intracellular carotenoids, reaching 13 ± 2.6 mg/L after 96 h, with a yield on consumed sugars of 0.108% (w/w) and on maximum quantity of sugars per biomass of 0.028% (w/w). Given that the amount of carotenoids extracted from *Camelina* meal with and without the addition of enzymes remained constant over time, the carotenoids measured in this and in the following experiments in the presence of WIS were due to microbial metabolism (Additional file 1: Figure S4).

Often proposed as an alternative to SHF, SSF is characterized by a single combined hydrolysis and microbial fermentation step. The two processes have several pros and cons in terms of efficiency, time, presence/release of inhibitory molecules, and downstream final product [42, 43]. SHF and SSF have been proposed and compared for several second-generation biorefineries that used *Arundo donax*, grass, or wheat straw as feedstocks [28, 44, 45]. A potential drawback of incubating enzymes and cells in the same environment is the compromise that needs to be reached allowing optimum operating conditions for both of them. In the present study, because 50 °C was not a viable temperature for *R. toruloides*, 30 °C was selected as the operative temperature. Thus, increased shaking was intended to partially compensate for the reduced activity by augmenting the probability of interactions between the matrix and the enzymes. Remarkably, the release of sugars in these conditions was comparable to that obtained by SHF or SSF + presaccharification (Additional file 1: Figure S5). As shown in Fig. 3c, after the first 6 h of hydrolysis, the amount of sugars in the medium was lower compared to that obtained by SHF, most likely due to the initial growth (and therefore sugar consumption) of *R. toruloides*. After 24 h, sugar consumption became clearly evident and was accompanied by the accumulation of carotenoids. After 96 h, the carotenoid concentration reached 16 ± 1.9 mg/L, with a maximum amount of sugars per biomass of 0.028% (w/w). In the case of SSF, it is not possible to measure the total sugar released during saccharification because of simultaneous fermentation. Importantly, the amount of carotenoids was significantly higher when WIS were left in the medium (SSF and SSF + presaccharification) compared to simple SHF (*t* test $p < 0.05$). While sub-lethal concentrations of insoluble solids might impair microbial growth, they could also

Table 2 Carotenoids production by *R. toruloides*

<i>R. toruloides</i> strain	Substrate	Time (h)	β -Carotene (mg/L)	References
ATCC 204091	WE ¹	72	62 \pm 1.70	[23]
	MM ²	100	57 \pm 2.18	
ATCC 10788	YPG ^a	288	3.6	[16]
AS 2.1389			4.3	
CBS 5490			6.8	
CCT 0783	SCBH ^b	72	1.2 \pm 0.1	[21]
	cSCBH	94	2.18 \pm 0.2	
NCYC 921 (alias ATCC 10788)	CPS100 ^c	48	0.41	[22]
	CPS75		0.47	
	SCM100 ^d		0.04	
	SCM75		0.18	
DSM 4444	CM SHF ^e	96	5.5 \pm 0.7	This study
	CM SSF + presaccharification		12.6 \pm 2.6	
	CM SSF		16.0 \pm 1.9	

Comparison of data obtained from different media and fermentation modes

¹ WE = waste extract from mandis (road-side vegetable markets)

² MM = minimal media with 5 g/L glucose

^a YPG = 20 g peptone, 10 g yeast extract, 60 g glycerol

^b SCBH = sugarcane bagasse hydrolysate, cSCBH = concentrated SCBH

^c CPS = carob pulp syrup

^d SCM = sugarcane molasse

^e CM = *Camelina* meal

^{1,2} Bioreactor, ^{a, b, c, d, e} shake flasks. Data from other studies are reported with the original digits and standard deviation

trigger the accumulation of metabolites important for the microalgae and yeasts' own defense systems [41, 46]. For example, β -phenol was shown to trigger carotenoid production in yeast [47].

The titers achieved by SSF indicate the efficacy of concurrent hydrolysis and fermentation, suggesting that a simplified procedure involving a single vessel could be used. Because productivity remained similar over time, the initial sugar released in the presence of cells did not seem to speed up the overall process. Overall, data from SSF and SSF + presaccharification reveal that the often mandatory detoxification step, indicated also for *R. toruloides* [48], is avoidable with this type of residual biomass. Moreover, the final product obtained by both SSF and SSF + presaccharification is a *Camelina* meal enriched with carotenoids, which can be used directly in the animal feed industry.

Therefore, different products, such as pure carotenoids and carotenoids-enriched *Camelina* meal, can be recovered from the tested processes. *Camelina* meal, in particular, would be an innovative product on the market, as carotenoids are commonly added to animal feed for nutritional and organoleptic reasons [3, 12]. In addition, the production of carotenoids from a residual biomass

of lower value may increase the economic attractiveness of the proposed process. Based on the logic of cascading [49, 50], the present work paves the way for the use of *Camelina* meal as an alternative feedstock in second-generation biorefineries exploiting microbial cell factories to produce fine chemicals.

Conclusions

Here, we demonstrate that *Camelina* meal could be employed as residual biomass for the development of novel biorefineries based on microbial cell factories. After enzymatic hydrolysis, this biomass was provided to the oleaginous yeast *R. toruloides* as a sole nutrient and energy source, and carotenoids production was assessed. A comparison of different processes revealed that the highest titer of carotenoids was obtained when *R. toruloides* was exposed to WIS and either SSF (16 \pm 1.9 mg/L) or SSF + presaccharification (13 \pm 2.6 mg/L). The presence of WIS seemed to play a positive role under these conditions, triggering the accumulation of the desired product and showing how common foes of biorefineries can turn into possible allies. To further investigate the pliancy of this study, we plan to analyze the titer of concurrently accumulated carotenoids (e.g., torulene and

torularhodin) and their relative ratio. We also intend to test alternative microbial cell factories to produce other high value-added molecules such as aromas. Moreover, biotransformation will be scaled-up from shake flasks to bioreactors, to generate data useful to calculate the competitiveness of a potential industrial process intended to further valorize *Camelina* meal, following the logic of cascading.

Materials and methods

Camelina meal composition

Flanat Research Italia S.r.l., Rho, Italy, provided *Camelina* meal derived from plants cultivated and harvested in Lombardy in 2018 and 2019. *C. sativa* seeds were processed to collect the oil, while the leftover meal was delivered to the laboratory and stored at $-20\text{ }^{\circ}\text{C}$. To measure the water content of *Camelina* meal, 0.9 g and 4.5 g of biomass were dried at $160\text{ }^{\circ}\text{C}$ for 3 h, and then weighted again to calculate the amount of evaporated water. The biomass was incubated at $160\text{ }^{\circ}\text{C}$ for an additional 3 h, but no further changes in weight compared to the value obtained after the initial treatment were observed. Hence, the initial treatment was deemed sufficient. To analyze chemical composition of *Camelina* meal, the biomass was treated following the protocols for the analysis of structural carbohydrates and lignin in biomass from the National Renewable Energy Laboratory (NREL, <https://www.nrel.gov/docs/gen/fy13/42618.pdf>) with some modifications. In brief, 300 mg of biomass was diluted in 3 mL H_2SO_4 72% (v/v), and then incubated at $30\text{ }^{\circ}\text{C}$ for 1 h, stirring thoroughly every 10 min. The solution was diluted to 4% (v/v) by adding 84 mL of distilled water, mixed by inversion, and autoclaved at $121\text{ }^{\circ}\text{C}$ for 1 h. The hydrolysis solution was vacuum-filtered through a previously weighted filtering crucible, and the insoluble components were measured gravimetrically on the filter paper. The filtered liquid was neutralized with NaOH until pH 5–6 was attained and then, the samples were analyzed by HPLC (as described below) after filtration with a $0.22\text{-}\mu\text{m}$ filter (Euroclone, Pero, Milan, Italy). Three independent experiments were performed.

Pretreatment and enzymatic hydrolysis of *Camelina* meal

Enzymatic hydrolysis of *Camelina* meal was performed using the enzyme mixture NS22119, kindly provided by Novozymes (Novozymes A/S, Copenhagen, Denmark). As described by the producer, NS22119 contains a wide range of carbohydrases, including arabinase, β -glucanase, cellulase, hemicellulase, pectinase, and xylanase from *Aspergillus aculeatus*. Without drying the biomass, different quantities of *Camelina* meal were weighted to a concentration of 3%, 6%, 9%, 12%, and 15% (w/v) into glass bottles, steeped in water with a final volume of

30 mL, and then autoclaved at $121\text{ }^{\circ}\text{C}$ for 1 h to both sterilize and pre-treat the biomass. Afterward, enzymes were added directly to the bottles and incubated at pH 5.5 and at $50\text{ }^{\circ}\text{C}$ in a water bath under mild agitation (105 rpm). A 1-mL aliquot was collected every 2, 4, 6, and 24 h from the start, and sugar content was analyzed by HPLC (see below). The following enzyme concentrations were tested: 11.9% w/w_{*Camelina* meal}, 23.8% w/w_{*Camelina* meal}, and 11.9% w/w_{*Camelina* meal} at 0 h plus at 6 h. Three independent experiments were performed. Low enzyme doses were intended to mimic commercially feasible hydrolysis, whereas high doses provided an indication of maximum enzymatically accessible sugar content. When implementing the suggested process at commercial scale, additional testing is recommended to refine the dose–response curve and determine the effect of time, solids loading, pretreatment protocol, cellulose conversion, and enzyme dosage.

Microbial strain and media

Rhodospiridium toruloides (DSM 4444) was purchased from DSMZ (German Collection of Microorganisms and Cell Cultures, GmbH) and stored in cryotubes at $-80\text{ }^{\circ}\text{C}$ in 20% glycerol (v/v). The composition of the medium for the pre-inoculum was as follows (per liter): 1 g yeast extract, 1.31 g $(\text{NH}_4)_2\text{SO}_4$, 0.95 g Na_2HPO_4 , 2.7 g KH_2PO_4 , and 0.2 g $\text{Mg}_2\text{SO}_4\cdot 7\text{H}_2\text{O}$. The medium was supplemented with 15 g/L of glycerol as main carbon source and a $100\times$ trace mineral stock solution consisting of (per liter) 4 g $\text{CaCl}_2\cdot 2\text{H}_2\text{O}$, 0.55 g $\text{FeSO}_4\cdot 7\text{H}_2\text{O}$, 0.52 g citric acid, 0.10 g $\text{ZnSO}_4\cdot 7\text{H}_2\text{O}$, 0.076 g $\text{MnSO}_4\cdot \text{H}_2\text{O}$, and 100 μL 18 M H_2SO_4 . Yeast extract was purchased from Biolife Italia S.r.l., Milan, Italy. All other reagents were purchased from Sigma-Aldrich Co., St Louis, MO, USA. After plating on rich medium, a pre-inoculum was run in rich medium until stationary phase. Then, cells were inoculated at 0.2 OD in shake flasks at $30\text{ }^{\circ}\text{C}$ and 160 rpm for both SHF and SSF processes (see below).

SHF and SSF

During both SHF and SSF processes, *R. toruloides* was grown in shake flasks at pH 5.5, supplemented with *Camelina* meal hydrolysate, with or without WIS. After 6 h of enzymatic hydrolysis at $50\text{ }^{\circ}\text{C}$, the hydrolysate was centrifuged at 4000 rpm for 10 min to separate the water-soluble components from WIS. Then, for SHF, the liquid fraction was collected and transferred into a shake flask for microbial growth at $30\text{ }^{\circ}\text{C}$. Alternatively, for the SSF + saccharification process, *Camelina* hydrolysate was provided directly to *R. toruloides* as growth medium, regardless of the presence of WIS. For the SSF process, *Camelina* meal was directly steeped and autoclaved in a shake flask, then supplemented with the enzymatic

cocktail at 11.9% w/w_{Camelina meal} and 0.2 OD of cells, and incubated at 30 °C and 160 rpm. Three independent experiments for each setting were performed.

Carotenoids extraction

Carotenoids were analyzed by acetone extraction from *R. toruloides* cells with a protocol adapted from [51]. In brief, 1 mL of culture broth was collected and harvested by centrifugation at 7000 rpm for 7 min at 4 °C, and the pellet was then resuspended in 1 mL acetone and broken using glass beads by thorough agitation with a FastPrep-24™ (MP Bio-medicals, LLC, Santa Ana, CA, USA). Carotenoids were extracted in the acetone phase, the suspension was centrifuged, and the supernatant collected. The extraction was repeated with fresh acetone until the biomass was colorless. Carotenoid content was measured spectrophotometrically (see below).

Analytical methods

HPLC analyses were performed to quantify the amount of glucose, sucrose, arabinose, fructose, and acetic acid. In brief, 1-mL samples from each of the three different streams of production (enzymatically hydrolyzed *Camelina* meal, SHF or SSF) were collected and centrifuged twice (7000 rpm, 7 min, and 4 °C), and then analyzed by HPLC using a Rezex ROA-Organic Acid column (Phenomenex, Torrance, CA, USA). The eluent was 0.01 M H₂SO₄ pumped at 0.5 mL/min and column temperature was 35 °C. Separated components were detected by a refractive index detector and peaks were identified by comparing with known standards (Sigma-Aldrich). Optical density (OD) of *R. toruloides* was measured spectrophotometrically at 600 nm. The pH was measured with indicator strips at the beginning and at the end of enzymatic hydrolysis to assess suitability of the initial conditions and to foresee possible toxic effects of the final medium.

The titer of carotenoids extracted in acetone from *R. toruloides* was determined spectrophotometrically (UV-1800; Shimadzu, Kyoto, Japan) based on the maximum absorption peak for β-carotene (455 nm). A calibration curve with standard concentration of β-carotene was obtained.

Calculations and statistical analyses

Sugar recovery (here S_r) was calculated as percentage of sugar yield obtained by enzymatic hydrolysis (here Y_{EH}) compared with the yield obtained from total acid hydrolysis of biomass (here Y_{AH}) (Eq. 1). Carotenoids yield on consumed sugars (here $Y_{c/s}$) and carotenoids yield on maximum quantity of sugars per biomass (here $Y_{c/b}$) measured with acid hydrolysis were calculated by Eqs. 2 and 3, respectively.

$$S_r = Y_{EH}/Y_{AH} \times 100 \quad (1)$$

$$Y_{c/s} = C_p/\Delta_{sug} \times 100 \quad (2)$$

$$Y_{c/b} = C_p/S_b \times 100 \quad (3)$$

where Δ_{sug} corresponds to consumed sugars, S_b to maximum quantity of sugars in the biomass, and C_p to carotenoids produced.

For statistical analysis, heteroscedastic two-tailed *t* test was applied.

Supplementary information

Supplementary information accompanies this paper at <https://doi.org/10.1186/s13068-020-01682-3>.

Additional file 1: Figure S1. Effect of enzymatic hydrolysis conditions on different concentrations of *Camelina* meal without addition of the NS22119 cocktail. **Figure S2.** Acetic acid released during enzymatic hydrolysis. The concentration of acetic acid released from 15% *Camelina* meal by treatment with the NS22119 cocktail (11.9% w/w_{Camelina meal}) was evaluated over time. **Figure S3.** *R. toruloides* production of carotenoids from 15% (w/v) *Camelina* meal hydrolysate. OD (dotted line), sugars consumption (dashed line), and β-carotene production (white bars) by *R. toruloides* during the SHF process are shown. **Figure S4.** Carotenoids' extraction from *Camelina* meal hydrolysate. **Figure S5.** Effect of enzymatic hydrolysis on 15% *Camelina* meal by the NS22119 cocktail (11.9% w/w_{Camelina meal}) at 30 °C.

Abbreviations

HPLC: High-performance liquid chromatography; OD: Optical density; SHF: Separate hydrolysis and fermentation; SSF: Simultaneous saccharification and fermentation; WIS: Water-insoluble solids.

Acknowledgements

The authors would like to thank Prof. Massimo Labra for fruitful discussions on the project and Chiara Cantù for technical support.

Authors' contributions

SB performed the experimental work, analyzed the data, and wrote the manuscript. SB and PB designed the experiments. PB and MB analyzed the data analysis and drafted the manuscript. PB and DP helped with funding acquisition. All authors read and approved the final manuscript.

Funding

This work was supported by "Sistemi Alimentari e Sviluppo Sostenibile: Creare sinergie tra ricerca e processi internazionali e africani" (SASS, 2016-NAZ-0228/L) and "Food Social Sensor Network" (FOODNET, 2016-NAZ-0143/A) to SB and PB, and partially by the University of Milano-Bicocca with the FA (Fondo di Ateneo) to DP and PB. The interdisciplinary cluster BEST4FOOD is also greatly acknowledged.

Availability of supporting data

Not applicable.

Ethics approval and consent to participate

Not applicable.

Consent for publication

All authors agree to submit the work to the journal.

Competing interests

The authors declare that they have no competing interests.

Author details

¹ Department of Biotechnology and Biosciences, University of Milano-Bicocca, Piazza della Scienza 2, 20126 Milan, Italy. ² Division of Industrial Biotechnology, Department of Biology and Biological Engineering, Chalmers University of Technology, Kemivägen 10, 412 96 Gothenburg, Sweden. ³ EviKrets Biobased Processes Consultants, Lunnävågen 87, 42834 Landvetter, Sweden.

Received: 10 December 2019 Accepted: 18 February 2020

Published online: 12 March 2020

References

- Azapagic A. Sustainability considerations for integrated biorefineries. *Trends Biotechnol.* 2014;32:1–4.
- Jönsson LJ, Martin C. Pretreatment of lignocellulose: formation of inhibitory by-products and strategies for minimizing their effects. *Bioresour Technol.* 2016;199:103–12.
- Food and Agriculture Organization of the United Nations (FAO). Utilization of lipid co-products of the biofuel industry in livestock feed in Biofuel co-products as livestock feed; 2012.
- Zubr J. Carbohydrates, vitamins and minerals of *Camelina sativa* seed. *Nutr Food Sci.* 2010;40:523–31.
- Cherian G. *Camelina sativa* in poultry diets : opportunities and challenges Biofuel co-products as livestock feed: opportunities and challenges. Rome: FAO; 2012.
- Murphy EJ. *Camelina (Camelina sativa)*. Industrial oil crops. Urbana: AOCS Press; 2016.
- Dharavath RN, Singh S, Chaturvedi S, Luqman S. *Camelina sativa* (L.) Crantz A mercantile crop with speckled pharmacological activities. *Ann Phytomed.* 2016;5:6–26.
- Sizmaz O, Gunturkun OB, Zentek J. A point on nutritive value of *Camelina* meal for broilers: a review. *Int J Vet Sci.* 2016;5:114–7.
- Li X, Mupondwa E. Production and value-chain integration of *Camelina sativa* as a dedicated bioenergy feedstock in the Canadian prairies. In: 24th European biomass conference & exhibition, Amsterdam Netherlands, 2016.
- Mohammad BT, Al-Shannag M, Alnaief M, Singh L, Singasaas E, Alkasrawi M. Production of multiple biofuels from whole *Camelina* material: a renewable energy crop. *BioResources.* 2018;13(3):4870–83.
- Wang C, Zhao S, Shao X, Park JB, Jeong SH, Park HJ, et al. Challenges and tackles in metabolic engineering for microbial production of carotenoids. *Microb Cell Fact.* 2019;18(1):1–8.
- Saini RK, Keum Y-S. Microbial platforms to produce commercially vital carotenoids at industrial scale: an updated review of critical issues. *J Ind Microbiol Biotechnol.* 2019;46:657–74.
- Yuan S-F, Alper HS. Metabolic engineering of microbial cell factories for production of nutraceuticals. *Microb Cell Fact.* 2019;18:46.
- Nagarajan J, Ramanan RN, Raghunandan ME, Galanakis CM, Krishnamurthy NP. Carotenoids. Nutraceutical and functional food components. Amsterdam: Elsevier Inc.; 2017.
- Guedes AC, Amaro HM, Malcata FX. Microalgae as sources of carotenoids. *Mar Drugs.* 2011;9(4):625–44.
- Lee JLL, Chen L, Shi J, Trzcinski A, Chen WN. Metabolomic profiling of *Rhodospiridium toruloides* grown on glycerol for carotenoid production during different growth phases. *J Agric Food Chem.* 2014;62(41):10203–9.
- Frengova GI, Beshkova DM. Carotenoids from *Rhodotorula* and *Phaffia*: yeasts of biotechnological importance. *J Ind Microbiol Biotechnol.* 2009;36(2):163.
- Kot AM, Blazejak S, Gientka I, Kieliszek M, Bryś J. Torulene and torularhodin: “New” fungal carotenoids for industry?. *Cell Fact: Microb; 2018.*
- Park YK, Nicaud JM, Ledesma-Amaro R. The engineering potential of *Rhodospiridium toruloides* as a workhorse for biotechnological applications. *Trends Biotechnol.* 2018;36(3):304–17.
- Sitepu I, Selby T, Lin T, Zhu S, Boundy-Mills K. Carbon source utilization and inhibitor tolerance of 45 oleaginous yeast species. *J Ind Microbiol Biotechnol.* 2014;41(7):1061–70.
- Bonturi N, Crucello A, Viana AJC, Miranda EA. Microbial oil production in sugarcane bagasse hemicellulosic hydrolysate without nutrient supplementation by a *Rhodospiridium toruloides* adapted strain. *Process Biochem.* 2017;57:16–25.
- Freitas C, Parreira TM, Roseiro J, Reis A, Da Silva TL. Selecting low-cost carbon sources for carotenoid and lipid production by the pink yeast *Rhodospiridium toruloides* NCYC 921 using flow cytometry. *Bioresour Technol.* 2014;158:355–9.
- Singh G, Sinha S, Bandyopadhyay KK, Lawrence M, Paul D. Triaxial growth of an oleaginous red yeast *Rhodospiridium toruloides* on waste “extract” for enhanced and concomitant lipid and β -carotene production. *Microb Cell Fact.* 2018;17(1):182.
- Dai X, Shen H, Li Q, Rasool K, Wang Q, Yu X, et al. Microbial lipid production from corn stover by the oleaginous yeast *Rhodospiridium toruloides* using the PreSSLP process. *Energies.* 2019;12:1053.
- Wahlström RM, Suurnäkki A. Enzymatic hydrolysis of lignocellulosic polysaccharides in the presence of ionic liquids. *Green Chem.* 2015;17:694–714.
- Khare SK, Pandey A, Larroche C. Current perspectives in enzymatic saccharification of lignocellulosic biomass. *Biochem Eng J.* 2015;102:38–44.
- Arevalo-Gallegos A, Ahmad Z, Asgher M, Parra-Saldivar R, Iqbal HMN. Lignocellulose: a sustainable material to produce value-added products with a zero waste approach—a review. *Int J Biol Macromol.* 2017;99:308–18.
- Ask M, Olofsson K, Di Felice T, Ruohonen L, Penttilä M, Lidén G, et al. Challenges in enzymatic hydrolysis and fermentation of pretreated *Arundo donax* revealed by a comparison between SHF and SSF. *Process Biochem.* 2012;47:1452–9.
- Kim JK, Yang J, Park SY, Yu JH, Kim KH. Cellulase recycling in high-solids enzymatic hydrolysis of pretreated empty fruit bunches. *Biotechnol Biofuels.* 2019;12:1–9.
- Dias C, Sousa S, Caldeira J, Reis A, da Silva TL. New dual-stage pH control fed-batch cultivation strategy for the improvement of lipids and carotenoids production by the red yeast *Rhodospiridium toruloides* NCYC 921. *Bioresour Technol.* 2015;189:309–18.
- Merino ST, Cherry J. Progress and challenges in enzyme development for biomass utilization. *Adv Biochem Eng Biotechnol.* 2007;108:95–120.
- Lenihan P, Orozco A, O’Neill E, Ahmad MNM, Rooney DW, Walker GM. Dilute acid hydrolysis of lignocellulosic biomass. *Chem Eng J.* 2010;156(2):395–403.
- Sousa MJ, Ludovico P, Rodrigues F, Leo C, Crte-Real M. Stress and cell death in yeast induced by acetic acid. *Cell metabolism—cell homeostasis and stress response.* Rijeka: InTech; 2012.
- Martani F, Marano F, Bertacchi S, Porro D, Branduardi P. The *Saccharomyces cerevisiae* poly(A) binding protein Pab1 as a target for eliciting stress tolerant phenotypes. *Sci Rep.* 2015;5:18318.
- Guldfeldt LU, Arneborg N. Measurement of the effects of acetic acid and extracellular pH on intracellular pH of nonfermenting, individual *Saccharomyces cerevisiae* cells by fluorescence microscopy. *Appl Environ Microbiol.* 1998;64(2):530–4.
- Pampulha ME, Loureiro-Dias MC. Energetics of the effect of acetic acid on growth of *Saccharomyces cerevisiae*. *FEMS Microbiol Lett.* 2000;184(1):69–72.
- Zhao X, Peng F, Du W, Liu C, Liu D. Effects of some inhibitors on the growth and lipid accumulation of oleaginous yeast *Rhodospiridium toruloides* and preparation of biodiesel by enzymatic transesterification of the lipid. *Bioprocess Biosyst Eng.* 2012;35(6):993–1004.
- Huang XF, Liu JN, Lu LJ, Peng KM, Yang GX, Liu J. Culture strategies for lipid production using acetic acid as sole carbon source by *Rhodospiridium toruloides*. *Bioresour Technol.* 2016;206:141–9.
- Hu C, Zhao X, Zhao J, Wu S, Zhao ZK. Effects of biomass hydrolysis by-products on oleaginous yeast *Rhodospiridium toruloides*. *Bioresour Technol.* 2009;100:4843–7.
- Singh G, Jawed A, Paul D, Bandyopadhyay KK, Kumari A, Haque S. Concomitant production of lipids and carotenoids in *Rhodospiridium toruloides* under osmotic stress using response surface methodology. *Front Microbiol.* 2016;7:1686.
- Mata-Gómez LC, Montañez JC, Méndez-Zavala A, Aguilar CN. Biotechnological production of carotenoids by yeasts: an overview. *Microb Cell Fact.* 2014;13(1):12.

42. Aditiya HB, Mahlia TMI, Chong WT, Nur H, Sebayang AH. Second generation bioethanol production: a critical review. *Renew Sustain Energy Rev.* 2016;66:631–53.
43. Srivastava N, Rawat R, Singh Oberoi H, Ramteke PW. A review on fuel ethanol production from lignocellulosic biomass. *Int J Green Energy.* 2015;12:949–60.
44. Burman NW, Sheridan CM, Harding KG. Lignocellulosic bioethanol production from grasses pre-treated with acid mine drainage: modeling and comparison of SHF and SSF. *Bioresour Technol Rep.* 2019;7:100299.
45. Tomás-Pejoj E, Oliva JM, Ballesteros M, Olsson L. Comparison of SHF and SSF processes from steam-exploded wheat straw for ethanol production by xylose-fermenting and robust glucose-fermenting *Saccharomyces cerevisiae* strains. *Biotechnol Bioeng.* 2008;100:1122–31.
46. Sun X-M, Ren L-J, Zhao Q-Y, Ji X-J, Huang H. Microalgae for the production of lipid and carotenoids: a review with focus on stress regulation and adaptation. *Biotechnol Biofuels.* 2018;11:272.
47. Kim BK, Park PK, Chae HJ, Kim EY. Effect of phenol on β -carotene content in total carotenoids production in cultivation of *Rhodotorula glutinis*. *Korean J Chem Eng.* 2004;21:689–92.
48. Matsakas L, Novak K, Enman J, Christakopoulos P, Rova U. Acetate-detoxification of wood hydrolysates with alkali tolerant *Bacillus* sp. as a strategy to enhance the lipid production from *Rhodospiridium toruloides*. *Bioresour Technol.* 2017;242:287–94.
49. IEA Bioenergy Task42. Sustainable and synergetic processing of biomass into marketable food & feed ingredients, chemicals, materials and energy (fuels, power, heat). *IEA Bioenergy.* 2014;66.
50. IEA Bioenergy Task40. Cascading of woody biomass: definitions, policies and effects on international trade. *IEA Bioenergy.* 2016;71.
51. Saenge C, Cheirsilp B, Suksaroge TT, Bourtoom T. Potential use of oleaginous red yeast *Rhodotorula glutinis* for the bioconversion of crude glycerol from biodiesel plant to lipids and carotenoids. *Process Biochem.* 2011;46:210–8.

Publisher's Note

Springer Nature remains neutral with regard to jurisdictional claims in published maps and institutional affiliations.

Ready to submit your research? Choose BMC and benefit from:


- fast, convenient online submission
- thorough peer review by experienced researchers in your field
- rapid publication on acceptance
- support for research data, including large and complex data types
- gold Open Access which fosters wider collaboration and increased citations
- maximum visibility for your research: over 100M website views per year

At BMC, research is always in progress.

Learn more biomedcentral.com/submissions



The *Saccharomyces cerevisiae* poly (A) binding protein (Pab1): Master regulator of mRNA metabolism and cell physiology

Marco Brambilla  | Francesca Martani  | Stefano Bertacchi  | Ilaria Vitangeli | Paola Branduardi 

Department of Biotechnology and Biosciences, University of Milano-Bicocca, Piazza della Scienza 2, 20126 Milan, Italy

Correspondence

Prof. Dr. Paola Branduardi, University of Milano-Bicocca, Department of Biotechnology and Biosciences, Piazza della Scienza 2, 20126, Milan, Italy.

Email: paola.branduardi@unimib.it

Funding information

FA (Fondo di Ateneo), post-Doctoral and PhD fellowships funded by the University of Milano-Bicocca

Abstract

Pab1, the major poly (A) binding protein of the yeast *Saccharomyces cerevisiae*, is involved in many intracellular functions associated with mRNA metabolism, such as mRNA nuclear export, deadenylation, translation initiation and termination. Pab1 consists of four RNA recognition motifs (RRM), a proline-rich domain (P) and a carboxy-terminal (C) domain. Due to its modular structure, Pab1 can simultaneously interact with poly (A) tails and different proteins that regulate mRNA turnover and translation. Furthermore, Pab1 also influences cell physiology under stressful conditions by affecting the formation of quinary assemblies and stress granules, as well as by stabilizing specific mRNAs to allow translation re-initiation after stress. The main goal of this review is to correlate the structural complexity of this protein with the multiplicity of its functions.

KEYWORDS

mRNA translation, mRNA turnover, Poly (A) binding protein, *Saccharomyces cerevisiae*

1 | INTRODUCTION

Cells have many ways to control and define the flux of information from genes to proteins (or, more generally, to macromolecules). Some mechanisms are direct, such as transcriptional regulation, whereas others are indirect, such as post-translational modification. These diverse mechanisms act not only at different levels but also at different times. Therefore, phenotypes can be obtained by triggering slow responses via transcriptional regulation, or very quick responses via post-translational control mechanisms that are effective on the order of fractions of seconds. Together, these networks are crucial for cells to respond to the environment and its fluctuations. A significant fraction of the long path from genes to proteins involves messenger RNA. The so-called mRNA cycle (Parker, 2012) adds complexity to this scenario, due to implications related to mRNA distribution, docking, storage and metabolism (Decker & Parker, 2012; Walters & Parker, 2014). Indeed, each mRNA can display unique properties that are dictated by the structural elements present on the mRNA molecules themselves (Kwok, Tang, Assmann, & Bevilacqua, 2015; Mitchell & Parker, 2014), in turn determining the specific interactions with cellular

machines. Nevertheless, all eukaryotic mRNAs share as common moiety: a poly (A) tail, which is the target of so-called poly (A) binding proteins (generically termed PABPs). PABPs function as scaffolds for the recruitment of various proteins that regulate gene expression at the post-transcriptional level (Goss & Kleiman, 2013). Interestingly, higher eukaryotes have specialized PABPs that show diverse localizations and functions (Smith, Blee, & Gray, 2014). For example, humans have one nuclear and three cytosolic PABPs, whereas plants have eight PABPs clustered into four classes that show different expression levels and/or tissue-specificities (Goss & Kleiman, 2013). The majority of PABPs display a conserved structure with four RNA recognition motifs (RRMs) at the N-terminus, a linker and a globular C-terminal domain; others lack both the linker and the C-terminal domain or have just one or two RRM (Goss & Kleiman, 2013; Smith et al., 2014).

The yeast *S. cerevisiae* possesses two essential poly (A) binding proteins that do not share sequence or structure homology: Pab1, which is predominantly distributed in the cytosol, and Nab2, which is found in the nucleus (Schmid et al., 2012). In contrast to Nab2, which only controls the poly (A) tail length of newly synthesized mRNAs and their proper export (Soucek, Corbett, & Fasken, 2012), Pab1 has a

broader range of action, including the regulation of mRNA deadenylation and translation. The goal of this review is to summarize the available information on *S. cerevisiae* Pab1, in terms of molecular structure and intracellular functions, offering a general overview of its relevance in the control of mRNA metabolism.

2 | Pab1 HAS A COMPLEX STRUCTURE THAT ACCOUNTS FOR ITS MULTIFUNCTIONAL BEHAVIOUR

Like most PABPs, *S. cerevisiae* Pab1 is composed of four RRMs, a linker and a globular C-terminal domain (Figure 1A) (Richardson et al., 2012). The full-length protein can be subjected to a proteolytic cleavage that releases two polypeptides of 53 and 17 kDa, which correspond to the four RRMs and the P-C domains, respectively (Sachs, Bond & Kornberg, 1986). The 53 kDa Pab1 isoform represents 10%–20% of the total Pab1 molecules (Yao et al., 2007) and is predominantly localized in the nucleus (Sachs, Bond, & Kornberg, 1986).

RRMs are highly conserved across species; they generally contain 90 to 100 residues that fold into a 3D structure consisting of four anti-parallel β -sheets flanked by two α -helices (Figure 1B) (Eliseeva, Lyabin, & Ovchinnikov, 2013; Maris, Dominguez, & Allain, 2005). The two highly conserved sequences RNP-1 (K/R)-G-(F/Y)-(G/A)-(F/Y)-(V/I/L)-X-(F/Y) and RNP-2 (I/V/L)-(F/Y)-(I/V/L)-X-N-L (where X can be any amino acid) are located in the β 3 and β 1 sheets, respectively, and are responsible for poly (A) tail binding (Maris et al., 2005). Deardorff and Sachs (1997) demonstrated by site-directed mutagenesis that RNA binding is directed by a single residue in the RNP-1 sequence and that equivalent residues in the RNP-1 of each RRM do not direct the same specificity of RNA binding. In the same work, RRM2 was identified as being involved in poly (A) binding, whereas RRM4 had a high affinity for non-specific polypyrimidine tracts; RRM1 and RRM3 appeared to contribute to RNA binding without being indispensable (Deardorff & Sachs, 1997).

In addition to RNP sequences, the RRM domains contain sequences that allow Pab1 to shuttle between the nucleus and the cytoplasm. The minimum putative nuclear localization sequence (NLS) that allows the entry of Pab1 into the nucleus (in association with the Kap108/Sxm1 importin) encompasses the amino acids 281–337 and is

located between the RRM3 and RRM4 domains (Brune, Munchel, Fischer, Podtelejnikov, & Weis, 2005). Recent findings, based on the overexpression of truncated versions of the *PAB1* gene in a wild-type background, suggest that nuclear localization might be favoured by the presence of the P domain together with the RRM3 domain (Brambilla, Martani, & Branduardi, 2017). The minimum putative nuclear export sequence (NES) is found within the RRM1 between residues 12 and 17 ("LENLNI") of Pab1 and is indispensable for interactions with the Xpo1/Crm1 exportin, which is involved in Pab1 export from the nucleus (Dunn, Hammell, Hodge, & Cole, 2005). Additionally, Pab1 can be exported into the cytoplasm by Mex67 (i.e., an mRNA export receptor) and/or by ongoing mRNA export (Figure 2) (Brune et al., 2005; Niño, Hérisant, Babour, & Dargemont, 2013). When export via Mex67 is compromised, there is no significant accumulation of Pab1 in the nucleus, suggesting the predominant role of an Xpo1/Crm1-mediated mechanism (Brune et al., 2005). Accordingly, Pab1 localizes in the nucleus in the absence of the Xpo1/Crm1 nuclear export pathway, and its nuclear localization is exacerbated by the absence of Mex67/mRNA-dependent export (Brune et al., 2005).

In contrast with RRMs, the linker is significantly divergent in length across species and a pattern of conserved residues can be found only among sequences of closely related organisms. The linker domain has a small number of charged amino acids, but is rich in proline (thus, called the P domain), methionine, glycine, glutamine and asparagine compared to the average yeast proteome (Riback et al., 2017). The linker domain exhibits an intrinsically disordered nature that results in a lack of a fixed 3D structure. Small-angle X-ray scattering (SAXS) analysis showed that, among all possible conformations, the P domain tends to be compact *in vitro*, with an estimated radius of gyration (R_g) of 20 Å (Riback et al., 2017).

Despite the validity of the descriptions mentioned above, they are biased by the absence of a complete 3D reconstruction of the entire protein structure and of the possible complexes. Considering the complexity of a multidomain and multifunctional protein, this deficiency impairs the possibility of an exhaustive description, but allows room for hypotheses and experimental validation. The C-terminal domain is the only domain of which the 3D structure was solved by NMR (Kozlov et al., 2002). In contrast from the human counterpart, this domain folds into four α -helices instead of five, contains two extra amino acids between the 2nd and the 3rd helices, and has a strongly

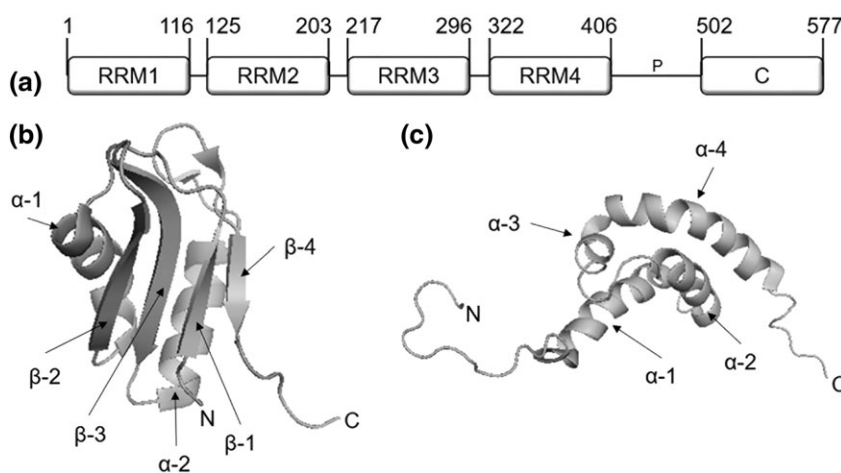


FIGURE 1 Pab1 structure. A) Schematic representation of the modular structure of the *S. cerevisiae* poly (A) binding protein Pab1. Numbers above the scheme indicate the beginning and the end of the corresponding domain according to Richardson et al., (2012). RRM: RNA recognition motives. P: P domain. C: C domain. B) 3D structure of the RRM2 domain of human PABPC generated using the program PyMOL (version 1.0.0.0) with Protein Data Bank (PDB) code 4F25. C) 3D structure of the C domain of the *S. cerevisiae* Pab1 generated using the program PyMOL (version 1.0.0.0) with PDB code 1IFW

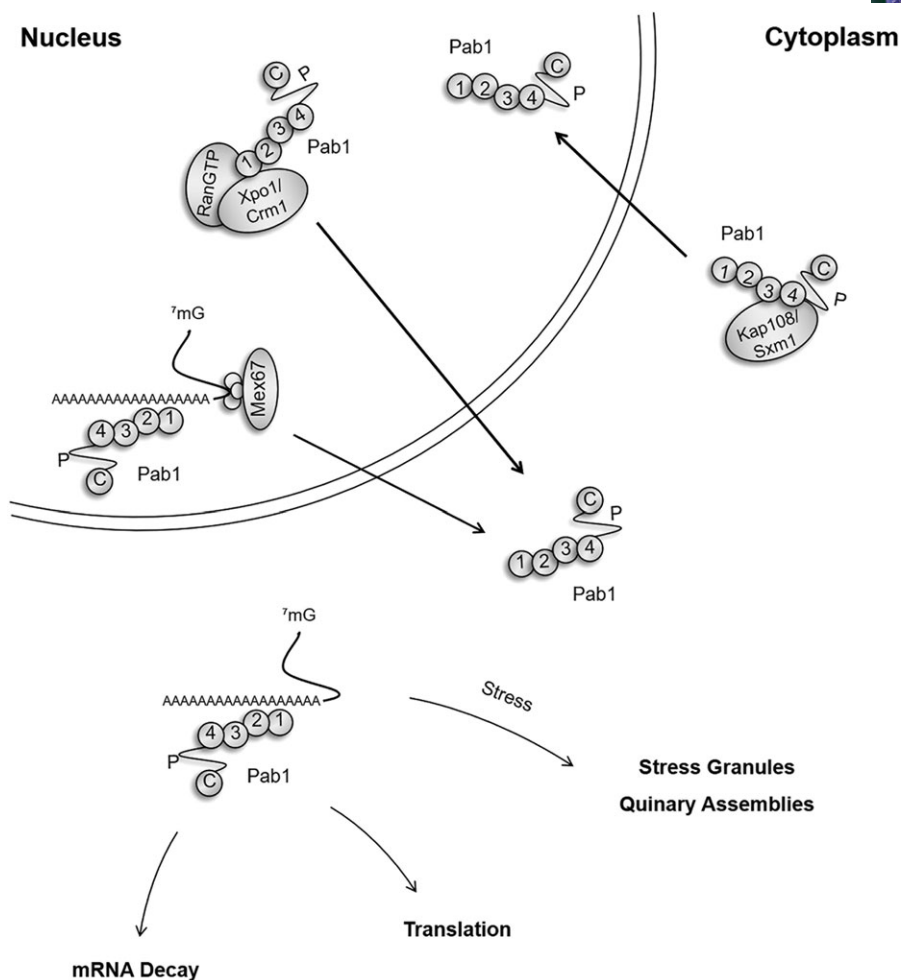


FIGURE 2 Pab1 and the mRNA fate. Pab1, predominately cytoplasmic, can enter the nucleus in association with the Kap108/Sxm1 importin, where it participates in the mRNA biogenesis. The export of Pab1 to cytoplasm occurs though the interaction with the Mex67/mRNA complex or with the exportin Xpo1/Crm1. Here Pab1 regulates the fate of mRNAs by targeting them to translation, decay or, when translation is inhibited, into stress granules

bent C-terminal helix (Figure 1C) (Kozlov et al., 2002). C-terminal domains of PABPs are also known as MLL (i.e., mademoiselle) because of the presence of the amino acid sequence KITGMLLE, which is responsible for the interaction of Pab1 with proteins containing the PAM2 motif (PABP-interacting motif 2) (Roque et al., 2015; Xie, Kozlov, & Gehring, 2014). In *S. cerevisiae*, this sequence is slightly divergent from the canonical sequence because the glutamate and one of the leucine residues are substituted by an aspartate and isoleucine, respectively (KITGMILD) (Roque et al., 2015).

The complex structure of this protein accounts for its interaction with different proteins involved in controlling mRNA metabolism and, consequently, for its different functions ranging from mRNA biogenesis to mRNA decay (as described in Figure 2, with additional details below).

3 | Pab1 IS AN ESSENTIAL PROTEIN IN THE CONTROL OF POLY (A) TAIL LENGTH AND TRANSLATION INITIATION

The first loss of function studies on Pab1, performed by inactivating the promoter and using a temperature-sensitive mutation (due to

lethality associated with the deletion of *PAB1*), revealed the importance of this protein in the control of poly (A) tail length and translation initiation (Sachs & Davis, 1989). Subsequently, many bypass suppressor mutations of the *PAB1* deletion were discovered. Suppressors can be divided into two groups: mutations or deletion of genes affecting the formation of the 60S ribosomal subunit (*SPB1*, *RPL39*, *SPB4*, *RPL35A*), and mutations or deletions of genes encoding enzymes responsible for mRNA turnover (*LSM1*, *DCP1*, *XRN1*, *RRP6*, *PAT1*, *MRT3*) (Table 1). Regarding the first group of suppressors, it has been proposed that under-accumulation of 60S subunits might sequester decreased amounts of 40S subunits into empty 80S ribosomes. The resulting excess of free 40S subunits, which are normally limited during translation initiation, may allow efficient translation in the absence of Pab1 (Chekanova & Belostotsky, 2003). In the second group of suppressors, the increased stability of transcripts due to defects in the mRNA decapping process and in general during mRNA turnover may counteract the decreased translation rate resulting from the absence of Pab1 (Boeck, Lapeyre, Brown, & Sachs, 1998; Wyers, Minet, Dufour, Vo, & Lacroute, 2000). Another mutation that suppresses the *PAB1* deletion is the *pbp1Δ* allele. Pbp1 (Pab1-binding protein 1) is the orthologue of human Ataxin-2 and is involved in stress granule

TABLE 1 Bypass suppressor mutations of *pab1Δ*

Gene	Description	Main function	Suppressor mutation	Mutant phenotype	References
SPB1	AdoMet-dependent methyltransferase	RNA processing and 60S ribosomal subunit maturation	<i>spb1-1</i> , cold-sensitive allele <i>spb1-2</i> , thermosensitive allele	-	Pintard, Kressler & Lapeyre, 2000; Sachs & Davis, 1989
RPL39 (SPB2, RPL46)	Ribosomal 60S subunit protein L39	Ribosome biogenesis	<i>spb2-1</i> , cold-sensitive allele; <i>spb2Δ</i>	-	Sachs & Davis, 1989; Sach and Davis, 1990
SPB4	ATP-dependent RNA helicase	Synthesis of 60S ribosomal subunit	<i>spb4-1</i> , cold-sensitive allele	-	Sachs & Davis, 1989
LSM1 (SPB8)	Lsm protein	Degradation of cytoplasmic mRNAs	<i>spb8-2</i>	accumulation of capped poly (A)-deficient mRNAs	Boeck, Lapeyre, Brown & Sachs, 1998
DCP1 (MRT2)	Subunit of the Dcp1p-Dcp2p decapping enzyme complex	mRNA decapping	<i>dcp1-1</i> <i>dcp1Δ</i>	reduce decapping activity; full length deadenylated mRNAs accumulation; no decapping activity; full length deadenylated mRNAs accumulation	Beelman et al., 1996; Hatfield, Beelman, Stevens & Parker, 1996 Beelman et al., 1996
XRN1	5'-3' exonuclease	mRNA decay	<i>xrn1Δ</i>	increased levels of full-length mRNA	Caponigro & Parker, 1995
RRP6	Nuclear exosome exonuclease component	3'-5' exonuclease involved in RNA processing, maturation, surveillance, degradation, tethering, and export	<i>rrp6Δ</i>	nuclear accumulation of polyadenylated RNA	Dunn, Hammell, Hodge & Cole, 2005
PAT1 (MRT1)	Deadenylation-dependent mRNA-decapping factor	mRNA decapping	<i>pat1-2</i> , <i>pat1-3</i> <i>pat1Δ</i>	accumulation of full-length deadenylated transcripts; reduced translation initiation	Hatfield, Beelman, Stevens & Parker, 1996 Wyers, Minet, Dufour, Vo & Lacroute, 2000
MRT3	-	mRNA decay	<i>mrt3-1</i>	accumulation of full-length deadenylated transcripts	Hatfield, Beelman, Stevens & Parker, 1996
PBP1	Pab1p-Binding Protein	mRNA polyadenylation	<i>pbp1Δ</i>	reduced polyadenylation	Mangus, Amrani & Jacobson, 1998
RPL35A (SOS1)	Ribosomal 60S subunit protein L35A	Ribosome biogenesis	<i>sos1Δ</i>	-	Zhong & Arndt, 1993

formation (Buchan, Muhrad, & Parker, 2008) and in the regulation of deadenylation (Mangus, Amrani, & Jacobson, 1998). The mechanisms by which the *pbp1Δ* allele suppresses the lethality associated with *PAB1* deletion are still unknown; in fact, *pbp1* deficient yeast did not show alterations in mRNA decay and translation, in the accumulation of ribosomal subunits, or in mRNA poly (A) tail length (Mangus et al., 1998). Although the use of bypass suppressor mutations allowed for the description of different phenotypes caused by the absence of Pab1, it is important to consider that the mutations used to suppress Δ *pab1* lethality can interfere with experimental observations. Therefore, complementary and alternative methods are necessary to validate the results.

Cross-species complementation approaches contributed to the elucidation of the essential functions of Pab1 for ensuring cell viability (Belostotsky & Meagher, 1996; Chekanova & Belostotsky, 2003; Chekanova, Shaw, & Belostotsky, 2001). The heterologous expression of the *Arabidopsis thaliana* PAB5 rescued the viability of *pab1Δ* yeast strains by partially restoring both poly (A) shortening and the translation initiation functions of PABP (Belostotsky & Meagher, 1996). However, Pab5 did not restore the linkage between deadenylation and decapping, two processes that are normally coupled in wild-type strains but occur independently in *pab1Δ* strains. This observation suggests that the coupling of deadenylation and decapping by Pab1 is not essential for cell viability (Belostotsky & Meagher, 1996). In another study, Chekanova and co-workers showed that the heterologous expression of the *A. thaliana* PAB3 rescued the viability of the *pab1Δ* strain by partially restoring the poly (A) tail length during polyadenylation in a PAN-dependent manner (Chekanova et al., 2001; Chekanova & Belostotsky, 2003). PAN is a deadenylase complex with an important function in mRNA biogenesis, which is described in the next paragraph. Because PAB3 does not function to protect the mRNA 5' cap from premature removal and does not stimulate translation in yeast, and because the *pan3Δ* mutation is synthetically lethal with the substitution of PAB3 for Pab1 (Chekanova et al., 2001; Chekanova & Belostotsky, 2003), this cross-complementation study demonstrated the essential role of Pab1 in mRNA biogenesis.

Together, these loss of function and cross-complementation studies indicate that the most important functions of Pab1 are linked to the end processing of 3' mRNA and translation, which are strictly coupled to control eukaryotic gene expression. Recently, Pab1 was described as a multifunctional scaffold protein that escorts transcripts from the beginning to the end of their life, indicating its essential function. Subsequently, we describe the interactions of Pab1 with the proteins involved in the regulation of mRNA metabolism as well as their biological relevance.

3.1 | Pab1 is essential for proper mRNA biogenesis

The relationship of Pab1 with mRNAs begins at the transcription site. Here, the binding of Pab1 to pre-mRNA plays an important role in 3'-end processing and thus, in the maturation of functional transcripts. In the nucleus, Pab1 interacts with Rna15, a component of the cleavage and polyadenylation factor CF I, which is involved in pre-mRNA 3'-end processing (Amrani, Minet, Le Gouar, Lacroute, & Wyers, 1997; Minvielle-Sebastia, Preker, Wiederkehr, Strahm, & Keller, 1997).

Amrani and co-workers observed that, in extracts from a thermosensitive *pab1* mutant and from a wild-type strain immunoneutralized for Pab1, cleavage activity was normal, but mRNAs had longer poly (A) tails (Amrani et al., 1997). These results indicated that Pab1 is not required for cleavage, although its presence inhibits the elongation of the poly (A) tail by the poly (A) polymerase Pap1. Interestingly, the behaviour of the fungal Pab1 is opposite to that of the mammalian nuclear poly (A) binding protein Pab II, which strongly stimulates Pap activity (Wahle, Lustig, Jenö, & Maurer, 1993). In addition to poly (A) elongation control, Pab1 contributes to the subsequent trimming of the poly (A) tail for mRNA export from the nucleus (Brown & Sachs, 1998; Dunn et al., 2005). This last step of mRNA maturation requires the presence of both Pab1 and the deadenylase complex Pan2/Pan3 (PAN). The PAN complex interacts with poly (A) tails benefitted by the interaction of the PAM2 motif of the Pan3 subunit with the C-terminal domain of Pab1 (Siddiqui et al., 2007). The recruitment of the PAN complex to mRNAs via interaction with Pab1 is essential to stimulate the exonucleolytic activity of the Pan2 subunit. In fact, yeast strains in which the Pab1 C-terminal domain is absent or mutated to prevent interaction with Pan3, contain a pool of mRNA with longer poly (A) tails compared to wild-type strains (Brown & Sachs, 1998; Martani, Marano, Bertacchi, Porro, & Branduardi, 2015; Simón & Séraphin, 2007). Accordingly, a reduced PAN-dependent deadenylation rate was observed in the absence of Pab1 *in vitro* (Wolf et al., 2014). Interestingly, Pab1 can also negatively regulate PAN-mediated deadenylation by recruiting Pbp1 to the poly (A) tail (Mangus et al., 2004). Although the residues involved in binding to Pan3 and Pbp1 are different (localized at the C domain and the P domain, respectively), Pab1 cannot bind to both proteins at the same time because of steric hindrance. Consequently, the efficiency of PAN-mediated deadenylation depends on which of the two proteins is interacting with Pab1 (Figure 3) (Mangus et al., 2004). In *pbp1Δ* cells, the 3' termini of pre-mRNAs are properly cleaved but lack full-length poly (A) tails, suggesting that Pbp1 may also repress Pab1's ability to negatively regulate polyadenylation (Mangus et al., 1998).

It was demonstrated that the deletion of *PAB1*, *PAN2* or *PAN3* resulted in inefficient release of mRNAs from the sites of transcription (Brown & Sachs, 1998; Dunn et al., 2005), indicating the importance of both Pab1 and the PAN complex to couple mRNA biogenesis to export. Whether Pab1 is also involved in the export of mRNAs from the nucleus is unclear because it is not possible to distinguish whether the nuclear accumulation of mRNAs occurring in the absence of Pab1 is due to improper biogenesis or export defects. However, it has been demonstrated that Pab1 bound to the poly (A) tail indirectly interacts with different nucleoporins of the nuclear pore complex and Mex67 (Niño et al., 2013). This evidence, together with Pab1's ability to move from the nucleus to the cytoplasm in association with the Mex67/mRNA complexes, suggests a possible role in mRNA export (Allen et al., 2002; Brune et al., 2005).

3.2 | Pab1 stabilizes mRNAs and promotes their translation

The first evidence of the requirement of the poly (A) tail and PABPs for translation was discovered in the 1980s (Grossi de Sa et al.,

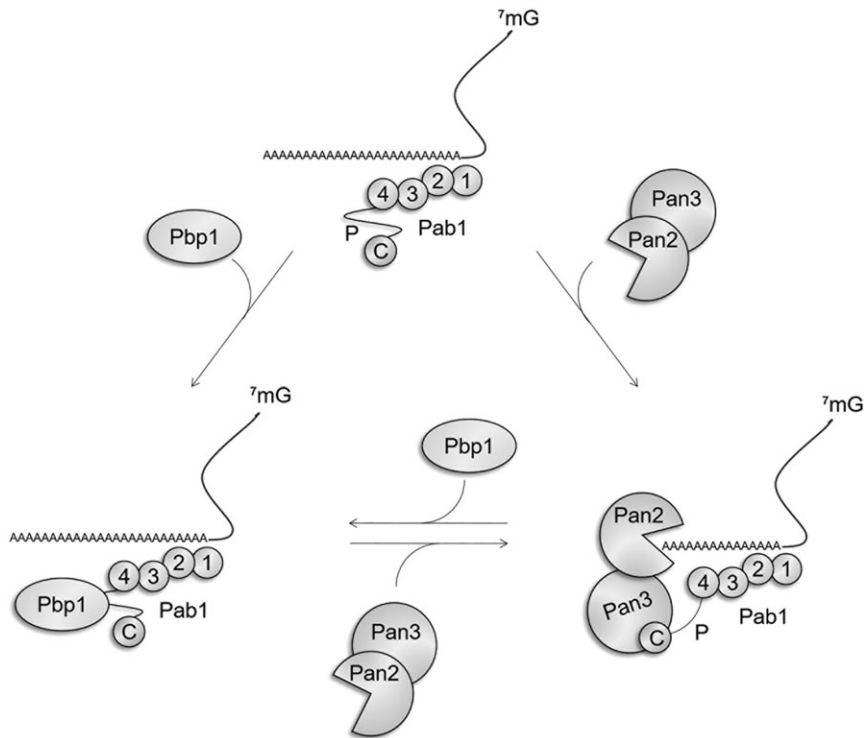


FIGURE 3 Positive and negative regulation of PAN-deadenylation by Pab1. Pab1 promotes PAN-deadenylation by binding Pan3 and therefore recruiting the Pan2/Pan3 complex to the poly (A) tail. When Pbp1 binds to Pab1 this interaction is hindered: the rate of deadenylation is dependent on the mutually exclusive interaction of Pab1 with Pan3 or Pbp1

1988; Jacobson & Favreau, 1983; Sachs & Davis, 1989). Subsequent studies in *S. cerevisiae* revealed that Pab1 has an important role in translation initiation because it promotes the assembly of ribosomal subunits onto the mRNAs. Different mechanisms require the presence of Pab1 to translate mRNAs into proteins. One mechanism is based on the closed-loop model, in which a circular mRNA structure is formed due to the joining of the 7-methylguanosine (m7G) 5' cap with the 3' poly (A) tail (Figure 4A) (Archer, Shirokikh, Hallwirth, Beilharz, & Preiss, 2015; Costello et al., 2015; Dever, Kinzy, & Pavitt, 2016; Melamed, Young, Miller, & Fields, 2015). The mRNA closed-loop restricts efficient translation of intact mRNAs, favours the assembly of polysomes, facilitates ribosome recycling and protects mRNAs from degradation (Archer et al., 2015; Costello et al., 2015; Huch & Nissan, 2014). This structure is formed with the help of simultaneous binding of eIF4G to eIF4E and Pab1, which are associated with the 5' cap and the 3' poly (A) tail, respectively. Pab1 association with eIF4G, which primarily occurs through the RRM2 domain of Pab1 (Dever et al., 2016; Melamed et al., 2015), stimulates the binding of the mRNA to the entire eIF4F complex (composed of eIF4E, eIF4G and the RNA helicase eIF4A) (O'Leary, Petrov, Chen, & Puglisi, 2013). The assembly of this structure facilitates the recruitment of the 43S preinitiation complex (composed of the 40S ribosomal subunit, eIF1, eIF2, eIF3, eIF5 and the methionyl-tRNA) at the mRNA, leading to formation of the 48S complex (Dever et al., 2016; Komar, Mazumder, & Merrick, 2012; Wang et al., 2012). Next, ribosome scanning occurs to identify the AUG start codon; subsequently, the 60S subunit joins the complex, leading to the formation of the 80S ribosome and to protein synthesis initiation (Costello et al., 2015; Dever et al., 2016; Farley, Powell, Weaver, Jennings, & Link, 2011; Komar et al., 2012; Wang et al., 2012). It has been proposed that the binding of Pab1 to the poly (A) tail stimulates the joining of the 60S ribosomal subunit by inhibiting

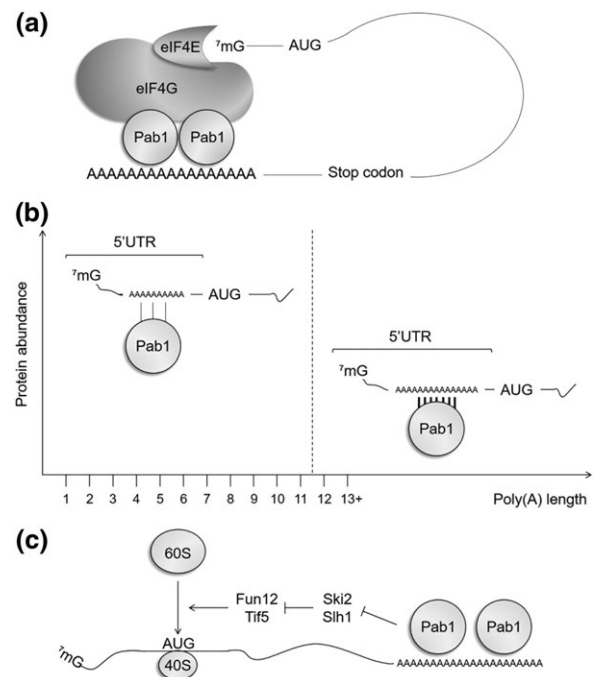


FIGURE 4 Pab1 promotes translation initiation. A) Representation of the closed loop structure: eIF4G bridges the two ends of the mRNA by binding eIF4E (associated to the 5' cap) and two molecules of Pab1 (associated to the 3' poly (A) tail), enabling the formation of a stable closed loop. B) The strength of Pab1 binding at 5' UTR IRES-mediated translation initiation. When poly (A) tracts at the 5'UTR of a mRNA are longer than or equal to 12 adenosines, Pab1 tightly binds them and the corresponding protein abundance is low; conversely, poly (A) tracts shorter than 12 adenosines are weakly bound by Pab1 and protein abundance is high. C) Pab1 binding to poly (A) tail blocks the Ski2/Sih1 inhibition on the translation initiation factors eIF5/eIF5B, thus stimulating 60S joining (redrawn from Searfoss et al., 2001)

the two RNA helicases Ski2 and Slh1 and, consequently, stimulates the activity of the translation initiation factors eIF5 and eIF5B (Figure 4C) (Searfoss, Dever, & Wickner, 2001).

Despite the physiological importance of the closed-loop in stimulating translation initiation, not all mRNAs require this structure for translation (Costello et al., 2015). In fact, a subset of efficiently translated transcripts (encoding, for example, proteins involved in amino acid and nucleotide metabolism, carbohydrate metabolism, energy generation, and tRNA amino-acylation and translation) has been found enriched with Pab1 but deficient for all other closed-loop related factors; hence, alternative Pab1-dependent mechanisms of translation might take place for these mRNAs (Costello et al., 2015). One possibility might be related to the presence of internal ribosome entry sites (IRESs) at the 5' UTR of mRNAs. IRESs can recruit ribosomes for translation initiation through a cap-independent mechanism (reviewed in Plank & Kieft, 2012) that might be relevant when cap-dependent translation initiation is repressed, such as during stressful conditions (Reineke & Merrick, 2009). Some IRESs in *S. cerevisiae* contain poly (A) tracts that can bind to Pab1, although the physiological role of this binding is unclear. It was suggested that the presence of Pab1 at the 5' UTR is a prerequisite for IRES activity because it might functionally substitute for the cap and eIF4E in recruiting eIF4G (Gilbert, Zhou, Butler, & Doudna, 2007). By contrast, when Pab1 binding to 5' UTR is too tight, such as for A-rich stretches equal to or longer than 12 adenosines (*i.e.*, the minimal length for efficient Pab1 binding (Sachs, Davis, & Kornberg, 1987)), the translation efficiency of the corresponding mRNA is reduced compared to that of transcripts with A-rich tracts shorter than 12 As (Figure 4B) (Xia et al., 2011). The presence of Pab1 tightly bound at the 5' UTR may interfere with ribosome scanning, thus reducing translation (Xia et al., 2011). Consequently, protein abundance and synthesis appear to be strongly dependent on the poly (A) length at the 5' UTR and on the efficiency of Pab1 binding. Interestingly, the mRNA encoding Pab1 contains an IRES in its 5' UTR with a poly (A) tract of 11 consecutive As that can escape the possible negative auto-regulation of the protein itself (Xia et al., 2011).

Pab1 can also stimulate translation independently from its binding to poly (A) tracts. *In vitro* studies showed that Pab1 significantly increases the affinity of eIF4E for the 5' cap of mRNAs lacking the poly (A) tail, leading to the formation of a stable eIF4E-mRNA complex (O'Leary et al., 2013). Pab1 may induce this structural rearrangement by binding to poly (A)-deficient mRNAs, taking advantage of the non-specific affinity of the RRM4 region to single-stranded RNA (Deardorff & Sachs, 1997). This hypothesis could be validated by assessing the conformational changes of the eIF4E-mRNA complex in the presence of a Pab1 mutant lacking the RRM4.

Despite its importance in stimulating translation, other studies suggest that Pab1 can also negatively regulate translation initiation by binding to 3' UTR sequences other than poly (A). *In vitro* translation assays demonstrated that Pab1 binding to AU-rich elements (AREs) at the 3' UTR represses translation of *MFA2* mRNAs in yeast cells growing on glucose (Vasudevan, Garneau, Tu Khounh, & Peltz, 2005). Furthermore, a Pab1-dependent mechanism of translation repression by Puf5 has been proposed (Chritton & Wickens, 2011).

In addition to binding to translation initiation proteins, Pab1 also interacts with the translation termination factor eRF3 (Sup35) by way of the P and C domains (Cosson et al., 2002; Roque et al., 2015).

Recently, it has been demonstrated that this interaction negatively regulates translation termination and maintains a basal level of translational read-through (Figure 5), a process in which the ribosome passes through the STOP codon by random insertion of a tRNA and continues translation to the next STOP codon in the same reading frame (Dabrowski, Bukowy-Bieryllo, & Zietkiewicz, 2015; Roque et al., 2015).

Together, these findings confirm that the mechanisms by which Pab1 intervenes in mRNA translation are multiple and far from being understood. Next, we discuss additional aspects of how Pab1 regulates the fate of mRNA.

3.3 | The dynamic binding of Pab1 to poly (A) tails regulates mRNA decay

In the cytoplasm, Pab1 also controls the mRNA deadenylation process. Its binding to the poly (A) tail regulates the activity of both the PAN and the Ccr4/Pop2/NOT deadenylation complexes. The physiological role of mRNA deadenylation in the cytoplasm is associated with the general mRNA decay pathway, differing from that which occurs in the nucleus. A sequential model has been proposed in which the Pan2/Pan3 complex is responsible for poly (A) tail shortening during the first

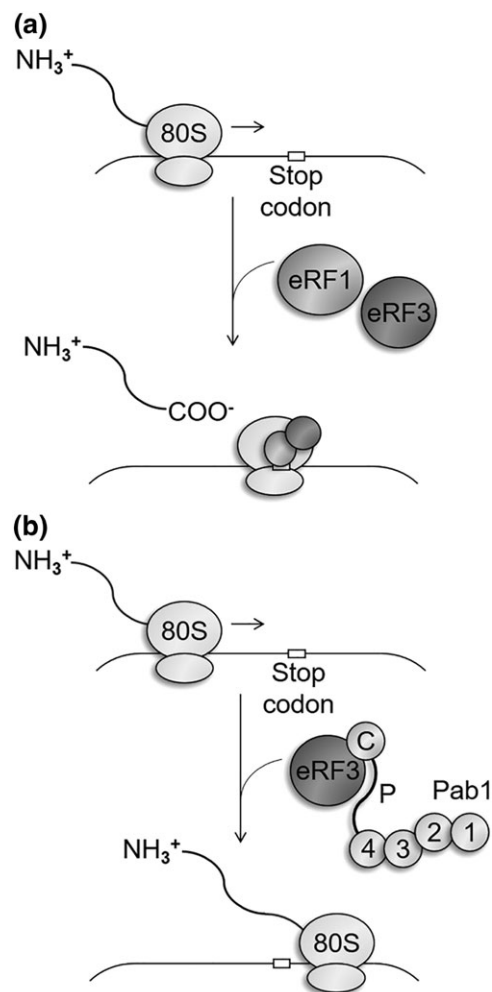


FIGURE 5 Pab1 effect on translation termination. A) eRF1-eRF3 association allows efficient stop codon recognition and translation arrest; B) Pab1 binding to eRF3 might impair translation termination, thus allowing a basal level of translational readthrough

distributive phase of deadenylation; successively, the more processive Ccr4/Pop2/NOT complex hydrolyses the remaining 20–25 residues (Brown & Sachs, 1998; Tucker, Staples, Valencia-Sanchez, Muhrad, & Parker, 2002; Wahle & Winkler, 2013; Wolf et al., 2014). The Ccr4/Pop2/NOT complex is composed of the scaffold subunits Not1, Not2 and Not3/5 and the two catalytic subunits Ccr4 and Pop2/Caf1. Pab1 inhibits Ccr4-mediated deadenylation *in vitro* (Tucker et al., 2002), but there is no evidence of direct contact between the two proteins. *In vivo*, it has been observed that Ccr4 shifts from a slow distributive to a rapid processive rate of deadenylation when the poly (A) tail is reduced to approximately 20–25 As, which corresponds to the number of residues protected by a Pab1 molecule (Yao et al., 2007). Therefore, the activity and recruitment of Ccr4 to mRNAs may be dependent on the binding state of Pab1 to poly (A) tails (Yao et al., 2007). In addition to poly (A) tail shortening, other mechanisms can impair Pab1 binding to mRNA and indirectly promote deadenylation by Ccr4. One mechanism consists of Pab1 self-circularization (Figure 6A) or oligomerization (Figure 6B), which lead to the formation of structures that are unable to bind poly (A) tails (Richardson et al., 2012; Yao et al., 2007). The RRM1 and P domains are both required for protein self-assembly (Yao et al., 2007). In addition to protein self-assembly, the interaction of Pab1 with Upf1 or Puf3, two factors involved in mRNA decay, can sequester Pab1 and favour Ccr4-mediated deadenylation (Figure 6C) (Lee et al., 2010; Richardson et al., 2012). The acceleration of deadenylation by Upf1 and Puf3 requires the RRM1 domain (Lee et al., 2010; Richardson et al., 2012). Accordingly, the mutation of some residues of this domain (Y41, C70, C109, and Y83) led to a reduction in the deadenylation rate (Zhang et al., 2013).

It has been proposed that Pab1 plays a role in mRNA degradation via nonsense-mediated decay (NMD). NMD is a surveillance pathway that guarantees the degradation of mRNAs with premature termination codons (PTCs) from which deleterious truncated proteins could be synthesized (Kervestin & Jacobson, 2012; Parker, 2012). The 'faux UTR' model suggests that the lack of termination factors that are normally present on canonical 3' UTRs induces an aberrant translation termination and consequently, NMD activation (Amrani et al., 2004).

This mechanism requires the core components of the surveillance complex Upf1, Upf2 and Upf3 as well as the two releasing factors eRF1 and eRF3 for stop codon recognition (Kervestin & Jacobson, 2012; Parker, 2012). It has been proposed that the proximity of Pab1 to the stop codon is necessary for the discrimination between normal and PTC-containing mRNAs. In fact, mRNAs with Pab1 tethered 37–73 nt downstream to the 3' of a PTC were particularly stable *in vivo* and were subjected to NMD when Pab1 was tethered 164 nt downstream to the PTC (Amrani et al., 2004). Accordingly, mRNAs with unusually long 3' UTRs are targeted to NMD, and the removal of a major part of the coding sequence downstream of a PTC stabilizes mRNAs (Kervestin & Jacobson, 2012). More recently, it has been demonstrated that PTC-containing mRNAs in yeast cells lacking Pab1, as well as PTC-containing mRNAs lacking the poly (A) tail, are still recognized as NMD substrates (Meaux, van Hoof, & Baker, 2008). Therefore, the role of Pab1 in discriminating premature from normal stop codons is ambiguous, suggesting that other factors may be involved in targeting mRNAs to NMD (Meaux et al., 2008).

Because of its importance in the control of deadenylation, Pab1 may also indirectly affect the regulation of cell cycle progression. Beilharz and Preiss (2007) found that mRNAs encoding elements relevant to the cell cycle have predominantly short tails in a mixed cell population. This evidence, together with the observation that the Ccr4 and Pan2 deadenylases genetically interact with cell cycle regulators (Hammett, Pike, & Heierhorst, 2002; Westmoreland et al., 2004; Woolstencroft et al., 2006), suggests that the temporal limitation of the expression of cell cycle-related proteins depends on proper deadenylase function (Beilharz & Preiss, 2007). The resulting delimited expression of cell cycle-related mRNAs to shorter intervals than suggested by changes in mRNA expression may be important for cell-cycle progression (Beilharz & Preiss, 2007). Although a direct interaction of Pab1 with cell cycle-related factors has not been identified, we cannot exclude that its role in the regulation of poly (A) tail length and mRNA translation might also contribute to cell cycle progression. Interestingly, Pab1 overexpression suppressed the

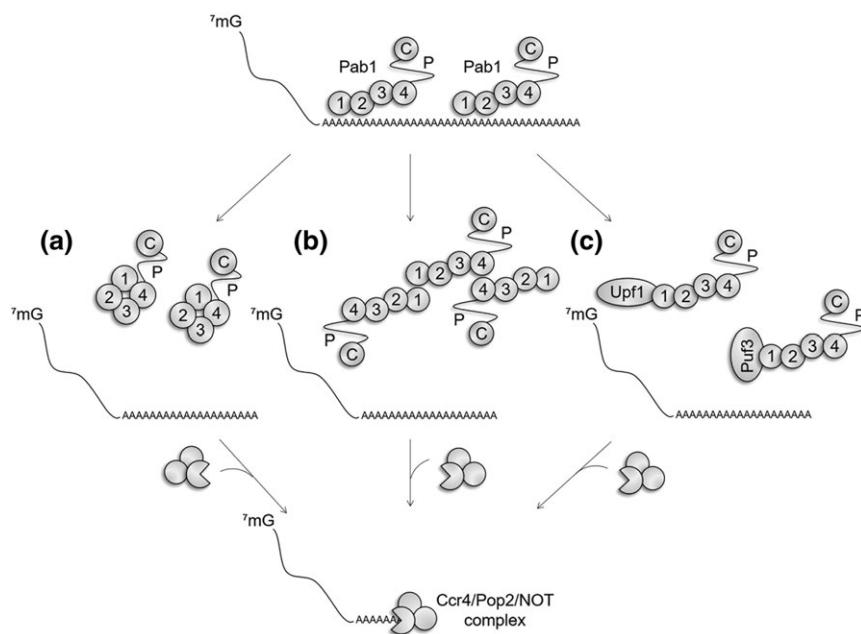


FIGURE 6 Mechanisms preventing the binding of Pab1 to poly (A) tails. Pab1 self-association into A) circular species or B) multimers, or C) Pab1 interaction with Upf1 or Puf3, prevents its binding to poly (A) and stimulates Ccr4 dependent deadenylation. (Figures A and B have been redrawn from Yao et al., 2007)

conditional lethality of *bck2 swi6-ts* cells, which are defective in a G1-specific transcriptional activator and are characterized by cell cycle arrest (Flick & Wittenberg, 2005). Two hypotheses have been formulated to explain this suppression: 1) Pab1 might influence the cell cycle by altering the regulation of G1-specific transcriptional targets as the result of an effect on the general translation rate; 2) Pab1 might directly antagonize the effect of Whi3 on specific mRNAs, including those encoding G1 cyclins (Flick & Wittenberg, 2005).

4 | Pab1 PARTICIPATES IN THE CELLULAR STRESS RESPONSE

By regulating mRNA metabolism, Pab1 plays an important role in the cellular response to stress. *S. cerevisiae* reacts to stressful conditions by reprogramming gene expression at the transcriptional and post-transcriptional levels (Arribere, Doudna, & Gilbert, 2011). Post-transcriptional regulation includes the export, translation and decay of mRNAs (Arribere et al., 2011), as well as the formation of intracellular protein aggregates with different sizes, compositions and physical properties (Buchan & Parker, 2009; Protter & Parker, 2016; Riback et al., 2017; Wallace et al., 2015). Pab1 participates in the cellular stress response by forming quinary assemblies, by promoting the formation of stress granules (SGs) and by stabilizing mRNAs to allow rapid re-initiation of translation after stress.

Quinary structures are transient protein assemblies that lack a fixed-stoichiometry and are kept together by multivalent interactions (Wallace et al., 2015). They are formed in response to mild heat-stress conditions and differ from misfolded-protein aggregates because they are beneficial and not deleterious (Riback et al., 2017; Wallace et al., 2015). Pab1 undergoes *in vivo* phase separation and forms these structures with the help of electrostatic forces associated with the RRM domains. The low-complexity region of the P domain is not required for the assembly of the quinary structures, but may act as a biophysical regulator. In fact, mutagenesis analyses showed that the reduction of the hydrophobicity of the P domain decreases the ability of the protein to phase separate and correlates with reduced cell fitness under mild heat-stress conditions (Riback et al., 2017).

When cells are challenged with severe stress (e.g., heat-shock at 46°C or glucose starvation), mRNAs can be delivered to mRNP granules referred to as processing bodies (PBs) and stress granules (SGs) (Buchan & Parker, 2009; Protter & Parker, 2016). According to the so-called "mRNA cycle", transcripts can be exchanged between these two aggregates and/or return to translation and/or be degraded (Buchan & Parker, 2009; Protter & Parker, 2016). The fate of transcripts stored in PBs is often degradation; indeed, PBs are composed of proteins involved in mRNA decay and translation repression (Buchan & Parker, 2009; Buchan, Yoon, & Parker, 2011; Decker & Parker, 2012; Giménez-Barcons & Díez, 2011; Grousl et al., 2009). Conversely, SGs are believed to be sites for promoting the formation of translation initiation complexes (Protter & Parker, 2016); accordingly, they typically contain proteins involved in protein synthesis initiation (Buchan et al., 2011; Buchan & Parker, 2009). Depending on the imposed stress, SG composition can be slightly different. For example, SGs of glucose-starved cells typically contain the translation initiation

factors eIF4E, eIF4G and Pab1, and for this reason, they have been referred to as EGP bodies (Hoyle, Castelli, Campbell, Holmes, & Ashe, 2007). By contrast, SGs of cells exposed to sodium azide or to heat-shock at 46°C contain eIF3, eIF1A and eIF5B (Buchan et al., 2011) or the 40S ribosomal subunits, eIF3 and proteins involved in the TOR pathway regulation (Grousl et al., 2009; Takahara & Maeda, 2012), respectively.

Despite these differences in protein composition (which probably account for specific response to a particular stress), Pab1 is a typical component of SGs and is commonly used as their indicator (Brambilla et al., 2017; Jain et al., 2016; Martani et al., 2015; Swisher & Parker, 2010; Wheeler, Matheny, Jain, Abrisch, & Parker, 2016). It has been proposed that this protein promotes SG formation (Swisher & Parker, 2010); however, the need for bypass suppressors of the *PAB1* deletion limits the possibility to accurately define its role in SG assembly. In fact, depending on the suppressor strain used, different phenotypes were observed in terms of the number of SGs and PBs formed in response to glucose starvation. In the *pab1Δ spb2Δ* strain, fewer SGs and more PBs were detected compared to the *spb2Δ* single deletion strain, suggesting that Pab1 might stimulate the transition of poly (A)⁺ mRNAs from PBs to SGs (Swisher & Parker, 2010). However, because SGs were still present in this strain and because no changes in their number were detected in another bypass suppressor strain (*pab1Δ pat1-2*), it was concluded that Pab1 is not required for SG formation (Swisher & Parker, 2010).

Arribere and colleagues (2011) observed that, after recovery from glucose starvation, cells contained translation-competent mRNAs with long poly (A) tails and were enriched with Pab1 (Arribere et al., 2011). Therefore, although Pab1 does not appear to be required to form SGs, under stressful conditions Pab1 might protect mRNAs from degradation by contributing to their delivery into SGs. According to this model, Pab1 assures translation re-initiation and consequently, cell recovery from stress.

5 | CONCLUSIONS AND FUTURE PERSPECTIVES

The *S. cerevisiae* poly (A) binding protein has been extensively studied to determine its cellular functions, revealing the complex network in which Pab1 is a master regulator of mRNA metabolism. Further insights into its functions and interactions will ensure a better comprehension of how it acts as a multifunctional scaffold protein in controlling mRNA dynamics. Novel findings on Pab1 functions are continuously emerging, indicating that the role of this protein in cell physiology could be larger than expected. For example, chromatin immunoprecipitation assays revealed that Pab1 binds DNA at the *ENO2* and *GAL1* promoter and that the carbon source can alter Pab1 enrichment at the promoter site (Guillen-Ahlers et al., 2016). This result suggests a possible role of Pab1 in the regulation of transcription and/or in the epigenetic control of chromatin function (Byrum, Raman, Taverna, & Tackett, 2012; Guillen-Ahlers et al., 2016).

In light of its broad role in controlling mRNA metabolism, we believe that Pab1 should be considered an important hub element whose modification could rearrange global gene-expression, leading to phenotypes of interest. We have recently demonstrated that the

modulation of its expression improves yeast stress tolerance and that its mutagenesis followed by the application of a specific screening protocol allows for the isolation of the ameliorated mutant *pab1* A60–9 (Martani et al., 2015). Nevertheless, we must consider that Pab1 has a complex modular structure, such that the positive effect of one mutation could be masked by other mutations or by other domains of the protein. As indicated by studies based on single domain deletions, some domains have a central role in protein self-association, deadenylation or translation, whereas others appear to be dispensable. These results imply that the modular structure of this protein accounts for the broad spectrum of Pab1 functions and represents an attractive platform for synthetic biology approaches aimed at rewiring mRNA metabolism. The addition, removal, or swapping of the modules inside the protein itself may allow for the creation of chimeras with altered properties that could improve cellular traits as well as increase our understanding of Pab1 function in controlling dynamic mRNA metabolism.

Finally, humanized versions of Pab1 have demonstrated that residues of the RRM2 are responsible for the species-specific binding of Pab1 to eIF4G1 (Melamed et al., 2015). In another study, Pab1 variants with long polyalanine tracts have been used to study the aggregation and the cellular dysfunctions associated with polyalanine-expansion occurring in some human disorders (Konopka et al., 2011).

We expect that further studies will better depict the roles and functions of Pab1 in yeast as well as in human cells, with possible applications in basic and in applied research.

ACKNOWLEDGMENTS

We wish to acknowledge Pooja Jayaprakash for language revision. This work was supported by the University of Milano-Bicocca with the FA (Fondo di Ateneo) to PB, the PhD fellowship to MB and the post-Doctoral fellowship to FM.

CONFLICT OF INTEREST

None declared.

ORCID

Marco Brambilla  <http://orcid.org/0000-0003-2022-803X>

Francesca Martani  <http://orcid.org/0000-0002-3553-3726>

Stefano Bertacchi  <http://orcid.org/0000-0002-8281-7625>

Paola Branduardi  <http://orcid.org/0000-0003-4115-7015>

REFERENCES

- Allen, N. P., Patel, S. S., Huang, L., Chalkley, R. J., Burlingame, A., Lutzmann, M., ... Rexach, M. (2002). Deciphering networks of protein interactions at the nuclear pore complex. *Molecular & Cellular Proteomics*, 1, 930–946.
- Amrani, N., Ganesan, R., Kervestin, S., Mangus, D. A., Ghosh, S., & Jacobson, A. (2004). A faux 3'-UTR promotes aberrant termination and triggers nonsense-mediated mRNA decay. *Nature*, 432, 112–118.
- Amrani, N., Minet, M., Le Gouar, M., Lacroute, F., & Wyers, F. (1997). Yeast Pab1 interacts with Rna15 and participates in the control of the poly (A) tail length *in vitro*. *Molecular and Cellular Biology*, 17, 3694–3701.
- Archer, S. K., Shirokikh, N. E., Hallwirth, C. V., Beilharz, T. H., & Preiss, T. (2015). Probing the closed-loop model of mRNA translation in living cells. *RNA Biology*, 12, 248–254.
- Arribere, J. A., Doudna, J. A., & Gilbert, W. V. (2011). Reconsidering movement of eukaryotic mRNAs between polysomes and P bodies. *Molecular Cell*, 44, 745–758.
- Beelman, C. A., Stevens, A., Caponigro, G., LaGrandeur, T. E., Hatfield, L., Fortner, D. M., & Parker, R. (1996). An essential component of the decapping enzyme required for normal rates of mRNA turnover. *Nature*, 382, 642–646.
- Beilharz, T. H., & Preiss, T. (2007). Widespread use of poly (A) tail length control to accentuate expression of the yeast transcriptome. *RNA*, 13, 982–997.
- Belostotsky, D. A., & Meagher, R. B. (1996). A pollen-, ovule-, and early embryo-specific poly (A) binding protein from *Arabidopsis* complements essential functions in yeast. *Plant Cell*, 8, 1261–1275.
- Boeck, R., Lapeyre, B., Brown, C. E., & Sachs, A. B. (1998). Capped mRNA degradation intermediates accumulate in the yeast *spb8-2* mutant. *Molecular and Cellular Biology*, 18, 5062–5072.
- Brambilla, M., Martani, F., & Branduardi, P. (2017). The recruitment of the *Saccharomyces cerevisiae* poly (A)-binding protein into stress granules: New insights into the contribution of the different protein domains. *FEMS Yeast Research*, 17(6).
- Brown, C. E., & Sachs, A. B. (1998). Poly (A) tail length control in *Saccharomyces cerevisiae* occurs by message-specific deadenylation. *Molecular and Cellular Biology*, 18, 6548–6559.
- Brune, C., Munchel, S. E., Fischer, N., Podtelejnikov, A. V., & Weis, K. (2005). Yeast poly (A)-binding protein Pab1 shuttles between the nucleus and the cytoplasm and functions in mRNA export. *RNA*, 11, 517–531.
- Buchan, J. R., Muhrad, D., & Parker, R. (2008). P bodies promote stress granule assembly in *Saccharomyces cerevisiae*. *The Journal of Cell Biology*, 183, 441–455.
- Buchan, J. R., & Parker, R. (2009). Eukaryotic stress granules: The ins and outs of translation. *Molecular Cell*, 36, 932–941.
- Buchan, J. R., Yoon, J. H., & Parker, R. (2011). Stress-specific composition, assembly and kinetics of stress granules in *Saccharomyces cerevisiae*. *Journal of Cell Science*, 124, 228–239.
- Byrum, S. D., Raman, A., Taverna, S. D., & Tackett, A. J. (2012). ChAP-MS: a method for identification of proteins and histone posttranslational modifications at a single genomic locus. *Cell Reports*, 2, 198–205.
- Caponigro, G., & Parker, R. (1995). Multiple functions for the poly (A)-binding protein in mRNA decapping and deadenylation in yeast. *Genes & Development*, 9, 2421–2432.
- Chekanova, J. A., & Belostotsky, D. A. (2003). Evidence that poly (A) binding protein has an evolutionarily conserved function in facilitating mRNA biogenesis and export. *RNA*, 9, 1476–1490.
- Chekanova, J. A., Shaw, R. J., & Belostotsky, D. A. (2001). Analysis of an essential requirement for the poly (A) binding protein function using cross-species complementation. *Current Biology*, 11, 1207–1214.
- Chritton, J. J., & Wickens, M. (2011). A role for the poly (A)-binding protein Pab1p in PUF protein-mediated repression. *The Journal of Biological Chemistry*, 286, 33268–33278.
- Cosson, B., Couturier, A., Chabelskaya, S., Kiktev, D., Inge-Vechtormov, S., Philippe, M., & Zhouravleva, G. (2002). Poly (A)-binding protein acts in translation termination via eukaryotic release factor 3 interaction and does not influence [PSI(+)] propagation. *Molecular and Cellular Biology*, 22, 3301–3315.
- Costello, J., Castelli, L. M., Rowe, W., Kershaw, C. J., Talavera, D., Mohammad-Qureshi, S. S., ... Ashe, M. P. (2015). Global mRNA selection mechanisms for translation initiation. *Genome Biology*, 16, 10.
- Dabrowski, M., Bukowy-Bieryllo, Z., & Zietkiewicz, E. (2015). Translational readthrough potential of natural termination codons in eucaryotes—The impact of RNA sequence. *RNA Biology*, 12, 950–958.
- Deardorff, J. A., & Sachs, A. B. (1997). Differential effects of aromatic and charged residue substitutions in the RNA binding domains of the yeast poly (A)-binding protein. *Journal of Molecular Biology*, 269, 67–81.

- Decker, C. J., & Parker, R. (2012). P-bodies and stress granules: Possible roles in the control of translation and mRNA degradation. *Cold Spring Harbor Perspectives in Biology*, 4, a012286.
- Dever, T. E., Kinzy, T. G., & Pavitt, G. D. (2016). Mechanism and Regulation of Protein Synthesis in *Saccharomyces cerevisiae*. *Genetics*, 203, 65–107.
- Dunn, E. F., Hammell, C. M., Hodge, C. A., & Cole, C. N. (2005). Yeast poly (A)-binding protein, Pab1, and PAN, a poly (A) nuclease complex recruited by Pab1, connect mRNA biogenesis to export. *Genes & Development*, 19, 90–103.
- Eliseeva, I. A., Lyabin, D. N., & Ovchinnikov, L. P. (2013). Poly (A)-binding proteins: structure, domain organization, and activity regulation. *Biochemistry (Mosc)*, 78, 1377–1391.
- Farley, A. R., Powell, D. W., Weaver, C. M., Jennings, J. L., & Link, A. J. (2011). Assessing the components of the eIF3 complex and their phosphorylation status. *Journal of Proteome Research*, 10, 1481–1494.
- Flick, K., & Wittenberg, C. (2005). Multiple pathways for suppression of mutants affecting G1-specific transcription in *Saccharomyces cerevisiae*. *Genetics*, 169, 37–49.
- Gilbert, W. V., Zhou, K., Butler, T. K., & Doudna, J. A. (2007). Cap-independent translation is required for starvation-induced differentiation in yeast. *Science*, 317, 1224–1227.
- Giménez-Barcons, M., & Díez, J. (2011). Yeast processing bodies and stress granules: self-assembly ribonucleoprotein particles. *Microbial Cell Factories*, 10, 73.
- Goss, D. J., & Kleiman, F. E. (2013). Poly (A) binding proteins: are they all created equal? *Wiley Interdiscip Rev RNA*, 4, 167–179.
- Grossi de Sa, M. F., Standart, N., Martins de Sa, C., Akhayat, O., Huesca, M., & Scherrer, K. (1988). The poly (A)-binding protein facilitates *in vitro* translation of poly (A)-rich mRNA. *European Journal of Biochemistry*, 176, 521–526.
- Grousl, T., Ivanov, P., Frýdlová, I., Vasicová, P., Janda, F., Vojtová, J., ... Hasek, J. (2009). Robust heat shock induces eIF2alpha-phosphorylation-independent assembly of stress granules containing eIF3 and 40S ribosomal subunits in budding yeast, *Saccharomyces cerevisiae*. *Journal of Cell Science*, 122, 2078–2088.
- Guillen-Ahlers, H., Rao, P. K., Levenstein, M. E., Kennedy-Darling, J., Perumalla, D. S., Jadhav, A. Y., ... Olivier, M. (2016). HyCCAPP as a tool to characterize promoter DNA-protein interactions in *Saccharomyces cerevisiae*. *Genomics*, 107, 267–273.
- Hammet, A., Pike, B. L., & Heierhorst, J. (2002). Posttranscriptional regulation of the RAD5 DNA repair gene by the Dun1 kinase and the Pan2-Pan3 poly (A)-nuclease complex contributes to survival of replication blocks. *The Journal of Biological Chemistry*, 277, 22469–22474.
- Hatfield, L., Beelman, C. A., Stevens, A., & Parker, R. (1996). Mutations in trans-acting factors affecting mRNA decapping in *Saccharomyces cerevisiae*. *Molecular and Cellular Biology*, 16, 5830–5838.
- Hoyle, N. P., Castelli, L. M., Campbell, S. G., Holmes, L. E., & Ashe, M. P. (2007). Stress-dependent relocalization of translationally primed mRNPs to cytoplasmic granules that are kinetically and spatially distinct from P-bodies. *The Journal of Cell Biology*, 179, 65–74.
- Huch, S., & Nissan, T. (2014). Interrelations between translation and general mRNA degradation in yeast. *Wiley Interdiscip Rev RNA*, 5, 747–763.
- Jacobson, A., & Favreau, M. (1983). Possible involvement of poly (A) in protein synthesis. *Nucleic Acids Research*, 11, 6353–6368.
- Jain, S., Wheeler, J. R., Walters, R. W., Agrawal, A., Barsic, A., & Parker, R. (2016). ATPase-Modulated Stress Granules Contain a Diverse Proteome and Substructure. *Cell*, 164, 487–498.
- Kervestin, S., & Jacobson, A. (2012). NMD: A multifaceted response to premature translational termination. *Nature Reviews. Molecular Cell Biology*, 13, 700–712.
- Komar, A. A., Mazumder, B., & Merrick, W. C. (2012). A new framework for understanding IRES-mediated translation. *Gene*, 502, 75–86.
- Konopka, C. A., Locke, M. N., Gallagher, P. S., Pham, N., Hart, M. P., Walker, C. J., ... Gardner, R. G. (2011). A yeast model for polyalanine-expansion aggregation and toxicity. *Molecular Biology of the Cell*, 22, 1971–1984.
- Kozlov, G., Siddiqui, N., Coillet-Matillon, S., Trempe, J. F., Ekiel, I., Sprules, T., & Gehring, K. (2002). Solution structure of the orphan PABC domain from *Saccharomyces cerevisiae* poly (A)-binding protein. *The Journal of Biological Chemistry*, 277, 22822–22828.
- Kwok, C. K., Tang, Y., Assmann, S. M., & Bevilacqua, P. C. (2015). The RNA structurome: Transcriptome-wide structure probing with next-generation sequencing. *Trends in Biochemical Sciences*, 40, 221–232.
- Lee, D., Ohn, T., Chiang, Y. C., Quigley, G., Yao, G., Liu, Y., & Denis, C. L. (2010). PUF3 acceleration of deadenylation *in vivo* can operate independently of CCR4 activity, possibly involving effects on the PAB1-mRNP structure. *Journal of Molecular Biology*, 399, 562–575.
- Mangus, D. A., Amrani, N., & Jacobson, A. (1998). Pbp1p, a factor interacting with *Saccharomyces cerevisiae* poly (A)-binding protein, regulates polyadenylation. *Molecular and Cellular Biology*, 18, 7383–7396.
- Mangus, D. A., Evans, M. C., Agrin, N. S., Smith, M., Gongidi, P., & Jacobson, A. (2004). Positive and negative regulation of poly (A) nuclease. *Molecular and Cellular Biology*, 24, 5521–5533.
- Maris, C., Dominguez, C., & Allain, F. H. (2005). The RNA recognition motif, a plastic RNA-binding platform to regulate post-transcriptional gene expression. *The FEBS Journal*, 272, 2118–2131.
- Martani, F., Marano, F., Bertacchi, S., Porro, D., & Branduardi, P. (2015). The *Saccharomyces cerevisiae* poly (A) binding protein Pab1 as a target for eliciting stress tolerant phenotypes. *Scientific Reports*, 5, 18318.
- Meaux, S., van Hoof, A., & Baker, K. E. (2008). Nonsense-mediated mRNA decay in yeast does not require PAB1 or a poly (A) tail. *Molecular Cell*, 29, 134–140.
- Melamed, D., Young, D. L., Miller, C. R., & Fields, S. (2015). Combining natural sequence variation with high throughput mutational data to reveal protein interaction sites. *PLoS Genetics*, 11, e1004918.
- Minvielle-Sebastia, L., Preker, P. J., Wiederkehr, T., Strahm, Y., & Keller, W. (1997). The major yeast poly (A)-binding protein is associated with cleavage factor IA and functions in premessenger RNA 3'-end formation. *Proceedings of the National Academy of Sciences of the United States of America*, 94, 7897–7902.
- Mitchell, S. F., & Parker, R. (2014). Principles and properties of eukaryotic mRNPs. *Molecular Cell*, 54, 547–558.
- Niño, C. A., Hérisant, L., Babour, A., & Dargemont, C. (2013). mRNA nuclear export in yeast. *Chemical Reviews*, 113, 8523–8545.
- O'Leary, S. E., Petrov, A., Chen, J., & Puglisi, J. D. (2013). Dynamic recognition of the mRNA cap by *Saccharomyces cerevisiae* eIF4E. *Structure*, 21, 2197–2207.
- Parker, R. (2012). RNA degradation in *Saccharomyces cerevisiae*. *Genetics*, 191, 671–702.
- Pintard, L., Kressler, D., & Lapeyre, B. (2000). Spb1p Is a Yeast Nucleolar Protein Associated with Nop1p and Nop58p That Is Able To Bind S-Adenosyl-L-Methionine *In Vitro*. *Molecular and Cellular Biology*, 20, 1370–1381.
- Plank, T. D., & Kieft, J. S. (2012). The structures of nonprotein-coding RNAs that drive internal ribosome entry site function. *Wiley Interdiscip Rev RNA*, 3, 195–212.
- Protter, D. S., & Parker, R. (2016). Principles and Properties of Stress Granules. *Trends in Cell Biology*, 26, 668–679.
- Reineke, L. C., & Merrick, W. C. (2009). Characterization of the functional role of nucleotides within the URE2 IRES element and the requirements for eIF2A-mediated repression. *RNA*, 15, 2264–2277.
- Riback, J. A., Katanski, C. D., Kear-Scott, J. L., Pilipenko, E. V., Rojek, A. E., Sosnick, T. R., & Drummond, D. A. (2017). Stress-Triggered Phase Separation Is an Adaptive, Evolutionarily Tuned Response. *Cell*, 168, 1028, e19–1040.
- Richardson, R., Denis, C. L., Zhang, C., Nielsen, M. E., Chiang, Y. C., Kierkegaard, M., ... Yao, G. (2012). Mass spectrometric identification

- of proteins that interact through specific domains of the poly (A) binding protein. *Molecular Genetics and Genomics*, 287, 711–730.
- Roque, S., Cerciat, M., Gaugué, I., Mora, L., Floch, A. G., de Zamaroczy, M., ... Kervestin, S. (2015). Interaction between the poly (A)-binding protein Pab1 and the eukaryotic release factor eRF3 regulates translation termination but not mRNA decay in *Saccharomyces cerevisiae*. *RNA*, 21, 124–134.
- Sachs, A. B., Bond, M. W., & Kornberg, R. D. (1986). A single gene from yeast for both nuclear and cytoplasmic polyadenylate-binding proteins: Domain structure and expression. *Cell*, 45, 827–835.
- Sachs, A. B., & Davis, R. W. (1989). The poly (A) binding protein is required for poly (A) shortening and 60S ribosomal subunit-dependent translation initiation. *Cell*, 58, 857–867.
- Sachs, A. B., & Davis, R. W. (1990). Translation initiation and ribosomal biogenesis: Involvement of a putative rRNA helicase and RPL46. *Science*, 247, 1077–1079.
- Sachs, A. B., Davis, R. W., & Kornberg, R. D. (1987). A single domain of yeast poly (A)-binding protein is necessary and sufficient for RNA binding and cell viability. *Molecular and Cellular Biology*, 7, 3268–3276.
- Schmid, M., Poulsen, M. B., Olszewski, P., Pelechano, V., Saguez, C., Gupta, I., ... Jensen, T. H. (2012). Rrp6p controls mRNA poly (A) tail length and its decoration with poly (A) binding proteins. *Molecular Cell*, 47, 267–280.
- Searfoss, A., Dever, T. E., & Wickner, R. (2001). Linking the 3' poly (A) tail to the subunit joining step of translation initiation: Relations of Pab1p, eukaryotic translation initiation factor 5b (Fun12p), and Ski2p-Slh1p. *Molecular and Cellular Biology*, 21, 4900–4908.
- Siddiqui, N., Mangus, D. A., Chang, T. C., Palermino, J. M., Shyu, A. B., & Gehring, K. (2007). Poly (A) nuclease interacts with the C-terminal domain of polyadenylate-binding protein domain from poly (A)-binding protein. *The Journal of Biological Chemistry*, 282, 25067–25075.
- Simón, E., & Séraphin, B. (2007). A specific role for the C-terminal region of the Poly (A)-binding protein in mRNA decay. *Nucleic Acids Research*, 35, 6017–6028.
- Smith, R. W., Blee, T. K., & Gray, N. K. (2014). Poly (A)-binding proteins are required for diverse biological processes in metazoans. *Biochemical Society Transactions*, 42, 1229–1237.
- Soucek, S., Corbett, A. H., & Fasken, M. B. (2012). The long and the short of it: the role of the zinc finger polyadenosine RNA binding protein, Nab2, in control of poly (A) tail length. *Biochimica et Biophysica Acta*, 1819, 546–554.
- Swisher, K. D., & Parker, R. (2010). Localization to, and effects of Pbp1, Pbp4, Lsm12, Dhh1, and Pab1 on stress granules in *Saccharomyces cerevisiae*. *PLoS One*, 5, e10006.
- Takahara, T., & Maeda, T. (2012). Transient sequestration of TORC1 into stress granules during heat stress. *Molecular Cell*, 47, 242–252.
- Tucker, M., Staples, R. R., Valencia-Sanchez, M. A., Muhlrud, D., & Parker, R. (2002). Ccr4p is the catalytic subunit of a Ccr4p/Pop2p/Notp mRNA deadenylase complex in *Saccharomyces cerevisiae*. *The EMBO Journal*, 21, 1427–1436.
- Vasudevan, S., Garneau, N., Tu Khounh, D., & Peltz, S. W. (2005). p38 mitogen-activated protein kinase/Hog1p regulates translation of the AU-rich-element-bearing MFA2 transcript. *Molecular and Cellular Biology*, 25, 9753–9763.
- Wahle, E., Lustig, A., Jenö, P., & Maurer, P. (1993). Mammalian poly (A)-binding protein II. Physical properties and binding to polynucleotides. *The Journal of Biological Chemistry*, 268, 2937–2945.
- Wahle, E., & Winkler, G. S. (2013). RNA decay machines: deadenylation by the Ccr4-not and Pan2-Pan3 complexes. *Biochimica et Biophysica Acta*, 1829, 561–570.
- Wallace, E. W., Kear-Scott, J. L., Pilipenko, E. V., Schwartz, M. H., Laskowski, P. R., Rojek, A. E., ... Drummond, D. A. (2015). Reversible, Specific, Active Aggregates of Endogenous Proteins Assemble upon Heat Stress. *Cell*, 162, 1286–1298.
- Walters, R., & Parker, R. (2014). Is there quality control of localized mRNAs? *The Journal of Cell Biology*, 204, 863–868.
- Wang, X., Zhang, C., Chiang, Y. C., Toomey, S., Power, M. P., Granoff, M. E., ... Denis, C. L. (2012). Use of the novel technique of analytical ultracentrifugation with fluorescence detection system identifies a 77S monosomal translation complex. *Protein Science*, 21, 1253–1268.
- Westmoreland, T. J., Marks, J. R., Olson, J. A., Thompson, E. M., Resnick, M. A., & Bennett, C. B. (2004). Cell cycle progression in G1 and S phases is CCR4 dependent following ionizing radiation or replication stress in *Saccharomyces cerevisiae*. *Eukaryotic Cell*, 3, 430–446.
- Wheeler, J. R., Matheny, T., Jain, S., Abrisch, R., & Parker, R. (2016). Distinct stages in stress granule assembly and disassembly. *eLife*, 5.
- Wolf, J., Valkov, E., Allen, M. D., Meineke, B., Gordiyenko, Y., McLaughlin, S. H., ... Passmore, L. A. (2014). Structural basis for Pan3 binding to Pan2 and its function in mRNA recruitment and deadenylation. *The EMBO Journal*, 33, 1514–1526.
- Woolstencroft, R. N., Beilharz, T. H., Cook, M. A., Preiss, T., Durocher, D., & Tyers, M. (2006). Ccr4 contributes to tolerance of replication stress through control of CRT1 mRNA poly (A) tail length. *Journal of Cell Science*, 119, 5178–5192.
- Wyers, F., Minet, M., Dufour, M. E., Vo, L. T., & Lacroute, F. (2000). Deletion of the PAT1 gene affects translation initiation and suppresses a PAB1 gene deletion in yeast. *Molecular and Cellular Biology*, 20, 3538–3549.
- Xia, X., MacKay, V., Yao, X., Wu, J., Miura, F., Ito, T., & Morris, D. R. (2011). Translation initiation: A regulatory role for poly (A) tracts in front of the AUG codon in *Saccharomyces cerevisiae*. *Genetics*, 189, 469–478.
- Xie, J., Kozlov, G., & Gehring, K. (2014). The "tale" of poly (A) binding protein: the MLE domain and PAM2-containing proteins. *Biochimica et Biophysica Acta*, 1839, 1062–1068.
- Yao, G., Chiang, Y. C., Zhang, C., Lee, D. J., Laue, T. M., & Denis, C. L. (2007). PAB1 self-association precludes its binding to poly (A), thereby accelerating CCR4 deadenylation *in vivo*. *Molecular and Cellular Biology*, 27, 6243–6253.
- Zhang, C., Lee, D. J., Chiang, Y. C., Richardson, R., Park, S., Wang, X., ... Denis, C. L. (2013). The RRM1 domain of the poly (A)-binding protein from *Saccharomyces cerevisiae* is critical to control of mRNA deadenylation. *Molecular Genetics and Genomics*, 288, 401–412.
- Zhong, T., & Arndt, K. T. (1993). The yeast SIS1 protein, a DnaJ homolog, is required for the initiation of translation. *Cell*, 73, 1175–1186.

How to cite this article: Brambilla M, Martani F, Bertacchi S, Vitangeli I, Branduardi P. The *Saccharomyces cerevisiae* poly (A) binding protein (Pab1): Master regulator of mRNA metabolism and cell physiology. *Yeast*. 2019;36:23–34. <https://doi.org/10.1002/yea.3347>



Article

Enzymatic Hydrolysate of Cinnamon Waste Material as Feedstock for the Microbial Production of Carotenoids

Stefano Bertacchi ¹, Stefania Pagliari ², Chiara Cantù ¹, Ilaria Bruni ², Massimo Labra ² and Paola Branduardi ^{1,*}

¹ BioIndTechLab, Department of Biotechnology and Biosciences, University of Milano—Bicocca, 20126 Milan, Italy; s.bertacchi@campus.unimib.it (S.B.); c.cantu@campus.unimib.it (C.C.)

² ZooPlantLab, Department of Biotechnology and Biosciences, University of Milano—Bicocca, 20126 Milan, Italy; stefania.pagliari@unimib.it (S.P.); ilaria.bruni@unimib.it (I.B.); massimo.labra@unimib.it (M.L.)

* Correspondence: paola.branduardi@unimib.it; Tel.: +39-02-64483418

Abstract: In the context of the global need to move towards circular economies, microbial cell factories can be employed thanks to their ability to use side-stream biomasses from the agro-industrial sector to obtain additional products. The valorization of residues allows for better and complete use of natural resources and, at the same time, for the avoidance of waste management to address our needs. In this work, we focused our attention on the microbial valorization of cinnamon waste material after polyphenol extraction (C-PEW) (*Cinnamomum verum* J.Presl), generally discarded without any additional processing. The sugars embedded in C-PEW were released by enzymatic hydrolysis, more compatible than acid hydrolysis with the subsequent microbial cultivation. We demonstrated that the yeast *Rhodospiridium toruloides* was able to grow and produce up to 2.00 (± 0.23) mg/L of carotenoids in the resulting hydrolysate as a sole carbon and nitrogen source despite the presence of antimicrobial compounds typical of cinnamon. To further extend the potential of our finding, we tested other fungal cell factories for growth on the same media. Overall, these results are opening the possibility to develop separate hydrolysis and fermentation (SHF) bioprocesses based on C-PEW and microbial biotransformation to obtain high-value molecules.

Keywords: microbial-based bioprocesses; cinnamon waste; separate hydrolysis and fermentation (SHF); *Rhodospiridium toruloides*; carotenoids



Citation: Bertacchi, S.; Pagliari, S.; Cantù, C.; Bruni, I.; Labra, M.; Branduardi, P. Enzymatic Hydrolysate of Cinnamon Waste Material as Feedstock for the Microbial Production of Carotenoids. *Int. J. Environ. Res. Public Health* **2021**, *18*, 1146. <https://doi.org/10.3390/ijerph18031146>

Academic Editor: Stefan Pflügl

Received: 16 December 2020

Accepted: 25 January 2021

Published: 28 January 2021

Publisher's Note: MDPI stays neutral with regard to jurisdictional claims in published maps and institutional affiliations.



Copyright: © 2021 by the authors. Licensee MDPI, Basel, Switzerland. This article is an open access article distributed under the terms and conditions of the Creative Commons Attribution (CC BY) license (<https://creativecommons.org/licenses/by/4.0/>).

1. Introduction

Biobased processes involve the exploitation of different renewable biomasses that possess a faster turnover compared to fossil resources and therefore have a reduced impact on the environment. The forestry, agriculture, and food industries are the main sectors involved in bioeconomy worldwide [1]. Sustainability and circularity are key features in this scenario, with the obtainment of products and energy from biomasses: indeed, the main aim of biorefineries is to exploit such resources as alternatives to fossil ones [2]. Agricultural biomasses are generally related to staple crops (e.g., cereals, tubers, corn, and sugarcane), which can satisfy the issue of circularity but cannot match all the criteria of sustainability. Therefore, there is an increasing need for utilizing side-stream materials that can be valorized in second-generation biorefineries, often by means of the so-called microbial cell factories [3,4]. These side-streams materials can be derived not only from staple crop processing but also from minor crops (for example, spice crops), which are often directly used in the food industry.

One of the main interesting strategies to enoble minor crops consists in the extraction of bioactive molecules by using chemical or biotechnological processes with low environmental impact [5,6]. In the case of the presence of residual biomasses after processing, these are mostly used to produce energy, which is a low-added value product usually obtained starting from abundant biomasses to compensate costs and market requirements.

Embedded in this approach, there is the aim to transform the entire biomass into a resource, potentially exploiting all the different portions of the plant: depending on composition and volumes, different innovative processes can be developed to obtain high added-value compounds, especially from these minor crops.

Given these considerations, in this work, we focused our attention on cinnamon (*Cinnamomum verum* J.Presl sin. *C. zeylanicum* Blume), a plant of Asian origin that has been exploited as a spice for centuries, with many nutraceutical properties and largely adopted as a food ingredient. At the botanical level, cinnamon bark is widely used by industries for the extraction of essential oils and secondary metabolites such as polyphenols to be used in food preparation, fragrances, and perfumes [7]. In these sectors, cinnamon can be deployed as an additive for both exploiting its antimicrobial properties and increasing the nutritional values of foods [8–10]. The global demand for cinnamon has been increasing during the last years also due to its possible antioxidant, anti-inflammatory, and antitumoral applications [11]. As a result of industrial processing, large quantities of waste vegetable matrix rich in cellulose and lignin [12] are obtained annually. Nevertheless, this loss has the potential to become a new resource as feedstock for the development of bioprocesses based on so-called microbial cell factories.

Indeed, microorganisms can transform different raw materials of plant (or animal) origin into valuable molecules such as biofuels, chemical platforms, biopolymers, and nutraceuticals [13]. Because of its lignocellulosic nature, the cellulose and hemicellulose content of cinnamon is an unmissable opportunity to be exploited as the main carbon and energy source for microbial growth possibly related to the biosynthesis of interest, given that other residual bioactive compounds are not expressing their antimicrobial properties. In fact, because of the presence of several antimicrobial molecules (i.e., cinnamaldehyde and cinnamic acid [14,15]), cinnamon-derived biomasses have never been considered as feedstock to be deployed in bioprocesses based on microbial cell factories; therefore, their biotechnological potential still needs to be explored.

For these reasons, the aim of this study focuses on the development of a novel bioprocess (*i*) by establishing and optimizing enzymatic hydrolysis of the cinnamon bark (CB) and of the derived residual biomass (polyphenols extraction waste, C-PEW) with varying chemico-physical parameters; (*ii*) by evaluating the criticisms in bioprocesses such as inhibitory molecules for microbial and, in particular, antifungal growth; and (*iii*) by identifying a potential cell factory and a product of interest.

With respect to the process developed, the oleaginous yeast *Rhodospiridium toruloides* was identified as a cell factory. It is naturally able to produce and accumulate carotenoids, valuable compounds with vast markets, with the food and feed sectors being the prominent ones [16–18]. In the present work, the enzymatic hydrolysis of C-PEW was matched with the ability of *R. toruloides* to produce carotenoids, and a separate hydrolysis and fermentation (SHF) process was run. The obtainment of 2.0 ± 0.23 mg/L of carotenoids starting from 9% (*w/v*) of initial biomass with a yield of $0.0053 \pm 0.0006\%$ on total sugars provided is a successful proof of concept of the possibility to provide an additional added value to the original biomass beyond the conventional extraction of nutraceuticals from cinnamon. Lastly, considering the promising results obtained on carotenoids production, other potential cell factories were tested for their ability to grow on C-PEW hydrolysate, expanding the industrial implications of our findings.

2. Materials and Methods

2.1. Plant Biomass: Feedstock Preparation and Composition

Epo S.r.l., Milano, Italy, provided cinnamon bark (*Cinnamomum verum* J.Presl, sin. *C. zeylanicum* Blume) grown in Madagascar. The cinnamon bark (CB) was stored at 25 °C away from heat and light sources until its use. Before extraction, the cinnamon bark was pulverized with an electric laboratory grinder. The cinnamon bark underwent an extraction process with water at 60 °C as described by [19] to obtain polyphenols. This extraction protocol was comparable with the one used by Epo S.r.l. in order to simulate

their industrial process and to obtain realistic waste material at the laboratory scale. At the end of the process, the cinnamon waste material after polyphenol extraction (C-PEW) was recovered, dried out to eliminate the water derived from the extraction, and stored at $-20\text{ }^{\circ}\text{C}$ until its use. To measure the water percentage of CB, 0.9 g of biomass was dried out at $160\text{ }^{\circ}\text{C}$ for 3 h and then weighed again to calculate the amount of evaporated water. The biomass was heat-incubated for additional 3 h to assess a lack of further changes in weight compared to the initial treatment. To analyze the chemical composition of CB and C-PEW, the biomass was processed following the protocol for the analysis of structural carbohydrates and lignin in the biomass of the National Renewable Energy Laboratory (NREL, <https://www.nrel.gov/docs/gen/fy13/42618.pdf>) with modifications as follows: 300 mg of biomass were diluted in 3 mL H_2SO_4 72% (*v/v*), and then incubated at $30\text{ }^{\circ}\text{C}$ for 1 h, stirring thoroughly every 10 min. The solution was diluted to 4% (*v/v*) by adding 84 mL of distilled water, mixed by inversion and autoclaved ($121\text{ }^{\circ}\text{C}$, 1 h). The hydrolysis mixture was vacuum filtered through one of the previously weighted filtering crucibles, and the insoluble components were measured gravimetrically on the filter paper. The filtered liquid was neutralized with NaOH to pH 5–6, and then, the samples were analyzed by High-Performance Liquid Chromatography (HPLC) (as described below). Three independent experimental replicates were performed.

2.2. Pretreatment and Enzymatic Hydrolysis of Cinnamon Bark and Waste Material

Enzymatic hydrolysis of the cinnamon bark powder and waste material was performed using the enzyme cocktail NS22119, kindly provided by Novozymes (Novozymes A/S, Copenhagen, Denmark). As described by the manufacturer, NS22119 contains a wide range of carbohydrases, including arabinase, β -glucanase, cellulase, hemicellulase, pectinase, and xylanase from *Aspergillus aculeatus*; 9% (*w/v*) of cinnamon bark and waste material were steeped in water with a final volume of 30 mL and then autoclaved ($121\text{ }^{\circ}\text{C}$, 1 h) in order to both sterilize and pretreat the biomass. Although mild physical pretreatment by autoclaving is less effective than chemical pretreatments, we decided not to involve their use because the overall processing, starting from the phenolic extraction that occurs upstream (and generate this waste), is intended to minimize environmental impacts.

Afterwards, the enzymes (11.9% *w/w*biomass) were added directly in the solution and incubated at pH 5.5 and at $50\text{ }^{\circ}\text{C}$ in a water bath under agitation (105 rpm). One milliliter of the sample was collected every 2, 4, and 6 h from the start, and the sugar content was analyzed by HPLC (see below). A high dosage provides an indication of the maximum enzymatically accessible sugar content, although low enzyme dosages provide a target for commercially feasible hydrolysis for further developments. Three independent experiments were performed.

2.3. Microbial Strains and Media

S. cerevisiae CEN.PK 102-5B was obtained from Peter Kötter (Institut für Mikrobiologie der Johann Wolfgang Goethe Universität, Frankfurt, Germany). The other strains used were *Komagataella phaffii* X-33 (formerly *Pichia pastoris*, ThermoFisher Scientific, Waltham, MA, USA); *Scheffersomyces stipitis* CBS 6054 (CBS Fungal Biodiversity Centre, Utrecht, The Netherlands); *Zygosaccharomyces bailii* ATCC 8766 and *Zygosaccharomyces parvibailii* ATCC 60483 (ATCC Virginia, Manassas, VA, USA); *Rhodosporidium toruloides* DSM 4444, *Rhodotorula glutinis* DSM 10134, *Cryptococcus curvatus* DSM 70022, and *Aureobasidium pullulans* DSM P268 from DSMZ (German Collection of Microorganisms and Cell Cultures, GmbH, Braunschweig, Germany); and *Kluyveromyces marxianus* NBRC1777 (Biological Resource Center, NITE, NBRC, Tokyo, Japan). All the strains were stored in cryotubes at $-80\text{ }^{\circ}\text{C}$ in 20% glycerol (*v/v*) and were pre-inoculated at $30\text{ }^{\circ}\text{C}$ on rich medium plates: 1% yeast extract (Biolife Italia S.r.l., Milan, Italy), 2% peptone, and 2% glucose (Sigma-Aldrich Co., St Louis, MO, USA). The enzymatic hydrolysate from C-PEW was used for formulating the media for the plates in order to test the ability of the aforementioned strains to grow in such substrates. This feature was qualitatively assessed after 72 h of growth at $30\text{ }^{\circ}\text{C}$.

2.4. *R. Toruloides* Cultivation and Carotenoids Production

R. toruloides was pre-inoculated in a synthetic medium constituting (per liter) 1 g of the yeast extract, 1.31 g of $(\text{NH}_4)_2\text{SO}_4$, 0.95 g of Na_2HPO_4 , 2.7 g of KH_2PO_4 , and 0.2 g of $\text{Mg}_2\text{SO}_4 \cdot 7\text{H}_2\text{O}$ and was supplemented with 15 g/L of glycerol as the main carbon source and a $100\times$ trace mineral stock solution as follows (per liter): 4 g of $\text{CaCl}_2 \cdot 2\text{H}_2\text{O}$, 0.55 g of $\text{FeSO}_4 \cdot 7\text{H}_2\text{O}$, 0.52 g of citric acid, 0.10 g of $\text{ZnSO}_4 \cdot 7\text{H}_2\text{O}$, 0.076 g of $\text{MnSO}_4 \cdot \text{H}_2\text{O}$, and 100 μL of 18 M H_2SO_4 . The yeast extract was purchased from Biolife Italia S.r.l., Milan, Italy. All other reagents were purchased from Sigma-Aldrich Co., St Louis, MO, USA. Pre-inoculum was run in that medium until stationary phase; then, cells were inoculated at an optical density (OD, 600 nm) of 0.2 in shake flasks at 30 °C and 160 rpm with C-PEW hydrolysate. After enzymatic hydrolysis, C-PEW hydrolysate was centrifuged at 4000 rpm for 10 min to separate the water insoluble components: the liquid medium obtained was used for the growth and the production of carotenoids by *R. toruloides*. Three independent experiments were performed.

2.5. Analytical Methods

HPLC analyses were performed to quantify the amount of glucose, sucrose, arabinose, fructose, and acetic acid. One milliliter of the liquid fraction was collected from each enzymatic hydrolysis, centrifuged twice (7000 rpm, 7 min, and 4 °C), and then analyzed at the HPLC using a Rezex ROA-Organic Acid (Phenomenex). The eluent was 0.01 M H_2SO_4 pumped at 0.5 mL min^{-1} , and column temperature was 35 °C. Separated components were detected by a refractive-index detector, and peaks were identified by comparison with known standards (Sigma-Aldrich, St Louis, MO, USA). HPLC analyses were performed to quantify also the amount of cinnamic acid, cinnamaldehyde, 4-hydroxybenzoic acid, and p-coumaric acid using the analysis protocol reported by [20]. The extracts were previously filtered with a 0.22 μm polytetrafluoroethylene (PTFE) filter. The column used for this chromatographic stroke was an Agilent Zorbax SB-C18 (4.6 \times 250 mm, 5 μm) composed of carbon chains of 18 carbon atoms and set to a temperature of 30 °C. Two mobile phases were used: phase A (aqueous solution of phosphoric acid H_3PO_4 at pH 3) and phase B (acetonitrile CH_3CN , 99.98% pure, HPLC grade). The volume of samples injected for analysis was 50 μL . The biomolecules were monitored by setting the diode array detector (DAD) detection signal to 280 nm.

The cellular dry weight (CDW) was measured gravimetrically after drying 1 mL of cell culture (Concentrator 5301, Eppendorf AG, Hamburg, Germany). The titer of carotenoids extracted in acetone from *R. toruloides*, as reported in [18], was determined spectrophotometrically (UV1800; Shimadzu, Kyoto, Japan) based on the maximum absorption peak for β -carotene (455 nm). A calibration curve with standard concentration of β -carotene was used for quantification.

A Urea/Ammonia Assay Kit (K-URAMR, Megazyme International Limited, Bray, Ireland) was used to determine the amount of ammonia and urea in the C-PEW hydrolysate.

The pH was measured with indicator strips in order to assess if the conditions were suitable for the enzymatic hydrolysis and to foresee possible detrimental effects on microbial growth of the final media.

2.6. Calculations

Sugar recovery (S_r) was calculated as a percentage of the sugar yield by enzymatic hydrolysis (Y_{EH}) when compared with the yield obtained from the total acid hydrolysis of the biomass (Y_{AH}).

$$S_r = \frac{Y_{EH}}{Y_{AH}} \times 100$$

For statistical analysis, heteroscedastic two-tailed *t* test was applied.

3. Results and Discussion

3.1. Evaluation of Total Composition of the CB and C-PEW by Acid Hydrolysis

The provided cinnamon bark (CB) and the related waste material derived from polyphenol extraction (C-PEW) were subjected to total acid hydrolysis to assess their composition in terms of water, insoluble components, acetate, and sugars. Insoluble components and acetate are among the main growth inhibitors commonly linked to residual biomasses, whereas sugars act as the main carbon and energy sources for microbial cell factories. As shown in Table 1, CB and C-PEW showed similar compositions among all the analyzed constituents, consistent with the fact that the components previously extracted (i.e., polyphenols) constitute only a limited amount of the whole biomass. These data are also in accordance with the few previously reported examples from both *C. verum* (formerly *C. zeylanicum*) and *C. cassia* [11,21]. Remarkably, the vast majority of sugars is composed by glucose (more than 65% *w/w*), being up to 27% *w/w* of the total biomass.

Table 1. Total hydrolysis of cinnamon: cinnamon bark and waste extract hydrolysate composition following acid treatment.

Total Acid Hydrolysis of Cinnamon		
Component	Cinnamon Bark (CB)	Cinnamon Waste Material (C-PEW)
Water	19.4 ± 1.34%	/
Insoluble fraction	41.1 ± 1.26%	44.5 ± 1.86%
Acetate	1.5 ± 1.03%	2.8 ± 0.13%
Sugars	37.3 ± 0.83%	41.5 ± 1.28%
of which		
Glucose	25.2 ± 0.53%	27.2 ± 0.99%
Fructose	9.1 ± 0.15%	10.7 ± 0.32%
Arabinose	3.0 ± 0.19%	3.6 ± 0.04%

Total acid hydrolysis was then no longer used for the experiments as it creates conditions that are detrimental (if not incompatible) with microbial growth and requires processing conditions that have a higher environmental impact if compared with enzymatic hydrolysis. In addition, its use is limited by the release of inhibitory compounds and a very low final pH that would need a neutralization step prior to use as the growth media [22,23].

3.2. Enzymatic Hydrolysis of CB and C-PEW and Composition of the Hydrolysates

After assessing the composition of both CB and C-PEW, enzymatic hydrolysis of such biomasses was performed. To the best of our knowledge, there is only a single accessible peer-reviewed example of enzymatic hydrolysis of cinnamon or cinnamon-derived biomasses [21], and it is not related to the development of a microbial-based bioprocess. We first assessed the effect of enzymatic cocktail NS22119 11.9% *w/w*biomass on CB or C-PEW 9% *w/v*: the exceeding amount of enzyme was proposed to maximize the hydrolysis of this novel substrate. The pH of both CB and C-PEW were measured between the pre-treatment and the hydrolysis step obtaining pH of 4.5 and 3.5, respectively. Both these values are lower than the optimum of the enzymatic cocktail (pH 6, as described by the manufacturer); therefore, we tested the saccharification at both the initial and the optimal pH.

As shown in Figure 1A, the enzymatic cocktail hydrolyzed CB at both pH during the first hours of saccharification. Prolonging the incubation beyond 6 h up to 24 h did not significantly increase the sugar release (data not shown): these observations are in accordance with previous applications of this enzymatic cocktail on a different residual biomass [18]. As shown in Table 2, in both cases, glucose is the main sugar released, in accordance with the data obtained from the total acid hydrolysis (Table 1). Figure 1A shows that the release of sugars from CB is higher (13%) when performed at pH 6 ($p < 0.05$).

Despite a technoeconomic analysis not yet performed, it is reasonable to conclude that this increase would not justify the additional neutralization step, considering that the difference was constituted by about 1 g/L of total sugars.

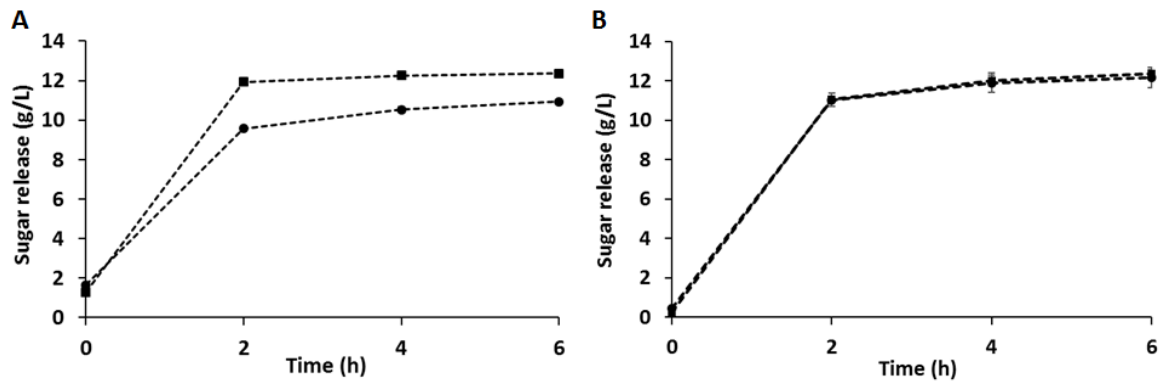


Figure 1. Enzymatic hydrolysis of cinnamon derived biomasses: the effect of the NS22119 cocktail (11.9% *w/w* biomass) on 9% *w/v* cinnamon bark (CB) (A) and cinnamon waste material after polyphenol extraction (C-PEW) (B) at pH 6 (squares) or at their original pH after pretreatment (pH 4.5 for panel A, pH 3.5 for panel B) (circles). The values are the means of three independent experiments. In panel A, standard deviations are included, despite being hardly visible as numerically very small.

Table 2. Effect of pH on enzymatic hydrolysis: the titer of sugars released by the NS22119 cocktail (11.9% *w/w* biomass) on 9% *w/v* CB or C-PEW at different pH after 6 h of treatment. The values are the means of three independent experiments.

Enzymatic Hydrolysis of Cinnamon-Derived Biomasses	Cinnamon Bark (CB)				Cinnamon Waste Material (C-PEW)				
	Component Titer (g/L)	pH 4.5	Yield	pH 6	Yield	pH 3.5	Yield	pH 6	Yield
Sucrose	0.9 ± 0.01	-	1.06 ± 0.00	0.8 ± 0.04	-	0.9 ± 0.01	-		
Glucose	7.5 ± 0.09	32.98%	8.2 ± 0.08	36.07%	8.8 ± 0.42	36.7%	9.0 ± 0.12	35.9%	
Fructose	2.6 ± 0.05	30.73%	2.4 ± 0.01	28.44%	1.8 ± 0.05	18.6%	1.8 ± 0.06	18.6%	
Arabinose	-	-	0.8 ± 0.01	25.65%	0.8 ± 0.02	8.4%	0.7 ± 0.06	5.6%	
Total sugars	10.9 ± 0.11	32.4%	12.4 ± 0.10	36.67%	12.2 ± 0.52	33%	12.4 ± 0.23	32.5%	

As shown in Figure 1B, increasing the pH did not affect the enzymatic hydrolysis of C-PEW. In addition, the sugar released from CB and C-PEW, at their original pH, are comparable: this means that polyphenol extraction did not impair the enzymatic activity. In order to reduce the use of neutralizing agents and therefore the operative steps, increasing both the economic and environmental sustainability of the process, the hydrolysis of C-PEW at pH 3.5 was chosen as the preferred one. In these conditions, considering the original sugar content, the yield of sugars from C-PEW was 33% on the total available, with a yield of glucose of 36.7% on the total available (see the Calculation subsection in the Materials and Methods section). In addition, 8.1 ± 2.1 mg/L of ammonia and 4.5 ± 1.35 mg/L of urea, which may act as nitrogen sources, were detected in the C-PEW hydrolysate.

The presence of aromatic compounds typical of cinnamon was evaluated too because of their known antimicrobial activity, concentrated in their essential oils. For example, cinnamaldehyde is known to possess a fungicidal activity [11,24,25]. Therefore, we investigated its presence together with cinnamic acid, p-coumaric acid, and 4-hydroxybenzoic acid in the hydrolysate without adjusting pH, since these molecules may impair microbial growth as well [22], reducing in return the applications of biomasses derived from the cinnamon supply chain. As shown in Table 3, cinnamaldehyde and cinnamic acid were the main aromatic compounds detected in the hydrolysate of CB. When compared with the same biomass hydrolyzed without the pretreatment, a reduction in the titer of most of

these molecules can be observed: heat is indeed known to have this kind of effect on such volatile compounds [11,26,27]. The titer of cinnamic acid and cinnamaldehyde detected in the C-PEW hydrolysate was inferior compared to the CB one (Table 3): this observation is consistent with the polyphenol extraction that cinnamon was subjected to.

Table 3. Aromatic compounds of cinnamon origin: evaluation of the presence of aromatic compounds typical of cinnamon in CB or C-PEW hydrolysates. The values are the means of three independent experiments.

Aromatic Compounds in Cinnamon-Derived Hydrolysates	CB Hydrolysate ZZZ(W/O Autoclave Pre-Treatment)	CB Hydrolysate	C-PEW Hydrolysate
Component	Titer (mg/L)	Titer (mg/L)	Titer (mg/L)
4-hydroxybenzoic acid	-	1.8 ± 0.52	4.8 ± 0.47
p-coumaric acid	6.7 ± 0.24	2.5 ± 1.27	0.8 ± 0.16
Cinnamic acid	35.6 ± 0.51	23.2 ± 2.88	6.7 ± 1.29
Cinnamaldehyde	155.5 ± 12.55	73.4 ± 2.82	5.5 ± 0.96

Taken together, these data confirmed that the C-PEW hydrolysate was comparable (in terms of sugars released) with the hydrolysate of the original edible biomass (CB), with an important reduced amount of growth inhibitors. Therefore, we excluded CB from the following experiments. Indeed, since C-PEW is a residual biomass not further valorized, it is a suitable feedstock to be considered in a microbial-based bioprocess: its hydrolysis can provide glucose as the main accessible carbon source, even without pH corrections.

3.3. Production of Carotenoids from C-PEW Hydrolysate

In order to valorize C-PEW as feedstock biomass in a bioprocess, we focused our attention on the yeast *Rhodospiridium toruloides*, known for being able to withstand residual biomasses when used as feedstock for both their growth and the production of carotenoids [16,18]. When tested on plates prepared with C-PEW as the growth medium, *R. toruloides* was able to grow and accumulate pigments (see Section 3.4); therefore, we tested the production in shake flasks as well. The type of process chosen was a separate hydrolysis and fermentation (SHF) in order to eliminate the water insoluble components (WIS) from the media. Figure 2 shows the growth of *R. toruloides* on sugars released from C-PEW hydrolysis at pH 3.5 and the co-current production of carotenoids. In particular, we could observe that the production reached its maximum after 48 h in concomitance with the beginning of the stationary phase. These data are in accordance with previous reports that carotenogenic microorganisms like *R. toruloides* produce carotenoids mainly in response to stressful or suboptimal conditions such as the stationary phase itself. In addition, only a limited amount of sugars was consumed: to analyze this phenomenon, we provided to *R. toruloides* the synthetic medium supplemented with the same amount of sugars present in C-PEW hydrolysate, setting the pH value at 3.5 or 5.5 (optimal for this yeast). As shown in Figure S1, *R. toruloides* was able to completely consume the sugars and to reach a higher CDW than in C-PEW hydrolysate regardless of the initial pH. The reduced growth and sugar consumption observed in the C-PEW hydrolysate could be ascribed to the low initial amount of nitrogen source, which resulted in depletion after 48 h (Figure S2), in correspondence to the stationary phase of growth. As the inhibitory compounds typical of cinnamon origin were not detected after 24 h, nitrogen depletion should be considered the main bottleneck for *R. toruloides* growth in C-PEW hydrolysate.

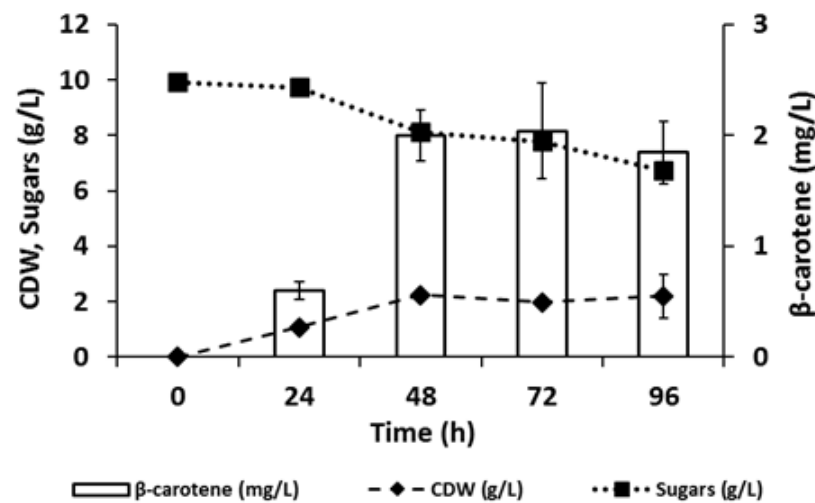


Figure 2. Production of carotenoids from the C-PEW hydrolysate by *R. toruloides*: cellular dry weight (CDW) in dashed line, total sugars in dotted line, and β -carotene in white bars. The values are the means of three independent experiments.

In SHF conditions with 9% (*w/v*) C-PEW hydrolysate, *R. toruloides* was able to accumulate up to 2.0 ± 0.23 mg/L of carotenoids after 48 h of growth, with a productivity of 0.04 ± 0.005 g/L/h and yields of $0.09 \pm 0.007\%$ on CDW, of $0.11 \pm 0.013\%$ on consumed sugars, and of $0.005 \pm 0.0006\%$ on the total sugars provided. When considering high added-value products, yields are not crucial but important to describe the process itself and to understand how to further improve it. In fact, although this titer of carotenoids is comparable with other recently reported bioprocesses based on the combination of *R. toruloides* and residual biomasses, like *Camelina sativa* meal, carob pulp syrup, sugarcane bagasse, and molasses [18,28,29], the possibility to increase glucose consumption might ameliorate the result obtained here.

This work focused on the valorization of cinnamon by-products by their exploitation as a substrate for microorganisms. Industries in this sector must eliminate large amounts of residues each year from the processing of cinnamon extraction of polyphenols and other residual biomasses derived from biomolecule extraction. Although this waste disposal cost may not be excessively high, it is important to consider it in the scenario of the reconversion to a circular economic model fostered by the European Union, promoting increasing attention towards the exploitation of industrial products following a biorefinery model, which aims to obtain more products starting from a single biomass [30–32]. This is also in line with the ambitious aims and goals of the Green Deal [33], where every activity can contribute to reaching the declared “carbon neutral” status. Additionally, other microbial cell factories might be deployed in bioprocesses involved in the conversion of C-PEW to compounds of industrial relevance, such as, as a matter of example, lipids and shikimate from species such as *Cryptococcus curvatus* and *Scheffersomyces stipitis*.

3.4. Testing the Growth of Other Fungal Cell Factories on C-PEW Hydrolysate

In order to widen the possible outcomes of the exploitation of C-PEW, we tested the ability of other yeast cell factories to grow on such biomass. Testing of possible candidates was needed since, to the best of our knowledge, there were no previous examples of cinnamon use for such purposes. In addition, cinnamon is known to possess a potent antimicrobial activity [11]; therefore, putative cell factories must be tested and selected for their ability to grow on this new medium. In fact, cinnamon antimicrobial activity has been studied with regard to several pathogenic microorganisms: in particular, the minimal inhibitory concentrations of cinnamaldehyde were 125 ± 25 g/L for *Candida albicans*, 88 ± 13 g/L for *Aspergillus niger*, 300 ± 0 g/L for *Escherichia coli*, and 250 ± 50 g/L for *Staphylococcus aureus* [34]. Nevertheless, considering the titers of antimicrobial compounds typical of cinnamon found

in C-PEW (Table 2), their amount may be considered neglectable or anyhow bearable by different fungal cell factories.

We focused our attention on the fungal species enlisted in Figure 3 (further details in the Materials and Methods section): all of them are classified as yeasts except for *Aureobasidium pullulans*, that is considered a yeast-like fungus [35]. The choice to test fungal clades that involve yeasts is related to the fact that those microorganisms are reliable and robust cell factories, able to convert residual biomasses into valuable compounds or to be used as chassis for further genetic modification, expanding the portfolio of putative products [36,37]. Although bacteria could be considered relevant microbial cell factories too, the higher general tolerance of yeasts towards low pH, likewise the biomass of interest, led them to be excluded in this study. As shown in Figure 3, all the tested strains were able to grow on agar plates containing C-PEW at pH 3.5, with a qualitative slower growth by *Komagataella phaffii* compared to the other tested species. These observations clearly highlight that C-PEW can be used as feedstock by a variety of fungal cell factories that possess peculiar characteristics of industrial interest. *A. pullulans* naturally produces antimicrobial compounds, industrial enzymes, and polymers such as pullulans and poly(β -L-malic acid) [35]. *K. marxianus*, *K. pastoris*, and *S. cerevisiae* are known to be chassis for recombinant molecules with several available tools for this purpose [38–40], therefore expanding the potential uses of C-PEW. *Z. bailii* and *Z. parabailii* were selected due to their ability to grow at low pH and to withstand weak organic acid: the availability of technologies for these species is increasing their applicability [41,42]. *S. stipitis* is known for producing shikimate, which can act as building blocks for high-value aromatics [43]. *C. curvatus* and *Rhodotorula glutinis* (together with *R. toruloides*) are oleaginous yeasts able to accumulate from 20% *w/w* lipids of their dry cell mass [44,45]. Therefore, the obtained single cell oils (SCOs) can be exploited for several applications, from biodiesel to waxes, as an alternative to both petrochemical and vegetable oil industries [46,47]. In addition, *R. glutinis* and *R. toruloides* are natural producers of carotenoids [17,48], a group of molecules widely used in the feed, food, dietary supplements, and dye industries with high market demand [49] that perfectly matches the bioeconomic logic of cascading [50]. Both these carotenogenic yeasts were able to produce carotenoids when fed with cinnamon waste material hydrolysate since their pinkish color was clearly visible (Figure 3). Due to the positive test of all these species, we can infer that they would be able to reproduce the same features in batch mode as well, providing a great added value to the residual biomass obtained from cinnamon processing.

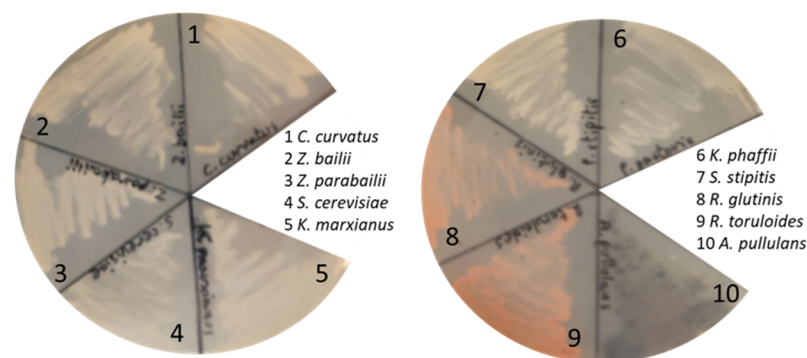


Figure 3. Testing of different fungal cell factories on agar plates containing only the enzymatic hydrolysate of 9% *w/v* C-PEW (pH 3.5) as a nutrient source: the picture was taken after 72 h of growth at 30 °C.

Taken together, the data obtained showed that a broad range of fungal species are phenotypically able to grow on the hydrolysate of cinnamon waste material and that therefore they can be considered a starting material for bioprocesses to obtain molecules of industrial relevance, from carotenoids to recombinant proteins.

4. Conclusions

The agri-food sector is leading to the accumulation of relevant amounts of residual biomasses, which are mainly burned for energy, used as animal feed, or disposed of as wastes. Nevertheless, these biomasses often contain energy-rich molecules that can still be exploited to obtain high-value products. Furthermore, the valorization of these biomasses fosters the transition from linear economies to circular ones, where the life cycle of natural resources is extended thanks to their further processing to extract additional values. In this work, we focused our attention on the waste material of the cinnamon supply chain, obtained from the polyphenol extraction (called C-PEW), which is not used for any purpose at the moment. Here, for the first time, a cinnamon-derived biomass was hydrolyzed using a commercial enzymatic cocktail, with a 33% yield of sugars on the total available, demonstrating its potentiality as feedstock for a bioprocess based on microbial cell factories.

We focused our attention on the yeast *Rhodospiridium toruloides*, naturally able to produce carotenoids and high-value molecules used in the food, the feed, the dye, and the cosmetic sectors. Since most of the carotenoid market is satisfied by chemical synthesis, there is an increasing demand for molecules of renewable origin. Here, in a separated hydrolysis and fermentation (SHF) process, *R. toruloides* was able to consume sugars from C-PEW and to accumulate up to 2.0 ± 0.23 mg/L of carotenoids. Although the obtained titer was comparable with those of other processes based on residual biomasses valorized by *R. toruloides*, the low sugar consumption in these conditions was a limiting element. An additional nitrogen source, preferentially of residual origin, might be considered to overcome this shortcoming.

In this work, it is shown for the first time the possibility to develop bioprocesses based on cinnamon-derived biomasses to provide additional production streams, such as carotenoids, to be applied as additive in sectors in which industries dealing with this residual biomass are already involved, thus increasing the value thereof. The successful test of several microorganisms of industrial relevance for their ability to grow on C-PEW hydrolysate (withstanding its low pH and anti-microbial compounds) widens the possible exploitations of this residual biomass. In addition, several new synthetic biology tools are becoming available for non-Saccharomyces fungal species, thus expanding the ability of these microbes to be tailored for industrial processes. In this case, a desirable implementation should be the engineering of *R. toruloides* to withstand antifungal molecules and to produce fine chemicals of industrial relevance. This in turn would increase the appeal of cinnamon derived biomasses, although it is a currently underrated feedstock for microbial cell factories.

Overall, this work can pave the way for further development of bioprocesses based on the exploitation of a side-stream biomass derived from the cinnamon industry, that usually would be disposed of as waste material, in order to produce not only high-value added products such as carotenoids in *R. toruloides* but also compounds from other yeast cell factories in the scenario of the cascading principles of biorefineries.

Supplementary Materials: The following are available online at <https://www.mdpi.com/1660-4601/18/3/1146/s1>, Figure S1. Growth of *R. toruloides* on synthetic media at pH 3.5 (panel A) and pH 5.5. Cellular dry weight (CDW) in dashed line, total sugars in dotted line. Values are the means of three independent experiments, Figure S2. Ammonium titer during *R. toruloides* growth on C-PEW hydrolysate. Values are the means of three independent experiments.

Author Contributions: Conceptualization, S.B., S.P., and I.B.; formal analysis, S.B. and C.C.; investigation, S.B., S.P., and C.C.; resources, M.L. and P.B.; data curation, S.B., S.P., and C.C.; writing—original draft preparation, S.B.; writing—review and editing, S.P., I.B., M.L., and P.B.; visualization, S.B. and C.C.; supervision, I.B., M.L., and P.B.; project administration, I.B., M.L., and P.B.; funding acquisition, M.L. and P.B. All authors have read and agreed to the published version of the manuscript.

Funding: This research was funded by the Food Social Sensor Network (FOOD NET) (grant number 2251551, POR FESR 2014-2020).

Institutional Review Board Statement: Not applicable.

Informed Consent Statement: Not applicable.

Data Availability Statement: Not applicable.

Acknowledgments: We thank Epo S.r.l., which directly collaborated with us for sample collection.

Conflicts of Interest: The authors declare no conflict of interest. The funders had no role in the design of the study; in the collection, analyses, or interpretation of data; in the writing of the manuscript; or in the decision to publish the results.

References

1. Bracco, S.; Calicioglu, O.; Juan, M.G.S.; Flammini, A. Assessing the contribution of bioeconomy to the total economy: A review of national frameworks. *Sustainability* **2018**, *10*, 1698. [[CrossRef](#)]
2. IEA Bioenergy Task42. *Sustainable and Synergetic Processing of Biomass into Marketable Food & Feed Ingredients, Chemicals, Materials and Energy (Fuels, Power, Heat)*; IEA Bioenergy: Wageningen, The Netherlands, 2014.
3. Dahiya, S.; Kumar, A.N.; Sravan, J.S.; Chatterjee, S.; Sarkar, O.; Mohan, S.V. Food waste biorefinery: Sustainable strategy for circular bioeconomy. *Bioresour. Technol.* **2018**, *248*, 2–12. [[CrossRef](#)] [[PubMed](#)]
4. Branduardi, P. Closing the loop: The power of microbial biotransformations from traditional bioprocesses to biorefineries, and beyond. *Microb. Biotechnol.* **2020**, 1–6. [[CrossRef](#)]
5. Magoni, C.; Bruni, I.; Guzzetti, L.; Dell’Agli, M.; Sangiovanni, E.; Piazza, S.; Regonesi, M.E.; Maldini, M.; Spezzano, R.; Caruso, D.; et al. Valorizing coffee pulp by-products as anti-inflammatory ingredient of food supplements acting on IL-8 release. *Food Res. Int.* **2018**, *112*, 129–135. [[CrossRef](#)] [[PubMed](#)]
6. Cavini, S.; Guzzetti, L.; Givoia, F.; Regonesi, M.E.; Di Gennaro, P.; Magoni, C.; Campone, L.; Labra, M.; Bruni, I. Artichoke (*Cynara cardunculus* var. *scolymus* L.) by-products as a source of inulin: How to valorise an agricultural supply chain extracting an added-value compound. *Nat. Prod. Res.* **2020**, 1–5. [[CrossRef](#)]
7. Goel, B.; Mishra, S. Medicinal and Nutritional Perspective of Cinnamon: A Mini-review. *Eur. J. Med. Plants* **2020**, 10–16. [[CrossRef](#)]
8. Muhammad, D.R.A.; Tuenter, E.; Patria, G.D.; Foubert, K.; Pieters, L.; Dewettinck, K. Phytochemical composition and antioxidant activity of *Cinnamomum burmannii* Blume extracts and their potential application in white chocolate. *Food Chem.* **2021**, *340*, 127983. [[CrossRef](#)]
9. Clemente, I.; Aznar, M.; Silva, F.; Nerín, C. Antimicrobial properties and mode of action of mustard and cinnamon essential oils and their combination against foodborne bacteria. *Innov. Food Sci. Emerg. Technol.* **2016**, *36*, 26–33. [[CrossRef](#)]
10. Nabavi, S.F.; Di Lorenzo, A.; Izadi, M.; Sobarzo-Sánchez, E.; Daglia, M.; Nabavi, S.M. Antibacterial effects of cinnamon: From farm to food, cosmetic and pharmaceutical industries. *Nutrients* **2015**, *7*, 7729–7748. [[CrossRef](#)]
11. Ribeiro-Santos, R.; Andrade, M.; Madella, D.; Martinazzo, A.P.; de Aquino Garcia Moura, L.; de Melo, N.R.; Sanches-Silva, A. Revisiting an ancient spice with medicinal purposes: Cinnamon. *Trends Food Sci. Technol.* **2017**, *62*, 154–169. [[CrossRef](#)]
12. Mehta, M.J.; Kumar, A. Green and Efficient Processing of *Cinnamomum cassia* Bark by Using Ionic Liquids: Extraction of Essential Oil and Construction of UV-Resistant Composite Films from Residual Biomass. *Chem. Asian J.* **2017**, *12*, 3150–3155. [[CrossRef](#)] [[PubMed](#)]
13. Lee, S.Y.; Kim, H.U.; Chae, T.U.; Cho, J.S.; Kim, J.W.; Shin, J.H.; Kim, D.I.; Ko, Y.-S.; Jang, W.D.; Jang, Y.-S. A comprehensive metabolic map for production of bio-based chemicals. *Nat. Catal.* **2019**, *2*, 18–33. [[CrossRef](#)]
14. Hameed, I.H.; Altameme, H.J.; Mohammed, G.J. Evaluation of antifungal and antibacterial activity and analysis of bioactive phytochemical compounds of *Cinnamomum zeylanicum* (Cinnamon bark) using gas chromatography-mass spectrometry. *Orient. J. Chem.* **2016**, *32*, 1769. [[CrossRef](#)]
15. OuYang, Q.; Duan, X.; Li, L.; Tao, N. Cinnamaldehyde exerts its antifungal activity by disrupting the cell wall integrity of *Geotrichum citri-aurantii*. *Front. Microbiol.* **2019**, *10*, 55. [[CrossRef](#)]
16. Wen, Z.; Zhang, S.; Odoh, C.K.; Jin, M.; Zhao, Z.K. *Rhodospiridium toruloides*—A potential red yeast chassis for lipids and beyond. *FEMS Yeast Res.* **2020**, *20*, 1–12. [[CrossRef](#)]
17. Park, Y.-K.K.; Nicaud, J.-M.M.; Ledesma-Amaro, R. The Engineering Potential of *Rhodospiridium toruloides* as a Workhorse for Biotechnological Applications. *Trends Biotechnol.* **2018**, *36*, 304–317. [[CrossRef](#)]
18. Bertacchi, S.; Bettiga, M.; Porro, D.; Branduardi, P. *Camelina sativa* meal hydrolysate as sustainable biomass for the production of carotenoids by *Rhodospiridium toruloides*. *Biotechnol. Biofuels* **2020**, *13*, 1–10. [[CrossRef](#)]
19. Cheng, D.M.; Kuhn, P.; Poulev, A.; Rojo, L.E.; Lila, M.A.; Raskin, I. In vivo and in vitro antidiabetic effects of aqueous cinnamon extract and cinnamon polyphenol-enhanced food matrix. *Food Chem.* **2012**, *135*, 2994–3002. [[CrossRef](#)]
20. Safafar, H.; Wagenen JVan Møller, P.; Jacobsen, C. Carotenoids, phenolic compounds and tocopherols contribute to the antioxidative properties of some microalgae species grown on industrial wastewater. *Mar. Drugs* **2015**, *13*, 7339–7356. [[CrossRef](#)]
21. Tang, P.; Hao, E.; Deng, J.; Hou, X.; Zhang, Z.; Xie, J. Boost anti-oxidant activity of yogurt with extract and hydrolysate of cinnamon residues. *Chin. Herb. Med.* **2019**, *11*, 417–422. [[CrossRef](#)]
22. Jönsson, L.J.; Martín, C. Pretreatment of lignocellulose: Formation of inhibitory by-products and strategies for minimizing their effects. *Bioresour. Technol.* **2016**, *199*, 103–112. [[CrossRef](#)] [[PubMed](#)]

23. Wahlström, R.M.; Suurnäkki, A. Enzymatic hydrolysis of lignocellulosic polysaccharides in the presence of ionic liquids. *Green Chem. R. Soc. Chem.* **2015**, *17*, 694–714. [[CrossRef](#)]
24. Ainane, A.; Elkouali, M. Cosmetic bio-product based on cinnamon essential oil “*Cinnamomum verum*” for the treatment of mycoses: Preparation, chemical analysis and antimicrobial activity. *MOJ Toxicol.* **2019**, *5*, 5–8.
25. Shreaz, S.; Wani, W.A.; Behbehani, J.M.; Raja, V.; Irshad, M.; Karched, M.; Ali, I.; Siddiqi, W.A.; Hun, L.T. Cinnamaldehyde and its derivatives, a novel class of antifungal agents. *Fitoterapia* **2016**, *112*, 116–131. [[CrossRef](#)] [[PubMed](#)]
26. Benkeblia, N. Free-radical scavenging capacity and antioxidant properties of some selected Onions (*Allium cepa* L.) and garlic (*Allium sativum* L.) extracts. *Braz. Arch. Biol Technol.* **2005**, *48*, 753–759. [[CrossRef](#)]
27. Settharaksa, S.; Jongjareonrak, A.; Hmadhlu, P.; Chansuwan, W.; Siripongvutikorn, S. Flavonoid, phenolic contents and antioxidant properties of thai hot curry paste extract and its ingredients as affected of pH, solvent types and high temperature. *Int. Food Res. J.* **2012**, *19*, 1581–1587.
28. Bonturi, N.; Crucello, A.; Viana, A.J.C.; Miranda, E.A. Microbial oil production in sugarcane bagasse hemicellulosic hydrolysate without nutrient supplementation by a *Rhodospiridium toruloides* adapted strain. *Process Biochem.* **2017**, *57*, 16–25. [[CrossRef](#)]
29. Freitas, C.; Parreira, T.M.; Roseiro, J.; Reis, A.; Da Silva, T.L. Selecting low-cost carbon sources for carotenoid and lipid production by the pink yeast *Rhodospiridium toruloides* NCYC 921 using flow cytometry. *Bioresour. Technol.* **2014**, *158*, 355–359. [[CrossRef](#)]
30. Zabaniotou, A. Redesigning a bioenergy sector in EU in the transition to circular waste-based Bioeconomy—A multidisciplinary review. *J. Clean. Prod.* **2018**, *177*, 197–206. [[CrossRef](#)]
31. European Commission. *Financing the Green Transition: The European Green Deal Investment Plan and Just Transition Mechanism*; European Commission: Brussels, Belgium, 2020.
32. United Nations. *Goal 9: Build Resilient Infrastructure, Promote Inclusive and Sustainable Industrialization, and Foster Innovation*; United Nations: New York, NY, USA, 2020; pp. 1–6.
33. European Commission. A European Green Deal. Available online: https://ec.europa.eu/info/strategy/priorities-2019-2024/european-green-deal_en (accessed on 10 December 2020).
34. Ooi, L.S.M.; Li, Y.; Kam, S.L.; Wang, H.; Wong, E.Y.L.; Ooi, V.E.C. Antimicrobial activities of Cinnamon oil and cinnamaldehyde from the Chinese medicinal herb *Cinnamomum cassia* Blume. *Am. J. Chin. Med.* **2006**, *34*, 511–522. [[CrossRef](#)]
35. Prasongsuk, S.; Lotrakul, P.; Ali, I.; Bankeeree, W.; Punnapayak, H. The current status of *Aureobasidium pullulans* in biotechnology. *Folia Microbiol.* **2018**, *63*, 129–140. [[CrossRef](#)] [[PubMed](#)]
36. Nandy, S.K.; Srivastava, R.K. A review on sustainable yeast biotechnological processes and applications. *Microbiol. Res.* **2018**, *207*, 83–90. [[CrossRef](#)] [[PubMed](#)]
37. Xu, X.; Liu, Y.; Du, G.; Ledesma-Amaro, R.; Liu, L. Microbial Chassis Development for Natural Product Biosynthesis. *Trends Biotechnol.* **2020**, *38*, 779–796. [[CrossRef](#)] [[PubMed](#)]
38. Fischer, J.E.; Glieder, A. Current advances in engineering tools for *Pichia pastoris*. *Curr. Opin. Biotechnol.* **2019**, *59*, 175–181. [[CrossRef](#)] [[PubMed](#)]
39. Li, M.; Borodina, I. Application of synthetic biology for production of chemicals in yeast *Saccharomyces cerevisiae*. *FEMS Yeast Res.* **2015**, *15*, 1–12. [[PubMed](#)]
40. Varela, J.A.; Gethins, L.; Stanton, C.; Ross, P.; Morrissey, J.P. Applications of *Kluyveromyces marxianus* in Biotechnology. In *Yeast Diversity in Human Welfare*; Satyanarayana, T., Kunze, G., Eds.; Springer: Singapore, 2017; pp. 1–486.
41. Kuanyshev, N.; Adamo, G.M.; Porro, D.; Branduardi, P. The spoilage yeast *Zygosaccharomyces bailii*: Foe or friend? *Yeast* **2017**, *34*, 359–370. [[CrossRef](#)]
42. Suh, S.O.; Gужjari, P.; Beres, C.; Beck, B.; Zhou, J. Proposal of *Zygosaccharomyces parabailii* sp. nov. and *Zygosaccharomyces pseudobailii* sp. nov., novel species closely related to *Zygosaccharomyces bailii*. *Int. J. Syst. Evol. Microbiol.* **2013**, *63*, 1922–1929. [[CrossRef](#)]
43. Gao, M.; Cao, M.; Suástegui, M.; Walker, J.; Quiroz, N.R.; Wu, Y.; Tribby, D.; Okerlund, A.; Stanley, L.; Shanks, J.V.; et al. Innovating a nonconventional yeast platform for producing shikimate as the building block of high-value aromatics. *ACS Synth. Biol.* **2017**, *6*, 29–38. [[CrossRef](#)]
44. Carsanba, E.; Papanikolaou, S.; Erten, H. Production of oils and fats by oleaginous microorganisms with an emphasis given to the potential of the nonconventional yeast *Yarrowia lipolytica*. *Crit. Rev. Biotechnol.* **2018**, *38*, 1230–1243. [[CrossRef](#)]
45. Sreeharsha, R.V.; Mohan, S.V. Obscure yet Promising Oleaginous Yeasts for Fuel and Chemical Production. *Trends Biotechnol.* **2020**, *38*, 873–887. [[CrossRef](#)]
46. Donot, F.; Fontana, A.; Baccou, J.C.; Strub, C.; Schorr-Galindo, S. Single cell oils (SCOs) from oleaginous yeasts and moulds: Production and genetics. *Biomass Bioenergy* **2014**, *68*, 135–150. [[CrossRef](#)]
47. Uemura, H. Synthesis and production of unsaturated and polyunsaturated fatty acids in yeast: Current state and perspectives. *Appl. Microbiol. Biotechnol.* **2010**, *95*, 1–12. [[CrossRef](#)] [[PubMed](#)]
48. Frengova, G.I.; Beshkova, D.M. Carotenoids from *Rhodotorula* and *Phaffia*: Yeasts of biotechnological importance. *J. Ind. Microbiol. Biotechnol.* **2009**, *36*, 163. [[CrossRef](#)] [[PubMed](#)]
49. Nagarajan, J.; Ramanan, R.N.; Raghunandan, M.E.; Galanakis, C.M.; Krishnamurthy, N.P. Carotenoids. In *Nutraceutical and Functional Food Components. Effects of Innovative Processing Techniques*; Galanakis, C.M., Ed.; Elsevier Inc.: Amsterdam, The Netherlands, 2017; pp. 259–296.
50. IEA Bioenergy Task40. *Cascading of Woody Biomass: Definitions, Policies and Effects on International Trade*; IEA Bioenergy: Wageningen, The Netherlands, 2016.

Chapter 9

RRI Approach for Development and Acceptance of Novel Fish Feed Formulations in Aquaculture

Chiara Magoni, Ausilia Campanaro, Andrea Galimberti, Chiara Pesciaroli, Stefano Bertacchi, Paola Branduardi and Massimo Labra

Abstract Stakeholders' involvement and public engagement in research processes are essential elements to obtain concrete impacts in society. In this context we tested the Responsible Research and Innovation (RRI) strategy in the aquaculture industry to improve fish quality by using the most suitable feeds. These could be obtained through biotechnological approaches starting from industrial waste, or by using flour with high nutritional values such as insect-meals. Both strategies were compared at the scientific level, to estimate their performance in terms of fish quality and health, and at the RRI impact. In this contest a pool of stakeholders was engaged to evaluate the economic, environmental and social aspects of both technological approaches and to steer research and technology transfer activities.

C. Magoni (✉) · A. Campanaro · A. Galimberti · C. Pesciaroli · S. Bertacchi
P. Branduardi · M. Labra
University of Milano-Bicocca, Milan, Italy
e-mail: chiara.magoni@unimib.it

A. Campanaro
e-mail: ausilia.campanaro@unimib.it

A. Galimberti
e-mail: andrea.galimberti@unimib.it

C. Pesciaroli
e-mail: chiara.pesciaroli@unimib.it

S. Bertacchi
e-mail: s.bertacchi@campus.unimib.it

P. Branduardi
e-mail: paola.branduardi@unimib.it

M. Labra
e-mail: massimo.labra@unimib.it

9.1 Problem Identification

Aquatic resources, with a total production of 167 million tons (FAO 2016), cover a significant percentage of the world proteins demand and almost completely the need for the rare Long Chain Fatty Acids omega-3, known to be essential in human nutrition (Evans and Burr 1927). In the last two decades, fishery has been over-exploited, and it no longer maintained the same worldwide consumption standard of 20.1 kg per capita (FAO 2016). Therefore, since only aquaculture can supply the growing fish demand, fish feed sector should be expanded in a sustainable way, including the adoption of more sustainable feed formulations. Generally, fish feed is composed of a mixture of fishmeal and fish oil. However, since their demand and costs are increasing, producers are substituting them with plants flour and other ingredients. As a consequence, feed formulations are deficient in several essential elements such as amino acids and show palatability problems. Over the years, many attempts have been made to find alternatives to traditional fish feed and recently waste biomass was evaluated as possible source of feed ingredients. This alternative source requires technical, economic, social and environmental evaluations through the RRI strategy to guarantee the innovation for aquaculture industry.

9.2 Analysis of Scientific Solutions and RRI Strategy for Biotechnological Process

In order to respond to the growing demand for alternative fish feed, a sustainable, viable, non-GMO biotransformation producing the key lipid ingredients (omega-3) through the transformation of the by-product glycerol was proposed. These ingredients will partially replace the components of current fish feed permitting to avoid, at the same time, the use of fish oil for intake of (ω -3). This is the main goal of MYSUSHI project (Microalgae and Yeasts SUSTainable fermentation for HIGH quality fish feed formulation, Cariplo Foundation, N°2015–0395) developed by a team of University of Milano-Bicocca and University of Insubria (Italy). Biotechnologies are pioneering tools for bringing innovation to society but, due to difficulties in the assess of economic feasibility and limits imposed by socio-ethical acceptance of novelties, scientific innovations are penalized in marketing. MYSUSHI project exploited the concept of RRI (Fisher et al. 2006) aiming at modeling the research process on industry expectations together with stakeholders of aquaculture industry. Some of the strategies, outcomes, and considerations on the use and success of RRI analysis applied to an aquaculture case study are presented.

9.3 Strategy and Results

In our activities, we consider the three phases of the RRI: Engagement phase, Communication phase and Technology Transfer phase. We focused our attention on the first two phases, which are based on interactions with stakeholders to define the most suitable technology transfer actions. Experiences integrating societal considerations into an academic research laboratory setting suggest that it may help research planning and stimulate creativity (Von Schomberg 2013). Therefore, our aim was to consider all aquaculture stakeholders feedback in order to shape the research in a better way and to plan the technology transfer.

9.3.1 Identification and Engagement Phase

In this first phase, we considered the largest freshwater fish producers in Europe. Aquaculture industry of Northern Italy was particularly investigated since it is one of the major producers of EU for trout. Therefore, we evaluated the trout industry stakeholders through bibliographic analysis, direct farms visiting and trade fair events. As a result of this extended analysis, three stakeholder classes were identified: industry actors, scientific community, and civil society (Table 9.1).

Table 9.1 Different types and numbers of engaged stakeholders are indicated in the table

Stakeholder classes		
Industry actors	Scientific community	Civil society
Aquaculture companies: 10	Ecologists: 12	Students: 6
Feed producers: 5	Fish physiologist: 13	Citizens: 18
Companies: 2	Veterinaries: 24	Category associations: 4
Intermediates: 7	Fish pathologists: 9	
Retailers: 1		
Industries magazine: 1		

9.3.2 Communication Phase

In order to critically evaluate the scientific solution proposed by MYSUSHI, we considered different RRI tools to interact with stakeholders: dedicated surveys, one-to-one meetings and web communication. Specific surveys were designed aiming to tackle three kinds of issues: socio-ethical, technical-scientific and economic. These surveys were firstly proposed during Aquafarm fair to reach industrial stakeholders (Pordenone, 26–27 January 2017). This fair represents the most suitable environment for engagement phase. Results are described in Fig. 9.1. Data suggested that most people were highly interested in the optimization of fish feed

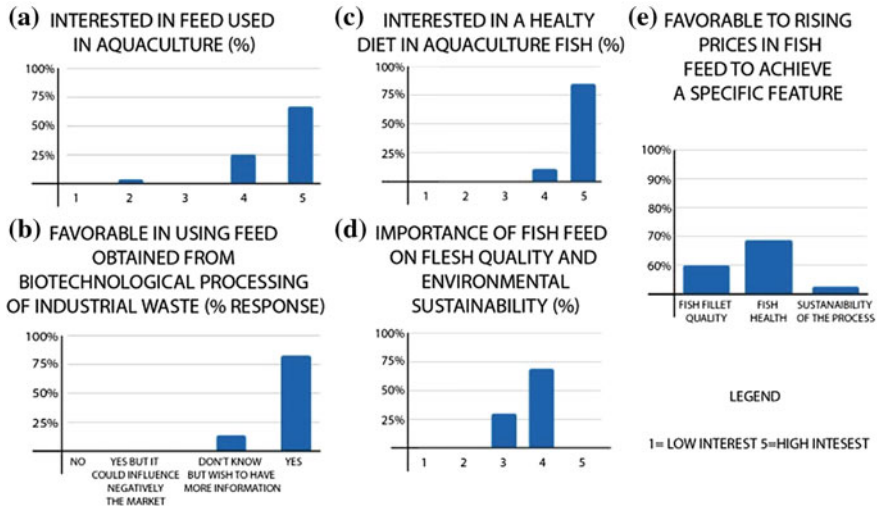


Fig. 9.1 Results of surveys' question. The stakeholder interest was expressed from 1 to 5 score. In **b** and **e** the specific features were indicated in the x-axis

(Fig. 9.1a) to enhance fish nutrition quality (Fig. 9.1c). The majority considered biotech processes a valuable tool to increase fish feed quality (Fig. 9.1b). Moreover, the environmental aspect represents a challenging issue of the aquaculture supply chain (Fig. 9.1d). Finally, almost a 70% of interviewed stakeholders were willing to pay for higher quality of fish fillet (Fig. 9.1e).

Industry actors were also engaged through one-to-one meetings to discuss all scientific project phases. Moreover, dedicated visits to the production facilities allowed us to better understand the organization of overall industrial process, guaranteeing the integration of research and technological goals. All tools adopted with industrial actors were very effective to improve research plan actions, to highlight the environmental impact of new feed formulations, to support bio-transformation in aquaculture and to enhance the fish quality aspects.

We planned the project considering local and European laws to design an innovation that could be implemented in the market. With more details about R&D innovation it will be possible to define the strategy with regulators. Among the stakeholders, scientists were reached through a strategy adopted by the grants office of Cariplo Foundation during MYSUSHI project evaluation. Three anonymous referees produced a technical report useful to improve scientific issues within the project, i.e. to identify a plan for biotechnological waste valorization phase. Moreover, one-to-one meetings were used specifically to evaluate the initial phase of the project during the selection of the most suitable strategy that could be used to improve fish feed formulation. In addition, MYSUSHI research team described the project during national and international conference through oral presentation and poster section (Aquafarm 2017, ASPA 2017). RRI action with scientific community

Table 9.2 Summary of possible feed alternative strategies, evaluated with scientific stakeholders

Source	Advantages	Disadvantages
Plant based products	<ul style="list-style-type: none"> • High availability • Good protein content 	<ul style="list-style-type: none"> • Palatability and pathological problems • High presence of fiber stimulate more excretion • Lipid fraction rich in ω-6 instead of ω-3 • Impact on use of soil
Animal based products	<ul style="list-style-type: none"> • Use of by-products • Amino acid profile more complete than vegetable one • Lower price than fish protein 	<ul style="list-style-type: none"> • Risk of disease transmission (TSE) • Need of mixing with polyunsaturated fats to avoid problem of fish digestibility • Consumer acceptance
GMO Trout	<ul style="list-style-type: none"> • Increased size of trout fillet (Medeiros et al. 2009) 	<ul style="list-style-type: none"> • In Europe, use of GM animals is prohibited • Public acceptance of GM trout is hard to achieve
Insect based products	<ul style="list-style-type: none"> • Very fast production rate • Legalized use of insect flour 	<ul style="list-style-type: none"> • Lipid content not sufficiently rich in omega-3 • Presence of chitin can interfere

allowed to evaluate alternative solutions of waste to produce feed as well as some scientist contributed to improve the nutritional quality of new feeds as described in Table 9.2. Civil society was reached through two different tools: a project dedicated website and social networks such as Facebook and Twitter. Facebook page “MySushi Biotech” has a total coverage of more than 9000 views while Twitter account (@MySushiBiotech) reached more than 38.000 views. We observed that citizens prefer to use Facebook to discuss about the aim of project while experts on specific issues (i.e. food systems) used Twitter to communicate with the project team. Those tools are also useful in order to contact non-commercial organizations since they provide full, yet simple explanation of the scientific solution and interaction with scientists. Initially, these tools were used to inform a wide public about MYSUSHI goals and strategy. Currently we are focusing on the presentation of critical issues of the project (ethical, social and economic) in order to stimulate a constructive debate to select the most active citizen-stakeholders.

9.4 Outcomes and Strategy for Next Phases

Our RRI analysis allowed to better identify the most suitable tools and strategies to reach several stakeholder classes. In the case of industrial actors we found one-to-one meeting the most promising strategy to drive research activities. However, considering that most of the industrial actors have a strong technical expertise, RRI team should involve not only experts in communication but also technical and scientific experts of the aquaculture sector. This could improve the relationships between industrial actors and scientists. Dedicated visits to the industrial facilities help the researchers in the identification of the main industrial

criticisms, for example on the strategy for handling waste material for biotransformation. Concerning scientific stakeholders, we considered the classical ways of scientific debate (meetings, conferences, papers) the most suitable tool to improve project's quality. Finally, citizens represent the most critical class of stakeholders due to their heterogeneity and lack of information about the criticism of aquaculture sector. On the whole, the RRI strategy adopted in our preliminary phase was suitable only for the communication phase but new tools should be identified to involve the citizen in the definition of innovation strategies, for example by defining a dedicated course for the more interested stakeholders, and to improve the role of citizen associations in the RRI evaluation of environmental impact, cost of production and future development.

References

- FAO (2016) The state of world fisheries and aquaculture 2016. Contributing to food security and nutrition for all, Rome, 200 p
- Evans HM, Burr GO (1927) A new dietary deficiency with highly purified diets. *Proc Soc Exp Biol Med* 24(8):740–743
- Fisher E, Mahajan RL, Mitcham C (2006) Midstream modulation of technology: governance from within. *Bull Sci Technol Soc* 26(6):485–496
- Von Schomberg R (2013) A vision of responsible research and innovation. In: Owen R, Bessant J, Heintz M (eds) *Responsible innovation: managing the responsible emergence of science and innovation in society*. Wiley, pp 51–74
- Medeiros EF, Phelps MP, Fuentes FD, Bradley TM (2009) Overexpression of follistatin in trout stimulates increased muscling. *Am J Physiol Regul Integr Comp Physiol* 297(1):R235–R242